# ELECTROPHYSIOLOGICAL STUDIES ON DORSAL ROOT GANGLIA NEURONS IN A SURGICAL KNEE DERANGEMENT MODEL OF OSTEOARTHRITIS IN THE RAT

By

QI WU, M.D., M.Sc

A Thesis

Submitted to the School of Graduate Studies

in Partial Fulfillment of the Requirements

for the Degree

Doctor of Philosophy

McMaster University

DOCTOR OF PHILOSOPHY (2010) McMaster University

(Medical Sciences) Hamilton, Ontario

TITLE: ELECTROPHYSIOLOGICAL STUDIES ON DORSAL ROOT GANGLIA NEURONS IN A SURGICAL KNEE DERANGEMENT MODEL OF OSTEOARTHRITIS IN THE RAT

AUTHOR: Qi Wu, M.D., M.Sc. (Second Military Medical University, P.R.China)

SUPERVISOR: Professor James, L. Henry

NUMBER OF PAGES: xx, 292

## ABSTRACT

Osteoarthritis (OA) is the most common arthritis, and the second most common diagnosis leading to disability. While loss of joint function is disabling, patients report that the greatest disabler of OA is the pain. Unfortunately, OA pain remains an unmet medical need. Numerous mechanisms have been proposed for the pathogenesis of OA pain. However, none of these mechanisms has led to satisfactory evidence-based treatment for OA pain. There is a critical need to address the mechanisms for OA pain due to the aging demographics and the prevalence of OA in older adults. This thesis project was aimed to study neural mechanisms for OA pain. The general hypothesis was that the pain of OA arises as a result of phenotypic changes in primary sensory neurons, especially in larger diameter A-fiber neurons. *In vivo* intracellular recordings were used to determine changes in specific populations of DRG neuron in a surgical knee derangement model of OA in the rat. It was found that Aß-fiber low threshold mechanoreceptors, particularly muscle spindle afferents underwent significant changes (including changes in action potential configurations and in responses to repetitive stimulation) one month following the model induction when histopathological changes of the knee joint and the nocifensive behaviors of the affected lower limb favor OA. Nociceptors, including C-, Aδ- and Aβ-fiber neurons remained largely unchanged at one month OA. Aβ-fiber high threshold mechanoreceptors exhibited significant changes at two month OA, a later phase during the progression of OA. The data demonstrate that distinct populations of dorsal root ganglia neuron are altered during the progression of OA, which might be the neuronal basis for clinical presentations of sensory deficit in OA

including pain and loss of proprioception. The data also suggest that the pain in OA might be a form of neuropathic pain.

## DEDICATION

This thesis is dedicated to my wife, Chang Ye. Your company and continuing support make this thesis a reality. You are the best wife, spiritual mate and friend.

## ACKNOWLEDGEMENTS

This thesis would be impossible without the help of many people who I would like to acknowledge here. The acknowledgements follow no particular order.

I have tremendous respect to my supervisor Dr. James L. Henry. You took me as your graduate student in 2004, which leads me to a completely different but ample life. I have greatly benefited from your mentorship. You are an outstanding scientist with superb vision and skills; you are a great thinker full of philosophy and knowledge and are keen to share; and you are an easy-going gardener full of love and care for your trainees. You have been training me to do science rather than do experiments. These five years with you would be the most valuable period in my life.

Most special thanks go to my parents (Dad, Tianzheng and Mom, Suhua). You contribution in this thesis is too important to be measured, as all my talents are from you. You have been taking very good care of yourself so that I could concentrate in this thesis project. The thesis is dedicated to Chang. But you will have your "souvenir", the convocation. I hope both of you will be sitting there and be honored. Qiang, my dear brother: thank you so much for the wonderful arrangements you have made for Dad and Mom. I owe you big!

I would also like to acknowledge the members of my supervisory committee: Drs. Alexander K. Ball, Jan Huizinga and Wolfgang Kunze. Thank you all for your critique during my committee meetings that boosted the chance to publish my data and for your very supportive references that made me successful in several prestigious scholarship applications.

Special thanks go to Dr. Alexander K. Ball for the pleasant collaboration that we have been through together, and for letting me use your space, equipments and chemicals. I am still amazed that the best images we got were those stained with the anti-substance P antibodies you stored in 80's!

I am grateful for Dr. Guozhong Chen, who is Head of the Department of Anesthesiology in Dongfang Hospital where I spent my four year of residency. You encouraged me to pursue study in pain, and let me go after my dream. Thank you for your understanding and continuing support.

I am also grateful for Dr. Yanguo Hong, who interviewed me and recommended me to Dr. Henry. I realize that the experience I gained in your lab later became very good orientation in the pain field. Thank you for your recommendation and your teaching.

I would like to thank Dr. Kiran Yashpal, the senior research scientist in our lab. You care about me and treat me like your child. I appreciate your efforts to create a better workplace and your efforts to bring in better equipments. I am especially grateful for Vasek Pitelka, our senior technician and my friend. You held my hand and comforted me when I arrived in Canada and experienced many forms of culture shock. You taught me lab skills and tricks. The skills remain in my brain, whereas the tricks in my heart. Thanks also go to my fellow graduate students and technicians, Liliane Dableh, Yongfang Zhu, Paolo De Ciantis, Chitra Lalloo, Yufang Wang and Sheila Bouseh, for your critique, discussion and any form of help in the lab.

## PREFACE

This thesis is a "sandwich" style thesis. Chapter 1 is the introduction, and Chapter 6 is the general discussion. Chapter 3 has been published as a research article prior to the completion of this thesis work. Chapters 2, 4 and 5 have been submitted for being published as peer-reviewed research papers, and are currently in the review process.

Preface of each chapter describes the details of the published or submitted article, as well as my contribution to the multiple-authored work.

All chapters have been reproduced with permission of all co-authors. Irrevocable, non-exclusive license has been granted to McMaster University and to the National Library of Canada from all publishers. Copies of permission and licenses have been submitted to the School of Graduate Studies.

# TABLE OF CONTENTS

# LIST OF TABLES

## CHAPTER 2



## CHAPTER 3

# LIST OF FIGURES

## CHAPTER 1



## CHAPTER 2



## CHAPTER 3

**CHAPTER 4**



**CHAPTER 5**

## LIST OF ABBREVIATIONS

**ACL:** anterior cruciate ligament
**AHP:** afterhyperpolarization
**AHP50, AHP80:** 50%, 80%AHP recovery time
**AP:** action potential
**APD:** action potential duration
**ATF-3:** activating transcription factor-3
**BDNF:** brain derived neurotrophic factor
**bHLH:** basic helix-loop-helix
**CGRP:** calcitonin gene related peptide
**CNS:** central nervous system
**COX:** cyclooxygenase
**CV:** conduction velocity
**DCMLS:** dorsal column -medial lemniscus system
**DEG/ENaC:** amiloride-sensitive sodium channels
**DRG:** dorsal root ganglia
**ERK:** extracellular signal-regulated kinase
**Epo:** erythropoietin
**EPSP:** excitatory postsynaptic potential
**ErbB:** erythroblastic leukemia viral oncogene homolog, also named as epidermal growth factor receptor family
**FFF:** fiber following frequency
**GDNF:** glial cell derived neurotrophic factor
**HMGB:** high-mobility group box
**HSP:** heat shock protein
**HTM:** high-threshold mechanoreceptor
**IB4:** isolectin I-B4
**IL:** interleukin
**JAK/STAT:** Janus kinases/ signal transducers and activators of transcription
**JNK:** c-Jun N-terminal kinase
**Kca:** calcium-activated potassium channel
**Kir:** inwardly rectifying potassium channel
**K2p:** two-pore potassium channel
**Kv:** voltage-gated potassium channel
**LIF:** leukemia inhibitory factor
**LTM:** low-threshold mechanoreceptor
**MAPK:** mitogen-activated protein kinase
**MFR:** maximum falling rate
**MHC:** major histocompatibility complex
**MIA:** mono iodoacetate
**MRI:** magnetic resonance imaging
**MRR**: maximum rising rate
**MyD:** myeloid differentiation

**Nav:** voltage-gated sodium channel
**NF-κB:** nuclear factor kappa-light-chain-enhancer of activated B cells
**NGF:** nerve growth factor
**NO:** nitric oxide
**NT-3, NT-4:** neurotrophin-3, 4
**NSAID:** non-steriodal anti-inflammatory drug
**OA:** osteoarthritis
**PI3K:** phosphoinositide 3 kinase
**PLC:** phospholipase C
**PKA, PKC, PKG:** protein kinase A, C, G
**PNS:** peripheral nervous system
**RI:** refractory interval
**Runx1:** Runt-related transcription factor
**TGF-β:** transforming growth factor beta
**TLR:** Toll-like receptors
**TNF-α:** tumor necrosis factor-α
**TRP:** transient receptor potential
**TTX:** tetrodotoxin
**VIP:** vasoactive intestinal polypeptide
**VPL:** ventral posterolateral nucleus
**VGCC:** voltage-gated calcium channel
**Vm:** resting membrane potential
**Trk:** tyrosine kinase
**WDR:** wide dynamic range

# CHAPTER 1.

# Introduction

Osteoarthritis (OA) is a degenerative joint disease that is projected to affect an astounding 18% of the population in the western world by the year 2020 (Lawrence et al., 1998). In addition, it has a cost of $15.5 billion per year in the US alone, taking into account the accompanying disability and social consequences (Yelin and Callahan, 1995). The features of OA constitute a group of conditions that are diagnosed upon common pathological and radiological characteristics (Felson et al., 1997) and are believed to be caused by material failure of the cartilage network leading to tissue breakdown (Poole, 1999) or by injury of chondrocytes with increased degradative responses (Aigner and Kim, 2002) (Figure 1.1).

Pain has been defined as the primary symptom of OA (Creamer, 2000). Physicians typically rely on scores of pain and measures of joint function to diagnose OA (Swagerty, Jr. and Hellinger, 2001), as pain rather than joint pathology is more pronounced in this disorder. Recently, Hawker et al. (2008) revealed two distinct types of OA pain: an early predictable dull, aching, throbbing "background" pain and an unpredictable short episode of intense pain that develops later (Hawker et al., 2008). During the progression of OA, pain evolves from the "background" pain that is use-related in early OA (Kidd, 2006), to unpredictable short episodes of intense pain on top of the "background" pain in advanced OA (Hawker et al., 2008). It is this

unpredictable intense pain that has the greatest impact on the quality of life and that results in the avoidance of social and recreational activities (Hawker et al., 2008).

Current investigations into the mechanisms of OA pain tend to focus on changes in excitability or activation of nerve terminals in the joint, including activation of sensitized nociceptors in the knee (McDougall et al., 2006;Schuelert and McDougall, 2006), bone marrow lesions or microfractures, increased intra-osseous pressure, inflammation of the synovium and changes in spinal sensory processing (Felson, 2005;Kidd, 2006;Niv et al., 2003;Rowbotham M.C et al., 2006), or try to explain the pain as due to central sensitization (Creamer et al., 1998;Bajaj et al., 2001;Melton, 2003). None of these mechanisms has led to satisfactory mechanism based treatments for the pain in OA.

Primary sensory neurons as a possible origin of OA pain are largely overlooked. Yet, clinical data implicate changes in primary sensory neurons in OA, including pain from areas remote from the arthritic joint in most OA patients (Kean et al., 2004), joint pain following total hip replacement (Nikolajsen et al., 2006), and the presentation of Aβ-fiber mediated symptoms, such as loss of proprioception in OA patients (Barrett et al., 1991;Hurley et al., 1997;Katz WA., 2001;Shakoor and Moisio, 2004;Sharma and Pai, 1997;Sharma, 1999). Thus, the objective of this thesis project is to investigate the possible role of primary sensory neurons in the pathogenesis of the pain in a surgical

knee derangement model of OA, which mimics the most common etiology in human OA. *In vivo* intracellular recording from functionally identified neurons forms the main technical basis of this thesis project, and is capable of pinpointing the sensory fiber type or types most affected in this model.

The following background section provides reviews of the animal model of OA, current understanding of the pain in OA, and fundamental knowledge about the physiological functions of the primary sensory system, which aims to help readers understand the findings from this thesis project. The rationale for the study is covered in each chapter.

**1.1. The animal model of OA**

There are several types of animal model of OA. One type of model is designed to elucidate molecular mechanisms underlying the pathogenesis of OA, including models induced by modulation of gene (Munoz-Guerra et al., 2004) or protein expression (Johnson and Terkeltaub, 2004), injection of inflammatory cytokines (Hui et al., 2003) or injection of proteolytic enzymes (Kikuchi et al., 1998). Another type is designed to model OA for pre clinical testing, and is generally based upon surgical induction (Liu et al., 2003) or excessive use of the joint (Pap et al., 1998).

The model selected for the present study is a surgically-induced derangement of the knee of one hind leg. OA can originate from a number of causes, of which injury is

the most common (Creamer et al., 1998). The procedure to induce the model involves transection of the ACL which is highly innervated (Krauspe et al., 1995;Haus and Halata, 1990), protects the joint from over extension, and is often ripped in sports injuries (Shirakura et al., 1995). The procedure also involves removal of the medial meniscus, another highly innervated structure (O'Connor and McConnaughey, 1978;Assimakopoulos et al., 1992) which distributes load evenly onto the articulating surfaces and is often damaged in a traumatic injury and commonly leads to the development of OA (Mitsou and Vallianatos, 1988). Removal of this structure therefore results in an approximate 65 % increase in the load on the articulating surfaces and thus increases the severity of the derangement (Noyes et al., 1980).

Previous work in our group showed that the model displays histological and imaging profiles resembling those in human knee OA, and the severity of the model can be regulated by forced mobilization on a slowly rotating treadmill (Appleton et al., 2007b;Appleton et al., 2007a;Appleton et al., 2007c). Dorsal horn wide dynamic range (WDR) neurons show expanded receptive fields and higher spontaneous discharge rates, and exhibit significantly different patterns of spontaneous activity in OA (Schwartz, 2005), indicating either increased peripheral drive or central hyperexcitability. Articulation of the deranged knee induces a brief heterosegmental pronociceptive effect in the tail flick test; in a modified open field test, this pronociceptive effect leads to a

decrease in voluntary use of the joint (Schwartz, 2005). Tests on a slowly rotating drum confirmed that this decrease is not due to a reduction in the mechanical viability of the joint and muscular strength (Schwartz, 2005;Appleton et al., 2007b). Repetitive articulation of the deranged knee within normal range also causes an increase in the spontaneous firing rate, an increase in low threshold spiking and an increase in the response to iontophoretic application of glutamate and substance P without altering the responsiveness to inhibitory amino acids (Schwartz, 2005).

**1.2. Current views of mechanisms of the pain in OA**

Pain in OA, like other chronic pain states is a complex process that involves abnormal cellular mechanisms at both peripheral and central levels of the nervous system. Several underlying mechanisms might be at play, and the relative contribution of these mechanisms determines the significant heterogeneity in OA patients. The following overview of the current literature mainly focuses at peripheral and spinal mechanisms.

1.2.1. OA is an inflammatory disease wherein peripheral sensitization of joint nociceptors initiates the pain

In contrast to rheumatoid arthritis where inflammation, both local and systemic, is a key feature, OA is traditionally considered as a primarily non-inflammatory condition. However, there is a growing acknowledgement that inflammation is of importance in OA pathophysiology. Pelletier et al. even propose that OA is an inflammatory disease

(Pelletier et al., 2001). There is mounting supportive evidence about the association between OA progression, the signs and symptoms of inflammation, and disease activity (Pelletier et al., 2001;Saxne et al., 2003). With the assumption that OA is an inflammatory disease, several hypotheses have been proposed to further explain the pathogenesis of the pain in OA.

1.2.1.1. Peripheral sensitization of joint nociceptors as a mechanism of joint pain in OA

Felson proposed that joint nociceptors could become a source of pain in OA (Felson, 2005). Nociceptors are distributed throughout the joint, and have been identified in the capsule, ligaments, menisci, periosteum and subchondral bone (McDougall, 2006). These nocicepotors are normally activated by noxious range movements of the joint. How do these nociceptors generate abnormal painful signals in OA? Some have proposed that it is due to abnormal innervation of these nociceptors, as some evidence shows the innervation of joint nociceptors extends to normally aneural tissues, such as cartilage (Suri et al., 2007). As a result, normal activity of the joint, such as standing or walking, could initiate abnormal painful signals due to the aberrant innervation of cartilage.

Another proposed mechanism of joint pain is that the activation threshold of joint nociceptors is reduced. These afferents become hypersensitive to both normal and noxious types of movement or even develop spontaneuous discharge in arthritic joints

(Grigg et al., 1986;Schaible and Schmidt, 1988;Schaible and Schmidt, 1985;Coggeshall et al., 1983).

Some others have proposed that the recruitment of "silent nociceptors" in OA contributes to joint pain (McDougall, 2006). These nociceptors are quiescent in normal joints, unable to be activated by noxious stimulation but become responsive when damage or inflammation occurs in the joint. In arthritic joints, these "silent nociceptors" are sensitized to increase responsiveness to even normal working range of movement of the joint (Schaible and Schmidt, 1985).

Then, what is the molecular basis of peripheral sensitization of joint nociceptors? It is generally agreed that pro-inflammtory mediators released into the joint in OA would sensitize joint afferents. However, people know too little to propose any potential molecule to be targeted. Recently, McDougall et al proposed that vasoactive intestinal polypeptide (VIP) is a modulator of joint pain in OA (McDougall et al., 2006). Peripherally administrated VIP causes peripheral sensitization of articular afferents in response to normal and noxious joint movement, and results in less hindlimb weight bearing as well as reduced hind paw withdrawal thresholds (McDougall et al., 2006;Schuelert and McDougall, 2006). Other evidence shows that VIP and two other neuropeptides commonly expressed by nociceptors, substance P and calcitonin gene related peptide (CGRP), are increased in content in the osteoarthritic joint (Saito and

Koshino, 2000;Saxler et al., 2007). Increased expression of these neuropeptides in sensory fibers leads to a hypersensitive state. Besides neuropetides, cytokines and other inflammatory mediators, such as nitric oxide (NO), prostaglandins, interleukin (IL)-1β, tumor necrosis factor (TNF)-α, IL-6, and IL-8 might also play a role in peripheral sensitization. Evidence shows that chondrocytes obtained from patients with OA actively produce these inflammatory mediators (De et al., 2004;Borzi et al., 1999). Thus, chondrocytes have been proposed to play an important role in initiating peripheral sensitization of joint nociceptors.

Peripheral sensitization of joint nociceptors is the dominating mechanism proposed for OA pain. However, this proposed mechanism cannot explain the pain that still remains in the 28% of patients after total hip replacement (Nikolajsen et al., 2006). Moreover, this proposed mechanism cannot account for the other sensory deficits commonly seen in OA patients, such as loss of proprioception, which is most likely mediated by large Aβ-fiber low-threshold mechanoreceptors (LTMs).

1.2.1.2. Local tissue pathology as a factor contributing to OA pain

Hunter et al. focused more on structural determinants of pain, and proposed that articular and peri-articular tissues constitute the source of pain in OA (Hunter et al., 2008). Synovial inflammation has been convincingly demonstrated in OA patients, at least during some phases of the disease. Periosteum, subchondral and marrow bone are

richly innervated with sensory fibers, lesions of which could be potential sources of OA pain. Peri-articular inflammation, which can arise secondary to deformity and lack of stability associated with OA, may also produce local pain that is difficult to distinguish from the pain in OA (Gnanadesigan and Smith, 2003).

In population studies there is a significant discordance between the severity of joint damage determined by knee radiography and the severity of pain experienced (Hannan et al., 2000). However, it is too early to conclude that there is no structural determinant of pain in OA. Evidence from imaging technologies, such as magnetic resonance imaging (MRI), has revealed some important correlations. Moderate or large effusions and synovial thickening occur more frequently in those with knee pain than those without, and synovial thickening has been identified associated with the severity of pain (Hill et al., 2001). MRI Evidence also shows significant association of several structural lesions, such as bone marrow lesions and subarticular bone attrition, with knee pain, as reviewed recently in (Hunter et al., 2008).

Evidence from other types of studies also supports a role of local tissue pathology in the pain in OA. Plebographic studies in OA identify impaired vascular clearance from bone and the resultant increase in intraosseous pressure in the bone marrow near the painful joint (reviewed in Simkin, 2004). Studies in knee pathology have revealed an association of OA with several peri-articular inflammation conditions, such as

trochanteric bursitis around the hip, pes anserine bursitis around the knee, medial collateral ligament syndromes and pes anserine tendinitis (Gnanadesigan and Smith, 2003;Creamer et al., 1998).

Local tissue pathology as a mechanism of pain in OA is an important complement for the peripheral sensitization theory, and is of particular importance for clinical practice in the management of OA pain, as peripheral sensitization is invisible whereas local tissue pathology is identifiable. However, the major limitation of this proposed mechanism of OA pain is that it fails to account for the referred pain and the loss of proprioception reported by OA patients, and it also cannot account for the chronic pain that persists in some patients that have undergone total joint replacement.

1.2.2. OA pain goes central

Gunnar Ordeberg, an orthopedic surgeon from Karolinska Institute, Sweden described the development of the pain in OA (Melton, 2003). "OA symptoms usually start with localised pain that responds to analgesics" , he explains. "Eventually the response to pain killers is lost and the area with pain spreads, to the thigh and knee, then the leg, and often there is pain all over the body." Many researchers agree, and central sensitization has been proposed as a critical mechanism for the full manifestation of the pain in OA (Felson, 2005;Kidd, 2006;Rowbotham M.C et al., 2006;Schaible and Grubb, 1993).

In chronic pain states, sustained or repetitive activation of primary afferents results in functional changes in the central nervous system (CNS), manifested as an increased response in spinal dorsal horn neurons to stimuli in areas adjacent to the inflamed tissue and even in the remote, non-inflamed "normal tissue, and the ensuing sustained increase in spinal excitability. This is known as central sensitization. Some people believed that nociceptive afferent input from joints sensitize spinal cord dorsal horn neurons in arthritic animals, giving rise to increased excitability, larger receptive fields and spontaneous activity (Hylden et al., 1989;Grubb et al., 1993). It has been proposed that increased excitability could mediate the pain felt during normal movements of the affected joint, while the spontaneous activity could be the afferent base of resting pain (Schaible and Grubb, 1993)

There are some observations implicating possible central mechanisms in the pathogenesis of OA pain. First, clinical observation has documented patient complaints of referred pain from areas outside osteoarthritic joints (Kean et al., 2004). Second, there is evidence of increased muscle hyperalgesia in OA patients (Bajaj et al., 2001). Third, patients with unilateral painful hip OA show lower pain thresholds for pressure stimulation even at the unaffected contralateral hip (Kosek and Ordeberg, 2000); unilateral administration of local anesthetic in the osteoarthritic joint can have bilateral effects in OA patients (Creamer et al., 1996).

.Other central mechanisms of pain in OA have been proposed, involving functional changes in the brain, for example, dysfunction of descending inhibitory control (Kosek and Ordeberg, 2000), and altered cortical processing of noxious information (Buffington et al., 2005).

Central mechanisms of the pain in OA are generally accepted to be in place, as each type of chronic pain is believed to develop a certain degree of central plasticity. It is a positive step that central sensitization as a cause of OA pain prompts us to look beyond the osteoarthritic joint because it shifts us to think of OA pain as being attributing to neural mechanisms. However, this theory is incomplete, as it does not tell us the fundamental difference in central sensitization in various chronic pain conditions, for example the difference between OA induced and rheumatoid arthritis induced central sensitization. This is critical to understand why some drugs are effective in one type of arthritis but not in another, which is critical for novel, effective mechanism based treatments. Finally, though, the proposal that central sensitization is the cause of OA pain also fails to account for the loss of proprioception in OA and fails to account for the lack of correlation between the severity of structural change and the severity of OA pain.

**1.3. Molecular and cellular bases for sensory specificity in primary sensory neurons**

The pleasant sensation of a gentle touch on skin or the pain from stepping on a nail is encoded by somatosensory neurons innervating skin. The peripheral terminals of

these neurons, whose cell bodies are located in the trigeminal ganglion and dorsal root ganglia (DRG), transduce various stimulus energies into APs that propagate to the CNS.

Somatosensory information is traditionally divided into three modalities – mechanical, thermal and chemical (Koerber HR and Mendell LM, 1992). DRG neurons are heterogenous in size, myelination and chemical composition. It has been suggested that these heterogeneities are the basis of sensory specificity. Different neuron types respond preferentially to a certain type of sensory modality. A number of classifications of DRG neurons have been proposed by several different labs (Burgess et al., 1968;Horch et al., 1977;Lynn and Carpenter, 1982;Iggo, 1985;Koerber et al., 1988;Leem et al., 1993a;Leem et al., 1993b;Cardenas et al., 1995;Koltzenburg et al., 1997;Lawson et al., 1997;Petruska et al., 2002;Petruska et al., 2000). Lawson's classification was modified, and served as the basis for any classification in this thesis project (Figure 1.2). In summary, detection of mechanical stimuli is served by neurons of all sizes (from small-sized C-fiber neurons to large-sized Aβ-fiber neurons). Most, but not all large-sized Aβ-fiber neurons detect low intensity, innocuous stimuli such as touch, movement over skin, shortening of muscle spindle and vibration etc. By contrast, most, but not all small-sized C-fiber and medium-sized Aδ-fiber neurons can only be activated by high intensity stimuli that are noxious in nature. However, it should be noted that there are significant numbers of Aβ-fiber neurons that respond only to high intensity,

noxious stimuli, and there is a small number of C-fiber and Aβ-fiber neurons that can be activated by very gentle touch/movement over skin. Thermosensation is encoded by a subpopulation of C-fiber and A-fiber neurons that exhibit responsiveness over a range of temperatures from extreme cold (about -10°C) to extreme hot (about 60°C). Mild temperatures produce a cool/warm sensation, and are encoded by non-nociceptive neurons, whereas extreme temperatures produce cold or heat pain, and are encoded by nociceptive neurons, in most cases polymodal neurons. Chemosensation to capsaicin, protons or ATP has been convincingly demonstrated in small to medium-sized C-fiber and A-fiber neurons (Petruska et al., 2002;Petruska et al., 2000;Cardenas et al., 1995). It has not been clearly stated whether or not large-sized Aβ-fiber neurons participate in chemosensation. However, Petruska et al. (2000) reported that all Type 4 neurons (diameter, 35-48μm) exhibit ATP-activated currents. This is supportive evidence for a role of fast-conducting Aβ-fiber neurons in chemosensation, at least to ATP, as our own *in vivo* observation confirming that many Aβ-fiber neurons fall within that size range.

Significant progress has been made in understanding the molecular basis of how sensory neurons convert environmental stimuli into propagating electrical signals. Several classes of ion channels have been proposed for sensory specificity, whose gating is controlled by mechanical, thermal and chemical stimuli (for reviews see Julius and Basbaum, 2001;Voets and Nilius, 2003;Lumpkin and Caterina, 2007;Belmonte and Viana,

2008). A model of molecular somatosensory specificity is shown in Figure 1.3. These encoding ion channel superfamilies include amiloride-sensitive sodium channels (DEG/ENaC) and transient receptor potential (TRP) channels. DEG/ENaCs are mainly involved in mechanical sensing and acidosis sensing, and might also act as cold sensors (Belmonte and Viana, 2008). TRPs are the superfamily consisting of seven subfamilies (TRPC, TRPV, TRPM, TRPN, TRPA, TRPP, and TRPML), and are cation-selective channels defined by six transmembrane-spanning domains and structural homology within these domains (Clapham et al., 2003;Huang, 2004). Unlike other ion channels, TRP channels have a diverse mode of activation and selectivity – gated by either biochemical ligands (e.g. capsicin, proton, menthol, etc.) or physical stimuli (e.g. heat or cold), and are the main players in transducing all three types of stimulus energies (mechanical, thermal and chemical). Here, we review ion channels critical for sensory encoding in mammals.

Several TRPV subunits, TRPA1 and TRPM8 have been implicated in thermal sensing, but with different yet overlapping optimal activating temperature. TRPV2 is activated by heat at the highest temperature range (> 52°C) (Caterina et al., 1999), followed by TRPV1 (> 42°C) (Tominaga et al., 1998), TRPV3 (30-39°C) (Smith et al., 2002;Xu et al., 2002;Peier et al., 2002b), and TRPV4 (25-35°C) (Guler et al., 2002). Activation of these channels leads to sensation from warmth to burning hot. However,

TRPM8 encodes cold, and it is activated at temperatures between 8 to 28°C (Peier et al., 2002a;McKemy et al., 2002). Temperature dropping below 17°C activates TRPA1, which causes a burning cold sensation (Story et al., 2003). Unlike thermal sensing, the molecular basis of somatic mechanosensation is less clear. Two DEG/ENaC members, ASIC2 and ASIC 3 are expressed in somata and peripheral terminals of DRG neurons including small and large diameter neurons (Garcia-Anoveros et al., 2001;Price et al., 2000;varez de la et al., 2002;Price et al., 2001). The firing rate of touch-evoked responses in low-threshold rapidly adapting mechanoreceptors is modestly decreased in the ASIC2 knockout mouse (Price et al., 2000). ASIC3 has a differential role in different neurons - in rapidly adapting mechanoreceptors the absence of ASIC3 enhances mechanosensitivity, whereas in A-fiber high-threshold mechoreceptors it reduces mechanosensitivity (Price et al., 2001). However, mechanical thresholds in both cases are basically unaffected. Several TRP channels including TRPC1, TRPA1, TRPV2, TRPV4, TRPP and TRPML3 have been implicated in other forms of mechnosensation such as hearing, osmolar sensing and flow sensing (Huang, 2004;Lumpkin and Bautista, 2005). However, a similar role of these channels in DRG neurons has yet to be confirmed. TRPV and ASIC channels are two main groups of chemosensors detecting changes in concentration of proton and other metabolic products (Belmonte and Viana, 2008).

Somatosensory encoding is an extremely complicated process, whose complexity is determined by several factors. First, there is limited sensory specificity associated with either DRG neurons or encoding channels. Most of C- and Aδ-fiber nociceptive neurons are polymodal, responding to heat, cold, chemicals and strong mechanical forces. The majority of TRP channels are polymodal. A good example is TRPV1, the founding channel of the TRP superfamily, which was recognized since its discovery as a polymodal transducing molecule for chemical (e.g. capsaicin) and heat stimuli (Caterina et al., 1997), and later for mechanical distention of the bladder (Birder et al., 2002). Second, there is a significant degree of sensory summation at the level of transducing molecules. A single event could simultaneously affect gating of several channels. For instance, temperature dropping from 37°C to 25°C increases the activation of TRPM8, but decreases the activation of background $K_{2P}$ channels (Reid and Flonta, 2001), TRPV3 and TRPV4. The final receptor potential is the result of the summation of separate ion channels activated by a specific stimulus in the same neuron. Third, sensory phenotype of a neuron is not just associated with a specific transduction molecule but instead results from a favorable blend with other ionic channels expressed in the neuron. For example, in a specific subpopulation of cold-insensitive DRG neurons, the application of 4-AP, a potassium channel blocker, induces a novel phenotype of cold-sensitivity (Viana et al., 2002). Fourth, there is significant modulation of the sensory initiation process at the

peripheral terminals. Potential mechanisms include combinatorial expression with voltage-gated sodium channels, intrinsic signaling, lipid metabolic products (Belmonte and Viana, 2008), and neighboring cells (e.g. keratinocytes) (Lumpkin and Caterina, 2007).

**1.4. Sensory pathways**

Primary afferent nociceptors project to spinothalamic projection neurons located in Rexed's laminae I, II and V. Rexed's laminae are shown in Figure 1.4. However, peptidergic and non-peptidergic nociceptors relay to different sensory pathways as depicted in Figure 1.5 (Braz et al., 2005;Hunt and Rossi, 1985). Peptidergic nociceptors terminate mainly in laminae I and $II_o$ (Hunt and Rossi, 1985). They directly contact projection neurons, and relay nociceptive information to the thalamus or to the amygdala via the parabrachial nucleus of the dorsolateral pons (Jasmin et al., 1997). Non-peptidergic nociceptors project to interneurons located in lamina $II_i$. These neurons contact projection neurons in laminae V, whose projections terminate in the amygdala, hypothalamus, bed nucleus of the stria terminalis and globus pallidus (Braz et al., 2005). The low-threshold cutaneous mechanoreceptors project mainly to laminae III-IV, including hair follicle afferents and glabrous rapidly adapting neurons (Wilson et al., 1986;Brown et al., 1977;Brown et al., 1978;Brown et al., 1980). However, Pacinian afferents and cutaneous slowly adapting neurons not only project to laminae III-IV, but

also to deeper laminae – Pacinian to laminae V and VI and slowly adapting neurons to laminae V. This tactile information is mainly conveyed by the spinocervical tract to higher centers in the ventrobasal thalamic nuclei (Brown, 1981). Group Ia and II proprioceptive afferents innervate muscle spindles, and Group Ib afferents innervate Golgi tendon organs (Inoue et al., 2002). The trajectory of group I proprioceptive afferents is somatotopically arranged both in the dorsal funiculus and in the grey matter. Ascending axons run in various regions of the dorsal funiculus – those from toe muscles in the ventral most part of the paramedian region, those from shank muscles in both dorsal and ventral paramedian regions, those from thigh muscles in both the paramedian and the more lateral regions, and those from hip muscles in the lateral region (Hongo et al., 1987). Proprioceptive afferents terminate in Clark's column in the intermediate zone and in the motor nucleus of the ventral horn of the spinal cord (Nakayama et al., 1998;Hongo et al., 1987). Collaterals of fibers from muscles ramify mostly in the dorsomedial one-third of the column. Collaterals of fibers from shank muscles terminate in its middle parts as well as in laminae V-VII. Collaterals of fibers from thigh muscles terminate in its ventrolateral part and in laminae V-VIII. Collaterals of fibers from hip muscles ramify mostly in laminae VII-IX. As the muscle of origin becomes more proximal, the proportion of termination outside Clarke's column progressively increases (Hongo et al., 1987). Proprioceptive information is mainly

relayed by the spinocerebellar tract, which also conveys tactile information (Bosco and Poppele, 2001;Edgley and Jankowska, 1988).

**1.5. The distribution of voltage-gated ion channels in primary sensory neurons**

1.5.1. Sodium channels

Voltage-gated sodium channels are critical for action potential (AP) initiation and propagation in excitable cells. Each sodium channel is comprised of a highly processed α subunit and one or more auxiliary β subunits. The pore-forming α subunit is sufficient for ion flow, but the kinetics and voltage dependence of channel gating are modified by the β subunits. So far, nine sodium channel isoforms (Nav1.1- Nav1.9) are defined. Further amino acid sequence and relatedness analyses reveal that Nav1.1, Nav1.2, Nav1.3, and Nav1.7 are closely interrelated and are tetrodotoxin (TTX)-sensitive. Nav1.5, Nav1.8, and Nav1.9 are closely interrelated and are TTX-resistant isoforms (Catterall et al., 2003). Nav1.4 and Nav1.6 do not belong to either group due to distinct phylogenetic relationship. However they are TTX-sensitive (Rush et al., 2007). Moreover, three auxiliary subunits of sodium channels have been defined – $\beta_1$, $\beta_2$, and $\beta_3$ (Catterall et al., 2003).

A recent study by Fukuoka, et. al. (2008) provided the most up-to-date understanding about the distribution of the sodium channel α subunit in DRG neurons. Nav1.4, the muscle isoform, in addition to Nav1.5, is not expressed in DRG neurons

(Catterall et al., 2003;Fukuoka et al., 2008;Kerr et al., 2007). Nav1.2 and Nav1.3 are expressed at a very low level in a very limited number of small neurons (Fukuoka et al., 2008;Black et al., 1996). Nav1.3 is the embryonic isoform, whose expression is very low in adult sensory neurons but is increased following axotomy (Waxman et al., 1994). Nav1.1 and Nav1.6 are exclusively expressed in $NF200^+$ neurons of all sizes, preferentially in TrkC positive neurons, more in isolectin I-B4 ($IB4^-$) neurons, and are A-fiber-neuron specific (Fukuoka et al., 2008). However, the expression of these channels in small diameter A-fiber neurons is controversial (Cummins et al., 2005;Black et al., 1996). It is notewothy that Nav1.6 is the channel highly expressed at nodes of Ranvier in A-fibers (Krzemien et al., 2000). Nav1.7 is expressed in ~ 70% of A-fiber neurons, forming various combinations of TTX-sensitive channels with Nav1.1 and Nav1.6. However, it is expressed in all C-fiber neurons, and it is the only TTX-sensitive channel in C-fiber neurons (Fukuoka et al., 2008). Nav1.8 and Nav1.9 are expressed in 60-70% of DRG neurons (almost all C-fiber neurons and 20-40% of medium to large diameter neurons) (Fukuoka et al., 2008;Sangameswaran et al., 1996;Dib-Hajj et al., 1998), which are mostly $TrkA^+$ neurons (Fukuoka et al., 2008). Almost all $IB4^+$ neurons express both Nav1.8 and Nav1.9 (Fukuoka et al., 2008;Fang et al., 2006), whereas only half of $IB4^-$ neurons express these channels (Fukuoka et al., 2008).

The sodium channel $\beta_1$ subunit is predominantly expressed in medium to large diameter neurons (Takahashi et al., 2003;Oh and Waxman, 1995;Black et al., 1996). The $\beta_2$ subunit is expressed in neurons of all sizes; the $\beta_3$ subunit is mainly expressed in small to medium size neurons (Takahashi et al., 2003).

1.5.2. Potassium channels

Potassium channels are a diverse group of ion channels with the largest number of subtypes. There are four major classes of potassium channel: Voltage-gate potassium channels ($K_v$) that open and close in response to trans-membrane voltage and play a crucial role during the AP in returning membrane potential back to the resting state; Calcium-activated potassium channels ($K_{ca}$) that are voltage-insensitive, open in response to the presence of internal calcium ion and are involved in calcium-dependant signaling; Inwardly rectifying potassium channels ($K_{ir}$) that are ligand-regulated (e.g. ATP), allow current flow in the inward direction, and play an important role in regulating resting level of neuronal activity; Two-pore potassium channels ($K_{2p}$) that are constitutively open or with high basal activation, are responsible for potassium leak current and stabilize membrane potential below firing threshold (Gutman et al., 2005;Wei et al., 2005;Goldstein et al., 2005;Kubo et al., 2005).

$K_v$ superfamily is the major group of potassium-selective channels consisting of 12 subfamilies forming 6 functional groups based on activation/inactivation properties –

delayed rectifier, A-type channel, outward-rectifying channel, inward-rectifying channel, slowly activating channel and modifier/silencer (Gutman et al., 2005). Delayed rectifiers and A-type channels are the dominant $K_v$ channels. Delayed rectifiers include $K_v$1.x (except $K_v$1.4), $K_v$2.x, $K_v$3.1, 3.2, $K_v$7.x, and $K_v$10.1, inactivate slowly, and are mainly involved in maintaining membrane potential and electrical excitability in cells (Gutman et al., 2005;Grissmer et al., 1994). A-type channels include $K_v$1.4, $K_v$3.3, 3.4 and $K_v$4.x, inactivate quickly, and are important in regulating afterhyperpolarization (AHP) and the frequency of repetitive spike firing (Gutman et al., 2005;Jerng et al., 1999). The expression of a variety of Kv currents in distinct populations of DRG neurons has been studied (Rasband et al., 2001;Yoshimura et al., 1996;Pearce and Duchen, 1994;Everill et al., 1998;Gold et al., 1996). Most $K_v$1.4-positive DRG neurons have a small cell body (18-30μm), do not express other $K_v$1.x subunits (suggesting the formation of homotetrameric Kv1.4 channels), and coexpress VR-1 and TTX-R Nav1.8 (Rasband et al., 2001;Pearce and Duchen, 1994). Three transient Kv currents have been described in small diameter DRG neurons, two of which are found in neurons sensitive to capsaicin (Gold et al., 1996). Moreover, bladder nociceptors coexpress TTX-R sodium channels and capsaicin receptors, a Kv1.4-like rapidly inactivating A-type current (Yoshimura et al., 1996). Large diameter DRG neurons (42-54μm) express a prominent DTX-sensitive delayed rectifier-type $K_v$ current (Pearce and Duchen, 1994). Moreover, Aβ-fiber

cutaneous DRG neurons identified by *in vivo* retrograde labeling exhibited three distinct DTX-sensitive $K_v$ currents, two sustained or slowly inactivating delayed rectifier-type currents (dominant currents), and a rapidly inactivating A-type current (Everill et al., 1998). The sustained current most probably corresponds to $K_v\alpha1.1,1.2/K_v\beta2.1$ channels, whereas the slowly and rapidly inactivating $K_v$ currents likely correspond to different heteromeric combinations of $K_v\alpha1.1,1.2$, $1.4/K_v\beta2.1$ and $K_v\alpha1.1,1.4/K_v\beta2.1$ (Rasband et al., 2001).

The $K_{ca}$ superfamily is the second major group of potassium channels, whose activation underlies the phenomenon of spike frequency firing adaptation (Sah and Faber, 2002;Mongan et al., 2005;Scholz et al., 1998). Studies regarding the expression of $K_{ca}$ in DRG focus more in $K_{ca}1.1$ (larger conductance), $K_{ca}2.x$ (small conductance) and $K_{ca}3.1$ (intermediate conductance), although 5 subfamilies of $K_{ca}$ have been identified (Wei et al., 2005). $K_{ca}1.1$ current is expressed in 63-95% of small diameter neurons (Li et al., 2007;Scholz et al., 1998). Further functional study reveals that ethanol-induced activation of $K_{ca}1.1$ is preferentially in $IB4^+$ neurons (Mongan et al., 2005). Moreover, calcium activated potassium currents are present in small to medium diameter neurons, but without further distinction (Sarantopoulos et al., 2007). $K_{ca}2.3$ is widely expressed in DRG neurons of all sizes (Bahia et al., 2005;Mongan et al., 2005), whereas $K_{ca}2.1$, 2.2, 3.1 are preferentially expressed in $IB4^+$ neurons with small cell bodies ($< 1000\ \mu m^2$)

(Mongan et al., 2005). Surprisingly, half of the $K_{ca}2.1$, 2.2, $3.1^+$ neurons also express CGRP (Mongan et al., 2005), which supports the ambiguous division of peptidergic and $IB4^+$ small DRG neurons (Mongan et al., 2005;Averill et al., 1995).

Functional studies of $K_{ir}$ and $K_{2p}$ superfamilies in DRG neurons have been reported only recently. However, limited studies have suggested that they might be important for neuronal excitability and polymodal pain perception (Kawano et al., 2009;Chi et al., 2007;Yin et al., 2007;Sarantopoulos et al., 2003;Noel et al., 2009;Rau et al., 2006;Alloui et al., 2006;Cooper et al., 2004;Maingret et al., 2000). Differential expression of these channels in distinct populations of DRG neurons is only partially revealed. ATP-sensitive $K_{ir}6.1$,6.2 are expressed in small to medium diameter neurons (Chi et al., 2007), but only $K_{ir}6.2$ is expressed in larger diameter neurons (Kawano et al., 2009). G-protein coupled $K_{ir}$ subunits are also expressed in DRG neurons (Gao et al., 2007). Small to medium diameter (< 25 μm) DRG neurons express $K_{2P}2.1$, $K_{2P}4.1$, $K_{2P}10.1$ and $K_{2P}18.1$. $K_{2P}10.1$ and $K_{2P}18.1$ are the major background potassium channels actived at 37°C and 25°C, respectively (Kang and Kim, 2006). Moreover, $K_{2P}2.1$ is highly expressed in small to median sensory neurons (< 35 μm), is present in both peptidergic and nonpeptidergic neurons and is extensively colocalized with $TRPV_1$ (Alloui et al., 2006). Differential expression of $K_{2P}3.1$, $K_{2P}5.1$, and $K_{2P}9.1$ has been shown in detail in nine functional subgroups in small to medium diameter neurons

classified by chemical responsiveness, histochemical phenotype and current signature (Rau et al., 2006).

1.5.3 Calcium channels

Based on activation voltage, voltage-gated calcium channels (VGCCs) are classified as low threshold T-type and high threshold L, N-, P/Q, and R-types. Based on the structure similarity of the $\alpha_1$ subunit (pore-forming) and the pharmacological characteristics, VDCCs form three subfamilies – $Ca_v1$ (L-type), $Ca_v2$ (N, P/Q and R-types) and $Ca_v3$ (T-type) (Catterall et al., 2005). Most types of VGCCs have 4 pore-forming $\alpha_1$ subunits and regulatory $\beta$, $\alpha_2\delta$ and $\gamma$ subunits. L-type calcium currents typically require a strong depolarization for activation, are long-lasting, and are blocked by organic antagonists including phenylalkylamines and benzothiazepines. N-type, P/Q-type and R-type calcium currents also require strong depolarization for activation. They are sensitive to specific polypeptide toxins from snail and spider venoms. They are expressed primarily in neurons, where they mediate calcium entry into cell bodies. T-type calcium currents are activated by weak depolarization and are transient. They are resistant to both organic antagonists and to the polypeptide toxins. They are expressed in a wide variety of cell types, where they are involved in shaping the action potential (AP) and controlling patterns of repetitive firing (Catterall et al., 2005).

The expression of various voltage-gated calcium channel (VGCC) α1 subunits has been confirmed in dorsal root ganglion neurons: $\alpha_{1A}$, $\alpha_{1B}$, $\alpha_{1C}$, $\alpha_{1D}$, $\alpha_{1E}$, $\alpha_{1I}$ and $\alpha_{1S}$ mRNA are expressed within all three types of neuron with $\alpha_{1A}$, $\alpha_{1D}$, $\alpha_{1E}$, $\alpha_{1I}$ and $\alpha_{1S}$ mRNA expressed at a higher level in the small diameter neurons (Yusaf et al., 2001). It has been suggested that $\alpha_{1C}$, $\alpha_{1D}$, and $\alpha_{1S}$ elicit L-type calcium currents while $\alpha_{1G}$, $\alpha_{1H}$, $\alpha_{1I}$ elicit T-type currents, $\alpha_{1A}$ for P/Q-type currents, $\alpha_{1B}$ for N-type and $\alpha_{1E}$ elicits R-type currents (Yusaf et al., 2001). Scroggs and Fox (1992b) classified DRG neurons as small diameter (20-27 μm), medium diameter (33-38 μm)and large diameter (45-51 μm), which is likely to correspond to DRG neurons which transmit different sensory modalities (Harper and Lawson, 1985). T-type calcium currents are observed in small and medium diameter, but not in large diameter neurons. Large diameter DRG cell bodies have a small low-threshold $Ca^{2+}$ current but this current does not inactivate and is insensitive to a change in holding potential from -80 to -90 mV, and thus does not appear to be conducted through T-type calcium channels. L-type calcium current is significantly larger in small diameter DRG cell bodies than in medium diameter or large diameter neurons. N-type calcium current is similar in small, medium and large diameter neurons. Nimodipine and ω-conotoxin GVIA-resistant (likely P/Q type) calcium currents are higher in medium diameter or large diameter neurons than in small diameter neurons (Scroggs and Fox, 1992a).

In small diameter neurons, only a small portion of the calcium influx is via the low threshold T-type calcium channel (~10%), whereas the majority of the calcium influx is via high threshold calcium channels (~30% via the L-type, ~50% via the N-type). In medium diameter neurons, T-type calcium current is prominent, about 0.9 nA, which is 8-9 time larger than that in small diameter neurons. The threshold of the T-type channel is around -50 mV. Approximately 37% (holding potential at -60 mV) or ~68% (holding potential at -80 mV) of calcium influx in medium diameter neuron is via the T-type channel, ~8% via the L-type, ~30% via the N-type channel. In large diameter neurons, the expression of L-, N-, and P-type channels is similar to that of the medium diameter neurons, but unlike medium diameter neurons, they are devoid of the T-type channel. Because of this, the duration of calcium current is much shorter than that of medium diameter neurons (Scroggs and Fox, 1992b).

**1.6. The ionic basis for action potential genesis in primary sensory neurons**

The resting membrane potential is largely near the potassium equilibrium potential. However, sodium channels also contribute to establishing the resting membrane potential, especially TTX-resistant $Na_v1.9$ sodium channels (Herzog et al., 2001). Sodium channels govern the depolarization phase of the AP. However, different subtypes of sodium channel serve different roles in different neuronal subsets. In small-sized nociceptors, TTX-resistant $Na_v1.8$ channels dominate the upstroke of the

AP, contributing to the majority of inward current during depolarization. TTX-sensitive sodium channels, likely $Na_v1.7$ also allow significant inward current especially at the initiation phase of the depolarization. However, inward calcium current is negligible during the depolarization of AP (Blair and Bean, 2002). TTX-resistant $Na_v1.8$ channels may account for longer AP duration and larger AP overshoots (Djouhri et al., 2003;Blair and Bean, 2002). Maximum rate of depolarization is positively correlated with the expression of the $Na_v1.8$ channel (Renganathan et al., 2001). Low threshold neurons, especially muscle spindle neurons usually exhibit a smaller AP overshoot and shorter AP duration (Djouhri and Lawson, 2001). Predominant TTX-sensitive sodium channels seem to account for these features in these non-nociceptive neurons.

Voltage-gated potassium channels play an integral role in the regulation of a number of neuronal response properties including spike repolarisation, interspike interval, and burst adaptation (Rudy, 1988). The repolarisation of the AP is largely determined by potassium channels, but can be modulated by other ion channels. A prominent shoulder during the falling phase of the AP is one of the characteristics of nociceptive neurons. The collective action of incomplete inactivation of TTX-resistant $Na_v1.8$ channels during repolarization and the opening of voltage-activated calcium channels produce this characteristic "hump" (Blair and Bean, 2002). Beside this, calcium channels also play an important role in setting the prominent AHP in C-fiber neurons,

which might be secondary to an increase in a potassium conductance (Gorke and Pierau, 1980).

**1.7. Action potential conduction in the peripheral nervous system**

The DRG neuron has features of a pseudo-unipolar structure - a single stem axon from its axon hillock-initial segment pole and a T or Y-shape bifurcation on the stem axon tens or hundreds of microns from the soma. The peripheral branch proceeds from the T-junction into the spinal nerve and then arborizes into sensory endings in skin, muscle, viscera etc. The central branch enters the dorsal root and then spinal cord. In some neurons the stem axon follows a tortuous, coiled path before extending to the T-junction, and sometimes spirals around the soma. This can sometimes end up with very long stem axon (Devor, 1999).

Activation of various transducing molecules on the peripheral terminals induces the receptor potential. When it is of sufficient amplitude this receptor potential generates an AP at the first node of Ranvier. Thus AP is conducted towards the spinal cord. There are important mechanisms regulating AP conduction along the axon, which shapes the information the spinal cord receives.

1.7.1. Myelinated vs. unmyelinated nerve conduction

There are two types of axons in the peripheral nervous system (PNS): myelinated and unmyelinated axons. The appearance is characterized by myelin ensheathing the axon

and nodes of Ranvier appearing as periodic interruptions in this myelin sheath (Figure 1.6). Moreover, the axonal membrane of myelinated fibers is differentiated into several structural and functional domains, including the nodes of Ranvier, the paranodal junction, the juxtaparanodes and the internodal region (Peles and Salzer, 2000).

Sodium channels are initiators for AP conduction along axons, whose distribution is highly focal at the nodes of Ranvier in myelinated axons (1000-2000 $\mu m^{-2}$) (Ritchie and Rogart, 1977), in contrast to the fairly even distribution in unmyelianted axons (100-200 $\mu m^{-2}$) (Pellegrino et al., 1984). Nav1.6 is the main sodium channel isoform responsible for impulse conduction, located in the nodes of Ranvier in mature peripheral axons (Caldwell et al., 2000) and in unmyelinated axons as well (Black et al., 2002). Expression of other sodium channel isoforms, such as Nav1.2, Nav1.8 and Nav1.9 has been found in axons. Nav1.2 is expressed in unmyelinated zone in adult axons, and at immature nodes of Ranvier during development, which is later replaced by Nav1.6 (Boiko et al., 2001). Nav1.8 and Nav1.9 are mainly expressed in unmyelinated axons, and some nociceptive myelinated fibers (Coward et al., 2000;Fjell et al., 2000). Each sodium channel isoform might contribute partially to impulse propagation, either via synergy or redundance, as lack of the dominant Nav1.6 in *med* mice does not lead to conduction block in unmyelinated fibers (Black et al., 2002).

Potassium channels are dampers for AP conduction, whose distribution along the axon is mainly restricted to the juxtaparanodes and internodes (Poliak and Peles, 2003), but exists at nodes of Ranvier as well (Devaux et al., 2004;Schwarz et al., 2006). Potassium channels present at juxtaparanodes are mainly fast kinetic delayed rectifying potassium channels (Kv1.1, Kv1.2 and Kv3.1) (Rasband et al., 1998;Poliak and Peles, 2003). Recently, two slowly activating and deactivating delayed rectifying potassium channels (Kv7.2 and Kv7.3) have been identified at nodes of Ranvier in peripheral myelinated fibers (Devaux et al., 2004;Schwarz et al., 2006). All nodes of myelinated axons have strong expression of Kv7.2. The nodes of about half the small to medium sized myelinated fibers express both Kv7.2 and Kv7.3, but nodes of large myelinated fibers express only Kv7.2 (Schwarz et al., 2006). Demyelination processes might lead to the redistribution of sodium and potassium channels along the axon, and therefore affects AP conduction as depicted in the model in Figure 1.7.

### 1.7.2. Modulation of AP propagation

Under physiological conditions, either function (e.g. kinetics of ion channels) or structure (geometry of axons) related electrical processes modulate AP propagation. The modulation mainly takes place in two areas: the shape of the AP and the reliability of conduction.

Two types of modulation of the shape of the AP are meaningful for the regulation of synaptic transmission – modulation of the width and modulation of the amplitude of the spike (Geiger and Jonas, 2000;Brody and Yue, 2000). The duration of the AP is not fixed. Activity-dependent short term broadening of the spike is commonly seen in repetitive firing along peripheral axons (Lu and Miletic, 1990;Luscher et al., 1994). Broadening of the presynaptic AP increases calcium influx into synaptic terminal and thus facilitates transmitter release. Reduction of the amplitude of the spike is another common phenomenon during repetitive stimulation of the axon (Lu and Miletic, 1990;Luscher et al., 1994). This decrease is the result of a decreased depolarizing force due to a number of mechanisms including sodium channel inactivation (Brody and Yue, 2000).

The reliability of conduction is determined by several geometric factors including branch points and swellings. In fact, it is the interplay of the AP and the input impedance beyond branch points and/or swellings that determines the fate of the propagation of the AP beyond branch and/or transforming points. If the combined impedance of both daughter branches equals that of the mother branch, the propagation of the AP continues without distortion; if it is smaller, the conduction is faster but without distortion; if it is larger, the conduction is delayed with distorted shape or even fails completely (Segev and Schneidman, 1999). Propagation failures also occur following

repetitive stimulation. Mechanisms for this type of conduction failure are related to the nature of repetitive stimulation, which can be grouped in two main categories – a result of either depolarization or hyperpolarization of the membrane. A depolarized membrane potential results from potassium accumulation in periaxonal space following repetitive activation, and this might contribute to the inactivation of certain sodium channel isoforms (Grossman et al., 1979), which impedes local AP genesis along the axon and may therefore block propagation. On the other hand, hyperpolarization of the membrane is against the spike generation, and may cause propagation failure (Bielefeldt and Jackson, 1993). Activity-dependent hyperpolarization of the membrane mainly results from activation of the $Na^+/K^+$ ATPase and/or calcium-dependent potassium channels (Poliak and Peles, 2003;Bielefeldt and Jackson, 1993).

### 1.8. Neurotrophin-dependence and sensory phenotype determination in primary sensory neurons

Different members of the neurotrophin family maintain specificity in subsets of sensory neurons, including nerve growth factor nerve growth factor (NGF), brain derived neurotrophic factor (BDNF), neurotrophin (NT)-3, NT-4, transforming growth factor (TGF)-β/ glial cell derived neurotrophic factor (GDNF) (Huang and Reichardt, 2001;Molliver et al., 1997;Bibel and Barde, 2000;Patapoutian and Reichardt, 2001). Sensory specificity of a sensory neuron is the collective action of neurotrophin supply

from peripheral tissues and receptors for neurotrophin expression in the neuron, manifesting as characteristic molecular trait, sensory modality and central projection pattern. Neurotrophins activate two distinct receptor classes, the tyrosine kinase (Trk) family of receptor tyrosine kinase and the p75 receptor (a member of TNF receptor superfamily). Three Trk receptors have been identified in mammals – TrkA, TrkB and TrkC. NGF is the preferred ligand for TrkA, BDNF and NT4 are preferred ligands for TrkB, and NT3 is the preferred ligand for TrkC, as well as for TrkA and TrkB but with less affinity. Through these receptors, neurotrophins activate many intracellular signaling pathways, including those via Ras, phosphoinositide 3 kinase (PI3K), phospholipase C (PLC)-γ, c-Jun N-terminal kinase (JNK) and nuclear factor kappa-light-chain-enhancer of activated B cells (NF-κB), and regulate the expression of a wide range of transcription factors (Figure 1.8). During development, neurotrophins function as survival factors. They also regulate axon growth and pattern of termination and the expression of proteins crucial for normal neuronal function, such as neurotransmitters and ion channels. In the mature nervous system, they control normal synaptic function and plasticity, while continuing to modulate neuronal survival. A defect in either neurotrophin production or neurotrophin receptors leads to very similar sensory phenotype, except for the NT-3/TrkC signaling. More neuron loss occurs in *nt*3-/- than in trkC-/- mutants, as NT3 utilizes both TrkA and TrkB for survival signaling

(Snider, 1994). NGF via TrkA is essential for small nociceptive neurons, particular CGRP containing neurons. Small neurons with ultimate phenotype of non-peptidergic/IB4$^+$ repress TrkA expression yet initiate the expression of Ret, the receptor tyrosine kinase for GDNF (Molliver et al., 1997). NT-3 via TrkC is essential for proprioceptive neurons, BDNF via TrkB for slowly adapting mechanoreceptors, and NT-4 via TrkB for down-hair neurons (Bibel and Barde, 2000;Huang and Reichardt, 2001).

Two basic helix-loop-helix (bHLH) transcription factors, *neurogenin1* (*ngn1*), *ngn*2, have been shown to play a central role in the determination of sensory subtype in DRG neurons. In chicken embryos, the neurogenesis of large sized TrkB$^+$, TrkC$^+$ sensory neurons starts first followed shortly by that of small sized TrkA$^+$ sensory neurons (Ma et al., 1999). Transcription factor ngn2 is required transiently during the early phase primarily by TrkB$^+$, TrkC$^+$ sensory neurons, whose role can be largely compensated by *ngn*1. Transcription factor ngn1 is required during the early phase and dominantly during the late phase, whose role can not be compensated by *ngn*2.

Another family of transcription factors, Runt-related transcription factor (Runx)1 and Runx3 also play critical roles in neuron differentiation, especially in the determination of central termination pattern. Runx1 and Runx3 are expressed in distinct neuron subpopulations. Runx3 is expressed by TrkC$^+$ precursor neurons which

differentiate into proprioceptive neurons. Runx1 is expressed in $TrkA^+$ precursor neurons, most likely being nociceptive neurons later (Inoue et al., 2002;Levanon et al., 2002;Theriault et al., 2004). Without these transcription factors, proper targeting of primary sensory neurons to the second order projection neurons or interneurons in the spinal cord fails (Kramer et al., 2006;Chen et al., 2006b;Inoue et al., 2002;Chen et al., 2006a;Levanon et al., 2002).

**1.9. Immune modulation of primary sensory neurons during chronic pain states**

Inflammtory pain and neuropathic pain are two main forms of persistent/chronic pain (Scholz and Woolf, 2002). The former results from various events, including exposure to microbial components (e.g. LPS and zymosan), irritant chemicals (e.g. carrageenan), whereas the latter arises as a result of nerve damage due to many etiologies, including traumatic mechanical injury (nerve transection), metabolic or nutritional injury (alcoholic neuropathy), viral infection (post-herpetic neuralgia), secondary to non-viral disease (diabetes neuropathy), neurotoxicity (chemotherapy neuropathy) (Sah et al., 2003). Resident or hemogenous immune cells, and/or immune-like cells (e.g. Schwann cells) are activated by various injuries, whose activation leads to the release of a plethora of histamine, prostaglandins, cytokines/chemokines and other proinflammtory mediators (Figure 1.9). As a result, nociception is greatly influenced by these non-neuronal immune cells.

Mast cells are one of the resident cells types in peripheral tissue or nerve tissue. These cells degranulate at the site of injury and release inflammatory mediators such as histamine, proteases and cytokines. Neutrophils are normally the earliest hemogenous inflammatory cells to infiltrate damaged tissues. Upon activation neutrophils release a wide range of microbe-killing effector molecules such as gemicidal proteins, cytokines, proteases and reactive oxygen species. However, another main function is to attract other inflammatory cell types via the release of chemokines, most importantly macrophages. Macrophages are the key immune and phagocytic resident cells. In response to tissue damage, these cells become the most important "hub" by releasing a variety of inflammatory mediators including TNF-α, interleukins, interferons, growth factors, nitric oxide and prostaglandins. T lymphocytes are normally recruited at a later time, and release cytokines in a T-helper-dependant manner. All these cell types are involved in the pathogenesis of both inflammatory and neuropathic pain (for reviews see Moalem et al., 2005;Marchand et al., 2005;Thacker et al., 2007;Watkins and Maier, 2002).

Schwann cells provide myelin encapsulation of peripheral axons and paracrine trophic factors to support nerves. Schwann cells are peripheral glia cells with potent immunoregulation capacity as they interact with the immune system in T-cell-mediated immune responses by expressing major histocompatibility complex (MHC) molecules

(Bergsteinsdottir et al., 1992;Gold et al., 1995). There is no known role of Schwann cells in inflammatory pain. In contrast, Schwann cells undergo dramatic phenotypic modulation in response to nerve damage. They transform into an activated form, begin to phagocytose myelin debris, and synthesize a wide range of inflammatory mediators, including NGF, BDNF, GDNF, TNF-α, IL-1β, IL-6, ATP and erythropoietin (Epo) (for reviews see Campana, 2007;Thacker et al., 2007). It has been suggested that erythroblastic leukemia viral oncogene homolog (ErbB)-dependent cellular signaling underlies this Schwann cell activation (Chen et al., 2003;Chen et al., 2006c).

There is a causal relationship between the release of cytokines and the onset of pain: cytokine release is increased in pain models (George et al., 1999;Murphy et al., 1999;Shamash et al., 2002); hyperalgesia is induced in naïve animals due to cytokine injections (Ferreira et al., 1988;Cunha et al., 1992); hyperalgesia in chronic pain is attenuated by suppressing cytokine release or effects (Cunha et al., 1992;Sommer et al., 1999;Schafers et al., 2001). Several mechanisms have been proposed about how cytokines modulate the processing of nociception. Cytokines can impose direct effects on sensory neurons, including neuronal sensitization that causes larger response to external stimuli (Brenn et al., 2007), modulation of ion channel current density (Czeschik et al., 2008) etc. Cytokines are also able to affect sensory neurons via indirect mechanisms, including promoting the production of prostaglandins during local

inflammation (Okuse, 2007); activating cellular signaling pathways in neurons, such as MAPKs (Schafers et al., 2003;Ji and Woolf, 2001); and activating glial cells that closely interact with neurons (Watkins et al., 2001).

**1.10. Figures 1-9**

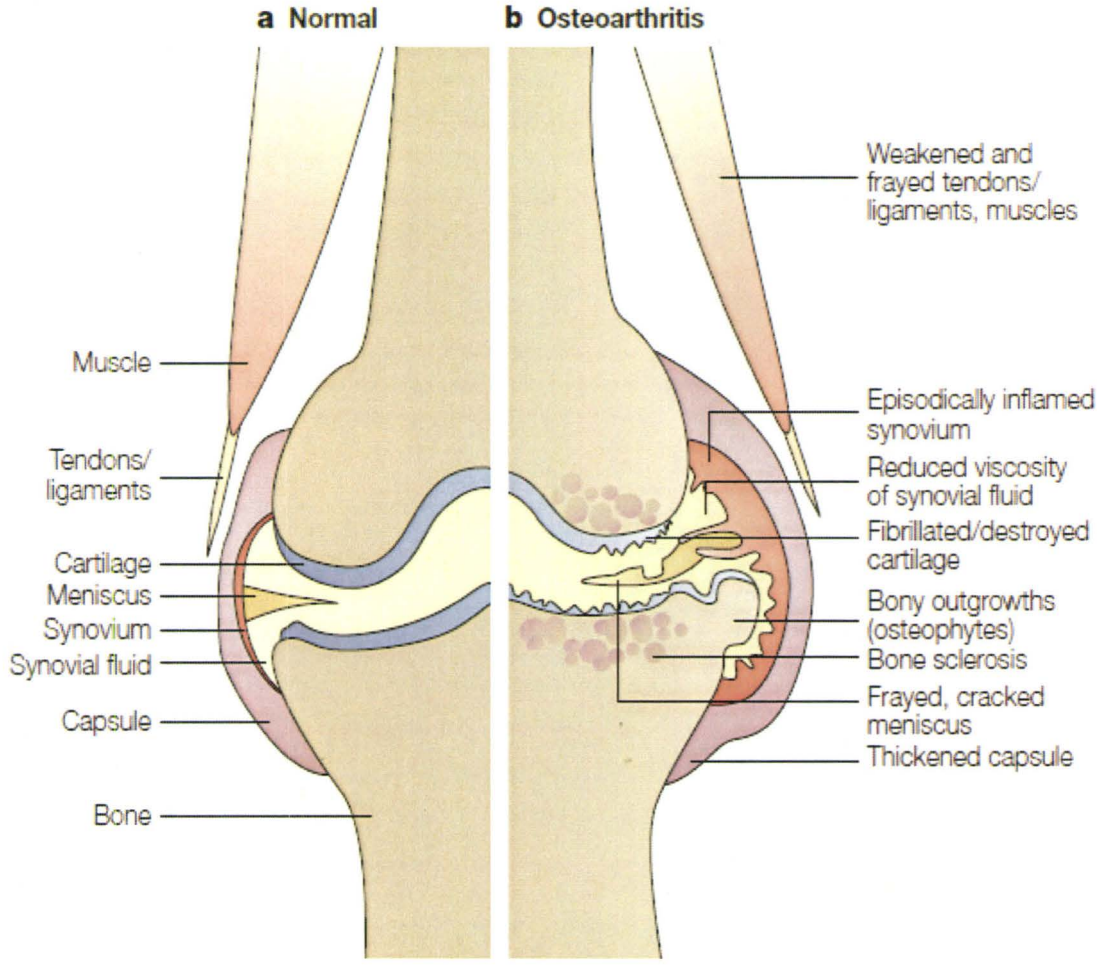


**Figure 1.1. Articular structures affected in osteoarthritis.** This figure is Figure 2 in (Wieland et al., 2005).

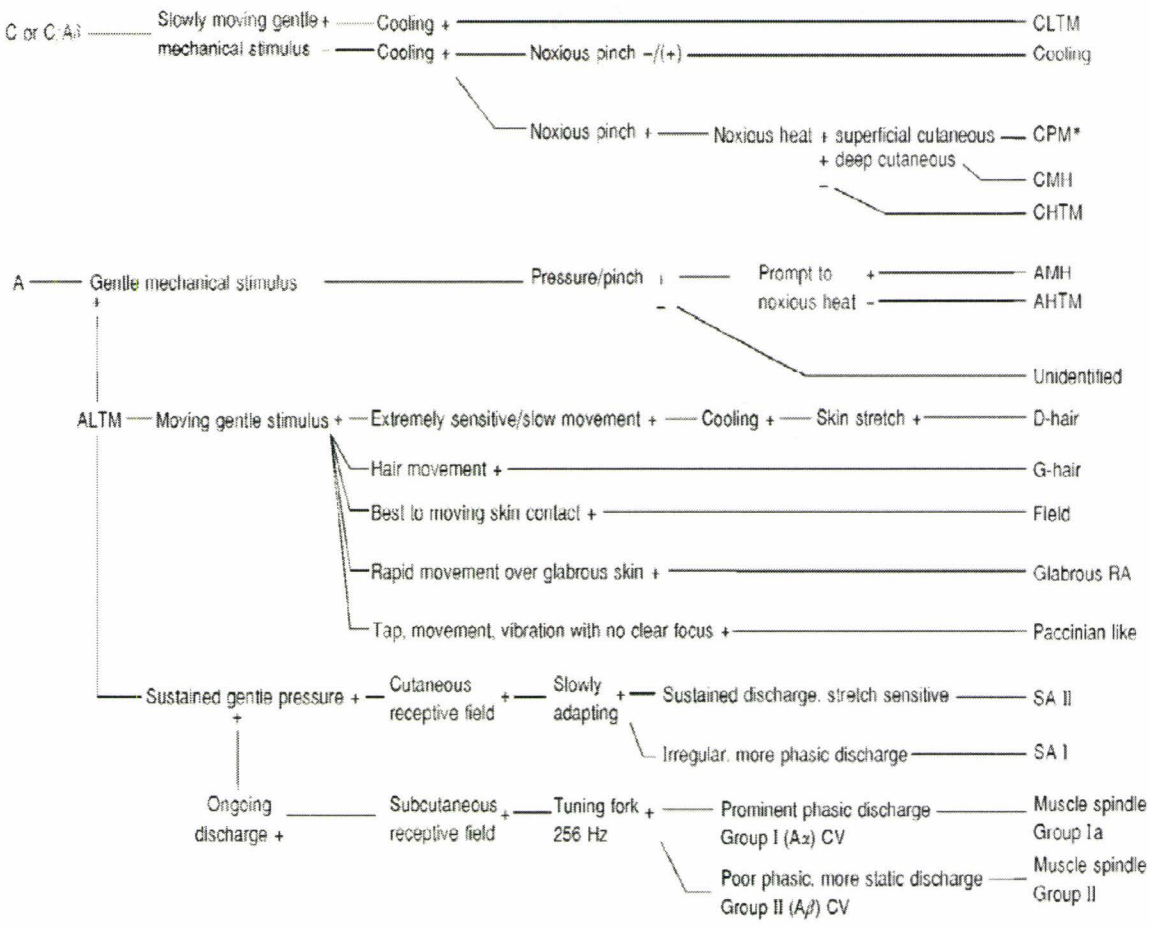


**Figure 1.2. Sensory properties and classification of dorsal root ganglia neurons.** Abbreviations: CLTM, C-fiber low threshold mechanoreceptor; CPM, C-fiber polymodal nociceptor; CMH, C-fiber mechno-heat neuron; CHTM, C-fiber high threshold mechanoreceptor; AMH, A-fiber mechano-heat neuron; AHTM, A-fiber high threshold mechanoreceptor; ALTM, A-fiber low threshold mechanorecepotor; RA, rapidly adapting; SA, slowly adapting. This figure is Figure 1 in (Lawson et al., 1997).

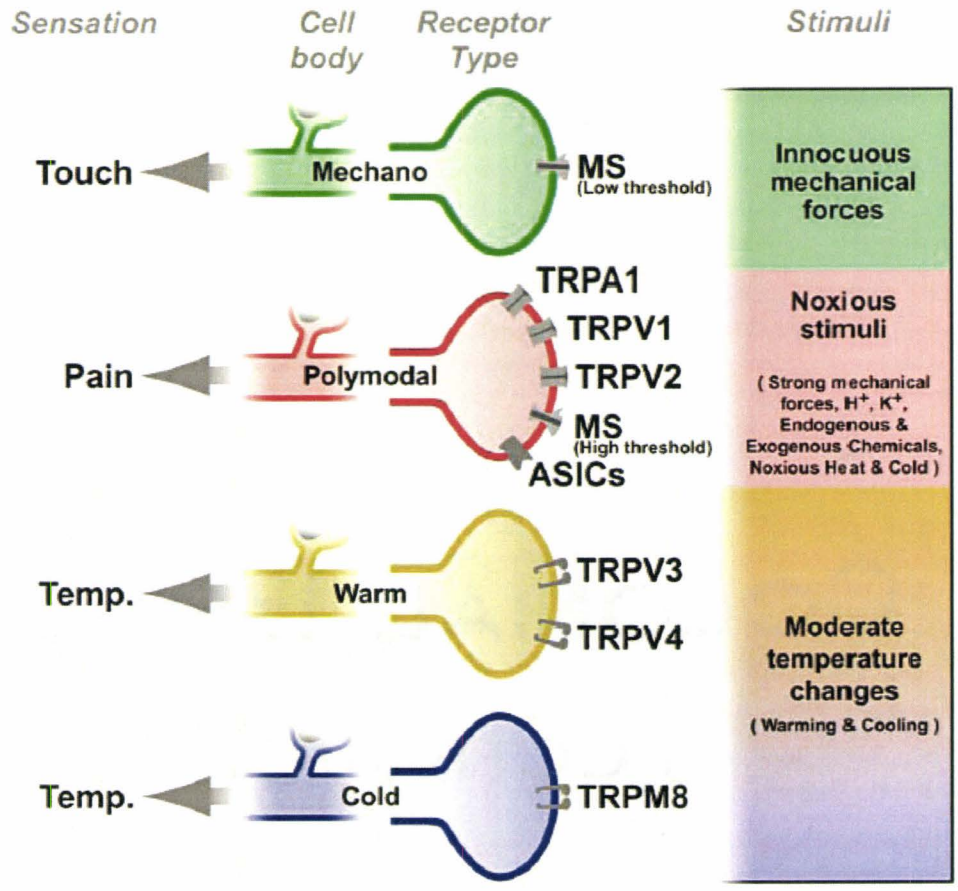


**Figure 1.3. Molecular basis of somatosensory specificity.** Schematic representation of various subpopulations of modality specific primary sensory neurons, and the putative specific transduction molecules involved in the detection of the different stimuli. This figure is Figure 4 in (Belmonte and Viana, 2008).

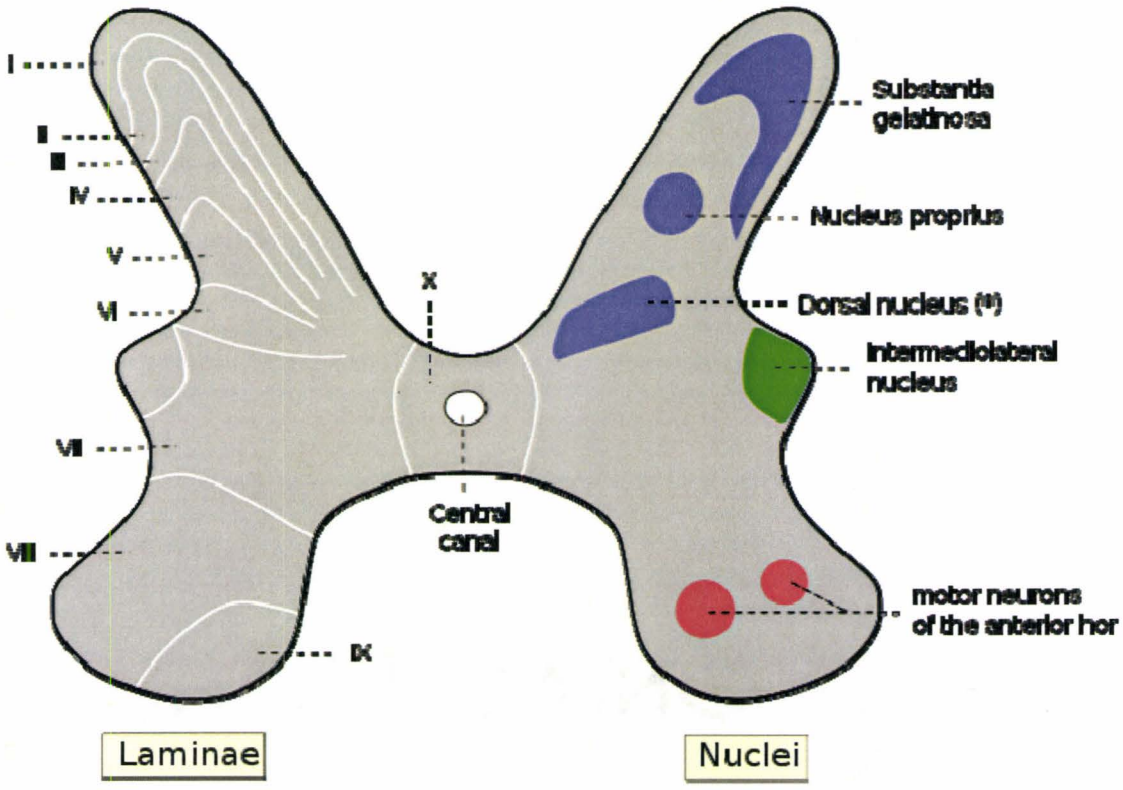


**Figure 1.4. Schematic representation of Rexed's laminae and nuclei in the spinal cord.** This picture is online material, whose link is as follows: http://en.wikipedia.org/wiki/File:Medulla_spinalis_-_Substantia_grisea_-_English.svg#file

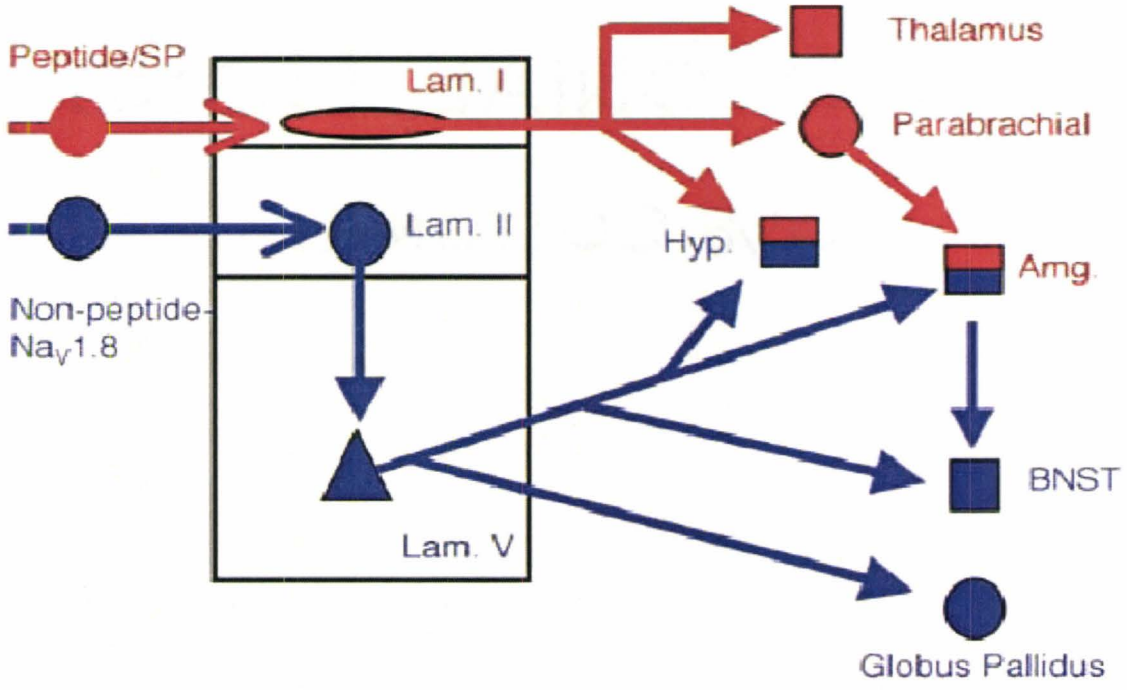


**Figure 1.5. Parallel "pain" pathways arise from subpopulations of primary afferent nociceptor.** Abbreviations: Lam, lamina; Amg, amygdala; BNST, bed nucleus of the stria terminalis; Hyp, hypothalamus. This figure is Figure 4 in (Braz et al., 2005).

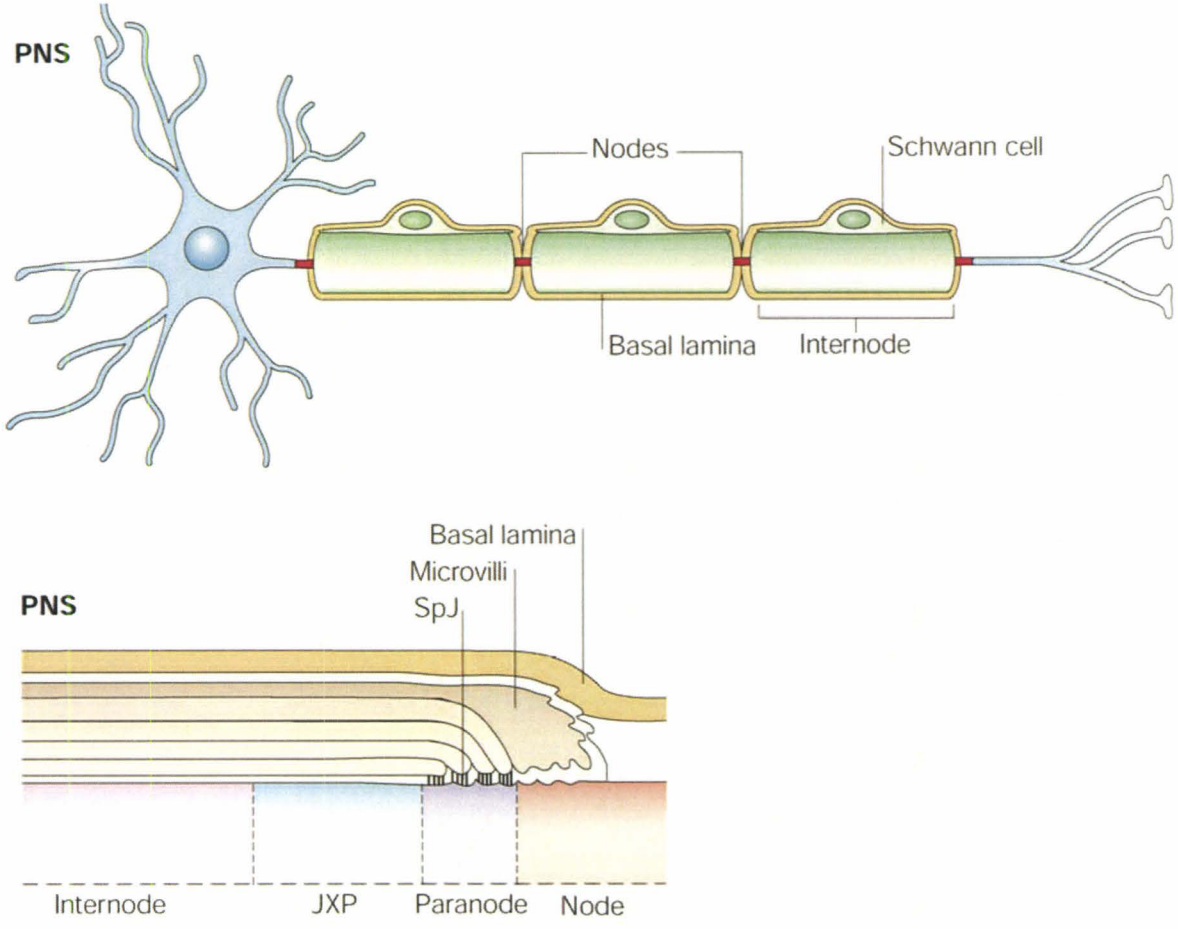


**Figure 1.6. Structure of myelinated axons.** Abbreviations: PNS, peripheral nervous system; JXP, juxtaparanode; SpJ, septate-like junction. This figure is modified from Figure 1 in (Peles and Salzer, 2000).

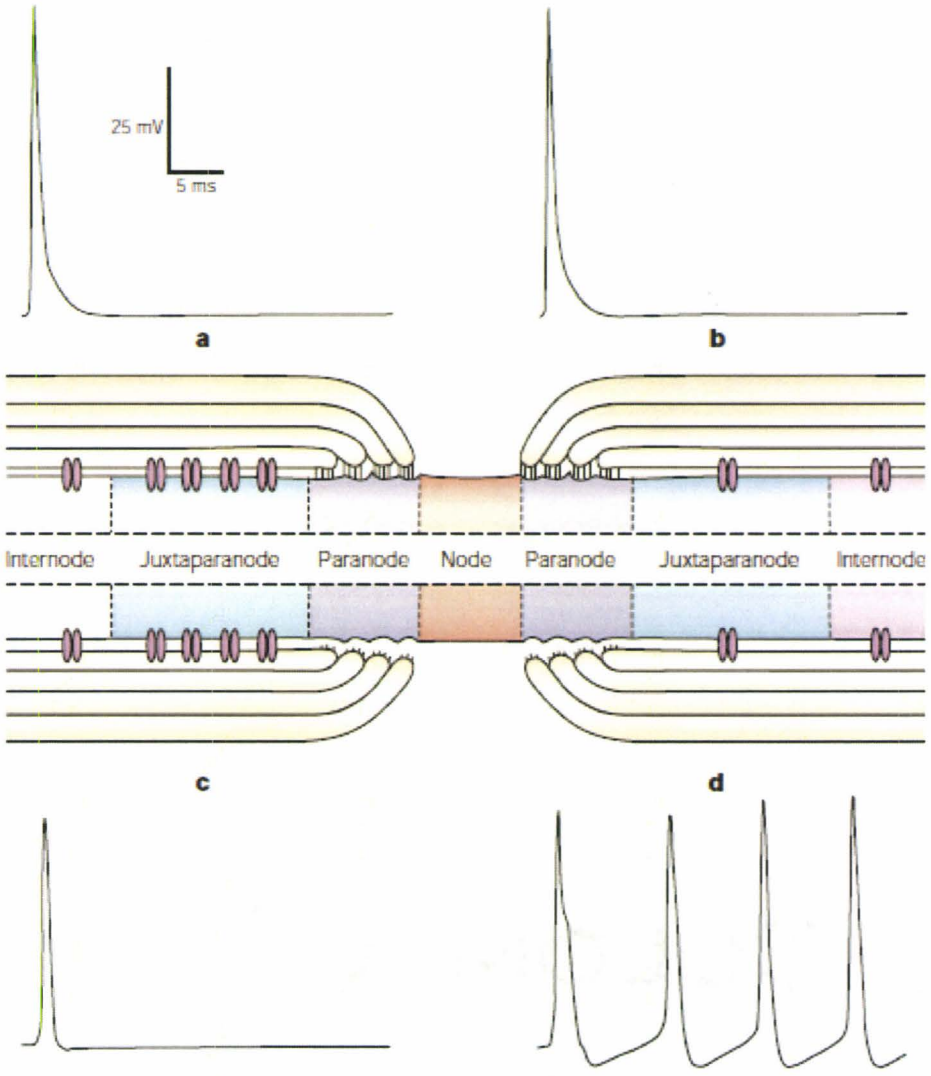


**Figure 1.7. A computational model illustrating a role for juxtaparanodal $K^+$ channels in myelinated fibers.**

Each part of the figure shows a schematic organization of the parnodal junction (black lines) and the distribution of $K^+$ channels (purple ovals), together with the corresponding action potential recorded after a single stimulus. **a** The axon has normal properties and responds normally to a single stimulus. **b** The paranodal junctions remain normal, but $K^+$ clusters have dissipated into the internode and conduction velocity remains normal. **c** The junctions are loosened, but the channels remain clustered. Conduction velocity is slowed, but is otherwise stable. **d** The junctions are loosened as in **c**, but the channels

are dispersed as in **b**, and the axon responds to a single stimulus with repetitive action potentials. This figure is modified from Figure 4 in (Peles and Salzer, 2000).

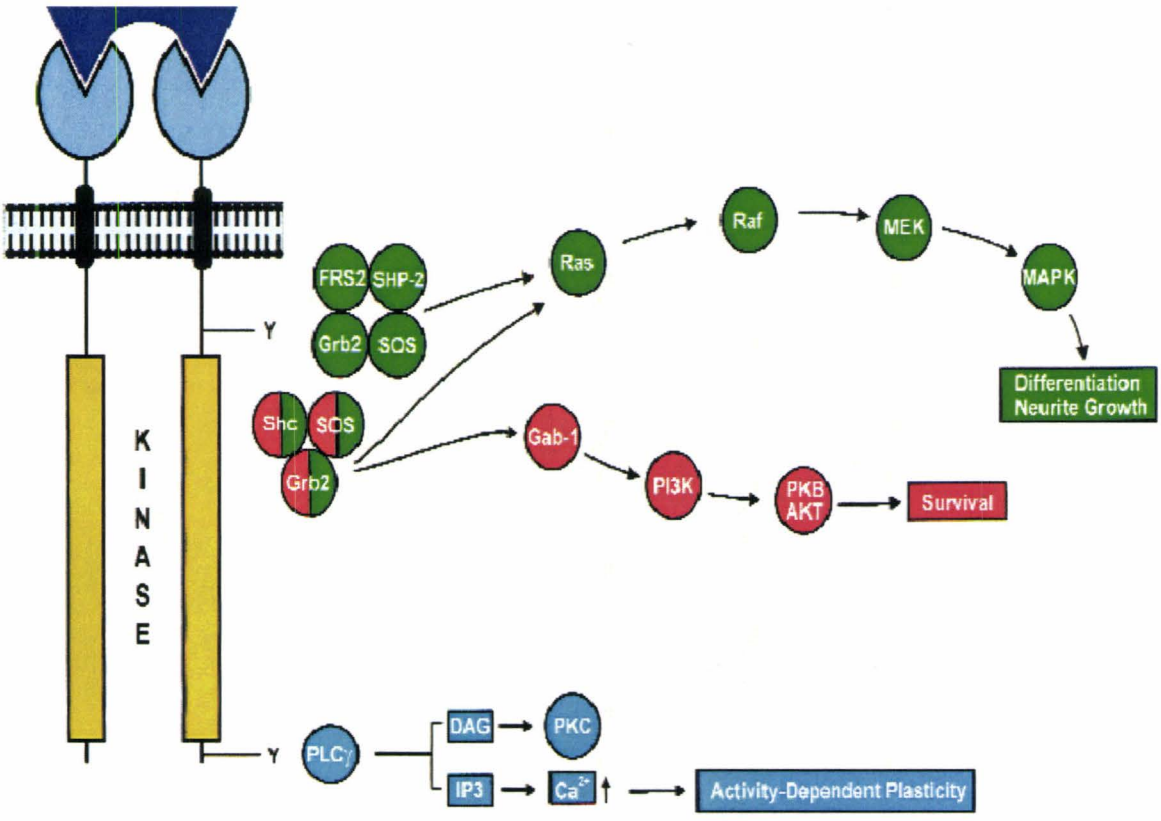


**Figure 1.8. Neurotrophin signaling pathways via Trk receptors.** This figure is Figure 2 in (Bibel and Barde, 2000)

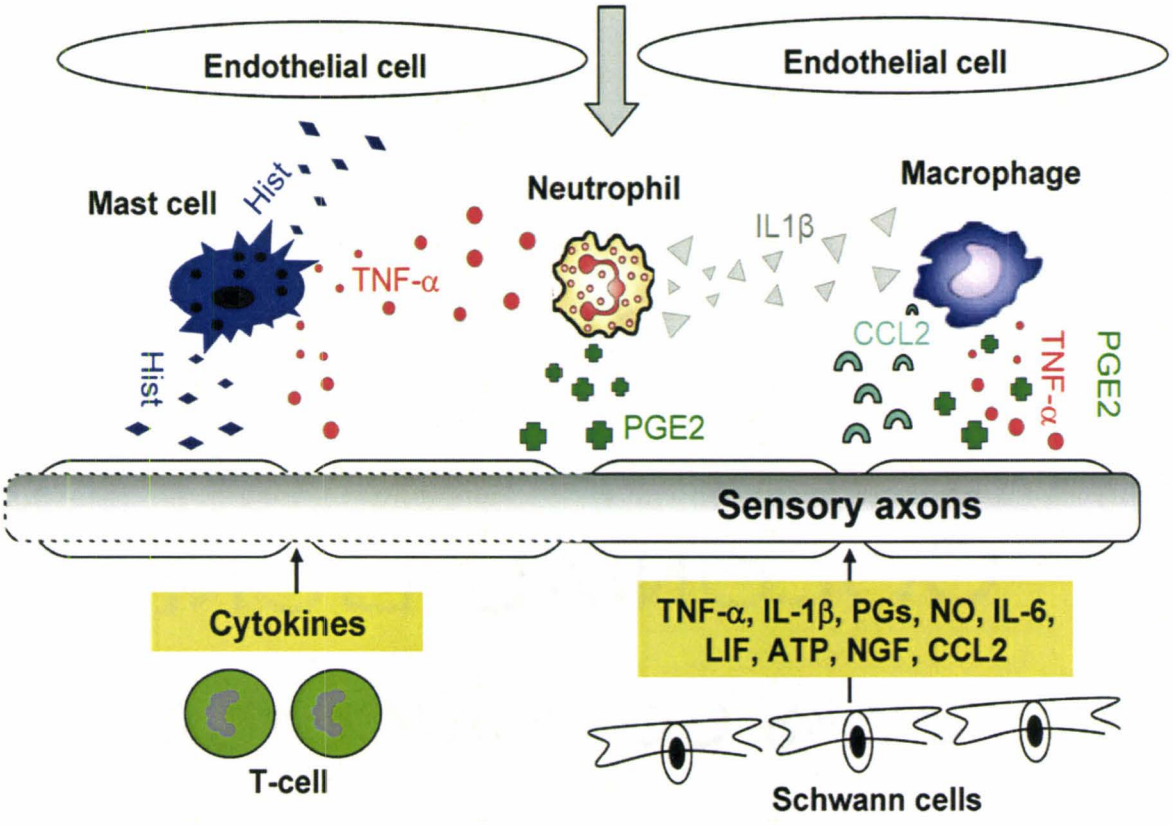


**Figure 1.9. Immune and glial cells contribute to pathological pain states.** After peripheral nerve injury, the site of damage is typified by the activation of resident immune cells and recruitment and proliferation of non-neuronal elements, which release inflammatory factors that initiate and maintain sensory abnormalities after injury. These factors may either induce activity in axons or are transported retrogradely to cell bodies in the dorsal root ganglia, where they may alter gene expression of the neurons. Abbreviations: Hist, histamine; TNF-α, tumor necrosis factor IL; interleukin; NO, nitric oxide; ATP, adenosine triphosphate; PGs, prostaglandins; NGF, nerve growth factor; CCL2, C-chemokine ligand 2. This figure is Figure 2 in (Thacker et al., 2007).

# CHAPTER 2.

## Changes in physiological properties of DRG neurons in a rat model of osteoarthritis: differences between Aβ non-nociceptors vs. C and Aδ nociceptors

**Authors:** Qi Wu, James L. Henry

**Corresponding author:** James L. Henry, Ph.D.
Michael G. DeGroote Institute for Pain Research and Care,
McMaster University,
1200 Main street West,
Hamilton, Ontario, Canada, L8N 3Z5,
Tel: +1-905-525-9140, extension 27704,
FAX: 905-522-8844,
E-mail address: jhenry@mcmaster.ca

This paper has been submitted to PAIN.

**Significance to thesis:**

This study demonstrated the successful reproduction of the knee derangement model of osteoarthritis (OA). This study documented structural changes in the knee joints characterized OA, changes in vascular permeabiligy in soft tissues of the joints, and changes in nocifensive behaviors at one month following model induction. More importantly, this study showed significant changes in Aβ-fiber low-threshold mechanoreceptors (LTMs) but not classical C-fiber nociceptors, which implicates a possible role of Aβ non-nociceptive primary sensory neurons in the pathogenesis of early OA pain.

**Author's contribution:**

Qi Wu did the electrophysiological experiments, the plasma extravasation experiments, and the tail flick tests, and prepared knee joint samples for histopathological examination. He also analyzed the data, performed statistical analyses, wrote the initial draft of the manuscript, and worked on refining this draft and the revision based on editorial review.

James L. Henry conceived of, designed, and coordinated the study. He also worked on refining this draft and the revision based on editorial review.

**Acknowledgements**

The authors are grateful to Dr. Sally N. Lawson for expert guidance during the earliest stages of this project. We thank Dr. Kiran Yashpal and Ms. Sheila Bouseh for the excellent technical support in behavior tests. We thank Mrs. Chang Ye for help in data input and statistical analysis. This work was generously supported by the Canadian Arthritis Network (CAN), the Canadian Institutes of Health Research (CIHR) and McMaster University. Qi Wu was a CIHR Strategic Training Fellow in Pain: Molecules to Community, and was also supported by CIHR, CAN and Canadian Pain Society.

**Abstract**

Clinical data on OA suggest widespread changes in the properties of sensory neurons. To determine changes in Aδ- and C-fiber neurons, and to compare any changes observed with those in Aβ-fiber LTMs. One month following unilateral surgical knee derangement in the rat, in vivo intracellular recordings were made in two main categories of L4 dorsal root ganglion neurons – Aβ-fiber LTMs, C- and Aδ-fiber nociceptive neurons in OA vs. naïve rats. Electrophysiological parameters included resting membrane potential (Vm), action potential (AP) amplitude, action potential duration (APD), AP rise time, maximum rising rate (MRR), AP fall time, maximum falling rate (MFR), conduction velocity (CV). The model displayed typical osteoarthritis pathology characterized by cartilage degeneration in the knee joint and also manifested knee pathophysiology (oedema and increased vasculature permeability of the joint) and altered nociception of the affected limb (hind paw tenderness and the knee articulation evoked reduction in the tail flick reflex latency). Neurons included in this report innervated regions throughout the entire hind limb. Aβ-fiber LTMs exhibited a slowing of the dynamics of AP genesis, including wider AP duration and slower maximum rising rate, and muscle spindle neurons were the most affected subgroup. Only minor AP configuration change was found in Aδ-fiber nociceptors. Our model successfully induced nociceptive changes one month after induction of the OA model.

At that stage, Aβ-fiber LTMs but not classical C- and Aδ-fiber nociceptors were altered, which implicates a possible role of Aβ-fiber non-nociceptive primary sensory neurons in the pathogenesis of early OA pain.

**Key words**

Animal model; arthritis; chronic pain; dorsal root ganglion; electrophysiology; intracellular

## 2.1. Introduction

Current investigations into the mechanisms of OA pain tend to focus on changes in excitability or activation of nerve terminals in the joint or on central sensitization, each of which may be at play. For example, several peripheral mechanisms have been suggested to account for OA pain, including activation of sensitized nociceptors in the knee by local inflammation (Schuelert and McDougall, 2006;McDougall et al., 2006;Schaible and Schmidt, 1985), bone marrow lesions or microfractures and increased intra-osseous pressure (Mach et al., 2002), as well as changes in spinal sensory processing (Felson, 2005;Kean et al., 2004;Niv et al., 2003).

Yet, many of the proposed mechanisms cannot account for clinical observations. For example, most OA patients experience pain from areas remote from the arthritic joint (Kean et al., 2004). Joint pain still persists in approximately 12% of patients months following total hip replacement (Nikolajsen et al., 2006). Most OA patients also experience loss of proprioception (Barrett et al., 1991;Hurley et al., 1997;Katz WA., 2001;Sharma, 1999), which is mediated by Aβ-fiber neurons, as well as loss of vibrational sense (Shakoor et al., 2008), which is also Aβ neuron-mediated.

Changes in the functional properties of primary afferent neurons may be able to initiate these changes but they are largely overlooked as possible origins of the pain of OA, even though such changes have been suggested in other models of chronic pain,

including models of inflammatory pain (Djouhri and Lawson, 1999;Djouhri and Lawson, 2001;Djouhri et al., 2006) and neuropathic pain (Djouhri et al., 2006;Michaelis et al., 2000;Newton et al., 2000;Rausch et al., 2000). Inflammatory pain models are associated with changes only in small dorsal root ganglia (DRG) neurons, possibly C- and Aδ-fiber neurons (Djouhri and Lawson, 1999;Xu et al., 2000), while in neuropathic models all neuronal populations appear to be changed, including large Aβ-fiber neurons (Abdulla and Smith, 2001;Kim et al., 1998;Liu and Eisenach, 2005;Liu et al., 2000;Ma et al., 2003;Sapunar et al., 2005;Stebbing et al., 1999;Zhang et al., 1999).

Therefore, the aim of the current study was to determine any changes in the electrophysiological properties of C- and Aδ-fiber nociceptive neurons, and to compare these with changes in Aβ-fiber LTMs in OA animals one month after model induction. We report here that significant changes in AP configuration were observed only in Aβ-fiber LTMs at a time during model development when the knee joint histopathology, knee pathophysiology and nociceptive responses of the affected limb confirmed that this was an animal model of OA and also an animal model of OA pain. The present findings do not support a role of C- or Aδ-fiber nociceptors in the pathogenesis of pain in this surgically-induced rat model of OA.

**2.2. Methods**

This study was carried out on female Sprague Dawley rats (180-225 g) obtained from Charles River Inc. (Saint Constant, QC, Canada). All experimental procedures were approved by the McMaster University Animal Review Ethics Board and conform to the Guide to the Care and Use of Laboratory Animals of the Canadian Council of Animal Care, Vols.1 and 2. Following model induction, animals were housed for one month before the acute electrophysiological experiment. At 28 days animals were tested for changes in nociceptive scores, and some animals were selected for histological and further physiological studies. After the end of the acute electrophysiological experiment each animal was euthanized by an overdose of anesthetic.

2.2.1. Induction of the model of OA

Surgically-induced derangement model of OA was used (Henry, 2004). Details of the surgical procedure to establish the model have been reported previously (Wu and Henry, 2009). In brief, each animal was anesthetized with a mixture of ketamine (100 mg/ml), xylazine (20 mg/ml) and acepromazine (10 mg/ml) – ketamine from Bioniche (Belleville, ON, Canada), xylazine from Bayer (Toronto, ON, Canada), acepromazine from Wyeth-Ayerst (Guelph, ON, Canada). After the animal was anesthetized, the tibial and medial ligament attachments of the medial meniscus were severed and the meniscus was removed. This exposed the anterior cruciate ligament (ACL), which was then cut. The incision was sutured in two layers and the animals were given the antibiotic Trimel

from Novopharm (Toronto, ON, Canada; 0.05ml once per day for 3 consecutive days), and the analgesic, Temgesic from Schering-Plough (Kenilworth, NJ, USA) twice per day for 2 consecutive days.

Following recovery from surgery, animals were housed in a climate-controlled room under a 12-h light/dark cycle. Animals were allowed to survive for 4-5 weeks as previous work in our group has suggested that typical signs of OA are entrenched by four weeks after surgery (Appleton et al., 2007).

2.2.2. Knee joint histopathology

Animals were anesthetized as described above, and perfused intracardially with 500 ml of physiological saline. The knee joints were harvested and decalcified in 5% formic acid. Histological processing and assessment of tissues were done by Bolder BioPATH Inc. (Boulder, CO, USA). Briefly, knees were trimmed into two approximately equal frontal halves, processed through graded alcohols, and embedded in paraffin. An initial section was cut, and two additional step sections were cut at 150μm for a total of three sections, which were stained with toluidine blue and evaluated microscopically for cartilage damage, osteophyte formation and the degree of joint instability. Cartilage degeneration in the tibia and femur was scored none to severe using the following criteria described by Janusz et al.: 1 = minimal superficial zone only; 2 = mild extends into the upper middle zone; 3 = moderate well into the middle zone; 4 =

marked into the deep zone but not to tidemark; 5 = severe full thickness degeneration to tidemark (Janusz et al., 2002). Cartilage degeneration scores were measured for the medial and lateral tibia and femur, and all values from all three slides were summed to provide a total joint cartilage degeneration sum.

Osteophytes were scored 1, 2, 3, 4 or 5 for small (< 299μm), moderate (300–399 μm), large (400–499 μm), very large (500–599 μm), or extremely large (> 600 μm) depending on the size using an ocular micrometer. Medial and lateral osteophyte scores were added to the total joint cartilage sum to derive a total joint score.

The degree of joint stability was determined based on fibroproliferative and chondrogenic changes in the synovium/collateral ligament as well as transected cruciate area, and the scoring system was as follows: mild = 1, moderate = 2, and severe = 3.

2.2.3. Tissue oedema and plasma extravasation of the knee joint

At four weeks following knee surgery, animals were anesthetized as above. Evan's blue dye (VWR, Mississauga, ON, Canada), dissolved at a concentration of 25 mg/ml in saline, was injected as 0.1mg/100g body weight through the jugular vein. Twenty minutes following Evan's blue injection, animals were perfused intracardially with 500 ml of physiological saline. Knee joints were dissected and dried in an oven at 60 °C for 24 h. To evaluate tissue oedema in the knee joint, the weight difference of each knee joint after the dehydration procedure was measured.

To measure any change in vascular permeability the degree of plasma extravasation was determined; dried knee joints were placed in vials each with 3ml of formamide (Fisher Scientific, Ottawa, ON, Canada) overnight in an oven at 60°C. Twenty-four hours later, fluids in the vials were filtered and evaluated by the absorbance measured by colour spectrophotometry (Biochrom Ltd.,Cambridge, UK), compared to pure formamide at wavelength 620 nm. The optical densities were calculated as follows: [ipsilateral absorbance/ipsilateral weigh]

2.2.4. von Frey test to determine hind paw mechanical withdrawal threshold

The customized testing chamber consisted of a 30x30x30 cm Plexiglas box with a clear Plexiglas floor. This floor contained 0.5 cm diameter holes that were spaced 1.5 cm apart, and was positioned over a mirror tilted 45 degrees that allowed an unobstructed view of the rat paws (Pitcher et al., 1999). Animals were placed in the testing chamber and allowed to acclimatize for 30 min prior to testing. von Frey filaments from Stoelting (Wood Dale, IL, USA) were applied to the soft tissue of the plantar surface of the hind paw to determine the withdrawal threshold. The first filament applied corresponded to a force of 4.31 grams. If a negative response (no response) was observed, a filament exerting greater force was applied, and if a positive response (paw withdrawal from platform) was observed, a filament of lesser force was used next. Each filament was applied three times, at 3 sec intervals. The response pattern described by

Chaplan was adopted to calculate 50% response threshold (Chaplan et al., 1994). The maximum score possible was 15 grams, and the minimum was 0.25 grams.

2.2.5. Effects of repeated flexion and extension of the OA knee on tail flick latency

We have found that noxious peripheral stimuli alter reaction time in the tail flick test (Pitcher et al., 1995;Romita and Henry, 1996;Cridland and Henry, 1988). Therefore, we applied a similar approach to determine whether repeated flexion and extension of the deranged knee would alter tail withdrawal latency.

Rats were gently wrapped in clean surgical drapes that covered the entire body to the base of the tail. They were acclimatized to the wrapping for 20-25 min, twice each day over a two-day period prior to surgery. Tail withdrawal latency was then determined on Model 33 tail flick Analgesia meter (IITC, Woodland Hills, CA, USA) at a point 10 cm from the tip that was blackened prior to the test. The intensity of light beam was set so that a baseline reaction time of 8-10 sec was achieved. Once stable baseline readings had been taken, the deranged knee was then articulated with a full extension-flexion mode through the normal plane of motion 20 times over a 30 sec period. Readings in the tail-flick test were then taken again 3 and 6 min after the articulation. The mean of the three baseline responses was taken as 100%. All subsequent responses were normalized as a percentage of the baseline value.

2.2.6. Animal preparation for acute electrophysiological recording

Full details of the animal preparation and intracellular recordings have been reported previously (Wu and Henry, 2009). Recordings were made from the L4 DRG partly because it is one of the DRGs which contains the largest number of the knee joint afferents. In brief, the L4 dorsal root was cut close to the spinal cord to allow a 12-15 mm length for electrical stimulation.

The rat was fixed in a stereotaxic frame, with the right femur further secured by a customized clamp onto the frame to minimize movements of the DRG during mechanical searching for receptive fields on the leg. The exposed spinal cord and DRG were covered with warm paraffin oil at 37°C to prevent drying. One pair of bipolar platinum stimulating electrodes (FHC, Bowdoinham, ME, USA) was placed beneath the $L_4$ dorsal root.

The animals were mechanically ventilated (Model 683, Harvard Apparatus, Saint Laurent, QC, Canada), and monitored with the CapStar-100 End-Tidal $CO_2$ Analyzer (CWE, Ardmore, PA, USA). Immediately before the start of recording, an initial 1 mg/kg dose of pancuronium from Sandoz (Boucherville, QC, Canada) was given to eliminate muscle tone. The effect of pancuronium was allowed to wear off periodically (normally within one hour of pancuronium administration) in order to confirm a surgical level of anesthesia by observing the pupil for dilation and testing for reflex withdrawal from a pinch to a forelimb. Throughout the experiments, 1/3 of the initial dose of

supplemental pentobarbital (CEVA SANTE ANIMALE, La Ballastière, Libourne, France) was added every hour to maintain a surgical level of anesthesia. This schedule of pentobarbital administration was confirmed to be effective and safe in maintaining a surgical level of anesthesia in non-paralyzed control rats in our pilot study. Rectal temperature was maintained at approximately 37°C using an in-house servo-controlled infrared heating lamp.

2.2.7. In vivo intracellular recording

Recordings were made intracellularly from somata in the DRG using sharp glass micropipettes fabricated from filament-containing borosilicate glass tubing (1.2 mm outer diameter, 0.68 mm inner diameter; Harvard Apparatus, Holliston, MA, USA). DC resistance of these pipettes was about 40-70MΩ filled with 3 M KCl solution.

The microelectrode was advanced into the $L_4$ DRG with an EXFO IW-800 micromanipulator (Montreal, QC, Canada) in steps of 1 μm until a Vm of at least -40 mV suddenly occurred and an AP could be evoked by stimulation of the dorsal root. Once this occurred the recording was allowed to stabilize over a five min period. Then, the stimulating electrode was used to deliver a single electrical pulse to evoke an AP for analysis. Recordings were made with a Multiclamp 700B amplifier (Molecular Devices, Union City, CA, USA) and digitized on-line via a Digidata 1322A interface (Molecular Devices) with *pClamp 9.2* software (Molecular Devices).

The first evoked AP in each neuron was used to determine any differences in configuration between control and OA animals. Measurements of the electrophysiological parameters have been demonstrated (Wu and Henry, 2009). These included CV, Vm, action potential duration (APD), AP half width, AP amplitude, AP rise time, AP fall time, MRR, MFR, afterhyperpolarization (AHP) amplitude, AHP50 and AHP80.

Analysis was done off-line using *pClamp 9.2* software.

2.2.8. Classification of DRG neurons

Response properties of neurons to natural stimuli of peripheral receptive fields were identified by various mechanical stimuli, and classified as previously described (Lawson et al., 1997). The criterion for the classification of C-, Aδ- and Aβ-fiber DRG neurons was mainly based on dorsal root conduction velocities: $\leq$ 0.8 m/s for C-fiber neurons, 1.5–6.5 m/s for Aδ-fiber neurons and $\geq$ 6.5 m/s for Aβ-fiber neurons (Fang et al., 2005).

Three major factors were considered in grouping Aβ-fiber LTMs: the threshold of activation, the depth of the receptive field and the pattern of adaptation. Non-nociceptive Aβ-fiber neurons were identified as low threshold mechanoreceptors using a soft brush, light pressure with a blunt probe and light manual tap. These neurons included various subtypes, such as guard hair, field hair, Pacinian, glabrous

rapidly adapting, slowly adapting types I and II, and muscle spindle types I and II. Guard and field hair neurons were both rapidly adapting cutaneous hair units and are included together. Pacinian and glabrous neurons were both rapidly adapting non-hair neurons, and were named rapidly adapting neurons. Slowly adapting neurons adapted slowly to light tactile stimuli to the cutaneous receptive fields. Muscle spindle neurons were slowly adapting neurons with subcutaneous receptive fields.

For C- and Aδ-fiber DRG neurons, only high threshold or unresponsive C- and Aδ-fiber neurons were recorded and included in the current electrophysiological study. High threshold neurons were those that were activated only by high intensity stimuli such as pinch and squeeze applied with a fine forceps, a coarse-toothed forceps or a sharp object such as a syringe needle. Unresponsive neurons were those not excited by any of the non-noxious or noxious mechanical stimuli listed above, and as defined by Lawson et al. (1997).

2.2.9. Acceptance criteria

A neuron was included in this study if it exhibited an evoked AP from dorsal root stimulation, had a Vm more negative than -40 mV and had an AP amplitude larger than 40 mV. Once impaled, and before sensory testing was begun, a continuous recording was obtained from each neuron for at least 5 min. Only neurons with stable Vm throughout recording and sensory testing were included.

2.2.10. Statistical analysis

Normality of electrophysiological data was done with the D'Agostino and Pearson omnibus test. Wherever appropriate, Student's *t*-test or the Mann-Whitney *U*-test was used for comparisons between OA and control animals in various neuronal subtypes and for various parameters. All statistical tests and graphing were done using Prism 4 software (GraphPad, La Jolla, CA, USA). *P*-values are indicated in the graphs and $P < 0.05$ was considered to indicate a significant difference.

**2.3. Results**

2.3.1. Histopathological changes in the knee joint

As determined by toluidine blue staining, knee joints in naïve control animals showed sporadic minimal cartilage degeneration on the inner part of the medial tibia, but without any osteophyte formation or any sign of joint instability (Figure 2.1. A,C). These minor changes are typical of common spontaneous medial tibial alterations in the cartilage area that is not protected by the meniscus. In animals with one month duration OA, lesions of the affected joint were observed, including cartilage degeneration ranging from superficial proteoglycan and chondrocyte loss (most joints) to focal marked to severe chondrocyte loss (less common, always medial; Figure. 2.1. B). The medial and lateral cartilage degeneration sums were significantly increased, as well as the total joint score. Total joint scores of $0.5 \pm 0.23$ in naïve control knees ($N = 7$) were significantly

lower than 12.2 ± 0.91 in OA knees ($N = 10$; $P < 0.001$; Figure 2.1. E). Moreover, the medial cartilage degeneration was more severe than lateral degeneration (4.5 ± 0.49, $N = 10$ vs. 2.4 ± 0.53, $N = 10$; $P = 0.008$; Figure 2.1. F). There was moderate to severe joint instability manifesting as varying amounts of damage to cruciate ligaments and medial menisci, as well as proliferative changes in both. The instability score was 2.3 ± 0.21 ($N = 10$). The medial joint capsule was thickened with proteoglycan deposition. The medial side of the joint typically exhibited osteophyte formation. Some joints exhibited a reshaping of the medial tibial epiphyseal marginal zone and subchondral bone (Figure 2.1. D).

2.3.2. Pathophysiological changes in the knee joint

As determined by the weight difference after the dehydration protocol, OA rats exhibited significantly more liquid in the ipsilateral knee joint than control rats. The weight difference by dehydration per knee was 0.5 ± 0.02 g in naïve control rats ($N = 7$), and the amount was significantly greater at 0.6 ± 0.02 g in OA rats ($N = 7$; $P = 0.002$; Figure 2.2. A).

Extravasation of Evans blue dye, usually taken as a measurement of vascular permeability, was greater in OA rats. The optical density of Evans blue dye in knees from control rats was 0.1 ± 0.01 ($N = 7$), and was 0.2 ± 0.02 in OA rats ($N = 7$; $P = 0.029$; Figure 2.2. B), suggesting a loss of vascular integrity in the knees from OA animals.

2.3.3. Nocifensive behaviors of the OA model

Paw withdrawal thresholds were measured only on the 28$^{th}$ day after surgical induction of the model.

The threshold to von Frey hair stimulation in controls was 14.6 ± 0.23 g ($N$ = 6). The OA group showed significantly higher sensitivity, the threshold was 8.8 ± 1.85 g ($N$ = 9; $P$ = 0.025; Figure 2.3. A). Interestingly, not every OA rat showed signs of hypersensitivity, and there was considerable individual variability. Three out of 9 OA rats showed no hypersensitivity (over the 15 g limit); another 2 showed moderate hypersensitivity (8-12 g); and the rest 4 OA rats showed high sensitivity (withdrawal from less than 5 g).

The latency to withdrawal of the tail in the tail-flick test was also determined in these animals on the 28$^{th}$ day after model induction. Repeated flexion and extension of the knee had no effect on the latency of the tail flick reflex in control rats (97.1 ± 5.18% of the baseline value). However, in OA rats the same manipulation significantly decreased the latency of the tail flick reflex to 64.7 ± 4.91% of the baseline reading ($P$ < 0.001; Figure. 2.3. B).

2.3.4. AP configurations in C- and Aδ-fiber neurons

Acute electrophysiological experiments were run between the 29$^{th}$ and the 35$^{th}$ day after model induction.

The C-fiber pool was comprised of 24 neurons (5 neurons with an identifiable receptive field) from 14 OA rats and 32 neurons (19 neurons with an identifiable receptive field) from 21 control rats. The Aδ-neuron pool was comprised of 15 neurons (5 neurons with an identifiable receptive field) from 10 OA rats and 18 neurons (9 neurons with an identifiable receptive field) from 15 control rats.

2.3.4.1. Conduction along dorsal root

No difference between control and OA model rats was found in the conduction velocity in either C- or Aδ-fibers: 0.5 ± 0.03 m/s in control C-fibers ($N$ = 33) vs. 0.6 ± 0.04 m/s in OA C-fibers ($N$ = 25; $P$ = 0.099), and 5.1 ± 0.04 m/s in control Aδ -fibers ($N$ = 18) vs. 4.4 ± 0.35 m/s in the OA Aδ-fibers ($N$ = 15; $P$ = 0.219). C- and Aδ-fiber neurons appeared to conduct in two widely separated ranges (Figure 2.4. A).

2.3.4.2. Resting membrane potential and AP amplitude

The Vm in C-fiber neurons was similar in control rats (-58.7 ± 1.76 mV; $N$ = 29) and in OA model rats (-56.7 ± 2.46 mV; $N$ = 25; $P$ = 0.497). However, Vm in Aδ-fibers in control rats (-65.1 ± 2.04 mV, $N$ = 17) was statistically less depolarized than in OA model rats (-58.7 ± 2.11 mV; $N$ = 15; $P$ = 0.038; Figure. 2.4. B).

AP amplitude was similar in both control and OA rats (86.6 ± 1.49 mV, $N$ = 33 in control C-fiber neurons vs. 84.1 ± 2.64 mV, $N$ = 25 in OA C-fiber neurons; $P$ = 0.387;

74.9 ± 2.48 mV, $N$ = 18 in control Aδ-fiber neurons vs. 77.7 ± 2.85 mV, $N$ = 15 in OA Aδ-fiber neurons; $P$ = 0.474; Figure 2.4. D).

2.3.4.3. Duration of the AP

The AP duration at base in C-fiber neurons in control rats (4.3 ± 0.28 ms; $N$ = 33) was similar to that in OA model rats (5.4 ± 0.93 ms; $N$ = 25; $P$ = 0.789; Figure. 2.4. C). It is also the case in Aδ-fiber neurons (2.2 ± 0.12 ms; $N$ = 18 in control vs. 2.6 ± 0.21 ms; $N$ = 15 in OA; $P$ = 0.069; Figure. 2.4. C).

For the duration at half amplitude in C-fiber neurons, no difference was identified between OA (2.3 ± 0.33 ms; $N$ = 24) and control rats (2.1 ± 0.14 ms; $N$ = 33; $P$ = 0.878), and no difference was found in Aδ-fiber neurons in control vs. OA rats (2.2 ± 0.12 ms; $N$ = 18 and 2.6 ± 0.21 ms; $N$ = 15, respectively; $P$ = 0.156).

2.3.4.4. AP rise time

AP rise time reflects the duration of the depolarization phase of the AP. No significant difference between OA and control animals was found in the AP rise time in either C-fibers or Aδ-fibers. AP rise time in C-fibers was 1.7 ± 0.14 ms in control ($N$ = 33) vs. 2.1 ± 0.41 ms in OA ($N$ = 25; $P$ = 0.47); AP rise time in Aδ-fibers was 0.9 ± 0.05 ms in control ($N$ = 18) vs. 1.1 ± 0.09 ms in OA ($N$ = 15; $P$ = 0.095).

2.3.4.5. Maximum rising rate

Maximum rising rate was derived from the differentiated conversion of the AP curve, which reflects the rate of depolarization over time. The maximum rising rate in C-fibers was similar in control and OA rats (154.5 ± 6.51 mV/ms in control, $N$ = 33 vs. 158.1 ± 9.95 mV/ms in OA, $N$ = 25; $P$ = 0.796). Similar is maximum rising rate in Aδ-fibers, 178.1 ± 11.08 mV/ms in control, $N$ = 18 vs. 171.7 ± 10.97 mV/ms in OA, $N$ = 15 ($P$ = 0.689). The data are shown in (Figure 2.4. E).

2.3.4.6. AP fall time

A similar rationale was adopted to determine the dynamics of repolarization, where AP fall time and maximum falling rate were used to measure the dynamics of the repolarization phase. Repolarization of the AP in either C-fibers or Aδ-fibers in OA animals was not different from that of control animals. AP fall time in C-fibers in control rats (2.6 ± 0.19 ms, $N$ = 33) was similar as that in OA rats (3.3 ± 0.62 ms, $N$ = 25; $P$ = 0.594), as was AP fall time in Aδ-fibers (1.3 ± 0.08 ms, $N$ = 18 in control vs. 1.6 ± 0.14 ms, $N$ = 15 in OA animals; $P$ = 0.084).

2.3.4.7. Maximum falling rate

Maximum falling rate in C-fibers in OA animals (65.1 ± 5.27 mV/ms ($N$ = 24) was similar to that in control animals (67.2 ± 4.84 mV/ms; $N$ = 33; $P$ = 0.734). Maximum falling rate in Aδ-fibers in OA animals (90.5 ± 6.35 mV/ms; $N$ = 15) was

similar to that in control animals (98.3 ± 5.54 mV/ms; $N = 18$; $P = 0.364$). The data are shown in (Figure. 2.4. F).

2.3.4.8. Afterhyperpolarization

Nociceptors have a longer AHP period than non-nociceptors (Fang et al., 2005). Therefore, measurements of the AHP associated parameters, particularly, 80% AHP recovery time, are liable to be compromised by noise signals during recording. In C-fiber neurons, a total of 16 out of 56 neurons (9 in OA and 7 in control groups) had at least one missing value for AHP, AHP50, or AHP80. A similar problem was observed in Aδ-fiber recordings, where 12 out of 33 neurons (6 in OA and 6 in control groups) lacked the full complement of AHP associated readings. Nonetheless, examination of these AHP associated parameters revealed no difference between OA and control rats, irrespective of the duration or the amplitude. AHP amplitude was 11.6 ± 0.82 mV ($N =$ 30) and 11.9 ± 1.08 mV ($N = 22$) in C-fiber control and OA neurons, respectively ($P =$ 0.831), and was 12.1 ± 0.84 mV ($N = 16$) and 10.3 ± 0.99 mV ($N = 12$) in Aδ-fiber control and OA neurons, respectively ($P = 0.191$). The AHP50 was 11.4 ± 0.93 ms ($N =$ 30 in control) vs. 12.8 ± 1.51 ms ($N = 21$ in OA) in C-fiber population ($P = 0.414$), and was 8.8 ± 1.54 ms ($N = 16$ in control) vs. 10.7 ± 2.28 ms ($N = 12$ in OA) in Aδ-fiber population ($P = 0.491$). The AHP80 was 27.5 ± 2.37 ms in control C-fiber neurons ($N =$ 24) vs. 30.4 ± 3.16 ms in OA C-fiber neurons ($N = 18$; $P = 0.451$), and was 20.4 ± 2.66

ms in control Aδ-fiber neurons ($N = 12$) vs. (21.1 ± 6.97 ms in OA Aδ-fiber neurons ($N = 8$; $P = 0.512$).

2.3.5. Aβ-fiber LTMs

For comparison of Aβ-fiber LTMs, 83 such neurons were recorded from 25 naïve control rats and 79 were recorded from 22 OA rats. In terms of the breakdown of different types of Aβ-fiber LTMs, both groups of animals yielded comparable numbers of each neuronal subtype. For example, guard/field hair neurons were recorded from 14 rats in the control group and 15 rats in the OA group. Similarly, muscle spindle (slowly adapting with subcutaneous receptive field) were recorded from 15 control rats and 20 OA rats.

Representative electrophysiological parameters of control A-fiber LTMs, such as Vm, APD, AP amplitude, MRR and MFR, were comparable to what has been reported in vivo (Djouhri and Lawson, 1999;Djouhri and Lawson, 2001;Fang et al., 2005), and also similar to what Ma et al. defined in the low threshold mechanoreceptor category in a modified in vitro recording that allowed activation of peripheral receptive fields (Ma et al., 2003). Aβ-fiber neurons were a focus of the current study. These are fast conducting medium to large size neurons. Electrophysiological parameters of the control neurons were also in the range of what has been reported in medium to large size

neurons in vitro (Sapunar et al., 2005;Stebbing et al., 1999;Villiere and McLachlan, 1996;Xu et al., 1997).

2.3.5.1. Receptive fields of Aβ-fiber LTMs

Receptive fields and sites of activation of Aβ-fiber LTMs studied were found throughout the entire hind leg. In the naïve control rats, receptive fields of 55.4% of all of A-fiber LTMs with identifiable receptive fields were on the foot, 19.3% on the calf, 20.5% on the thigh, 1.2% on the ankle joint and 3.6% on the knee joint. In the OA rats, the distribution was as follows: foot (50%), calf (31.8%), thigh (9.1%), ankle joint (3.8%) and knee joint (5.3%). Table 1 summarizes the locations of the receptive fields associated with each neuron type recorded.

Some neuronal subtypes only innervated the foot, such as glabrous skin type of rapidly adapting neurons and slowly adapting neurons. Based on our observations, cutaneous rapidly adapting neurons could only be activated by stimulating the glabrous skin of the paw and slowly adapting neurons only by stimulating narrow skin strips surrounding the nails. Receptive fields of the remainder of the neuronal subtypes (i.e. guard/field hair neurons, the Pacinian type of rapidly adapting neurons and muscle spindle neurons) were found ubiquitously innervating the hind leg.

The guard/field hair and muscle spindle neuronal subgroups contributed to thigh-to-calf receptive field shift following joint derangement. In control rats, 9% of

guard/field hair neurons and 54% of muscle spindle neurons projected to the calf region, while in OA rats the percentages were 27% in guard/field hair neuron subgroup and 74% in muscle spindle subgroup. Interestingly, the percentages of guard/field hair and muscle spindle neurons projecting to the thigh region was 30% and 36%, respectively, in control rats, but only 7% and 14%, respectively, in OA rats.

2.3.5.2. Changes in AP configuration in Aβ-fiber LTMs

In general, the dynamics of AP genesis were slower in the OA animals, particularly in the depolarization phase of the AP. The duration of the AP was longer in A-fiber LTMs in animals following knee derangement. Compared with the control group (1.0 ± 0.03 ms; $N = 83$), the AP duration at base was significantly wider in the OA group (1.1 ± 0.02 ms; $N = 79$; $P = 0.028$; Figure 2.5. A). Half width was significantly longer in neurons in OA animals (0.4 ± 0.02 ms, $N = 83$ in control vs. 0.5 ± 0.01 ms, $N = 79$ in OA; $P = 0.046$). In contrast to the control group (0.4 ± 0.01 ms; $N = 83$), AP rise time was significantly longer in the OA group (0.5 ± 0.01 ms; $N = 79$; $P < 0.001$; Figure 2.5. B). Maximum rising rate was 291.9 ± 9.41 mV/ms in the control group ($N = 83$), which was significantly faster than in the OA group (254.3 ± 6.22 mV/ms, $N = 79$; $P = 0.001$; Figure 2.5. E).

However, the AP fall time was not significantly different between the control group and the OA group ($P = 0.262$); readings were 0.6 ± 0.02 ms ($N = 83$) in the control

group and 0.6 ± 0.02 ms ($N$ = 79) in the OA group (Figure 2.5. C). Maximum falling rate was similar in the control and the OA group, at 173.3 ± 8.77 mV/ms ($N$ = 82) vs. 145.1 ± 4.39 mV/ms ($N$ = 79), respectively ($P$ = 0.114; Figure 2.5. F).

The AP amplitude was not different in the control vs. the OA group (58.9 ± 1.10 mV, $N$ = 83 vs. 57.6 ± 0.98 mV, $N$ = 79, respectively; $P$ = 0.527; Figure 2.5. D).

The remaining parameters, including CV, Vm, AHP50 and AHP80, were also not different between the two groups (data not shown).

2.3.5.3. Changes in AP configuration in subgroups of Aβ-fiber LTMs

Further comparison was made between the OA group and the control group for each subset of Aβ-fiber LTMs based on the 4 subsets described above: guard/field hair, rapidly adapting, slowly adapting and muscle spindle neurons. Muscle spindle neurons were the most affected, followed by guard/field hair neurons. Surprisingly, no significant difference was identified between control and OA groups in either the rapidly adapting neurons or the slowly adapting neurons. The relatively small number of slowly adapting neurons may have contributed to the lack of a significant difference between the OA neurons and the control neurons.

In muscle spindle neurons, the slower dynamics of the AP was the most obvious of all of the parameters studied. In contrast with 0.8 ± 0.06 ms ($N$ = 23) in the control group, AP duration at base was significantly wider in the OA group (0.9 ± 0.04 ms, $N$ =

24; $P$ = 0.04). The AP rise time was 0.3 ± 0.02 ms in control ($N$ = 23), which is significantly shorter than that in the OA group (0.4 ± 0.02 ms, $N$ = 24; $P$ = 0.002). Correspondingly, the maximum rising rate was significantly decreased in OA (307.2 ± 19.73 mV/ms, $N$ = 23 in control vs. 246.8 ± 11.34 mV/ms, $N$ = 24 in OA; $P$ = 0.01). The remaining parameters were not different between the OA and the control groups.

In guard/field hair neurons, the slowing of the AP rise time in OA rats was the only statistically significant change that related to the duration of the AP (0.4 ± 0.02 ms, $N$ = 24 in control vs. 0.5 ± 0.02 ms, $N$ = 20 in OA; $P$ = 0.038). No other significant difference was identified in the remaining parameters related to the duration of AP, such as AP duration at base, AP half width and AP fall time.

Vm of neurons in the control neurons (-66.3 ± 1.55 mV, $N$ = 23) was significantly less depolarized than that of the OA group (-61.1 ± 2.15 mV, $N$ = 19; $P$ = 0.047).

**2.4. Discussion**

In the present *in vivo* study using intracellular recording techniques in rat DRG neurons, the electrophysiological properties of Aβ-fiber LTMs (non-nociceptive) and classic C- and Aδ-fiber nociceptive primary sensory neurons were systematically evaluated in a rat model of OA at one month following model induction. This model was confirmed with fully established osteoarthritic characteristics, namely characteristic cartilage degeneration within the knee joint, increased permeability of the knee

vasculature and tenderness of the affected lower limb. Several important observations were made. Even the primary sensory neurons innervating non-articular structures were affected by the injury initiated in the knee joint. There was a slowing of the dynamics of AP generation in Aβ-fiber LTMs, consisting of a wider duration of the AP, and a slower maximum rising rate; there were barely any obvious changes in AP configuration in C- and Aδ-fiber nociceptors. Our study revealed that Aβ-fiber LTMs are greatly altered in AP configuration in OA, which might imply their role in the pathogenesis of abnormal pain sensation in OA.

2.4.1. The neuropathic pattern of affected neuronal types in OA

Ironically, the distinction between the pathophysiology of inflammation and neuropathic pain diminishes, as knowledge of the peripheral and central mechanisms of nociception accumulates (Bennett et al., 1998). Evidence aiding the classification is of little clarity and may even be overlapping. For example, complete Freund's adjuvant has been reported to cause both inflammatory pain and neuropathic pain depending on the types of tissue affected (Djouhri and Lawson, 1999;Eliav et al., 1999). Both tactile allodynia and thermal hyperalgesia can occur in both types of pain (Nagakura et al., 2003;Xie et al., 2005). Central sensitization is observed in both types of pain (Nakatsuka et al., 1999;Woolf et al., 1992). Therefore, it is possible that for both

inflammatory and neuropathic pain, changes at the spinal and supraspinal levels follow a common pathway, and the real differentiation lies in the pattern of peripheral drive.

It has been suggested that inflammation and neuropathic aetiologies likely affect distinct populations of DRG neurons in various chronic pain models. In superficial inflammation models as induced by injecting complete Freund's adjuvant subcutaneously (Djouhri and Lawson, 1999;Xu et al., 2000), only Aδ-fiber neurons and C-fiber neurons undergo significant changes in electrophysiological properties, with those in C-fiber neurons more severe. In adjuvant-induced joint inflammation, no studies on the properties of DRG neurons are available. However, indirect evidence has suggested that the effects of the joint inflammation do not invade the large, non-nociceptive A-fiber neurons, as indicated by the lack of expression of two pain-related peptides, calcitonin gene-related peptide and substance P in those neuronal types (Bulling et al., 2001;Hanesch et al., 1993). On the contrary, in classic neuropathic models, such as the complete sciatic nerve transection model (Abdulla and Smith, 2001), partial sciatic nerve transection model (Liu and Eisenach, 2005), and the lumbar spinal nerve transection model (Kim et al., 1998;Liu et al., 2000;Ma et al., 2003;Sapunar et al., 2005;Stebbing et al., 1999), changes in AP configurations in A-fiber neurons characterize changes in primary sensory system, and are common. Although in some studies (Abdulla and

Smith, 2001;Kim et al., 1998;Ma et al., 2003), changes in C-fiber neurons are also reported, changes are less prominent than those in A-fiber neurons.

In the present study, no changes were found in C- or Aδ-fiber nociceptors with identifiable receptive fields in OA rats. We can not preclude that the relatively small number of those neurons might cause too weak power of *t*-tests to reveal potential differences. It is compelling for us to combine C- or Aδ-fiber nociceptors with or without identifiable receptive fields mainly for two reasons. First, by doing so, it is unlikely to include a significant number of low threshold units. During our extensive receptive field search, it is uncommon to leave a low threshold unit not activated, but it is common to "run over" a high threshold unit, especially C- or Aδ-fiber nociceptors without triggering it. Moreover, in one previous study, C-fiber low threshold units were estimated to be only 8% of C-fiber neurons (Djouhri et al., 1998). Second, changes in C- and Aδ-fiber neurons in some *in vitro* recordings are presented as changes in small to medium cell neurons in various chronic pain models without further functional division (Abdulla and Smith, 2001;Liu and Eisenach, 2005;Ma et al., 2003). By combining C- or Aδ-fiber neurons with or without identifiable receptive fields, comparison with previous studies is more parallel.

One of the surprising findings in the present study is that Aβ-fiber LTMs (non-nociceptors) are affected in OA rats, manifesting as changes in AP configurations.

These neurons correspond to medium to large neurons in previous studies. The pattern of prominent changes in large Aβ-fiber neurons and less prominent or no change in small C-fiber neurons is commonly seen in neuropathic model of chronic pain, and is rarely seen in inflammation model of chronic pain. Therefore, we propose that the electrophysiological changes in our OA rats result from the neuropathic etiology that follows knee surgery.

2.4.2. Neuropathic etiology likely accounting for the slowed dynamics of AP genesis in Aβ-fiber non-nociceptors

In the present study, changes in AP configurations in Aβ-fiber non-nociceptors, such as wider AP duration, longer AP rise time and slower maximum rising rate are presentations of slowed dynamics of AP genesis, especially slower dynamic of depolarization. Even in nociceptive neurons characteristic with prominent calcium current during repolarization, the voltage-activated calcium current only accounts for about 2% of the depolarization, while two classes of sodium channel contribute to the remaining current - about 58% tetrodotoxin (TTX)-resistent current and about 40% TTX-sensitive current (Blair and Bean, 2002). Therefore, our results could be attributted to changes in sodium channel in those neurons, either functional or expressional. However, the detailed ionic mechanism remains unknown, partly because a detailed sodium channel composition has not yet been revealed in functionally

classified sensory subtypes, such as hair, paccinian, glabrous rapid adapting or muscle spindle neurons (all examples of Aβ-fiber LTMs). Deduced from a recent paper by Fukuoka et. al, naive control large A-fiber neurons might express both TTX-sensitive sodium channels (Nav 1.1, Nav 1.6 and Nav 1.7) and TTX-resistent sodium channels (Nav 1.8, Nav 1.9) (Fukuoka et al., 2008). Moreover, after axotomy, 75% of A-fiber neurons (implication of the involvement of Aβ-fiber non-nociceptors) re-express the embryonic TTX-sensitive Nav 1.3 (Fukuoka et al., 2008). In neuropathic pain animals, particularly after axotomy, there are complicated changes in the sodium channel expression, including up-regulation of Nav1.3 and down-regulation of Nav 1.8, Nav 1.9 (Devor, 2006). Therefore, the significance of our data should be discussed in the context of the summation effect of various changes in sodium channels Nav 1.1, Nav 1.3, Nav 1.6, Nav 1.7, Nav 1.8, and Nav 1.9.

In DRG neurons, slowed dynamics of the AP, such as a widened AP duration and decreased maximum rising and falling rates are believed to be typical in neuropathy type of changes in primary sensory neurons (Abdulla and Smith, 2001;Kim et al., 1998;Liu and Eisenach, 2005;Liu et al., 2000;Ma et al., 2003;Sapunar et al., 2005;Stebbing et al., 1999;Zhang et al., 1999). Yet, accelerated dynamics are also a feature of neuropathy, which has been reported in intact neurons in the spinal ligation model (Sapunar et al., 2005). Furthermore, the possibility of diverse physiological changes in intact and

axotomized primary sensory neurons is strengthened by the fact that different signalling pathways are employed (Obata et al., 2004), and different chemical phenotype switches are observed (Fukuoka and Noguchi, 2002). This "diverse-change" phenomenon also gets support from another experiment looking at the effects of nerve ligation on calcium-activated potassium currents in axotomized and neighbouring intact neurons, in which these currents are reduced by axotomy, but are increased in intact neurons (Sarantopoulos et al., 2007). Therefore, both slowed dynamics and accelerated dynamics of the AP are possible outcome following a neuropathic aetiology.

2.4.3. Mechanisms that functional changes in Aβ-fiber LTMs induce chronic pain.

What prompts us to challenge the accountability of C- or Aδ-fiber neurons for OA pain is the lack of correlation of the onset of various changes in nociception at 4 weeks following model induction with changes in the function of those neurons. It is obvious that some other mechanisms should account for the changes in nociception, such as lowered activation threshold of the hind paw and painful articulation of affected knee joint. We then see simultaneous changes in nociception (mainly mechanical sensitivity) and in the function of Aβ-fiber LTMs. Previous studies also suggest a possible role of such large myelinated neurons in sensory deficits, such as allodynia (Abdulla and Smith, 2001;Devor, 2006;Kim et al., 1998;Liu et al., 2000;Ma et al., 2003;Sapunar et al., 2005), although detailed mechanism has not yet been revealed. One possible explanation is

that some Aβ-fiber non-nociceptors take up a new role in nociception and begin to convey signals along novel pathway leading to nociception/pain. Various neurotrophic factors play important role in the rewiring of sensory pathway at the first synapse at spinal cord. Normally, TrkA positive neurons project to the dorsal spinal cord, whereas TrkC neurons extend neuronal processes to the intermediate (Ia and Ib afferents) and ventral spinal cord (Ia afferents). However, the "wiring" in the spinal cord is dynamic responding to alterations in signalling of neurotrophic factors (Moqrich et al., 2004). We speculate that there is altered supply of various neurotrophic factors, such as brain derived neurotrophic factor (BDNF), GDNF, neurotrophin (NT)-3 etc. These changes constitute a common pathway leading to two parallel changes in Aβ-fiber LTMs – changes in sodium channel expression and changes in the pattern of projection to the spinal cord.

2.4.4. Conclusion

We agree with Ivanavicius (2007) who referred to OA pain as having a neuropathic component. Ivanavicius did not support a role of inflammation in OA pain considering mild immune cell infiltration and poor efficacy of non-steroidal anti-inflammatory drugs (Ivanavicius et al., 2007). Similarly, our observation that heavily myelinated A fibers were affected is hard to be explained by inflammatory

pathogenesis.

**2.5. Tables, Figures**

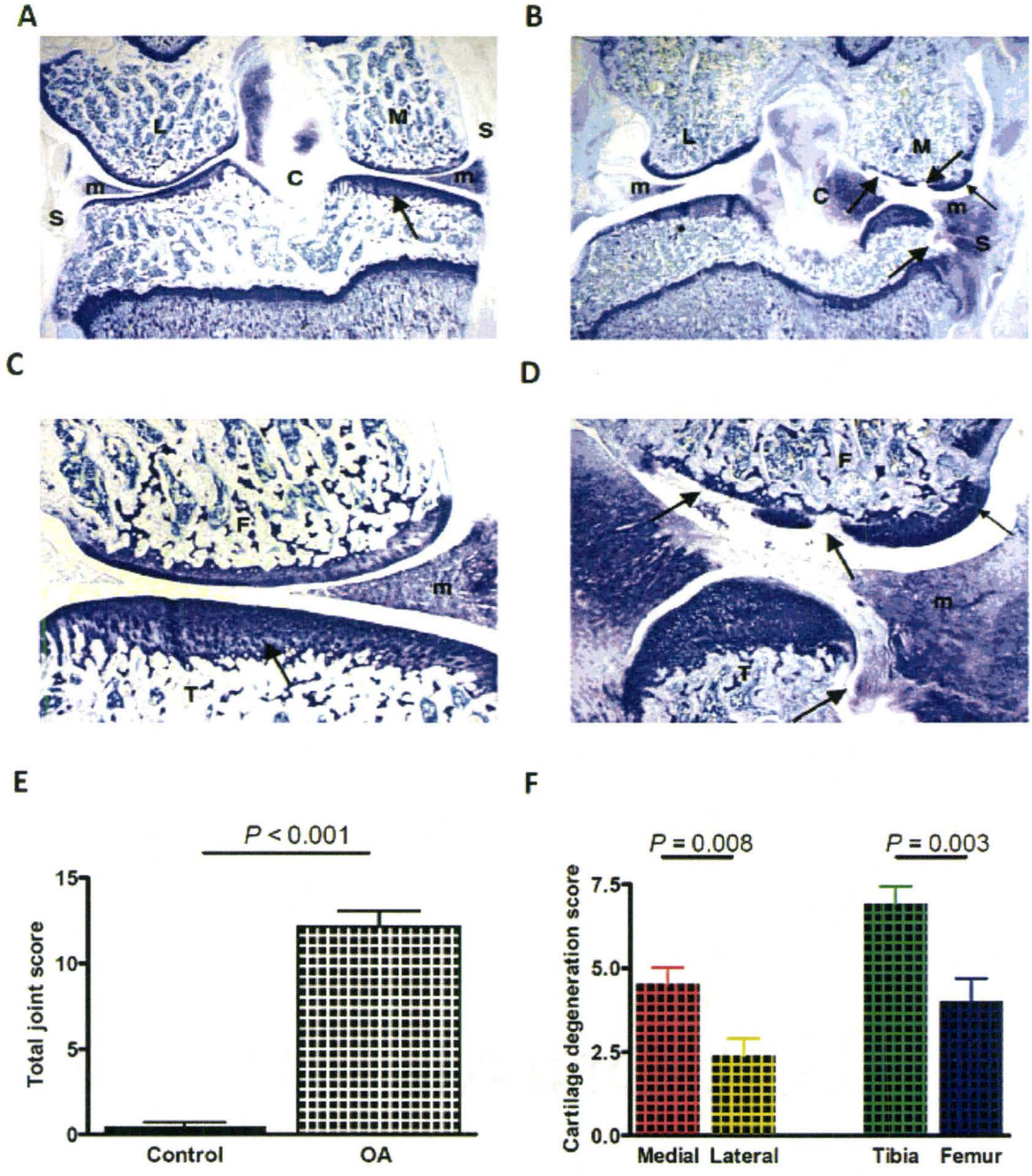


**Figure 2.1. Histology of OA and naïve control knee joints.** ***A***, ***C***, knee from a naive animal has normal cartilage (arrow). Higher magnification of medial compartment from naive animal shows normal cartilage (arrow). ***B***, ***D***, knee from one month OA animal has

minimal to marked cartilage degeneration on all articulating surfaces, with the greatest lesion severity on the medial femur (large arrows). There is severe atrophy of the medial tibia, as well as marked a reshaping of the medial tibial plateau and tibial epiphyseal bone. Additionally, there is a medium-sized osteophyte on the medial femur (small arrow). There is severe thickening/fibrous repair with proteoglycan on the medial side of the synovium and joint capsule. M = Medial; L = Lateral; S = Synovium; m = Meniscus; C = Cruciate ligaments. ***E***, total joint score was significantly increased in OA knees (0.47 ± 0.23; $N = 7$ in naïve control vs. 12.17 ± 0.9, $N = 10$ in OA; $P < 0.001$; Mann-Whitney *U*-test). ***F***, Medial cartilage degeneration was more severe than that of the lateral cartilage (4.53 ± 0.49, $N = 10$ vs. 2.4 ± 0.53, $N = 10$, respectively; $P = 0.008$; Student's *t*-test). Moreover, tibia cartilage degeneration was more severe than femur cartilage degeneration (4.53 ± 0.49, $N = 10$ vs. 2.4 ± 0.53, $N=10$, respectively; $P = 0.003$; Student's *t*-test).

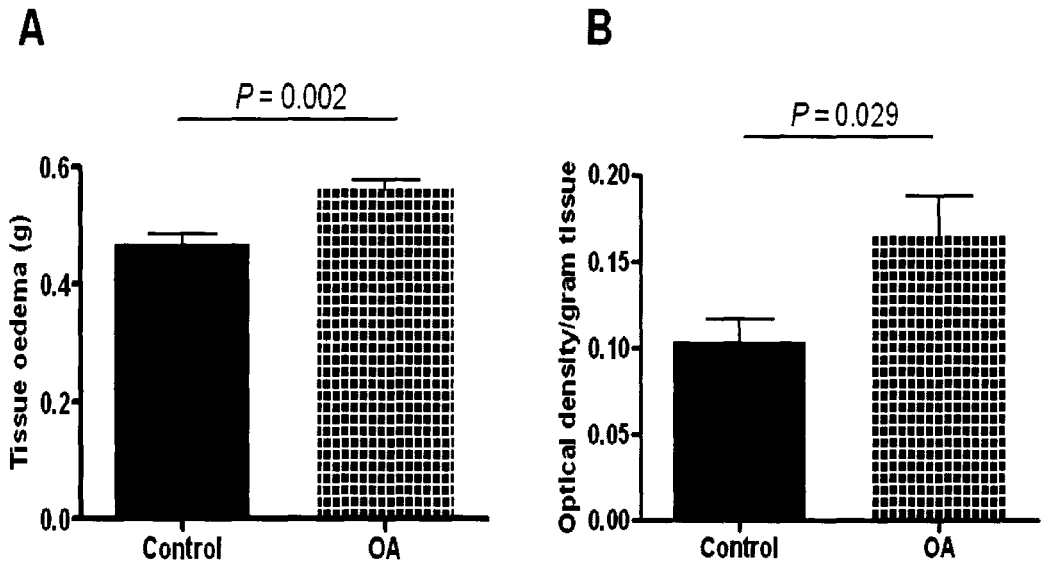


**Figure 2.2. Tissue edema and plasma extravasation of the knee joint in naïve control rats and OA rats.** ***A***, significantly increased oedema was found in OA knee joints (0.47 ± 0.01g, $N = 7$ in control vs. 0.56 ± 0.02g, $N = 7$ in OA ; $P = 0.002$; Student's *t*-test). ***B***, optical densities of Evan's blue in knee joint soft tissue were significantly higher than that of the naïve control knee (0.1 ± 0.01g, $N = 7$ in control vs. 0.17 ± 0.02g, $N = 7$ in OA; $P = 0.029$; Student's *t*-test).

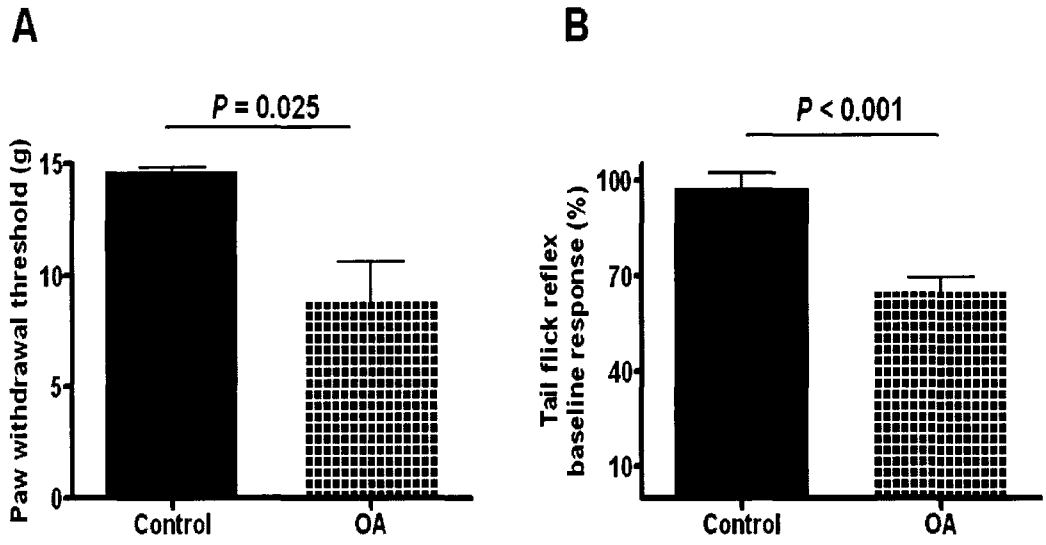


**Figure 2.3. Pronociceptive effects in sensory tests in OA models run one month following model induction.** **A**. OA rats displayed a significantly decreased threshold to the von Frey hair stimulation to the affected hind paw (14.63 ± 0.23 g, $N = 6$ in control vs. 8.78 ± 1.85 g, $N = 9$ in OA, $P = 0.025$; Student's $t$-test). **B.** Repetitive flexion and extension of the knee had no significant effect on the latency of the tail flick reflex in control rats (97.1 ± 5.2% of the baseline latency, $N = 6$). However, the same manipulation significantly decreased the latency of the tail flick reflex in OA rats (64.7 ± 4.9% of the baseline readings, $N = 9$; $P < 0.001$; Student's $t$-test).

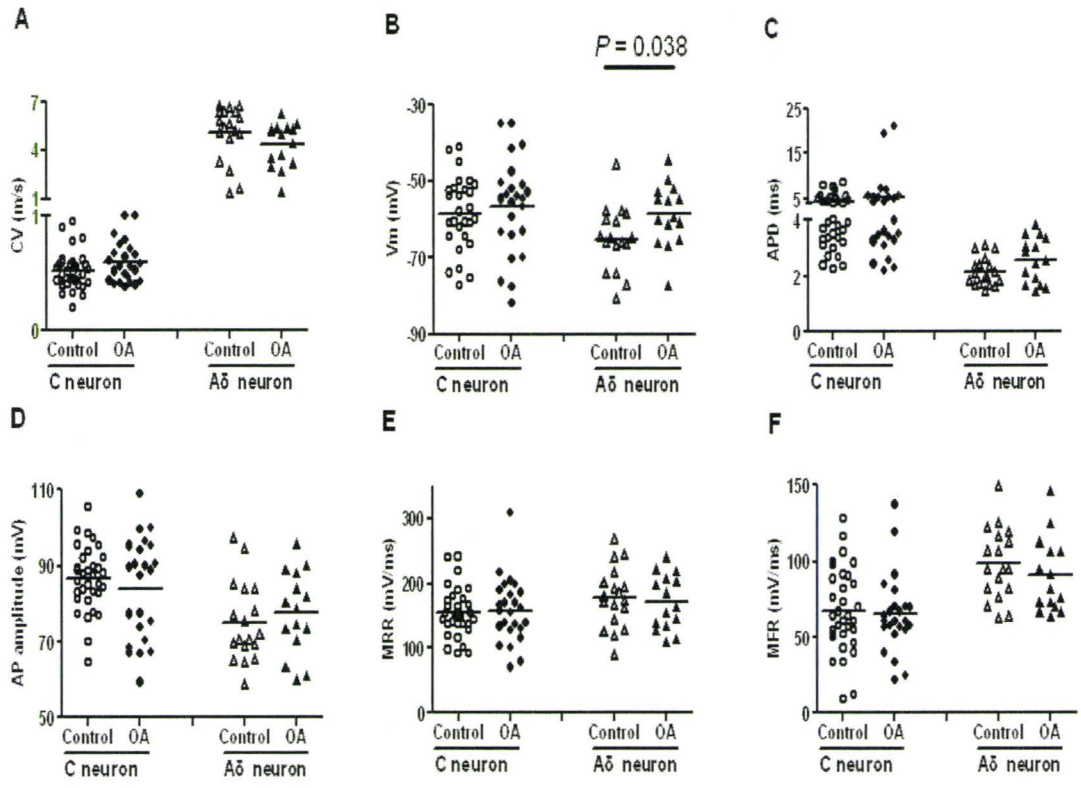


**Figure 2.4. C- and Aδ-fiber nociceptive DRG neurons.** Scatter plots indicating AP properties of individual neurons in control animals, and in OA animals at one month following model induction. "C neuron" stands for C-fiber DRG neurons which include C-fiber high threshold mechanoreceptors and C-fiber non-responsive neurons. Similarly, "Aδ neuron" represents Aδ-fiber DRG neurons which include Aδ-fiber high threshold mechanoreceptors and Aδ-fiber non-responsive neurons. The parameters that bear most of the documented changes are presented, including ***A*** AP duration at base, ***B*** AP rise time, ***C*** AP fall time, ***D*** AP amplitude, ***E/F*** maximum rising and falling rates. The only

difference between OA and control rats was a more depolarized resting membrane potential in Aδ-fiber DRG neurons in model animals (-65.11 ± 2.04, $N$ = 17 mV in control vs. -58.72 ± 2.11 mV; $N$ = 15 in OA; $P$ = 0.038; Student's $t$-test).

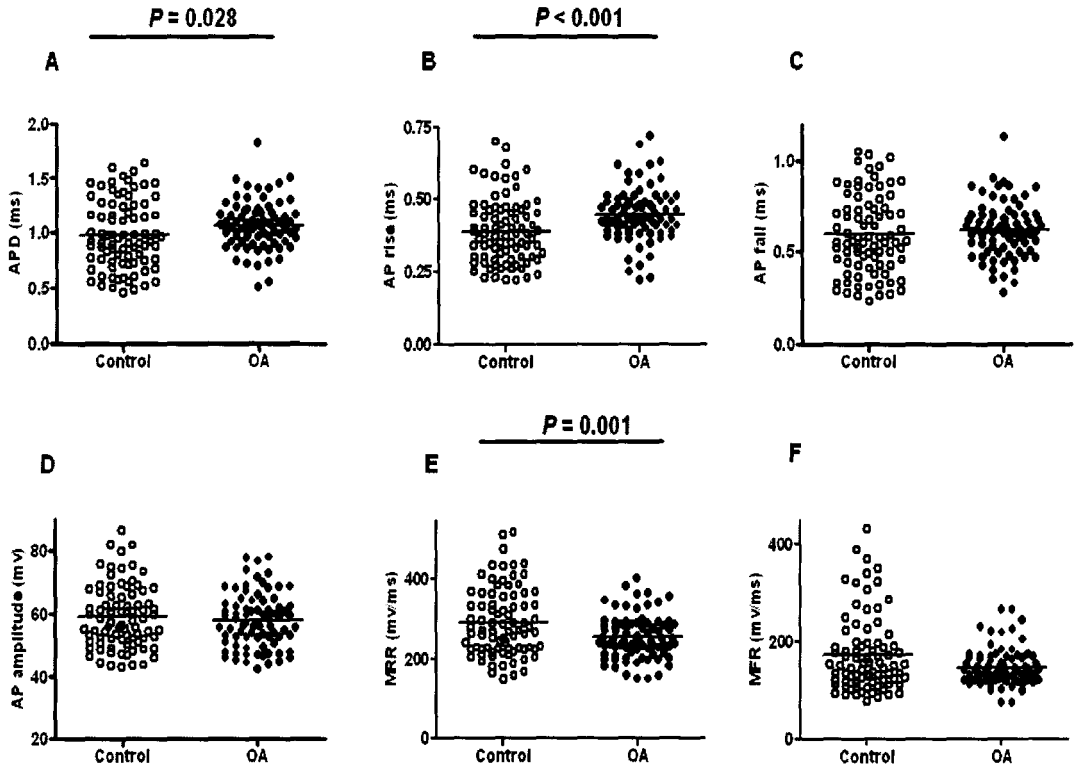


**Figure 2.5. Aβ-fiber low threshold mechanoreceptors.** Scatter plots of AP properties of individual neurons in control animals, and in OA animals at one month after model induction. The parameters that bear most of the documented changes are presented, including ***A*** AP duration at base, ***B*** AP rise time, ***C*** AP fall time, ***D*** AP amplitude, ***E/F*** maximum rising and falling rates. In each case the median (horizontal line) is superimposed. The D'Agostino and Pearson omnibus normality test was run in all data groups in order to assign the data to parametric or non-parametric *t* tests. APD (AP duration at base) was significantly wider in the OA group (0.98 ± 0.03 ms, $N = 83$ in control vs. 1.07 ± 0.02 ms, $N = 79$ in OA; $P = 0.028$; Mann-Whitney *U*-test). AP rise

time was significantly longer in the OA group (0.39 ± 0.01 ms, $N = 83$ in control vs. 0.45 ± 0.01 ms, $N = 79$ in OA; $P < 0.001$; Student's *t*-test). MRR (Maximum rising rate) was significantly slower in the OA group (291.9 ± 9.41 mV/ms, $N = 83$ in control vs. 254.3 ± 6.22 mV/ms, $N = 79$ in OA; $P = 0.001$; Student's *t*-test).

**Table 2.1. Locations of receptive fields of Aβ-fiber low threshold mechanoreceptors recorded in both the OA rats and the naive control rats.**

| | Foot | Calf | Thigh | Ankle | Knee |
|---|---|---|---|---|---|
| **G/F CTL (*N*)** | 14 | 2 | 7 | 1 | / |
| **G/F OA (*N*)** | 20 | 8 | 2 | 2 | 4 |
| **RA CTL (*N*)** | 25 | 2 | 2 | | 2 |
| **RA OA (*N*)** | 34 | 3 | 4 | 3 | 3 |
| **MS CTL (*N*)** | 2 | 12 | 8 | / | 1 |
| **MS OA (*N*)** | 5 | 31 | 6 | / | / |
| **SA CTL (*N*)** | 5 | / | / | / | / |
| **SA OA (*N*)** | 7 | / | / | / | / |
| **A LTM CTL** | 46 | 16 | 17 | 1 | 3 |
| **A LTM OA** | 66 | 42 | 12 | 5 | 7 |

The locations of receptive fields of neurons included are summarized. The classification adopts only the major anatomical regions, including foot, calf, thigh, ankle joint and knee joint. Abbreviations: CTL, naïve control; OA, osteoarthritis; G/F, neurons which include field neurons and guard hair neurons; RA, rapidly adapting neurons, which include glabrous RA neurons and Pacinian neurons; MS, muscle spindle neurons; SA, slowly adapting neurons; A LTM, A type low threshold mechanoreceptors which include G/F, RA, MS, and SA neurons.

**References**

Abdulla FA, Smith PA (2001) Axotomy- and autotomy-induced changes in the excitability of rat dorsal root ganglion neurons. J Neurophysiol 85:630-643.

Appleton CT, McErlain DD, Henry JL, Holdsworth DW, Beier F (2007) Molecular and histological analysis of a new rat model of experimental knee osteoarthritis. Ann N Y Acad Sci 1117:165-174.

Barrett DS, Cobb AG, Bentley G (1991) Joint proprioception in normal, osteoarthritic and replaced knees. J Bone Joint Surg Br 73:53-56.

Bennett DL, Michael GJ, Ramachandran N, Munson JB, Averill S, Yan Q, McMahon SB, Priestley JV (1998) A distinct subgroup of small DRG cells express GDNF receptor components and GDNF is protective for these neurons after nerve injury. J Neurosci 18:3059-3072.

Blair NT, Bean BP (2002) Roles of tetrodotoxin (TTX)-sensitive Na+ current, TTX-resistant Na+ current, and Ca2+ current in the action potentials of nociceptive sensory neurons. J Neurosci 22:10277-10290.

Bulling DG, Kelly D, Bond S, McQueen DS, Seckl JR (2001) Adjuvant-induced joint inflammation causes very rapid transcription of beta-preprotachykinin and alpha-CGRP genes in innervating sensory ganglia. J Neurochem 77:372-382.

Chaplan SR, Bach FW, Pogrel JW, Chung JM, Yaksh TL (1994) Quantitative assessment of tactile allodynia in the rat paw. J Neurosci Methods 53:55-63.

Cridland RA, Henry JL (1988) Facilitation of the tail-flick reflex by noxious cutaneous stimulation in the rat: antagonism by a substance P analogue. Brain Res 462:15-21.

Devor M (2006) Sodium channels and mechanisms of neuropathic pain. J Pain 7:S3-S12.

Djouhri L, Bleazard L, Lawson SN (1998) Association of somatic action potential shape with sensory receptive properties in guinea-pig dorsal root ganglion neurones. J Physiol 513:857-872.

Djouhri L, Koutsikou S, Fang X, McMullan S, Lawson SN (2006) Spontaneous pain, both neuropathic and inflammatory, is related to frequency of spontaneous firing in intact C-fiber nociceptors. J Neurosci 26:1281-1292.

Djouhri L, Lawson SN (2001) Differences in the size of the somatic action potential overshoot between nociceptive and non-nociceptive dorsal root ganglion neurones in the guinea-pig. Neuroscience 108:479-491.

Djouhri L, Lawson SN (1999) Changes in somatic action potential shape in guinea-pig nociceptive primary afferent neurones during inflammation in vivo. J Physiol 520:565-576.

Eliav E, Herzberg U, Ruda MA, Bennett GJ (1999) Neuropathic pain from an experimental neuritis of the rat sciatic nerve. Pain 83:169-182.

Fang X, McMullan S, Lawson SN, Djouhri L (2005) Electrophysiological differences between nociceptive and non-nociceptive dorsal root ganglion neurones in the rat in vivo. J Physiol 565:927-943.

Felson DT (2005) The sources of pain in knee osteoarthritis. Curr Opin Rheumatol 17:624-628.

Fukuoka T, Kobayashi K, Yamanaka H, Obata K, Dai Y, Noguchi K (2008) Comparative study of the distribution of the alpha-subunits of voltage-gated sodium channels in normal and axotomized rat dorsal root ganglion neurons. J Comp Neurol 510:188-206.

Fukuoka T, Noguchi K (2002) Contribution of the spared primary afferent neurons to the pathomechanisms of neuropathic pain. Mol Neurobiol 26:57-67.

Hanesch U, Pfrommer U, Grubb BD, Heppelmann B, Schaible HG (1993) The proportion of CGRP-immunoreactive and SP-mRNA containing dorsal root ganglion cells is increased by a unilateral inflammation of the ankle joint of the rat. Regul Pept 46:202-203.

Henry JL (2004) Molecular events of chronic pain: from neuron to whole animal in an animal model of osteoarthritis. Novartis Found Symp 260:139-145.

Hurley MV, Scott DL, Rees J, Newham DJ (1997) Sensorimotor changes and functional performance in patients with knee osteoarthritis. Ann Rheum Dis 56:641-648.

Ivanavicius SP, Ball AD, Heapy CG, Westwood FR, Murray F, Read SJ (2007) Structural pathology in a rodent model of osteoarthritis is associated with neuropathic pain: increased expression of ATF-3 and pharmacological characterisation. Pain 128:272-282.

Janusz MJ, Bendele AM, Brown KK, Taiwo YO, Hsieh L, Heitmeyer SA (2002) Induction of osteoarthritis in the rat by surgical tear of the meniscus: Inhibition of joint damage by a matrix metalloproteinase inhibitor. Osteoarthritis Cartilage 10:785-791.

Katz WA. (2001) Osteoarthritis: clinical presentations. In: Osteoarthritis: diagnosis and medical/surgical management (Moskowitz RW, Howell DS, Altman RD, Buckwalter JA, Goldberg V, eds), pp 231-238. W.B. Saunders.

Kean WF, Kean R, Buchanan WW (2004) Osteoarthritis: symptoms, signs and source of pain. Inflammopharmacology 12:3-31.

Kim YI, Na HS, Kim SH, Han HC, Yoon YW, Sung B, Nam HJ, Shin SL, Hong SK (1998) Cell type-specific changes of the membrane properties of peripherally-axotomized dorsal root ganglion neurons in a rat model of neuropathic pain. Neuroscience 86:301-309.

Lawson SN, Crepps BA, Perl ER (1997) Relationship of substance P to afferent characteristics of dorsal root ganglion neurones in guinea-pig. J Physiol 505:177-191.

Liu B, Eisenach JC (2005) Hyperexcitability of axotomized and neighboring unaxotomized sensory neurons is reduced days after perineural clonidine at the site of injury. J Neurophysiol 94:3159-3167.

Liu CN, Wall PD, Ben-Dor E, Michaelis M, Amir R, Devor M (2000) Tactile allodynia in the absence of C-fiber activation: altered firing properties of DRG neurons following spinal nerve injury. Pain 85:503-521.

Ma C, Shu Y, Zheng Z, Chen Y, Yao H, Greenquist KW, White FA, LaMotte RH (2003) Similar electrophysiological changes in axotomized and neighboring intact dorsal root ganglion neurons. J Neurophysiol 89:1588-1602.

Mach DB, Rogers SD, Sabino MC, Luger NM, Schwei MJ, Pomonis JD, Keyser CP, Clohisy DR, Adams DJ, O'Leary P, Mantyh PW (2002) Origins of skeletal pain: sensory and sympathetic innervation of the mouse femur. Neuroscience 113:155-166.

McDougall JJ, Watkins L, Li Z (2006) Vasoactive intestinal peptide (VIP) is a modulator of joint pain in a rat model of osteoarthritis. Pain 123:98-105.

Michaelis M, Liu X, Janig W (2000) Axotomized and intact muscle afferents but no skin afferents develop ongoing discharges of dorsal root ganglion origin after peripheral nerve

lesion. J Neurosci 20:2742-2748.

Moqrich A, Earley TJ, Watson J, Andahazy M, Backus C, Martin-Zanca D, Wright DE, Reichardt LF, Patapoutian A (2004) Expressing TrkC from the TrkA locus causes a subset of dorsal root ganglia neurons to switch fate. Nat Neurosci 7:812-818.

Nagakura Y, Okada M, Kohara A, Kiso T, Toya T, Iwai A, Wanibuchi F, Yamaguchi T (2003) Allodynia and hyperalgesia in adjuvant-induced arthritic rats: time course of progression and efficacy of analgesics. J Pharmacol Exp Ther 306:490-497.

Nakatsuka T, Park JS, Kumamoto E, Tamaki T, Yoshimura M (1999) Plastic changes in sensory inputs to rat substantia gelatinosa neurons following peripheral inflammation. Pain 82:39-47.

Newton RA, Bingham S, Davey PD, Medhurst AD, Piercy V, Raval P, Parsons AA, Sanger GJ, Case CP, Lawson SN (2000) Identification of differentially expressed genes in dorsal root ganglia following partial sciatic nerve injury. Neuroscience 95:1111-1120.

Nikolajsen L, Brandsborg B, Lucht U, Jensen TS, Kehlet H (2006) Chronic pain following total hip arthroplasty: a nationwide questionnaire study. Acta Anaesthesiol Scand 50:495-500.

Niv D, Gofeld M, Devor M (2003) Causes of pain in degenerative bone and joint disease: a lesson from vertebroplasty. Pain 105:387-392.

Obata K, Yamanaka H, Kobayashi K, Dai Y, Mizushima T, Katsura H, Fukuoka T, Tokunaga A, Noguchi K (2004) Role of mitogen-activated protein kinase activation in injured and intact primary afferent neurons for mechanical and heat hypersensitivity after spinal nerve ligation. J Neurosci 24:10211-10222.

Pitcher GM, Ritchie J, Henry JL (1999) Paw withdrawal threshold in the von Frey hair test is influenced by the surface on which the rat stands. J Neurosci Methods 87:185-193.

Pitcher GM, Yashpal K, Coderre TJ, Henry JL (1995) Mechanisms underlying antinociception provoked by heterosegmental noxious stimulation in the rat tail-flick test. Neuroscience 65:273-281.

Rausch O, Newton RA, Bingham S, Macdonald R, Case CP, Sanger GJ, Lawson SN, Reith AD (2000) Nerve injury-associated kinase: a sterile 20-like protein kinase up-regulated in dorsal root ganglia in a rat model of neuropathic pain. Neuroscience

101:767-777.

Romita VV, Henry JL (1996) Intense peripheral electrical stimulation differentially inhibits tail vs. limb withdrawal reflexes in the rat. Brain Res 720:45-53.

Sapunar D, Ljubkovic M, Lirk P, McCallum JB, Hogan QH (2005) Distinct membrane effects of spinal nerve ligation on injured and adjacent dorsal root ganglion neurons in rats. Anesthesiology 103:360-376.

Sarantopoulos CD, McCallum JB, Rigaud M, Fuchs A, Kwok WM, Hogan QH (2007) Opposing effects of spinal nerve ligation on calcium-activated potassium currents in axotomized and adjacent mammalian primary afferent neurons. Brain Res 1132:84-99.

Schaible HG, Schmidt RF (1985) Effects of an experimental arthritis on the sensory properties of fine articular afferent units. J Neurophysiol 54:1109-1122.

Schuelert N, McDougall JJ (2006) Electrophysiological evidence that the vasoactive intestinal peptide receptor antagonist VIP6-28 reduces nociception in an animal model of osteoarthritis. Osteoarthritis Cartilage 14:1155-1162.

Shakoor N, Agrawal A, Block JA (2008) Reduced lower extremity vibratory perception in osteoarthritis of the knee. Arthritis Rheum 59:117-121.

Sharma L (1999) Proprioceptive impairment in knee osteoarthritis. Rheum Dis Clin North Am 25:299-314.

Stebbing MJ, Eschenfelder S, Habler HJ, Acosta MC, Janig W, McLachlan EM (1999) Changes in the action potential in sensory neurones after peripheral axotomy in vivo. Neuroreport 10:201-206.

Villiere V, McLachlan EM (1996) Electrophysiological properties of neurons in intact rat dorsal root ganglia classified by conduction velocity and action potential duration. J Neurophysiol 76:1924-1941.

Woolf CJ, Shortland P, Coggeshall RE (1992) Peripheral nerve injury triggers central sprouting of myelinated afferents. Nature 355:75-78.

Wu Q, Henry JL (2009) Delayed onset of changes in soma action potential genesis in nociceptive A-beta DRG neurons in vivo in a rat model of osteoarthritis. Mol Pain 5:57.

Xie W, Strong JA, Meij JT, Zhang JM, Yu L (2005) Neuropathic pain: early spontaneous

afferent activity is the trigger. Pain 116:243-256.

Xu GY, Huang LY, Zhao ZQ (2000) Activation of silent mechanoreceptive cat C and Adelta sensory neurons and their substance P expression following peripheral inflammation. J Physiol 528:339-348.

Xu ZQ, Zhang X, Grillner S, Hokfelt T (1997) Electrophysiological studies on rat dorsal root ganglion neurons after peripheral axotomy: changes in responses to neuropeptides. Proc Natl Acad Sci U S A 94:13262-13266.

Zhang JM, Song XJ, LaMotte RH (1999) Enhanced excitability of sensory neurons in rats with cutaneous hyperalgesia produced by chronic compression of the dorsal root ganglion. J Neurophysiol 82:3359-3366.

# CHAPTER 3.

## Delayed onset of changes in soma action potential genesis in nociceptive A-beta DRG neurons in vivo in a rat model of osteoarthritis

**Authors:** Qi Wu, James L. Henry

**Corresponding author:** James L. Henry, Ph.D.
Michael G. DeGroote Institute for Pain Research and Care,
McMaster University,
1200 Main street West,
Hamilton, Ontario, Canada, L8N 3Z5,
Tel: +1-905-525-9140, extension 27704,
FAX: 905-522-8844,
E-mail address: jhenry@mcmaster.ca

This paper is published on Molecular Pain. Full citation of this paper is as follows:

Wu Q, Henry JL (2009) Delayed onset of changes in soma action potential genesis in nociceptive A-beta DRG neurons in vivo in a rat model of osteoarthritis. Mol Pain 5:57.

**Significance to thesis:**

This study demonstrated significant changes in electrophysiological properties in Aβ-fiber high-threshold mechanoreceptors (HTMs) at one month after unilateral derangement of the knee by cutting the ACL and removing the medial meniscus. These late onset changes, well beyond the time that changes in structure and in nociceptive scores appear, may relate to the episodes of intense pain that characterize advanced osteoarthritis (OA).

**Author's contribution:**

Qi Wu did the electrophysiological experiments, analyzed the data, performed statistical analyses, wrote the initial draft of the manuscript, and worked on refining this draft and the revision based on editorial review.

James L. Henry conceived of, designed, and coordinated the study. He also worked on refining this draft and the revision based on editorial review.

**Acknowledgments**

This work was generously supported by the Canadian Arthritis Network, the Canadian Institutes of Health Research and McMaster University. James L. Henry was Chair in Central Pain in the Faculty of Health Sciences, McMaster University. Qi Wu was a CIHR Strategic Training Fellow in Pain: Molecules to Community. The authors thank Mrs. Chang Ye for help in data input and statistical analysis. The authors are grateful to Dr. S. N. Lawson for expert guidance during the earliest stages of this project.

**Abstract**

Background: Clinical data on OA suggest widespread changes in sensory function that vary during the progression of OA. In previous studies on a surgically-induced animal model of OA we have observed that changes in structure and gene expression follow a variable trajectory over the initial days and weeks. To investigate mechanisms underlying changes in sensory function in this model, the present electrophysiological study compared properties of primary sensory nociceptive neurons at one and two months after model induction with properties in naïve control animals. Pilot data indicated no difference in C- or Aδ-fiber associated neurons and therefore the focus is on Aß-fiber nociceptive neurons.

Results: At one month after unilateral derangement of the knee by cutting the ACL and removing the medial meniscus, the only changes observed in Aß-fiber dorsal root ganglia (DRG) neurons were in nociceptor-like unresponsive neurons bearing a hump on the repolarization phase; these changes consisted of longer half width, reflecting slowed dynamics of action potential (AP) genesis, a depolarized resting membrane potential (Vm) and an increased AP amplitude. At two months, changes observed were in Aβ-fiber HTMs, which exhibited shorter AP duration at base and half width, shorter rise time and fall time, and faster maximum rising rate/maximum falling rate, reflecting accelerated dynamics of AP genesis.

Conclusions: These data indicate that Aß nociceptive neurons undergo significant changes that vary in time and occur later than changes in structure and in nociceptive scores in this surgically-induced OA model. Thus, if changes in Aβ-fiber nociceptive neurons in this model reflect a role in OA pain, they may relate to mechanisms underlying pain associated with advanced OA.

### 3.1. Background

OA afflicts an estimated 12-27% of adults over the age of 26 (Lawrence et al., 1998) and is characterized by alterations in sensory function, including pain (Wieland et al., 2005;Felson, 2005). Recently, a multi-center study led by Hawker et al. (2008) revealed two distinct types of OA pain: an early predictable dull, aching, throbbing "background" pain and an unpredictable short episode of intense pain that develops later (Hawker et al., 2008). During the progression of OA, pain evolves from the "background" pain that is use-related in early OA (Kidd, 2006). Later, this evolves into unpredictable short episodes of intense pain on top of the "background" pain in advanced OA. It is this unpredictable intense pain that has the greatest impact on the quality of life and that results in the avoidance of social and recreational activities (Hawker et al., 2008). Chronicity of OA (Oddis, 1996) suggests that this is a progressive disorder that develops longitudinally in time.

In addition to this clinical evidence, further evidence from animal models of OA supports the idea that nociception varies longitudinally and, as a result, different mechanisms may come into play at different times. To address mechanisms underlying these functional changes in OA we have been studying an animal model of OA that exhibits changes in cartilage and bone closely matching the human condition, including cartilage edema and collage turnover (Appleton et al., 2007a;McErlain et al., 2008) and

that demonstrates significant changes in gene expression of joint tissues (Appleton et al., 2007c). We have found that development of the typical changes that are observed may follow a variable trajectory (Appleton et al., 2007b). Some changes occur early but subside later in model development, including genes in the chemokine, endothelin and epidermal growth factor signaling pathways (Appleton et al., 2007a;Appleton et al., 2007c). Further, a recent study done in a surgically-induced OA model in the guinea pig has reported an augmentation in the joint movement-evoked discharge selectively in C-fibers at one week after model induction and in Aδ neurons at one day, one week and three weeks after model induction (Gomis et al., 2007). Importantly, the change in C-fibers is transient, and reverses by three weeks.

The fact that there is a progression of the pain and of nociceptive signals raises the possibility of a succession of mechanisms involved in changes in sensory function. Among the sites to investigate changes in the neural substrate of nociception is the DRG, which contains the cell bodies of primary sensory neurons that project from the periphery to the spinal cord. With the idea that a change in sensitivity or function of primary afferent neurons is reflected in the configuration of the AP in these neurons, we undertook a study to determine whether changes occur in DRG neurons following induction of OA in our rat model, whether changes observed followed any particular time course of development, and whether changes were associated with a particular functional

type of neuron. Several proposals have been made previously to account for the pain of OA, such as activation of sensitized nociceptive neurons in the knee (Niv et al., 2003;Kean et al., 2004;Felson, 2005). Nociceptive primary sensory neurons are those having receptive endings with a high stimulus threshold and that respond preferentially to noxious stimuli (Campbell JN et al., 1989). These nociceptive neurons actually conduct in all three velocity ranges of sensory neurons, C-, Aδ- and Aα/β, but in many studies are often considered to conduct only in the C- or Aδ-range of velocities, and Aα/β primary sensory neurons are generally thought to be only non-nociceptive. Our pilot data, however, did not reveal significant changes in AP configuration in C- or Aδ-fiber associated neurons, yet changes were seen in Aβ neurons (Wu and Henry, 2006).

A perusal of the literature indicates that there is a considerable number of nociceptive neurons that conduct in the Aβ range: approximately 12% of A-fibers innervating hairy skin in the monkey (Treede et al., 1998), 20% of Aβ-fibers in cats (Burgess and Perl, 1967;Koerber et al., 1988) and 30% of Aβ-fibers in rodents (Lynn and Carpenter, 1982;Djouhri et al., 1998;Fang et al., 2005;Ritter and Mendell, 1992). HTMs are the main type of A-fiber nociceptor, and the other two less common types are mechano-heat nociceptors, and mechano-cold nociceptors (Djouhri and Lawson, 2004;Treede et al., 1998). Moreover, A-fiber neurons have been suggested to be involved in models of chronic pain (Ossipov et al., 1999;Shir and Seltzer, 1990).

Therefore, the present study was done to identify any changes specifically in high threshold Aβ-fiber neurons, and to determine whether there is a progression of change in A-fiber nociceptors through early and later stages of the progression of the model. The present OA model was designed to mimic the most prevalent etiology in human knee OA, which is destabilization of the joint due to an injury (Creamer et al., 1998). Results from the present study suggest that following surgically-induced knee derangement nociceptive neurons in the Aβ range may undergo important changes in physiology. Changes in other types of primary sensory neuron in this model are the subject of other studies.

**3.2. Methods**

Experiments were done on female Sprague Dawley rats (180-225g) obtained from Charles River Inc. (St. Constant, QC, Canada). All protocols were approved by the McMaster University Animal Review Ethics Board and all experimental procedures conformed to the Guide to the Care and Use of Laboratory Animals of the Canadian Council of Animal Care, Vols.1 and 2. Upon completion of the acute electrophysiological experiment each animal was euthanized by an overdose of anesthetic.

3.2.1. Induction of the animal model of OA

The model of OA used was based on mechanical derangement of the knee (Henry, 2004). For surgical induction of the model, animals were anesthetized with a mixture of ketamine (100 mg/ml), xylazine (20 mg/ml) and acepromazine (10 mg/ml) – ketamine from Bioniche (Belleville, ON, Canada), xylazine from Bayer (Toronto, ON, Canada), acepromazine from Wyeth-Ayerst (Guelph, ON, Canada). The joint capsule was exposed and the tibial and medial ligament attachments of the medial meniscus were severed to allow removal of the meniscus. The ACL then became clearly visible and was cut. The incision was then sutured in two layers. Naive animals served as controls. Following the surgery, animals were sequentially given Trimel from Novopharm (Toronto, ON, Canada) 0.05ml once per day for 3 consecutive days, and the analgesic, Temgesic from Schering-Plough (Kenilworth, NJ, USA), twice per day for 2 consecutive days.

We have previously found that in this model, mild cartilage degeneration, such as surface discontinuity, is observed 2-4 weeks after surgery (Appleton et al., 2007b), yet severe cartilage degeneration, such as vertical fissure formation and chondrocytes clusters appears 8 weeks after surgery (Appleton et al., 2007b). Therefore, 2-4 weeks after knee surgery in the present OA model can be considered the initiation phase, whereas 8 weeks after surgery may represent a more advanced phase. To determine whether there would be temporal changes in electrophysiological properties of Aβ

nociceptive primary sensory neurons that would correlate with these phases, acute electrophysiological recordings were carried out at two time points, early, at 4 weeks, and late, at 8 or more weeks following the surgery. Recordings were not made at 2 weeks after surgery in OA rats to avoid any acute surgical effect on neuronal properties.

3.2.2. Animal preparation for acute electrophysiological recording

At one or two months after model induction each animal was initially anesthetized with the ketamine mixture described above. The right jugular vein was cannulated for i.v. infusion of drugs. An initial 1 mg/kg dose of pancuronium from Sandoz (Boucherville, QC, Canada) was given to eliminate muscle tone; the effect of pancuronium was allowed to wear off periodically (normally within one hour of pancuronium administration) in order to confirm a surgical level of anesthesia by observing the pupil for dilation and testing for reflex withdrawal from a pinch to a forelimb. Supplements of pentobarbital (CEVA SANTE ANIMALE, La Ballastière, Libourne, France; 20 mg/kg) and pancuronium (1/3 of the initial dose) were added every hour; this schedule of pentobarbital administration was confirmed to be effective in maintaining a surgical level of anesthesia in non-paralyzed control rats in our pilot study. An in-house servo-controlled infrared heating lamp maintained rectal temperature at approximately 37°C. The animals were mechanically ventilated (Model 683, Harvard Apparatus, QC, Canada); the ventilation parameters were adjusted to maintain the $CO_2$

concentration at approximately 40 mmHg using end-tidal CO2 monitoring (CapStar-100 End-Tidal $CO_2$ Analyzer, CWE, Ardmore, PA, USA).

The L4 DRG was selected for study. While $L_3$ and $L_4$ receive the most knee afferents (Salo and Theriault, 1997) our pilot studies suggested that not only knee afferents were changed in this model, but changes were also in neurons innervating neighboring territories. In addition, in some cases it was important to stimulate the sciatic nerve and, as the majority of $L_3$ afferents do not supply the sciatic nerve, the L4 DRG was selected for this study.

The rat was fixed in a stereotaxic frame and the vertebral column was rigidly clamped at the $L_2$ and $L_6$ vertebrae. The right femur was fixed by a customized clamp to avoid movements of the DRG during mechanical searching for peripheral receptive fields. Connective tissue over $L_4$ DRG was removed with care. Exposed spinal cord and DRG were covered with warm paraffin oil to prevent drying. Direct heating of the DRG by the light source for the surgical microscope was carefully avoided. A pair of bipolar platinum stimulating electrodes (FHC, Bowdoinham, ME, USA) was placed beneath the $L_4$ dorsal root that had been exposed and cut close to the spinal cord. The distance from the stimulation site (cathode) to the recording site (center of the DRG) was measured at the end of the experiment to determine the conductance distance and thereby calculate the

conduction velocity of the fibers associated with each DRG neuron recorded. This conduction distance was normally between 12 and 16 mm.

3.2.3. In vivo intracellular recording

The configuration of the AP is characteristic of each particular functional type of DRG neuron and thus can be used as one parameter for classification of each neuron recorded. For example, myelinated afferents that display a hump on the falling phase of the AP are considered to be nociceptors, while those that do not bear the hump innervate hairs, muscles, etc. and respond to innocuous stimulation (Koerber et al., 1988;Rose et al., 1986). Nociceptive neurons also exhibit other electrophysiological features, such as a broad AP duration, a relatively large AP amplitude and a long AHP duration (Fang et al., 2005). Changes in the physiology of DRG neurons can be identified through changes in AP configuration. Thus, AP configuration was compared between control and model animals with the aim to identify changes in physiological properties of the neurons.

Thus, APs were obtained by intracellular recordings from somata in the DRG using micropipettes fabricated from filament-containing borosilicate glass tubing (1.2 mm outer diameter, 0.68 mm inner diameter; Harvard Apparatus, Holliston, MA, USA). The electrodes were pulled using a Brown-Flaming puller (Model P-87; Sutter Instrument Co., Novota, CA, USA) and filled with a 3 M KCl solution (DC resistance: about 40-70MΩ).

During the acute electrophysiological experiment the microelectrode was advanced using an EXFO IW-800 micromanipulator (EXFO, Montreal, QC, Canada) until a hyperpolarization of at least -40 mV suddenly occurred and an AP could be evoked by stimulation of the dorsal root; APs were recorded with a Multiclamp 700B amplifier (Molecular Devices, Union City, CA, USA) and digitized on-line via a Digidata 1322A interface (Molecular Devices) with pClamp 9.2 software (Molecular Devices).

Measurement of electrophysiological parameters has been reported previously (Kim et al., 1998;Djouhri et al., 1998). These include conduction velocity (CV), Vm, action potential duration (APD), AP duration at half AP amplitude (AP half width), AP amplitude, AP rise time, AP fall time, maximum rising rate (MRR), maximum falling rate (MFR), AHP amplitude, AHP50 and AHP80. Each of these parameters reflects a different mechanism contributing to the electrical properties of the neuron. Analysis was done offline using pClamp 9.2.

3.2.4. Classification of dorsal root ganglion neurons

The criteria for neuron classification based on conduction velocity followed those reported in a previous *in vivo* study, in which Aβ-fiber conduction velocity was defined as greater than 6.5 m/s along the dorsal root in female Wistar rats (Fang et al., 2005). We adopted this criterion because it most closely applied to the present studies compared with criteria from other labs (Leem et al., 1993;Handwerker et al., 1991;Ritter and

Mendell, 1992), including the same gender (female), a comparable age at experiment (~ 160 g in Lawson's vs. ~ 250 g in ours), similar recording temperature due to similar surgical exposure, heating strategy and core temperature set-point.

The sensory receptive properties of DRG neurons were identified using specific mechanical stimuli, and classified as previously described (Fang et al., 2005) and as outlined below. HTMs were considered to be nociceptive neurons if they were activated by high intensity stimuli such as pinch or squeeze applied with a fine or coarse-toothed forceps, or a sharp object such as the tip of a syringe needle. Neurons included in this study did not show a response evoked by innocuous stimuli such as gentle pressure or brush with a camel hair brush.

Some neurons were the so-called "unresponsive neurons". These have been identified in earlier studies as those neurons that are not excited by any of the non-noxious or noxious mechanical stimuli listed above (Lawson et al., 1997). Among these, some might be nociceptive neurons based on the fact that they had a prominent inflection on the repolarization phase of the AP in differentiated recordings, which is considered to be a feature unique to nociceptive neurons (Caffrey et al., 1992;Ritter and Mendell, 1992) and which has been adopted as a criterion to differentiate nociceptive neurons from non-nociceptive neurons in *in vitro* electrophysiological studies where

sensory property testing is not possible (Ma et al., 2003;Stebbing et al., 1999;Koerber et al., 1988;Ritter and Mendell, 1992).

3.2.5. Acceptance criteria

All neurons included in this study met the following criteria: they exhibited an evoked AP from dorsal root stimulation, had a Vm more negative than -40 mV and had an AP amplitude larger than 40 mV. In addition, for each neuron, before sensory testing was begun a continuous recording was obtained for ≥5 min after electrode penetration; only those neurons that maintained a stable Vm throughout recording and sensory testing are included in this report.

3.2.6. Statistical analysis

The D'Agostino and Pearson omnibus test was carried out to determine normality of the electrophysiological data. In addition, wherever appropriate, one way analysis of variance (ANOVA) with Newman-Keuls post test or non-parametric Kruskal-Wallis test with Dunn's post test was used for comparison of parameters in control animals and at both stages of development of the OA model. *Fisher*'s exact test was used to analyze count data. Statistical tests and graphing were done using Prism 4 software (GraphPad, La Jolla, CA, USA), and $P < 0.05$ was considered to be significant.

**3.3. Results**

All neurons included in this study were Aβ nociceptive neurons judged by sensory testing and by AP features. Electrophysiological properties of Aβ-fiber HTMs in control animals were comparable to those that have been reported from other research groups for this type of neuron (Djouhri et al., 1998;Fang et al., 2005;Koerber et al., 1988;Ritter and Mendell, 1992). Successful recordings that met the acceptance criteria were from a total of 23 neurons from 17 control animals and 47 neurons from 19 OA model animals. Following the criteria of Lawson et al. (1997) these were further differentiated into the following groups: Aβ-fiber nociceptor-like unresponsive neurons at one-month after model induction ($N$ = 14), Aβ-fiber HTMs at one-month after model induction ($N$ = 18) and Aβ-fiber HTMs at two months after model induction ($N$ = 15). Very few Aβ-fiber nociceptor-like unresponsive neurons were observed in two-month OA animals. Therefore, no separate group was formed based on this type of neuron.

3.3.1. Aβ-fiber nociceptor-like unresponsive neurons and Aβ-fiber HTMs

Typical examples of an Aβ-fiber HTM and of an Aβ-fiber nociceptor-like unresponsive neuron are illustrated in Figure 3.1. Note the prominent inflection observed in the representative Aβ-fiber nociceptor-like unresponsive neuron shown in Figure 3.1. (B,E). This is consistent with earlier reports on this type of neuron from other laboratories and characterizes nociceptive neurons as described above (Caffrey et al., 1992;Koerber et al., 1988;Ritter and Mendell, 1992;Rose et al., 1986).

The grouping of Aβ-fiber nociceptor-like unresponsive neurons might be heterogeneous having a mixture of nociceptive and non-nociceptive neurons. However, this is the only group that might include hypothetical axotomized neurons. The proportion of Aβ-fiber nociceptor-like unresponsive neurons in all unresponsive neurons was compared in the control vs. OA groups, and was 6 out of 21 neurons (28.6%) in control and 14 out of 31 neurons (45.2%) in OA animals at one month. This seemly large increase in the proportion of Aβ-fiber nociceptor-like unresponsive neurons in OA was not significantly different ($P$ = 0.26). Let us assume that nociceptor-like unresponsive neurons are actual nociceptors. Next, we calculated the proportion of "unresponsive nociceptors" in the nociceptor population between OA and control animals. Again, there was no difference in this proportion: 6 out of 29, 20.7% in control vs. 14 out of 32, 43.8% in one month OA (P = 0.064). In conclusion, our observation was insufficient to substantiate an increase in the number of nociceptor-like unresponsive neurons in OA.

All Aβ-fiber HTMs in the present study were recorded from $L_4$ DRG. Receptive fields of these neurons encompassed every major compartment of the ipsilateral lower limb: from knee joint ($N$ = 3 each in control, OA at one month and OA at two months), from ankle joint ($N$ = 3 in control, 2 in OA at one month, and 1 in OA at two months), from the leg (N = 5 in control, 1 in OA at one month, and 3 in OA at two months), from

calf ($N$ = 1 in control, none in OA at one month, and 1 in OA at two months), and from foot ($N$ = 11 in control, 12 in OA at one month, and 4 in OA at two months). There were two general observations. First, most Aβ-fiber HTMs innervated deep tissues, such as joint, muscle and/or periosteum of the leg, and deep tissue of the foot. Second, the foot receives a rich innervation from Aβ-fiber HTMs with a comparable distribution in either hairy or glabrous skin.

3.3.2. Changes in Aβ-fiber nociceptor-like unresponsive neurons and HTMs at one month

To examine the possible effects of direct nerve damage on AP configuration in the OA model, we compared Aβ-fiber nociceptor-like unresponsive neurons at one month OA with naïve control Aβ-fiber HTMs. Aβ-fiber nociceptor-like unresponsive neurons were the primary type significantly altered in AP configuration at one month. In these neurons, Vm was significantly depolarized compared with values from naïve controls (-56.3 ± 1.23 mV, $N$ = 13 in OA and -64.7 ± 1.71 mV, $N$ = 23 in control; $P$ = 0.002; Figure 3.2. A). However, in this early phase of the model no change in Vm was observed in Aβ-fiber HTMs (Table 1).

AP amplitude is the net effect of depolarization and rectification forces, and was significantly less in nociceptive neurons of OA animals. At one month of the model no difference in AP amplitude was observed in Aβ-fiber HTMs. In Aβ-fiber nociceptor-like unresponsive neurons in OA animals, AP amplitude was 84.0 ± 2.33 mV

($N = 14$). This is 11.5 mV more hyperpolarized than that of the Aβ-fiber HTMs in naïve control animals, which was 72.5 ± 2.04 mV ($N = 23$; $P = 0.001$; Figure 3.2. B).

APD reflects the net effect of overall ion flow. This did not differ in either type of nociceptive neuron between control and model animals at one month after model induction (Figure 3.3. A). Compared with the control animals, a significantly longer AP half width was found in Aβ-fiber nociceptor-like unresponsive neurons in OA model animals (1.0 ± 0.09 ms, $N = 14$ vs. 0.8 ± 0.05 ms, $N = 23$ in control; $P = 0.027$; Figure 3.3. B).

AP rise time is taken as a measure of the time for depolarization from baseline to peak and largely reflects $Na^+$ flux. No difference in AP rise time was found in Aβ-fiber HTMs or in Aβ-fiber nociceptor-like unresponsive neurons at one month after model induction (data not shown). MRR, used as an additional measure of the dynamics of depolarization, was derived by mathematical conversion of the AP waveform as the differentiated derivative of the AP. Thus, the curve represents the rate of voltage change over time. MRR reflects the maximum depolarization driving force, mostly generated by sodium influx current. MRR in Aβ-fiber HTMs in OA animals was not significantly different from control values (Table 1).

A similar rationale was adopted to determine the dynamics of repolarisation, where AP fall time and MFR were used as measures of the dynamics of the repolarisation

phase of the AP. Significant differences in AP fall time and MFR were not seen between control and OA animals in Aβ-fiber HTMs or nociceptor-like unresponsive neurons (Table 1).

Basically, there are three types of AHP following the spike – a fast AHP (immediate activation during the spike having a duration of several tens of milliseconds), a medium AHP (immediate activation during the spike having a duration of several hundreds of milliseconds) and a slow AHP (slow activation over hundreds of milliseconds having a duration of several seconds) (Sah and Faber, 2002). Different calcium-activated potassium channels underlie different AHPs, such as BK-type channels for fast AHP, SK-type channels for medium AHP (Sah and Faber, 2002). The AHP80 in control Aβ-fiber HTMs was 30.9 ± 4.9 ms ($N$ = 22), suggesting that the AHP in the present study was likely to be a fast AHP. However, none of the parameters of the AHP, including amplitude and duration, showed any difference between either OA Aβ-fiber HTMs or Aβ-fiber nociceptor-like unresponsive neurons and naive control Aβ-fiber HTMs, including duration or amplitude (Table 1).

Unlike the other parameters measured, which reflect properties of the soma, conduction velocity reflects properties of the axon. There were no statistically significant differences in conduction velocity between Aβ-fiber HTMs in controls vs.

Aβ-fiber HTMs or Aβ-fiber nociceptor-like unresponsive neurons in OA animals (Table 1).

3.3.3. Changes in Aβ-fiber HTMs at two months

At two months of model development, only a few Aβ-fiber nociceptor-like unresponsive neurons were recorded. Thus, the following data are from Aβ-fiber HTMs. Vm was similar in Aβ-fiber HTMs from control vs. model animals in this later phase of the model (Table 1). However, a significantly larger AP amplitude was seen in these neurons at this phase of model development (83.2 ± 2.40 mV, $N$ = 15) compared to controls (72.5 ± 2.04 mV, $N$ = 23; $P$ = 0.002; Figure 3.2. B).

APD was significantly shorter in the OA model rats at two months compared with the control rats (1.1 ± 0.09 ms, $N$ = 15 vs. 1.6 ± 0.11 ms, $N$ = 23 in control; $P$ = 0.007; Figure 3.3. A). AP half width was also significantly shorter in OA model rats in the late phase compared to control rats (0.6 ± 0.05 ms, $N$ = 15 vs. 0.8 ± 0.05 ms, $N$ = 23 in control; $P$ = 0.007; Figure 3.3. B).

As shown in Figure 3.4. (A), AP rise time was shorter in OA animals at two months of model development compared to control rats (0.5 ± 0.04 ms, $N$ = 15 vs. 0.7 ± 0.06 ms, $N$ = 23 in control; $P$ = 0.021). MRR was 350.4 ± 28.09 mV/ms ($N$ = 15) in Aβ-fiber HTMs in the late phase, which was significantly faster than the 339.1 ± 19.23 mV/ms ($N$ = 23) in control rats ($P$ = 0.002; Figure 3.4. B).

Similarly, as shown in Figure 3.5. (A), a significantly shorter AP fall time was observed in Aβ-fiber HTMs at two months compared to control rats (0.7 ± 0.05 ms, $N$ = 15 vs. 0.9 ± 0.05 ms, $N$ = 23 in control; $P$ = 0.004). Also, as shown in Figure 3.5. B, MFR was faster in the late phase OA animals compared to control rats (197.5 ± 14.66 mV/ms, $N$ = 15 vs. 135.7 ± 10.23 mV/ms, $N$ = 23 in control; P = 0.001).

In Aβ-fiber HTMs, there were no difference in conduction velocity or afterhyperpolarization (AHP) associated parameters between control and OA animals at two months (Table 1).

**3.4. Discussion**

The present study provides evidence that unilateral knee derangement induces changes in the AP recorded from Aβ-fiber nociceptive primary sensory neurons in the ipsilateral L4 DRG. Interestingly, the neuron types exhibiting changes differentiate into two groups, Aβ-fiber HTMs and Aβ-fiber nociceptor-like unresponsive neurons. These changes were also different in animals tested at two months after model induction vs. those tested at one month.

3.4.1. Rationale for model selection and control

Several types of animal models of OA exist, including those induced by modulation of gene (Munoz-Guerra et al., 2004) or protein expression (Johnson and Terkeltaub, 2004), injection of inflammatory cytokines (Hui et al., 2003) or injection of

photolytic enzymes (Kikuchi et al., 1998) as well as surgical induction (Liu et al., 2003) or excessive use of the joint (Pap et al., 1998). The model selected for the present study is a surgically-induced derangement of the knee of one hind leg; while OA can originate from a number of causes, injury is the most common (Creamer et al., 1998). We have shown that our OA model successfully mimic changes in cartilage and bone closely matching the human condition, including cartilage edema and collagen turnover (Appleton et al., 2007a;McErlain et al., 2008).

Controls for this study were naïve rats. Simple surgical exposure of the joint capsule, regardless of the size of the surgical exposure has been reported to cause joint instability (Hsu et al., 1997) and articular cartilage degeneration (Hsu et al., 2003), which would result in an unwanted comparison between severe and mild osteoarthritis. Even a surgical incision normally induces a brief inflammatory phase lasting only days (Rook et al., 2008;Baum and Arpey, 2005), but is fully repaired with scar tissue devoid of inflammatory infiltration by the end of the first month (Mitchell and Cotran, 2003).

3.4.2. Changes in neuronal physiology in model animals at one month

The changes at one month were observed only in Aβ-fiber nociceptor-like unresponsive neurons bearing a hump on the repolarization branch. The changes observed reflect greater excitability, such as a relatively depolarized resting membrane potential and increased AP amplitude, as well as slowed dynamics of AP genesis,

illustrated as longer AP half width. These changes might be able to be explained by nerve injury.

The in vivo intracellular recording technique is a sensitive means of identifying changes in intact neurons, but is less sensitive in differentiating between axotomised neurons from otherwise unresponsive neurons. If the receptive field of a neuron cannot be identified, there are two possibilities: either the neuron is axotomised or its receptive field is not sufficiently activated. The unresponsive neuron group might thus be heterogeneous. They could be neurons with a very high stimulation threshold, neurons with inaccessible receptive fields, neurons unexcitable from any receptive field, neurons that are only responsive to chemical stimuli (Djouhri et al., 1998), or neurons that have lost their receptive fields due to axotomy. Our OA model involves transection of the ACL, which is innervated mostly by large size neurons from L7 (main sciatic nerve root) and L5-6 (main femoral nerve roots) in cats (Haus and Halata, 1990), as well as removal of the medial meniscus for which the anterior and posterior horns are highly innervated by several different mechanoreceptors (Assimakopoulos et al., 1992;O'Connor and McConnaughey, 1978). As both structures are innervated, following surgery mechanical derangement of the joint may be accompanied by nerve trauma and may represent a source of pain (Michaelis et al., 2000).

Moreover, Aβ-fiber nociceptor-like unresponsive neurons were the only group that could include hypothetical axotomised nociceptors. The time course of the earliest irreversible stage of DRG neuron death following axotomy, peaks at two weeks, and continues to lead to the elimination of neurons, which peaks at one to two months (McKay et al., 2002). The fact that this type of neuron was rarely encountered in model animals studied at two months after model induction in the present study (data not shown) might agree with the marked apoptosis of DRG neurons by two months (McKay et al., 2002).

3.4.3. Changes in neuronal physiology in model animals at two months

The changes at two months after model induction were quite different from those at one month. The major changes reported here occur at two months or more after model induction; changes at one month are relatively minor compared to the later changes. Changes at this more advanced phase of OA reflected accelerated rather than slowed dynamics of AP genesis, including shorter APD and AP half width, shorter AP rise time and fall time, and faster MRR and MFR. The diverse changes in AP configuration in Aβ-fiber nociceptive neurons at different phases of OA might be attributed to transcriptional regulation of a variety of ion channels by neurotrophic factors (Lesser et al., 1997) and/or other inflammatory mediators. Our previous microarray data indicate a dynamic change in gene expression during the progression of the model, which involves

cytokine, chemokine, and growth factor signaling pathways (Appleton et al., 2007c). However, detailed pathways leading to the specific changes are simply unknown at present. These changes in sensory neurons over such a prolonged period of time suggest that studies on sensory neuron changes in animal models should include later time points in model induction. Moreover, it is possible that these late-developing changes in sensory neurons may relate in some way to the types of pain associated with more advanced OA in humans (Hawker et al., 2008).

3.4.4. Conclusions

Results from the present study suggest that Aß nociceptive neurons undergo changes in this surgically-induced model of OA. If these changes are representative of changes in injury-induced joint OA, these neurons may play an important role in OA pain. Importantly, there is a late onset of electrophysiological changes in these neurons, well beyond the time that changes in structure and in nociceptive scores appear, and these may relate to the episodes of intense pain that characterize advanced OA.

## 3.5. Tables, Figures

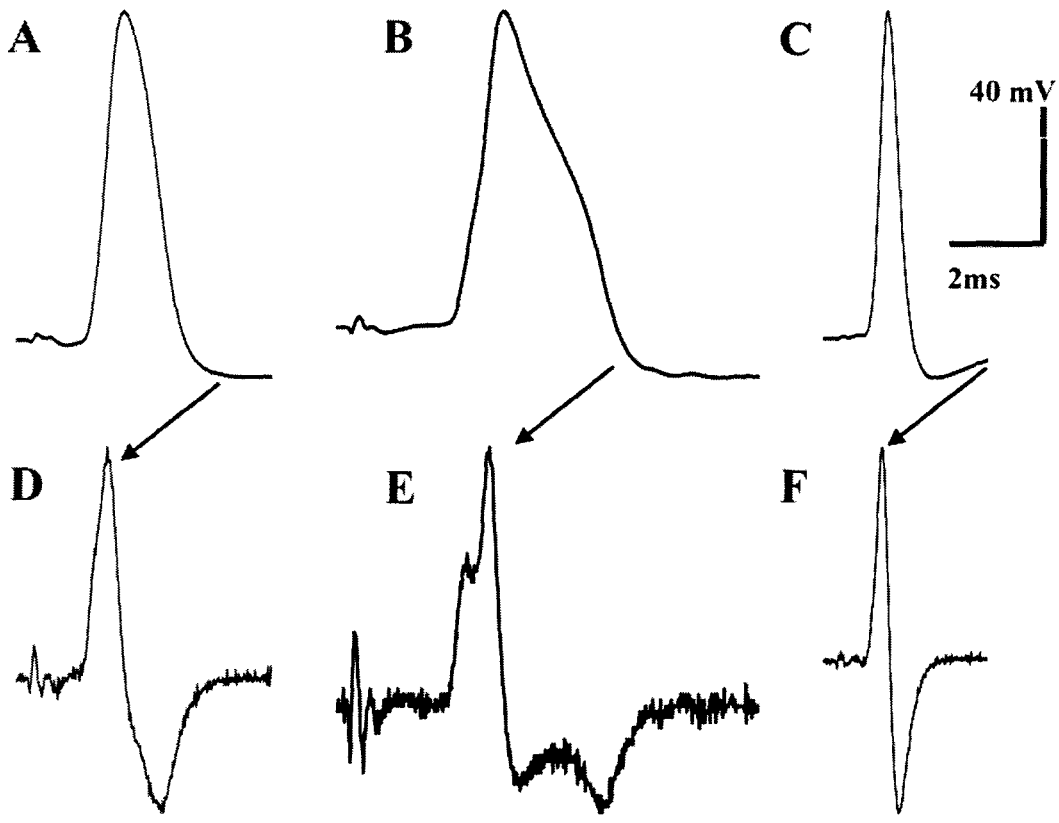


**Figure 3.1 - Representative APs evoked in Aβ nociceptive neurons by dorsal root stimulation.** **A-C**, evoked APs; D-F, differentiated derivatives of these APs to determine rate of change. **A** and **D** are from a nociceptive neuron that could be activated only by high intensity stimuli, including firm pinch applied to the ankle joint; conduction velocity was 12.4 m/s. **B** and **E** are from an unresponsive neuron classified as an Aβ fiber on the basis of conduction velocity, which was 8 m/s, and a plateau was identified on the repolarisation branch of the AP in the differentiated recording, which is

indicative of a nociceptive neuron. **C** and **F** are from another unresponsive neuron, with a conduction velocity of 18.8 m/s, but with no inflection on the falling phase in the differentiated recording, which is considered a non-nociceptive neuron.

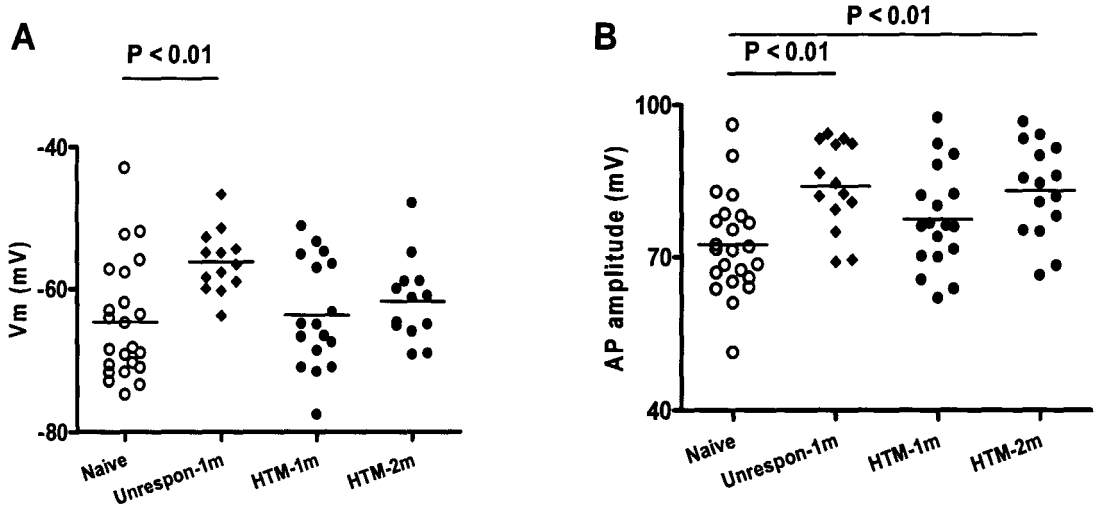


**Figure 3.2 - Resting membrane potential (Vm) and action potential (AP) amplitude in Aβ nociceptive DRG neurons in osteoarthritis (OA) animals at one month and at two months, and in naïve control animals.** "Naive" represents Aβ-fiber HTMs in control animals. "Unrespon" represents nociceptor-like Aβ-fiber unresponsive neurons in one month OA animals; an inflection on the falling phase of the differentiated recording was used to classify these neurons (Caffrey et al., 1992;Ritter and Mendell, 1992). "HTM-1m" and "HTM-2m" represent Aβ-fiber HTMs from the OA group tested one month or two months after model induction, respectively. One way ANOVA with Newman-Keuls post-hoc test was used for multiple comparisons among "Naive" (N = 23), "Unrespon" (N = 13 for Vm and N = 14 for AP amplitude), "HTM-1m" (N = 17 for Vm and N = 18 for AP amplitude), "HTM-2m" (N = 13 for Vm and N = 15 for AP amplitude). In each case the mean (horizontal line) is presented.

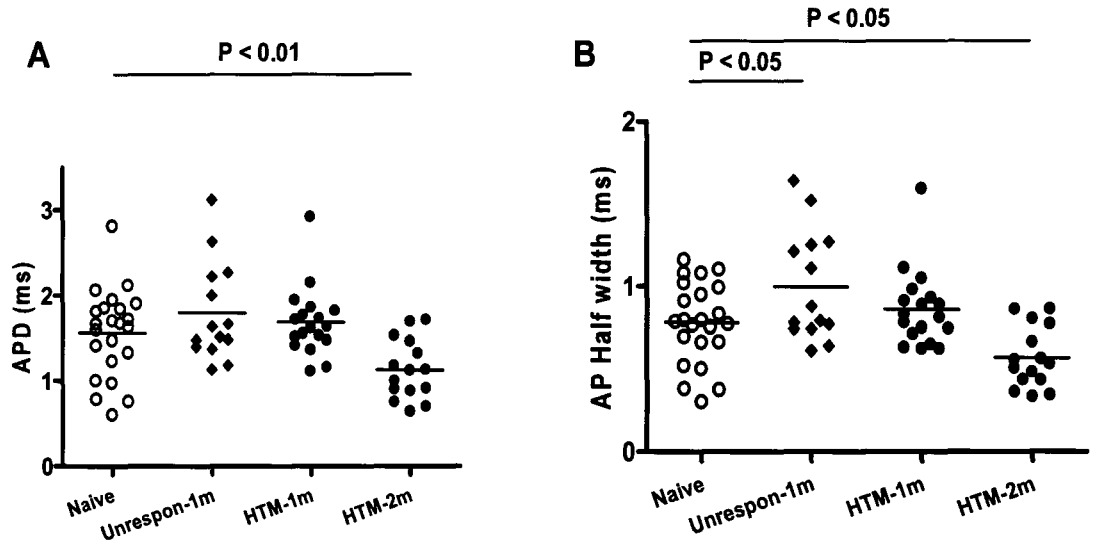


**Figure 3.3 - Action potential duration at base (APD) and AP width at half amplitude (AP half width) in Aβ nociceptive DRG neurons in OA animals at one month and at two months, and in naïve control animals.** Labeling is otherwise the same as in Figure 3.2. One-way ANOVA with Newman-Keuls post test was used for multiple comparisons among groups as follows: "Naive" (N = 23), "Unrespon" (N = 14), "HTM-1m" (N = 18) and "HTM-2m" (N = 15).

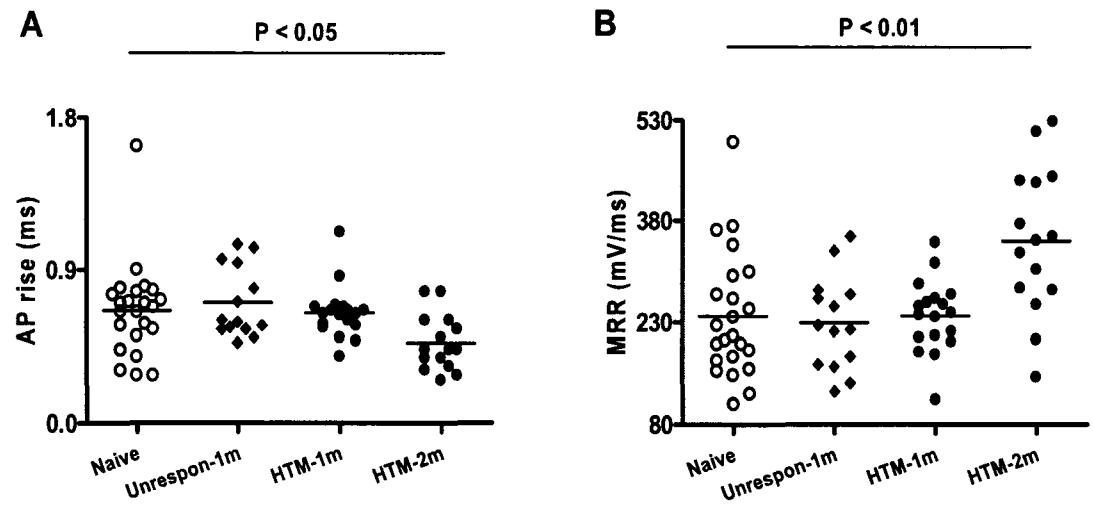


**Figure 3.4 - Action potential rise time (AP rise) and maximum rising rate (MRR) in Aβ nociceptive DRG neurons in OA animals at one month and at two months, and in control animals.** Labeling is otherwise the same as in Figure 3.2. Kruskal-Wallis test with Dunn's post test was used for multiple comparisons among "Naive" (N = 23), "Unrespon" (N = 14), "HTM-1m" (N = 18) and "HTM-2m" (N = 15).

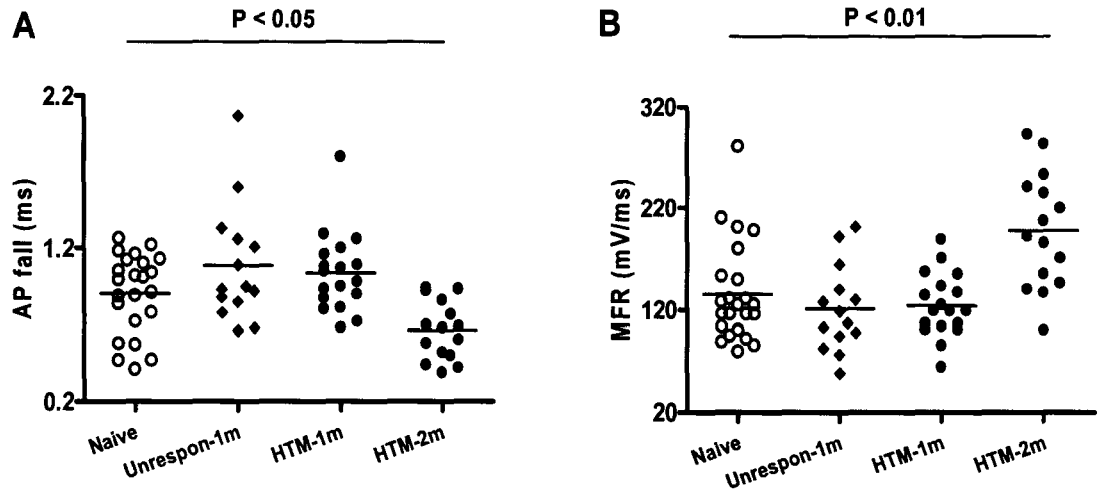


**Figure 3.5 - Changes in action potential fall time (AP fall) and maximum falling rate (MFR) in Aβ nociceptive DRG neurons in OA animals at one month and two months, and in naïve control animals.** Labeling is otherwise the same as in Figure 3.2. Kruskal-Wallis test with Dunn's post test was used for multiple comparisons among the "Naive" (N = 23), "Unrespon" (N = 14), "HTM-1m" (N = 18) and "HTM-2m" (N = 15).

**Table 3.1. Properties of all the nociceptive DRG neurons recorded in control and osteoarthritis animals**

| Parameter | Naïve | Unrespon-1m | HTM-1m | HTM-2m |
|---|---|---|---|---|
| **Vm (mV)** | -64.66 ± 1.71, $N = 23$ | -56.25 ± 1.23, $N = 13$ | -63.65 ± 1.85, $N = 17$ | -61.72 ± 1.62, $N = 13$ |
| **Amplitude (mV)** | 72.47 ± 2.04, $N = 23$ | 84.01 ± 2.33, $N = 14$ | 77.52 ± 2.35, $N = 18$ | 83.19 ± 2.4, $N = 15$ |
| **APD (ms)** | 1.56 ± 0.11, $N = 23$ | 1.79 ± 0.16, $N = 14$ | 1.68 ± 0.1, $N = 18$ | 1.13 ± 0.09, $N = 15$ |
| **Half width (ms)** | 0.78 ± 0.05, $N = 23$ | 1 ± 0.09, $N = 14$ | 0.86 ± 0.06, $N = 18$ | 0.56 ± 0.05, $N = 15$ |
| **Rise time (ms)** | 0.66 ± 0.06, $N = 23$ | 0.71 ± 0.06, $N = 14$ | 0.64 ± 0.04, $N = 18$ | 0.47 ± 0.04, $N = 15$ |
| **MRR (mV/ms)** | 239.1 ± 19.23, $N = 23$ | 228.8 ± 18.52, $N = 14$ | 239.1 ± 12.49, $N = 18$ | 350.4 ± 28.09, $N = 15$ |
| **Fall time (ms)** | 0.9 ± 0.05, $N = 23$ | 1.09 ± 0.1, $N = 14$ | 1.04 ± 0.06, $N = 18$ | 0.66 ± 0.05, $N = 15$ |
| **MFR (mV/ms)** | 135.7 ± 10.23, $N = 23$ | 121.1 ± 11.29, $N = 14$ | 124.3 ± 7.33, $N = 18$ | 197.5 ± 14.66, $N = 15$ |
| **AHP (mV)** | 10.7 ± 0.68, $N = 23$ | 11.78 ± 1.05, $N = 13$ | 12.19 ± 0.69, $N = 15$ | 10.11 ± 0.71, $N = 14$ |
| **AHP80 (ms)** | 30.95 ± 5, $N = 22$ | 35.9 ± 7.46, $N = 13$ | 34.71 ± 4.82, $N = 15$ | 21.01 ± 4.92, $N = 14$ |
| **AHP50 (ms)** | 8.99 ± 1.29, $N = 22$ | 9.6 ± 1.73, $N = 13$ | 8.67 ± 1.48, $N = 15$ | 5.71 ± 1.62, $N = 14$ |
| **CV (mm/ms)** | 14.1 ± 1, $N = 23$ | 11.69 ± 0.8, $N = 14$ | 13.24 ± 0.66, $N = 18$ | 16.38 ± 1.42, $N = 15$ |

"Naive" represents Aβ-fiber HTMs in control animals. "Unrespon-1m" represents nociceptior-like Aβ-fiber unresponsive neurons in one month OA animals. "HTM-1m" and "HTM-2m" represent Aβ-fiber HTMs from the OA group tested one month or two

months after model induction, respectively. Values are presented as mean ± S.E.M. "N" represents the number of neurons.

**References**

Appleton CT, McErlain DD, Henry JL, Holdsworth DW, Beier F (2007a) Molecular and histological analysis of a new rat model of experimental knee osteoarthritis. Ann N Y Acad Sci 1117:165-174.

Appleton CT, McErlain DD, Pitelka V, Schwartz N, Bernier SM, Henry JL, Holdsworth DW, Beier F (2007b) Forced mobilization accelerates pathogenesis: characterization of a preclinical surgical model of osteoarthritis. Arthritis Res Ther 9:R13.

Appleton CT, Pitelka V, Henry J, Beier F (2007c) Global analyses of gene expression in early experimental osteoarthritis. Arthritis Rheum 56:1854-1868.

Assimakopoulos AP, Katonis PG, Agapitos MV, Exarchou EI (1992) The innervation of the human meniscus. Clin Orthop Relat Res232-236.

Baum CL, Arpey CJ (2005) Normal cutaneous wound healing: clinical correlation with cellular and molecular events. Dermatol Surg 31:674-686.

Burgess PR, Perl ER (1967) Myelinated afferent fibres responding specifically to noxious stimulation of the skin. J Physiol 190:541-562.

Caffrey JM, Eng DL, Black JA, Waxman SG, Kocsis JD (1992) Three types of sodium channels in adult rat dorsal root ganglion neurons. Brain Res 592:283-297.

Campbell JN, Raja SN, Cohen RH, Manning DC, Meyer RA (1989) Peripheral neuronal mechanisms of nociception. In: Textbook of pain (Wall PD, Melzack R, eds), pp 22-45. London: Churchill Livingstone.

Creamer P, Lethbridge-Cejku M, Hochberg MC (1998) Where does it hurt? Pain localization in osteoarthritis of the knee. Osteoarthritis Cartilage 6:318-323.

Djouhri L, Bleazard L, Lawson SN (1998) Association of somatic action potential shape with sensory receptive properties in guinea-pig dorsal root ganglion neurones. J Physiol 513:857-872.

Djouhri L, Lawson SN (2004) Abeta-fiber nociceptive primary afferent neurons: a review of incidence and properties in relation to other afferent A-fiber neurons in mammals. Brain Res Brain Res Rev 46:131-145.

Fang X, McMullan S, Lawson SN, Djouhri L (2005) Electrophysiological differences between nociceptive and non-nociceptive dorsal root ganglion neurones in the rat in vivo. J Physiol 565:927-943.

Felson DT (2005) The sources of pain in knee osteoarthritis. Curr Opin Rheumatol 17:624-628.

Gomis A, Miralles A, Schmidt RF, Belmonte C (2007) Nociceptive nerve activity in an experimental model of knee joint osteoarthritis of the guinea pig: effect of intra-articular hyaluronan application. Pain 130:126-136.

Handwerker HO, Kilo S, Reeh PW (1991) Unresponsive afferent nerve fibres in the sural nerve of the rat. J Physiol 435:229-242.

Haus J, Halata Z (1990) Innervation of the anterior cruciate ligament. Int Orthop 14:293-296.

Hawker GA, Stewart L, French MR, Cibere J, Jordan JM, March L, Suarez-Almazor M, Gooberman-Hill R (2008) Understanding the pain experience in hip and knee osteoarthritis--an OARSI/OMERACT initiative. Osteoarthritis Cartilage 16:415-422.

Henry JL (2004) Molecular events of chronic pain: from neuron to whole animal in an animal model of osteoarthritis. Novartis Found Symp 260:139-145.

Hsu HC, Luo ZP, Cofield RH, An KN (1997) Influence of rotator cuff tearing on glenohumeral stability. J Shoulder Elbow Surg 6:413-422.

Hsu HC, Luo ZP, Stone JJ, Huang TH, An KN (2003) Correlation between rotator cuff tear and glenohumeral degeneration. Acta Orthop Scand 74:89-94.

Hui W, Rowan AD, Richards CD, Cawston TE (2003) Oncostatin M in combination with tumor necrosis factor alpha induces cartilage damage and matrix metalloproteinase expression in vitro and in vivo. Arthritis Rheum 48:3404-3418.

Johnson K, Terkeltaub R (2004) Upregulated ank expression in osteoarthritis can promote both chondrocyte MMP-13 expression and calcification via chondrocyte extracellular PPi excess. Osteoarthritis Cartilage 12:321-335.

Kean WF, Kean R, Buchanan WW (2004) Osteoarthritis: symptoms, signs and source of pain. Inflammopharmacology 12:3-31.

Kidd BL (2006) Osteoarthritis and joint pain. Pain 123:6-9.

Kikuchi T, Sakuta T, Yamaguchi T (1998) Intra-articular injection of collagenase induces experimental osteoarthritis in mature rabbits. Osteoarthritis Cartilage 6:177-186.

Kim YI, Na HS, Kim SH, Han HC, Yoon YW, Sung B, Nam HJ, Shin SL, Hong SK (1998) Cell type-specific changes of the membrane properties of peripherally-axotomized dorsal root ganglion neurons in a rat model of neuropathic pain. Neuroscience 86:301-309.

Koerber HR, Druzinsky RE, Mendell LM (1988) Properties of somata of spinal dorsal root ganglion cells differ according to peripheral receptor innervated. J Neurophysiol 60:1584-1596.

Lawrence RC, Helmick CG, Arnett FC, Deyo RA, Felson DT, Giannini EH, Heyse SP, Hirsch R, Hochberg MC, Hunder GG, Liang MH, Pillemer SR, Steen VD, Wolfe F (1998) Estimates of the prevalence of arthritis and selected musculoskeletal disorders in the United States. Arthritis Rheum 41:778-799.

Lawson SN, Crepps BA, Perl ER (1997) Relationship of substance P to afferent characteristics of dorsal root ganglion neurones in guinea-pig. J Physiol 505:177-191.

Leem JW, Willis WD, Chung JM (1993) Cutaneous sensory receptors in the rat foot. J Neurophysiol 69:1684-1699.

Lesser SS, Sherwood NT, Lo DC (1997) Neurotrophins differentially regulate voltage-gated ion channels. Mol Cell Neurosci 10:173-183.

Liu W, Burton-Wurster N, Glant TT, Tashman S, Sumner DR, Kamath RV, Lust G, Kimura JH, Cs-Szabo G (2003) Spontaneous and experimental osteoarthritis in dog: similarities and differences in proteoglycan levels. J Orthop Res 21:730-737.

Lynn B, Carpenter SE (1982) Primary afferent units from the hairy skin of the rat hind limb. Brain Res 238:29-43.

Ma C, Shu Y, Zheng Z, Chen Y, Yao H, Greenquist KW, White FA, LaMotte RH (2003) Similar electrophysiological changes in axotomized and neighboring intact dorsal root ganglion neurons. J Neurophysiol 89:1588-1602.

McErlain DD, Appleton CT, Litchfield RB, Pitelka V, Henry JL, Bernier SM, Beier F,

Holdsworth DW (2008) Study of subchondral bone adaptations in a rodent surgical model of OA using in vivo micro-computed tomography. Osteoarthritis Cartilage 16:458-469.

McKay HA, Brannstrom T, Wiberg M, Terenghi G (2002) Primary sensory neurons and satellite cells after peripheral axotomy in the adult rat: timecourse of cell death and elimination. Exp Brain Res 142:308-318.

Michaelis M, Liu X, Janig W (2000) Axotomized and intact muscle afferents but no skin afferents develop ongoing discharges of dorsal root ganglion origin after peripheral nerve lesion. J Neurosci 20:2742-2748.

Mitchell RN, Cotran RS (2003) Tissue repair: Cell regeneration and fibrosis. In: Robbins and Cotran: Pathologic Basis of Disease (Kumar V, Cotran RS, Robbins SL, eds), pp 61-78. Philadelphia: ELSEVIER SAUNDERS.

Munoz-Guerra MF, gado-Baeza E, Sanchez-Hernandez JJ, Garcia-Ruiz JP (2004) Chondrocyte cloning in aging and osteoarthritis of the hip cartilage: morphometric analysis in transgenic mice expressing bovine growth hormone. Acta Orthop Scand 75:210-216.

Niv D, Gofeld M, Devor M (2003) Causes of pain in degenerative bone and joint disease: a lesson from vertebroplasty. Pain 105:387-392.

O'Connor BL, McConnaughey JS (1978) The structure and innervation of cat knee menisci, and their relation to a "sensory hypothesis" of meniscal function. Am J Anat 153:431-442.

Oddis CV (1996) New perspectives on osteoarthritis. Am J Med 100:10S-15S.

Ossipov MH, Bian D, Malan TP, Jr., Lai J, Porreca F (1999) Lack of involvement of capsaicin-sensitive primary afferents in nerve-ligation injury induced tactile allodynia in rats. Pain 79:127-133.

Pap G, Eberhardt R, Sturmer I, Machner A, Schwarzberg H, Roessner A, Neumann W (1998) Development of osteoarthritis in the knee joints of Wistar rats after strenuous running exercise in a running wheel by intracranial self-stimulation. Pathol Res Pract 194:41-47.

Ritter AM, Mendell LM (1992) Somal membrane properties of physiologically identified sensory neurons in the rat: effects of nerve growth factor. J Neurophysiol 68:2033-2041.

Rook JM, Hasan W, McCarson KE (2008) Temporal effects of topical morphine application on cutaneous wound healing. Anesthesiology 109:130-136.

Rose RD, Koerber HR, Sedivec MJ, Mendell LM (1986) Somal action potential duration differs in identified primary afferents. Neurosci Lett 63:259-264.

Sah P, Faber ES (2002) Channels underlying neuronal calcium-activated potassium currents. Prog Neurobiol 66:345-353.

Salo PT, Theriault E (1997) Number, distribution and neuropeptide content of rat knee joint afferents. J Anat 190:515-522.

Shir Y, Seltzer Z (1990) A-fibers mediate mechanical hyperesthesia and allodynia and C-fibers mediate thermal hyperalgesia in a new model of causalgiform pain disorders in rats. Neurosci Lett 115:62-67.

Stebbing MJ, Eschenfelder S, Habler HJ, Acosta MC, Janig W, McLachlan EM (1999) Changes in the action potential in sensory neurones after peripheral axotomy in vivo. Neuroreport 10:201-206.

Treede RD, Meyer RA, Campbell JN (1998) Myelinated mechanically insensitive afferents from monkey hairy skin: heat-response properties. J Neurophysiol 80:1082-1093.

Wieland HA, Michaelis M, Kirschbaum BJ, Rudolphi KA (2005) Osteoarthritis - an untreatable disease? Nat Rev Drug Discov 4:331-344.

Wu Q, Henry JL (2006) Electrophysiological properties of dorsal root ganglion neurons in vivo in a derangement rat model of osteoarthritis. pp http://www.abstractsonline.com/viewer/viewAbstractPrintFriendly.asp?CKey={62CC52E5-A052-4CBF-993D-078F39D1E5AD}&SKey={0FC269E7-500A-45A8-8180-8C63E377FA93}&MKey={D1974E76-28AF-4C1C-8AE8-4F73B56247A7}&AKey={3A7DC0B9-D787-44AA-BD08-FA7BB2FE9004}.

# CHAPTER 4.

## Proprioceptive primary afferent neurons: changes in properties in a rat osteoarthritis model

**Authors:** Qi Wu, James L. Henry

**Corresponding author:** James L. Henry, Ph.D.
Michael G. DeGroote Institute for Pain Research and Care,
McMaster University,
1200 Main street West,
Hamilton, Ontario, Canada, L8N 3Z5,
Tel: +1-905-525-9140, extension 27704,
FAX: 905-522-8844,
E-mail address: jhenry@mcmaster.ca

This paper has been revised and submitted to Neuroscience.

**Significance to thesis:**

This study demonstrated significant changes in electrophysiological properties in muscle spindle neurons in the derangement model of osteoarthritis (OA) established by cutting the ACL and removing the medial meniscus. These changes in proprioceptive neurons were associated with loss of proprioception indicated by altered hind paw weight bearing pattern. Thus, this study may provide a possible avenue to understand loss of proprioception in human OA.

**Author's contribution:**

Qi Wu did the electrophysiological experiments and the incapacitance tests, analyzed the data, performed statistical analyses, wrote the initial draft of the manuscript, and worked on refining this draft and the revision based on editorial review.

James L. Henry conceived of, designed, and coordinated the study. He also worked on refining this draft and the revision based on editorial review.

**Acknowledgements**

This work was generously supported by a New Emerging Team grant from the Canadian Arthritis Network (CAN) and the Canadian Institutes of Health Research (CIHR), and funds from McMaster University. J.L. Henry was Chair in Central Pain in the Faculty of Health Sciences at McMaster University. Q. Wu was a CIHR Strategic Training Fellow in Pain: Molecules to Community, and was also supported by the Canadian Pain Society, CAN and CIHR graduate awards. The authors thank Mrs. Chang Ye for help in data input and statistical analysis. The authors are grateful to Dr. S. N. Lawson for expert guidance during the earliest stages of this project.

**Abstract**

OA is associated with a loss of proprioception in humans. To determine whether specific changes occur in primary sensory neurons and to obtain a better understanding of possible peripheral mechanisms contributing to loss of proprioception, we recorded intracellularly in vivo in proprioceptive dorsal root ganglia (DRG) neurons in a rat model of OA four weeks after surgical knee derangement, and evaluated proprioception in term of changes in weight bearing pattern as well. From intracellular recordings from individual DRG proprioceptive neurons in vivo, components of the action potential (AP) configuration and number of spikes following direct current injection were compared between OA and naïve control female Sprague Dawley rats. We found that at four weeks after knee surgery, when a electrophysiological evaluation is run, the incapacitance test demonstrated a differential hind paw weight distribution with less weight put on the arthritic leg compared with the weight distribution in the pre-surgical period in the OA group. Significantly more spikes were elicited by depolarizing current injection after knee derangement. AP properties differed in OA rats, including longer APD, slower rise time, slower maximum rising rate (MRR). Axonal conduction velocity in model animals was slower. The present study demonstrates that significant changes in proprioceptive neurons occur in this derangement model of OA, and this may provide a possible avenue to understand loss of proprioception in human OA.

**Key words:**

Dorsal root ganglion, proprioception; electrophysiology; action potential

## 4.1. Introduction

OA is a degenerative joint disease caused by material failure of the cartilage network leading to tissue breakdown (Poole, 1999) or by injury of chondrocytes with increased degradative responses (Aigner and Kim, 2002). OA is associated with changes in sensory function, particularly pain (Felson, 2005;Wieland et al., 2005) and loss of proprioception (Barrett et al., 1991;Garsden and Bullock-Saxton, 1999;Koralewicz and Engh, 2000;Hurley et al., 1997;Pai et al., 1997). Deficits in proprioception have been linked to functional instability (Sharma and Pai, 1997;van der Esch et al., 2007) and increased risk of falls (Hurley et al., 1997;Lephart et al., 1997), and have even been suggested to be pathophysiologically related to the progression of knee OA (Shakoor and Moisio, 2004;Sharma, 1999). In fact, it has been advocated that to promote improved functional outcomes in OA patients rehabilitation strategies should be aimed at decreasing the loss of proprioception (Bernauer et al., 1994;Schaible and Grubb, 1993), particularly in early OA (Vad et al., 2002;Lephart et al., 1997;Pai et al., 1997).

Sherrington, in 1906, described proprioception as the sensory information contributing to a sense of actions and movements of the organism itself (Sherrington, 1906). Compared to kinesthesia, the conscious sense of movements of limbs and body, proprioception serves the unconscious sense of the position, location and orientation of the body and its parts (Bosco and Poppele, 2001). Proprioception is due to the activation

of proprioceptors, a distinct class of sensory receptors (Evarts, 1981) for which adequate stimuli arise from the actions of the organism itself, including the muscle spindles, Golgi tendon organs, and joint receptors (Hasan and Stuart, 1988).

Sensory impressions are due to changes in neurons. A virtual soup of chemicals is generated in the region of the degenerating joint and these may generate persisting changes in the physiology of sensory neurons innervating the joint (Herbert and Schmidt, 2001). Thus, to pursue the possibility that functional changes are induced in this model of OA, and the possibility that these changes can be detected in electrophysiological studies, the present study was undertaken. Through recording intracellularly from dorsal root ganglion (DRG) neurons, the aim was to determine whether changes occur specifically in proprioceptive neurons in a surgical derangement model of OA in order to obtain a better understanding of possible peripheral mechanisms contributing to loss of proprioception.

**4.2. Materials and methods**

All experimental procedures were approved by the McMaster University Animal Review Ethics Board and conform to the Guide to the Care and Use of Laboratory Animals of the Canadian Council of Animal Care, Vols.1 and 2. At the end of the acute electrophysiological experiment each animal was euthanized without recovery by an overdose of the anesthetic.

4.2.1. Induction of the animal model of OA

Procedure for the induction of the animal model of OA have been described previously (Wu and Henry, 2009). Briefly, female Sprague Dawley rats (180-225 g) from Charles River Inc. (St. Constant, QC, Canada) were used. Animals were anesthetized with a ketamine based anesthetics (ketamine, 100 mg/ml; xylazine, 20 mg/ml; and acepromazine, 10 mg/ml). The medial meniscus was removed, and the ACL was cut. After surgery, the animals were given 0.05ml antibiotics Trimel (Sulfamethoxazole plus Trimethoprim; Novopharm, Toronto, ON, Canada) once per day for 3 consecutive days, and analgesics Buprenorphine hydrochloride (Temgesic, Schering-Plough, Kenilworth, NJ, USA) twice per day for 2 consecutive days.

4.2.2. Experimental setup for in vivo intracellular recording

Four weeks after the model induction, the animal was anesthetized. Then the right jugular vein was cannulated for i.v. infusion of drugs. Rectal temperature of the animal was maintained at around 37°C, and was mechanically ventilated to achieve an end tide $CO_2$ concentration around 40 mmHg. An initial 1 mg/kg dose of pancuronium was given to eliminate muscle tone. Supplements of pentobarbital were added as needed to maintain a surgical level of anesthesia. Principle of decision making for pentobarbital and pancuronium supplements has been described in detail previously (Wu and Henry, 2009)

A laminectomy was performed to expose the $L_4$ dorsal root ganglion (DRG) ipsilateral to the surgical derangement. The animal was fixed and suspended in a stereotaxic frame. The exposed spinal cord and DRG were covered with warm paraffin oil to prevent drying. The dorsal root of the $L_4$ DRG was cut to allow a 12-15 mm length for electrical stimulation, and one pair of bipolar platinum stimulating electrodes was placed underneath.

Intracellular recordings from somata in the $L_4$ DRG were made with micropipettes fabricated from filament-containing borosilicate glass tubing filled with 3 M KCl solution, with DC resistance about 40-70MΩ. The microelectrode was advanced by an EXFO IW-800 micromanipulator (EXFO, Montreal, QC, Canada). Intracellular recording is established when a hyperpolarization of at least -40 mV suddenly occurred and an AP could be evoked by electrical stimulation of the dorsal root. Evoked APs were recorded with a Multiclamp 700B amplifier (Molecular Devices, Union City, CA, USA) and digitized on-line via a Digidata 1322A interface (Molecular Devices) with *pClamp 9.2* software (Molecular Devices).

Figure 4.1 illustrates the electrophysiological parameters that were measured in each neuron, including resting membrane potential (Vm), APD, AP half width, AP amplitude, AP rise time, AP fall time, MRR, maximum falling rate (MFR), afterhyperpolarization (AHP), AHP50 and AHP80. After each experiment the

conduction distance was measured for each neuron recorded, as the distance from the center of the DRG to the stimulation site (cathode). Conduction velocity (CV) was then calculated from this value. Analysis was done offline using the *pClamp 9.2* software.

Neuronal excitability was measured by electrical stimulation of the dorsal root as well as by injection of a depolarizing current into the neuron. To measure electrical threshold along the dorsal root, a series of 0.04 ms rectangular pulse stimuli, starting from 0.1 mA with increment of 0.1 mA, were delivered along the nerve until an AP could be evoked. The minimal current strength for an evoked AP was recorded as the threshold. As multiple direct current injection may change the composition of intracellular fluid and the dynamic properties of ion channels, to minimize these effects multiple injections were avoided. Neurons tested for rheobase were different from those used to determine repetitive firing frequency because in each case the character of the physiological properties is changed by the experimental procedure. Therefore, it was decided to focus on repetitive firing frequency. Thus, once the sensory properties of a neuron had been identified a 20 ms, 2 nA depolarizing current was injected into the neuron and the number of spikes following injection was recorded.

4.2.3. Sensory properties of proprioceptive neurons

Proprioceptive neurons include muscle spindle neurons and tendon organ neurons. These neurons sense the length or the tension of the muscle spindle, respectively. Lawson

et al. described the sensory properties of proprioceptive neurons (Lawson et al., 1997), which served as the theoretical basis for the classification we used. Thus a neuron was classified as a proprioceptive neuron if it could be activated by touching along the muscle belly or changing joint position or if it had a subcutaneous receptive field, and if it could not be activated by touch or pressure stimuli to the skin only.

4.2.4. Acceptance criteria

Neurons were included in this study if they exhibited an evoked AP from dorsal root stimulation, had a Vm more negative than -40 mV and had AP amplitude larger than 40 mV. For each neuron, before sensory testing was begun a continuous recording was obtained for $\geq$ 5 min after electrode penetration. Only neurons with stable Vm throughout recording and sensory testing were included.

4.2.5. Hind paw weight distribution

Differential hind paw weight distribution was recently used as a measurement of proprioceptive performance (Liu et al., 2009). An incapacitance tester from Linton Instrumentation (Palgrave Diss, Norfolk, UK) was used to determine hind paw weight distribution. Incapacitance tests were conducted in naive and in OA animals at one day before surgery and 4 weeks after surgery. The quantification system described by Pomonis et al. was used (Pomonis et al., 2005). Briefly, the percent weight on the right leg (ipsilateral to the derangement) was calculated using the following formula:

**% weight on the ipsilateral leg =**

**[Weight on the right leg /(weight on the right leg + weight on the left leg)] × 100**

4.2.6. Statistical analysis

Numerical data are presented as mean ± S.E.M. Differences between the weight bearing prior to model induction and 4 weeks after model induction in the OA group were analyzed with the paired *t*-test. Differences in numbers of neurons between control and OA animals, such as number evoked at a specific stimulus strength to the dorsal root or the number of neurons with specific evoked responses following 2nA direct current injection, were analyzed with the Chi-square test. Electrophysiological data were tested for normality using the D'Agostino and Pearson omnibus normality test. Student's *t*-test or Mann-Whitney *U*-test was used in comparisons between the control and OA model animals, where appropriate. All tests and graphing were done using Prism 4 software from Graphpad (La Jolla, CA, USA). The *P* values of the *t*-tests are indicated in the figures, where appropriate, and $P < 0.05$ was set as the level of statistical significance.

**4.3. Results**

4.3.1. Effects of knee derangement on hind paw weight distribution

Differential hind paw weight distribution was measured one day before surgery and then on day 28 after surgery; control animals were run at the same times for the purpose of temporal control. Baseline readings taken before surgery demonstrated equal weight distribution on both hind legs in both groups of animals and there was no difference between the groups. There was also no change in the percentage of weight bearing on either leg in control animals after 4 weeks of housing (data not shown). However, at 4 weeks after surgery, the time at which animals were used in *in vivo* electrophysiological experiments, 47.9 ± 0.19 % of the total hind paw load was placed on the ipsilateral hind leg ($n = 9$), and this percentage was significantly reduced compared to the baseline values before model induction (49.2 ± 0.46 %; $n = 9$; paired $t$-test, $P = 0.02$; Figure 4.2.)

4.3.2. Response of proprioceptive neurons to direct current injection

To determine the electrical threshold of the dorsal root, rectangular pulse stimuli were delivered at a current strength sufficient to evoke an AP. This value in control rats was 0.35 ± 0.12 mA ($N = 21$), which was not different from that in OA rats, which was 0.17 ± 0.11 mA ($N = 35$; Mann-Whitney $U$-test, $P = 0.1$; Figure 4.3. e). Moreover, there was no difference in the number of neurons activated at different current strengths between control and OA animals (Chi-square test, $P = 0.29$). Detailed composition information is shown in Figure 4.3. (c).

To determine the repetitive firing frequency, direct current was injected into the neuron via a glass recording pipette. Twenty-five neurons from 15 control animals and 37 neurons from 17 OA animals were included in the study. The study was done independent of the project to investigate AP configurational changes in the somata of proprioceptive neurons. Examples of repetitive firing following direct current injection from a control and an OA proprioceptive neuron are shown in Figure 4.3. (a,b); 68% of control proprioceptive neurons exhibited one spike (36.1 %) or no spike (32.2 %) following 20 ms, 2nA depolarizing current injection. In OA neurons this percentage was considerably less, at 32.4%: one spike (18.9%), no spike (13.5%). In addition, there was a dramatic increase in the percentage of neurons exhibiting seven or more spikes in OA neurons: 45.9% vs. 16.1% in control. These differences indicate a significant swift towards greater firing following current injection in OA animals (Chi-square test, $P = 0.02$). A detailed composition of spikes in both groups of neurons is shown in Figure 4.3 (d). The average number of spikes following the 20 ms, 2nA depolarizing current injection was 2.28 ± 0.59 in the control proprioceptive neurons. This number was greater in OA proprioceptive neurons, at 4.73 ± 0.57 (Mann-Whitney *U*-test, $P = 0.01$; Figure 4.3. f), suggesting a greater neuronal excitability in proprioceptive neurons in the OA animals.

4.3.3. Electrophysiological properties of the somata of proprioceptive neurons

Properties of proprioceptive DRG neurons in control animals were similar to those in previous *in vivo* reports in guinea-pigs (Djouhri and Lawson, 2001;Djouhri and Lawson, 1999), and are also within the range reported from *in vitro* studies (Ma et al., 2003;Oyelese and Kocsis, 1996). Successful recordings that met the acceptance criteria were from a total of 35 neurons from 17 control animals and 40 neurons from 14 OA model animals.

4.3.3.1. Axonal conduction velocity

Conduction velocity in OA model rats (20.72 ± 0.38 m/s, $n$ = 40) was significantly slower compared with that in control rats (22.88 ± 0.92 m/s, $n$ = 35; Student's $t$-test, $P$ = 0.04). The data are shown in Figure 4.4 (a). While there is some systematic error in the estimation of conduction velocity, this type of error is unlikely to result in the difference of conduction velocity between control rats and OA model rats. This difference in conduction velocity may suggest a change in myelination in sensory neurons in the OA model.

4.3.3.2. Resting membrane potential and action potential amplitude in proprioceptive neurons in OA

The Vm was particularly stable in this type of neuron, mainly because of a relatively large cell diameter, of approximately 50 μm (Oyelese and Kocsis, 1996). Vm

was similar in control rats (-61.07 ± 1.21 mV, $n$ = 35) and in OA model rats (-61.65 ± 1.02 mV, $n$ = 40; Student's $t$-test, $P$ = 0.72).

The AP amplitude in proprioceptive neurons seldom exhibited an overshoot, unlike some of the smaller neurons. This is in agreement with properties of DRG neurons reported earlier (Djouhri and Lawson, 2004). In low threshold neurons, a smaller AP overshoot and a shorter duration of the AP have been reported, especially in muscle spindle neurons (Djouhri and Lawson, 2001). These characteristics seem to be attributable to the fact that tetrodotoxin (TTX)-sensitive $Na^+$ channels are the predominant $Na^+$ channel in this type of DRG neuron, especially proprioceptive neurons. AP amplitude was the same in both control and OA rats (OA model rats, 54.46 ± 1.15 mV, $n$ = 40; control rats 55.7 ± 1.55 mV, $n$ = 35; Student's $t$-test, P = 0.51).

4.3.3.3. Duration of the action potential

Due to the proximity of the recording and stimulating electrodes, in some cases the stimulus artifact overlapped the onset of the spike. Thus, in order to determine the point of onset, two techniques were used in our study: a) using the pre-sweep Vm as the baseline, b) determining the point of AP onset with the aid of the differentiated curve of the recording, in which the point of onset of the AP should have a near 0 reading. Compared with the APD in the control rats (0.73 ± 0.03 ms, $n$ = 35), this parameter was

significantly longer in the OA model rats (0.85 ± 0.03 ms, $n$ = 40; Student's $t$-test, $P$ = 0.006; Figure 4.4. b).

In addition, another way to evaluate the duration of the AP is to measure the width of the AP at half amplitude. However, half width was statistically not different between OA model rats and control rats (0.38 ± 0.01 ms, $n$ = 40 vs. 0.34 ± 0.01 ms, $n$ = 35, respectively; Student's $t$-test, $P$ = 0.06).

4.3.3.4. Dynamics of depolarization

AP rise time was taken as a measure of the time for depolarization from baseline to peak amplitude. As shown in Figure 4.4 (c), there was a longer AP rise time in OA model animals (0.38 ± 0.01 ms, $n$ = 40) compared to control rats (0.32 ± 0.01 ms, $n$ = 35; Student's $t$-test, $P$ = 0.001).

MRR was used as a second measure of the dynamics of depolarization. It was derived by mathematical conversion of the AP configuration as the differentiated derivative of the AP. Thus, the curve represents the rate of voltage change over time. MRR reflects the maximum depolarization driving force, mostly generated by sodium influx current. Figure 4.4 (d) shows that MRR was 277.7 ± 9.81 mV/ms ($n$ = 40) in the OA rats, which was significantly slower than the 313.8 ± 12.63 mV/ms in control rats ($n$ = 35; Student's $t$-test, $P$ = 0.03).

4.3.3.5. Dynamics of repolarization

A similar rationale was adopted to determine the dynamics of repolarization, where AP fall time and MFR were used to measure the dynamics of the repolarization phase. AP fall time had larger individual variance than AP rise time. AP fall time tended to be different from neuron to neuron. This heterogeneity might partly explain the lack of statistical difference revealed in the repolarization phase compared with the depolarization phase. As shown in Figure 4.4 (e), no statistical difference in AP fall time was observed in OA model neurons (0.47 ± 0.02 ms, $n$ = 40) compared to control rats (0.41 ± 0.02 ms; $n$ = 35; Mann-Whitney $U$-test, $P$ = 0.06).

Similarly, as shown in Figure 4.4 (f), MFR was not significantly less in the OA model rats (186.1 ± 9.14 mV/ms, $n$ = 40) compared to control rats (218.2 ± 13.89 mV/ms, $n$ = 35; Mann-Whitney $U$-test, $P$ = 0.1).

4.3.3.6. Afterhyperpolarization phase

AHP is generated predominantly by potassium efflux creating a relatively refractory period. Examination of the parameters of the AHP showed no difference between model and control rats, irrespective of the duration or the amplitude. The AHP amplitude was 8.94 ± 0.67 mV ($n$ = 39) in OA model rats, similar to the values in control rats (9.4 ± 0.56 mV, $n$ = 35; Student's $t$-test, $P$ = 0.61). Furthermore, the AHP50 in OA model rats was similar to that in control rats (1.74 ± 0.14 ms, $n$ = 39 vs. 1.89 ± 0.16 ms, $n$ = 35, respectively; Mann-Whitney $U$-test, $P$ = 0.34), as was the AHP80 (3.42 ± 0.41 ms,

$n$ = 35 vs. 4.13 ± 0.58 ms, $n$ = 33, respectively; Mann-Whitney $U$-test, $P$ = 0.29). In 7 neurons (5 OA and 2 control neurons), measurements of the AHP associated parameters, particularly AHP80 could not be completed because of greater baseline fluctuation due to higher noise level during recording.

**4.4. Discussion**

We report here properties of proprioceptive neurons in normal rats, including duration and amplitude of action potential. In addition, we report that surgical derangement of the ipsilateral limb leads to significant differences between proprioceptive neurons in control rats vs. OA model rats. These differences include increased number of spikes following direct current injection, slower CV, wider APD and slower AP rise time, as well as slower dynamics of depolarization, including slower MRR. These functional changes in proprioceptive neurons are correlated with changes in hind paw weight bearing in OA rats, which may reflect changes in proprioception or proprioceptor-motor integration. .

4.4.1. Changes in AP configurations in proprioceptive neurons are consistent with changes associated with peripheral neuropathy

The configurational changes in proprioceptive neurons observed in the current study resemble typical changes that have been characterized in classic neuropathic models in terms of the nature of the changes and the cell type affected.

Proprioceptive neurons account for a large portion of large and medium sized DRG neurons. According to a recent observation, 49% of large neurons and 25% of medium neurons are muscle spindle afferents (Ma et al., 2003). Therefore, it is reasonable to deduce that a large proportion of these neurons reported in various neuropathic models are actually proprioceptive neurons. The changes reported include slowed dynamics of AP genesis, such as broad APD, slow rising/falling rate, and increased excitability, such as depolarized Vm and spontaneous discharge (Zhang et al., 1999;Kim et al., 1998;Ma et al., 2003).

Moreover, clearly identified proprioceptive neurons have been reported to be altered in neuropathic models. For example, following spinal nerve injury there is an increased low-amplitude subthreshold oscillation mainly in muscle spindle afferents retrogradely labeled with true blue (Liu et al., 2002). Increased firing frequency and/or spontaneous firing has also been reported in muscle spindle afferents following nerve cut (Michaelis et al., 2000). Proprioceptive neurons have been reported to undergo changes in their AP configuration in the sciatic nerve injury model (Oyelese and Kocsis, 1996); in this case retrogradely labeled muscle spindle afferents exhibited more depolarized resting membrane potential and a longer APD. Therefore, the nature of the changes in proprioceptive neurons in the present study, such as broadening of AP duration and

slowing of the rate of depolarization are the same as the nature of changes previously reported in classic neuropathic models.

Heavily myelinated neurons, particularly non-nociceptors are most likely to be affected only in neuropathic type of changes. This is also consistent with what is reported here. Proprioceptive neurons are low threshold A-fiber mechanoreceptors (non-nociceptors) and are heavily myelinated. Such evidence has been demonstrated in the complete sciatic nerve transection model (Abdulla and Smith, 2001), the partial sciatic nerve transection model (Liu and Eisenach, 2005), and the lumbar spinal nerve transection model (Liu et al., 2000;Sapunar et al., 2005;Stebbing et al., 1999;Kim et al., 1998;Ma et al., 2003) of peripheral neuropathic pain.

This contrasts with peripheral inflammation models such as that induced by injecting complete Freund's adjuvant subcutaneously (Xu et al., 2000;Djouhri and Lawson, 1999), where only lightly myelinated A δ neurons and C neurons undergo significant changes in electrophysiological properties. Therefore, as the changes in proprioceptive neurons in the present study are similar to changes in neuropathic models but not inflammation models, we suggest that the changes in the OA model may be due to or represent a neuropathic etiology.

4.4.2. Possible mechanisms contributing to loss of proprioception in OA

OA is defined classically as mechanical failure of the articular cartilage and thus any condition leading to a long-term increase in loading stress per unit area may result in the development of OA. The model used in this study was selected because the most common cause of OA in humans is mechanical destabilization of the joint due to injury (Creamer et al., 1998;Mitsou and Vallianatos, 1988). The OA model chosen for study exhibits signs of clinical OA, including changes in cartilage and bone (Appleton et al., 2007a;Appleton et al., 2007b;McErlain et al., 2008) and a difference in weight-bearing pattern seen in this study as well as in other studies (Fernihough et al., 2004;Bove et al., 2006). A sham-operated control, such as exposure of the joint capsule was not adopted in the study because this has also been reported to induce a mild OA of the joint. It has been shown that a small capsule tear could cause significant joint instability (Hsu et al., 1997). Moreover, a tight correlation has been found between capsule tear and articular cartilage degeneration, regardless of the size of the tear (Hsu et al., 2003).

Evarts (1981) states, in his re-interpretation of Sherrington's concept of proprioception: "Most of what we know about proprioceptive systems has been gained by observing the reflex consequences of externally produced changes of muscle length and tension". This remains the case even in current animal studies regarding proprioception. As a result, evaluation of weight-bearing pattern was chosen as a measurement of proprioception.

An explanation does not easily come to mind to account for how the changes in the configuration of the AP that occur in proprioceptive neurons in our OA model could be related to loss of proprioception in OA. The phenotype of sensory neurons is under the control of trophic factors (Pezet and McMahon, 2006) and a change in phenotype development has been proposed where a larger number of proprioceptive neurons occur as a result of TrkC overexpression (Fukuoka et al., 2008). Inviting though this concept might be, such a change in phenotype has yet to be demonstrated in mature DRGs. In any case, if there were to be a change in phenotype, whereby neurons previously serving a proprioceptive function, perhaps by virtue of their projection pattern in the spinal cord, were to undergo a phenotypic change and serve a nociceptive function, it would be possible that they would serve a dual function, proprioception and nociception, or they would lose their proprioceptive function in difference to a nociceptive function. Thus, a shift or loss of proprioceptive primary afferent neurons due to this change in function might account for the compromised proprioception in people with OA.

An alternative mechanism is that neuropathic type of changes in proprioceptive neurons in the current OA model could result in changes in reflex response that might eventually manifest as loss of proprioception as observed in people with OA. A proprioceptive reflex is a muscular response elicited by sensory input from proprioceptors, which is mild (Evarts, 1981), contrasted to large-scale stretch reflexes.

Sanes reported loss of physiological tremor in patients who had sensory neuropathy affecting large myelinated afferents (Sanes, 1985). Physiological tremor is more likely to be a proprioceptive reflex, as Brown et al. have implied that the frequency range of physiological tremor (8-12 Hz) makes it unlikely to be caused by a stretch reflex (Brown et al., 1982).

The functional significance of decreased axonal conduction velocity in proprioceptive DRG neurons after knee derangement remains unclear. However, this decrease is consistent with the decrease in conduction velocity of peripheral axons in diabetic patients with peripheral polyneuropathy compared to diabetic patients without peripheral polyneuropathy and that of matched control healthy volunteers (Watanabe et al., 2009) and is therefore consistent with our suggestion that the present model exhibits signs of peripheral neuropathy. The decrease in conduction velocity is also consistent with the loss of vibratory perception, which is mediated via large diameter afferents (Salter and Henry, 1990), in diabetic patients compared to normal controls (Hyllienmark et al., 2009). Thus, at the very least, the slowing of conduction velocity may represent a loss of myelination of the large diameter afferent neurons, including proprioceptive neurons. As Wallerian degeneration has been suggested to contribute to axonal conduction failure (Moldovan et al., 2009), this slowing of conduction velocity in proprioceptive neurons may thus indicate changes in the dynamic properties of the axons,

and future studies should be directed at whether the present data could reflect the early stages of axonal failure at high frequencies of APs. Such failure could account for a loss of proprioception in people with OA.

Besides a possible causal relationship between changes in proprioceptive neurons and loss of proprioception reported in humans with OA it is possible that changes in AP configuration and loss of proprioception are two parallel events that result from a common etiology. Nonetheless, the present results demonstrating changes in proprioceptive neurons in this derangement model of OA may be considered a first step in understanding the neurological basis for changes in proprioceptive acuity in people who suffer OA.

In conclusion, we present evidence for functional changes in proprioceptive neurons indicated by significantly altered electrophysiological properties following OA induced by knee trauma. Given the prominent loss of proprioception in OA patients, the present results provide a possible avenue to explore in understanding mechanisms underlying this sensory loss and its resultant motor sequelae.

**4.5. Tables, Figures**

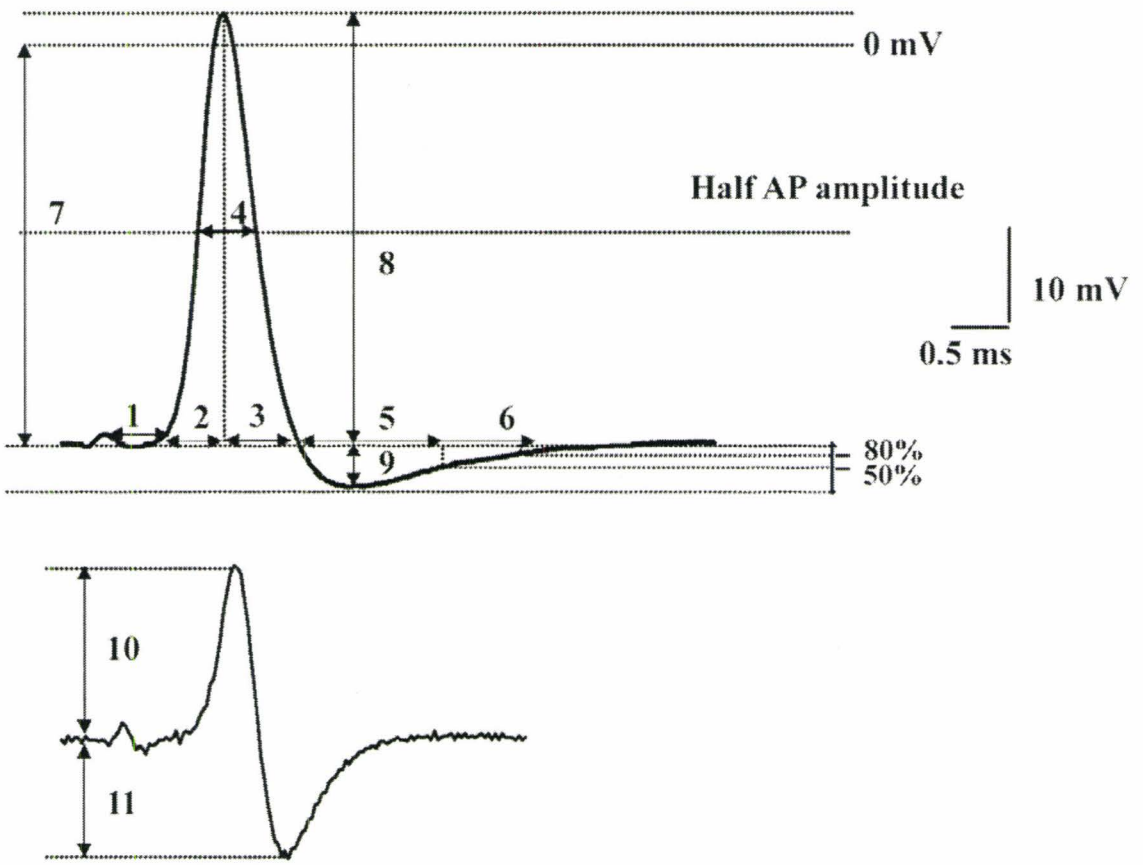


**Figure 4.1. Action potential recorded intracellularly from a proprioceptive neuron, illustrating parameters measured in each neuron studied.** The AP in the upper trace was elicited in a muscle spindle neuron by electrical stimulation of the L4 dorsal root. 1, latency (by measuring the distance from the stimulating site to the center of DRG after each experiment, the conduction velocity is calculated); 2, AP rise time; 3, AP fall time; AP duration at base (the value equals AP rise time plus AP fall time); 4, AP half width; 5, 50% afterhyperpolarization recovery time; 6, 80% afterhyperpolarization recovery time; 7, resting membrane potential; 8, AP amplitude; 9, afterhyperpolarization amplitude.

Lower trace is the differentiated derivative of the upper trace recording, and plots the change of voltage over time: 10, maximum rising rate; 11, maximum falling rate.

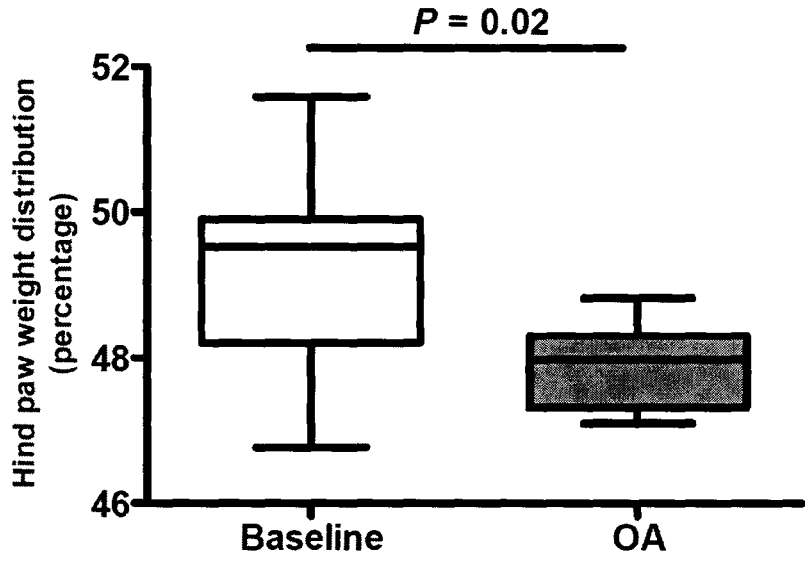


**Figure 4.2. Effects of knee derangement on differential hind paw weight distribution in the incapacitance test.** The percentage of weight bearing of the right hind paw (ipsilateral) was compared between one day before surgery (baseline) and 4 weeks after surgery. In each case the median (horizontal line) is superimposed. Paired *t*-test was used in the comparison. Significant difference in the percentage of weight bearing of the right hind paw prior to and after model induction in OA animals was found at 4 weeks after surgery.

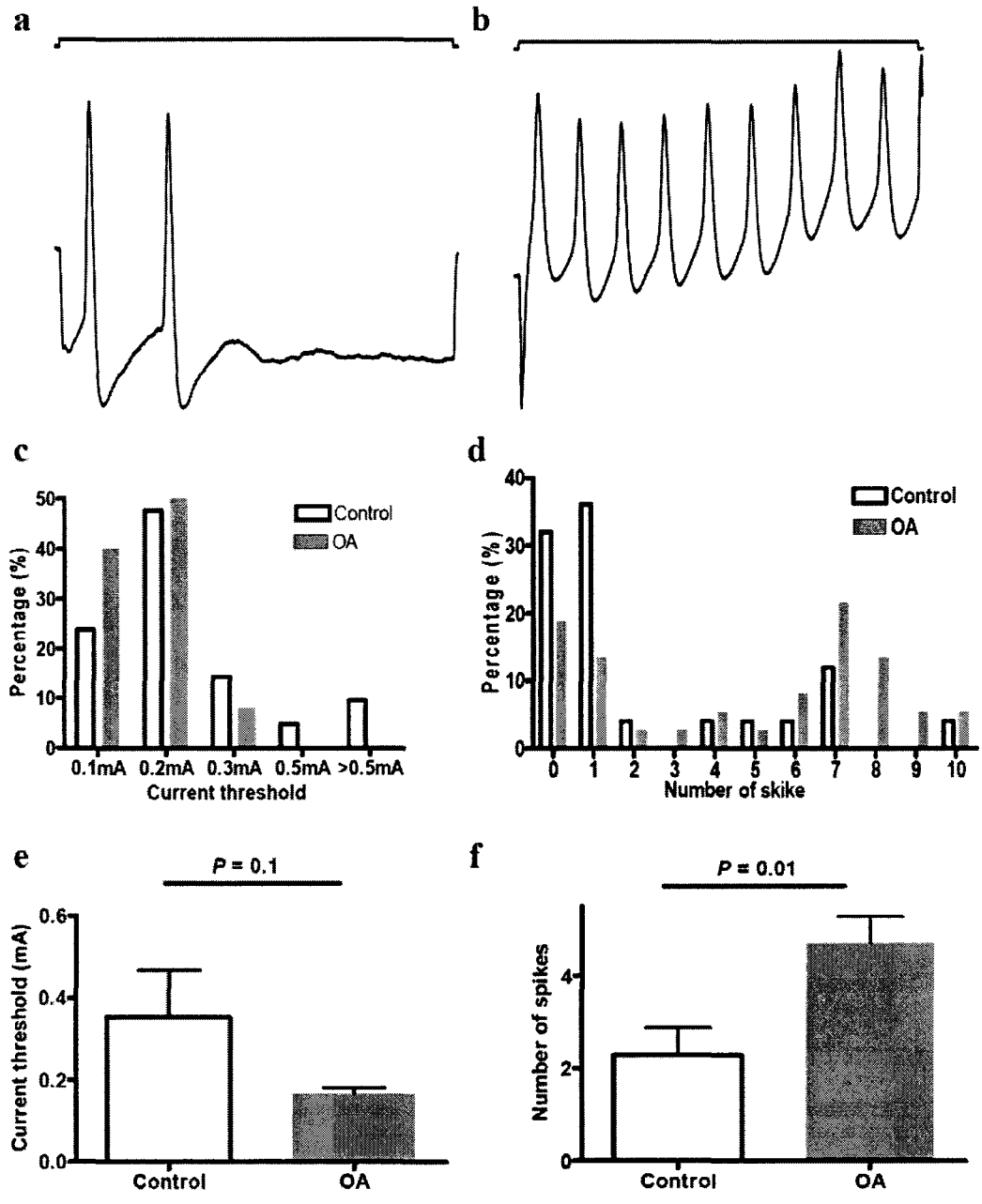


**Figure 4.3. Excitability of proprioceptive DRG neurons determined by electrical stimulation to the dorsal root and by depolarizing current injection in control and OA animals.** A 0.04 ms rectangular pulse stimulus was delivered to dorsal roots and 20

ms, 2nA direct current was injected into neurons at 4 weeks after surgery in control and in OA animals. **(a, and b)** show repetitive firing in a control and an OA proprioceptive neuron, respectively. In both recordings, the upper trace indicates the 2 nA depolarizing current, and the lower trace is the intracellular recording signal. **(c and d)** are the histograms showing the number of neurons evoked at various current strengths to the dorsal root and the number of neurons with various evoked spikes following depolarizing current injection in both control and OA proprioceptive neurons. **(e)** shows the comparison of minimal electrical current sufficient to evoke a spike between OA ($n$ = 25) and control proprioceptive neurons ($n$ = 21). **(f)** shows the comparison of the number of spikes evoked by 2 nA direct current injection between OA ($n$ = 37) and control ($n$ = 25) proprioceptive neurons. The Mann-Whitney $U$-test was used.

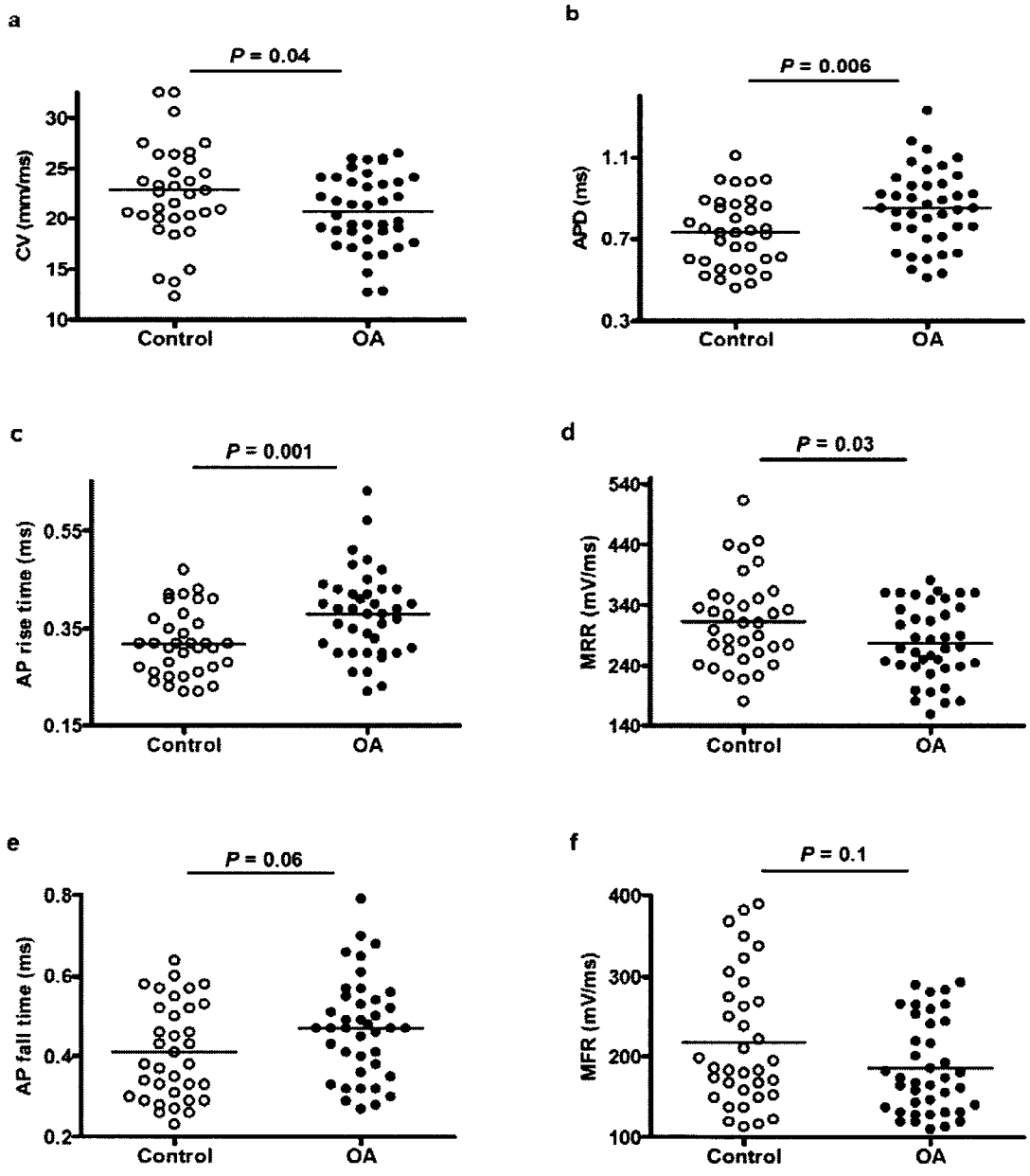


**Figure 4.4. Scatter plots of conduction velocity (a), AP duration (b), AP rise time (c), maximum rising rate (d), fall time (e) and maximum falling rate (f) of individual proprioceptive DRG neurons in control and OA animals.** In each case the median

(horizontal line) is superimposed. Student's *t*-tests were used in the comparisons between OA ($n$ = 40) and control ($n$ = 35) proprioceptive neurons, except that Mann-Whitney *U*-tests were used in the comparison for the AP fall time and maximum falling rate, because the control AP fall time and OA maximum falling rate data failed the D'Agostino and Pearson omnibus normality test. The data indicate slower axonal conduction velocities and slower dynamics of AP spike generation particularly depolarization in neurons in OA animals.

**References**

Abdulla FA, Smith PA (2001) Axotomy- and autotomy-induced changes in the excitability of rat dorsal root ganglion neurons. J Neurophysiol 85:630-643.

Aigner T, Kim HA (2002) Apoptosis and cellular vitality: issues in osteoarthritic cartilage degeneration. Arthritis Rheum 46:1986-1996.

Appleton CT, McErlain DD, Pitelka V, Schwartz N, Bernier SM, Henry JL, Holdsworth DW, Beier F (2007a) Forced mobilization accelerates pathogenesis: characterization of a preclinical surgical model of osteoarthritis. Arthritis Res Ther 9:R13.

Appleton CT, Pitelka V, Henry J, Beier F (2007b) Global analyses of gene expression in early experimental osteoarthritis. Arthritis Rheum 56:1854-1868.

Barrett DS, Cobb AG, Bentley G (1991) Joint proprioception in normal, osteoarthritic and replaced knees. J Bone Joint Surg Br 73:53-56.

Bernauer EM, Walby WF, Ertl AC, Dempster PT, Bond M, Greenleaf JE (1994) Knee-joint proprioception during 30-day 6 degrees head-down bed rest with isotonic and isokinetic exercise training. Aviat Space Environ Med 65:1110-1115.

Bosco G, Poppele RE (2001) Proprioception from a spinocerebellar perspective. Physiol Rev 81:539-568.

Bove SE, Laemont KD, Brooker RM, Osborn MN, Sanchez BM, Guzman RE, Hook KE, Juneau PL, Connor JR, Kilgore KS (2006) Surgically induced osteoarthritis in the rat results in the development of both osteoarthritis-like joint pain and secondary hyperalgesia. Osteoarthritis Cartilage 14:1041-1048.

Brown TI, Rack PM, Ross HF (1982) Different types of tremor in the human thumb. J Physiol 332:113-123.

Creamer P, Lethbridge-Cejku M, Hochberg MC (1998) Where does it hurt? Pain localization in osteoarthritis of the knee. Osteoarthritis Cartilage 6:318-323.

Djouhri L, Lawson SN (1999) Changes in somatic action potential shape in guinea-pig nociceptive primary afferent neurones during inflammation in vivo. J Physiol 520:565-576.

Djouhri L, Lawson SN (2001) Differences in the size of the somatic action potential

overshoot between nociceptive and non-nociceptive dorsal root ganglion neurones in the guinea-pig. Neuroscience 108:479-491.

Djouhri L, Lawson SN (2004) Abeta-fiber nociceptive primary afferent neurons: a review of incidence and properties in relation to other afferent A-fiber neurons in mammals. Brain Res Brain Res Rev 46:131-145.

Evarts EV (1981) Sherrington's concept of proprioception. Trends Neurosci 4:44-46.

Felson DT (2005) The sources of pain in knee osteoarthritis. Curr Opin Rheumatol 17:624-628.

Fernihough J, Gentry C, Malcangio M, Fox A, Rediske J, Pellas T, Kidd B, Bevan S, Winter J (2004) Pain related behaviour in two models of osteoarthritis in the rat knee. Pain 112:83-93.

Fukuoka T, Kobayashi K, Yamanaka H, Obata K, Dai Y, Noguchi K (2008) Comparative study of the distribution of the alpha-subunits of voltage-gated sodium channels in normal and axotomized rat dorsal root ganglion neurons. J Comp Neurol 510:188-206.

Garsden LR, Bullock-Saxton JE (1999) Joint reposition sense in subjects with unilateral osteoarthritis of the knee. Clin Rehabil 13:148-155.

Hasan Z, Stuart DG (1988) Animal solutions to problems of movement control: the role of proprioceptors. Annu Rev Neurosci 11:199-223.

Herbert MK, Schmidt RF (2001) Sensitisation of group III articular afferents to mechanical stimuli by substance P. Inflamm Res 50:275-282.

Hsu HC, Luo ZP, Cofield RH, An KN (1997) Influence of rotator cuff tearing on glenohumeral stability. J Shoulder Elbow Surg 6:413-422.

Hsu HC, Luo ZP, Stone JJ, Huang TH, An KN (2003) Correlation between rotator cuff tear and glenohumeral degeneration. Acta Orthop Scand 74:89-94.

Hurley MV, Scott DL, Rees J, Newham DJ (1997) Sensorimotor changes and functional performance in patients with knee osteoarthritis. Ann Rheum Dis 56:641-648.

Hyllienmark L, Jonsson B, Ekberg K, Lindstrom P (2009) Abnormal cold perception in the lower limbs: A sensitive indicator for detection of polyneuropathy in patients with type 1 diabetes mellitus. Diabetes Res Clin Pract.

Kim YI, Na HS, Kim SH, Han HC, Yoon YW, Sung B, Nam HJ, Shin SL, Hong SK (1998) Cell type-specific changes of the membrane properties of peripherally-axotomized dorsal root ganglion neurons in a rat model of neuropathic pain. Neuroscience 86:301-309.

Koralewicz LM, Engh GA (2000) Comparison of proprioception in arthritic and age-matched normal knees. J Bone Joint Surg Am 82-A:1582-1588.

Lawson SN, Crepps BA, Perl ER (1997) Relationship of substance P to afferent characteristics of dorsal root ganglion neurones in guinea-pig. J Physiol 505:177-191.

Lephart SM, Pincivero DM, Giraldo JL, Fu FH (1997) The role of proprioception in the management and rehabilitation of athletic injuries. Am J Sports Med 25:130-137.

Liu B, Eisenach JC (2005) Hyperexcitability of axotomized and neighboring unaxotomized sensory neurons is reduced days after perineural clonidine at the site of injury. J Neurophysiol 94:3159-3167.

Liu CN, Devor M, Waxman SG, Kocsis JD (2002) Subthreshold oscillations induced by spinal nerve injury in dissociated muscle and cutaneous afferents of mouse DRG. J Neurophysiol 87:2009-2017.

Liu CN, Wall PD, Ben-Dor E, Michaelis M, Amir R, Devor M (2000) Tactile allodynia in the absence of C-fiber activation: altered firing properties of DRG neurons following spinal nerve injury. Pain 85:503-521.

Liu S, Bohl D, Blanchard S, Bacci J, Said G, Heard JM (2009) Combination of microsurgery and gene therapy for spinal dorsal root injury repair. Mol Ther 17:992-1002.

Ma C, Shu Y, Zheng Z, Chen Y, Yao H, Greenquist KW, White FA, LaMotte RH (2003) Similar electrophysiological changes in axotomized and neighboring intact dorsal root ganglion neurons. J Neurophysiol 89:1588-1602.

McErlain DD, Appleton CT, Litchfield RB, Pitelka V, Henry JL, Bernier SM, Beier F, Holdsworth DW (2008) Study of subchondral bone adaptations in a rodent surgical model of OA using in vivo micro-computed tomography. Osteoarthritis Cartilage 16:458-469.

Michaelis M, Liu X, Janig W (2000) Axotomized and intact muscle afferents but no skin afferents develop ongoing discharges of dorsal root ganglion origin after peripheral nerve

lesion. J Neurosci 20:2742-2748.

Mitsou A, Vallianatos P (1988) Meniscal injuries associated with rupture of the anterior cruciate ligament: a retrospective study. Injury 19:429-431.

Moldovan M, Alvarez S, Krarup C (2009) Motor axon excitability during Wallerian degeneration. Brain 132:511-523.

Oyelese AA, Kocsis JD (1996) GABAA-receptor-mediated conductance and action potential waveform in cutaneous and muscle afferent neurons of the adult rat: differential expression and response to nerve injury. J Neurophysiol 76:2383-2392.

Pai YC, Rymer WZ, Chang RW, Sharma L (1997) Effect of age and osteoarthritis on knee proprioception. Arthritis Rheum 40:2260-2265.

Pezet S, McMahon SB (2006) Neurotrophins: mediators and modulators of pain. Annu Rev Neurosci 29:507-538.

Pomonis JD, Boulet JM, Gottshall SL, Phillips S, Sellers R, Bunton T, Walker K (2005) Development and pharmacological characterization of a rat model of osteoarthritis pain. Pain 114:339-346.

Poole AR (1999) An introduction to the pathophysiology of osteoarthritis. Front Biosci 4:D662-D670.

Salter MW, Henry JL (1990) Physiological characteristics of responses of wide dynamic range spinal neurones to cutaneously applied vibration in the cat. Brain Res 507:69-84.

Sanes JN (1985) Absence of enhanced physiological tremor in patients without muscle or cutaneous afferents. J Neurol Neurosurg Psychiatry 48:645-649.

Sapunar D, Ljubkovic M, Lirk P, McCallum JB, Hogan QH (2005) Distinct membrane effects of spinal nerve ligation on injured and adjacent dorsal root ganglion neurons in rats. Anesthesiology 103:360-376.

Schaible HG, Grubb BD (1993) Afferent and spinal mechanisms of joint pain. Pain 55:5-54.

Shakoor N, Moisio K (2004) A biomechanical approach to musculoskeletal disease. Best Pract Res Clin Rheumatol 18:173-186.

Sharma L (1999) Proprioceptive impairment in knee osteoarthritis. Rheum Dis Clin North Am 25:299-314.

Sharma L, Pai YC (1997) Impaired proprioception and osteoarthritis. Curr Opin Rheumatol 9:253-258.

Sherrington CS (1906) The Integrative Action of the Nervous System. New Heaven: YALE UNIVERSITY PRESS.

Stebbing MJ, Eschenfelder S, Habler HJ, Acosta MC, Janig W, McLachlan EM (1999) Changes in the action potential in sensory neurones after peripheral axotomy in vivo. Neuroreport 10:201-206.

Vad V, Hong HM, Zazzali M, Agi N, Basrai D (2002) Exercise recommendations in athletes with early osteoarthritis of the knee. Sports Med 32:729-739.

van der Esch M, Steultjens M, Harlaar J, Knol D, Lems W, Dekker J (2007) Joint proprioception, muscle strength, and functional ability in patients with osteoarthritis of the knee. Arthritis Rheum 57:787-793.

Watanabe T, Ito H, Morita A, Uno Y, Nishimura T, Kawase H, Kato Y, Matsuoka T, Takeda J, Seishima M (2009) Sonographic evaluation of the median nerve in diabetic patients: comparison with nerve conduction studies. J Ultrasound Med 28:727-734.

Wieland HA, Michaelis M, Kirschbaum BJ, Rudolphi KA (2005) Osteoarthritis - an untreatable disease? Nat Rev Drug Discov 4:331-344.

Wu Q, Henry JL (2009) Delayed onset of changes in soma action potential genesis in nociceptive A-beta DRG neurons in vivo in a rat model of osteoarthritis. Mol Pain 5:57.

Xu GY, Huang LY, Zhao ZQ (2000) Activation of silent mechanoreceptive cat C and Adelta sensory neurons and their substance P expression following peripheral inflammation. J Physiol 528:339-348.

Zhang JM, Song XJ, LaMotte RH (1999) Enhanced excitability of sensory neurons in rats with cutaneous hyperalgesia produced by chronic compression of the dorsal root ganglion. J Neurophysiol 82:3359-3366.

# CHAPTER 5.

## Recovery from sodium channel inactivation is altered in Aβ-fiber neurons in a knee derangement model of osteoarthritis in the rat

**Authors:** Qi Wu, James L. Henry

**Corresponding author:** James L. Henry, Ph.D.
Michael G. DeGroote Institute for Pain Research and Care,
McMaster University,
1200 Main street West,
Hamilton, Ontario, Canada, L8N 3Z5,
Tel: +1-905-525-9140, extension 27704,
FAX: 905-522-8844,
E-mail address: jhenry@mcmaster.ca

This paper is submitted to Neuroscience.

**Recovery from sodium channel inactivation is altered in Aβ-fiber neurons in a knee derangement model of osteoarthritis in the rat**

**Significance to thesis:**

This study demonstrated significant changes in responses to repetitive stimulation in heavily myelinated Aβ-fiber dorsal root ganglia (DRG) neurons at one month following the induction of the knee derangement model of osteoarthritis (OA). These changes might be important in the initiation and maintenance of central plasticity, and thus contribute to chronic pain in OA.

**Author's contribution:**

Qi Wu did the electrophysiological experiments, analyzed the data, performed statistical analyses, wrote the initial draft of the manuscript, and worked on refining this draft and the revision based on editorial review.

James L. Henry conceived of, designed, and coordinated the study. He also worked on refining this draft and the revision based on editorial review.

**Acknowledgements**

This work was generously supported by the Canadian Arthritis Network (CAN), the Canadian Institutes of Health Research (CIHR), and McMaster University. J.L.H was Chair in Central Pain in the Faculty of Health Sciences at McMaster University. Q.W was a CIHR Strategic Training Fellow in Pain: Molecules to Community, and was supported by the Canadian Pain Society, CAN and CIHR. The authors thank Mrs. Chang Ye for help in data input and statistical analysis.

**Abstract**

In chronic pain conditions, conduction failure regulates peripheral drive from DRG neurons, which plays an important role in spinal plasticity. Our previous studies revealed significant changes in the upstoke branch of evoked action potential (AP) in Aβ-fibre neurons in OA animals, suggesting changes in sodium channel kinetics. Thus, this study was aimed to investigate the role of sodium channel inactivation in conduction failure in Aβ-fibre neurons in a surgical derangement model of OA in the rat. Sprague-Dawley rats were used, forming two groups - OA and naïve control. Four weeks after cutting the anterior cruciate ligament (ACL) and removing the medial meniscus to induce the model, intracellular in vivo recordings were made in ipsilateral L4 DRG neurons in the anaesthetized paralyzed rat, and dorsal roots were stimulated to determine the refractory interval (RI; pairs of stimuli are delivered with variable interval), fibre following frequency (FFF; a train of 200 ms stimuli at variable frequency). Paired pulse recordings were differentiated to determine the dynamics of the two evoked APs and the residual AP. It was found that RI was increased in Aβ-fibre high-threshold mechanoreceptors (HTMs), but was decreased in Aβ-fibre low-threshold mechanoreceptors (LTMs) in OA animals compared to control. The extent of decay in maximum rising rate (MRR) during paired pulse and the MRR of the residual AP were greater in OA Aβ-fibre LTMs, suggesting that the decrease in refractory interval was due

to a shift towards more prominent fast kinectics tetrodotoxin (TTX)-sensitive currents. Conduction failure during train pulse was well fitted with a single exponential decay function. Maximum FFF in Aβ-fibre LTMs was greater in OA animals. Compared with paired pulse, train pulse caused additional decay in MRR, due to other mechanisms including sodium channel slow inactivation. However, no difference in sodium channel slow inactivation was observed between control and OA neurons. Moreover, a difference was observed in the conduction failure between peripheral and central processes in the OA model. The data show significant changes in responses to repetitive stimulation in Aβ-fiber neurons, which might be important for the initiation and maintenance of central plasticity, and therefore chronic pain in OA.

**Key words**:

Dorsal root ganglion, repetitive firing; electrophysiology; conduction failure; spike frequency adaption neuron

## 5.1. Introduction

It is believed that primary sensory neurons contribute to the plasticity in second order spinal neurons partly via frequency-dependant modulation of the synaptic transmission in these neurons (Kadekaro et al., 1985;Jeftinija and Urban, 1994;Fields, 2006;Udina et al., 2008). Under physiological conditions, DRG neurons are able to discharge trains of APs, which only partially arrive at the spinal cord under some conditions, such as in response to high frequency or repetitive stimulation. Conduction failure has been attributed to the cell morphology of DRG neurons, for example the low safety factor T-junction region (Luscher et al., 1994b).

In chronic pain models, peripheral drive from DRG neurons has been reported to play an important role in developing and maintaining spinal plasticity (Pitcher and Henry, 2008;Dalal et al., 1999;Pitcher and Henry, 2004;Seltzer et al., 1991;Sotgiu et al., 1994). CFA induced hind limb inflammation leads to increased maximum FFF along dorsal root in nociceptive DRG neurons (Djouhri et al., 2001), implying attenuated conduction failure. It is possible that changes in discharge properties of primary afferent neurons may contribute to altered activity in nociceptive pathways.

A variety of ionic mechanisms of spike-frequency adaptation have also been proposed to explain this conduction failure. These include a calcium-activated

potassium conductance (Viana et al., 1993), a hyperpolarisation-activated inward current (Ih) (Momin and McNaughton, 2009), intracellular accumulation of calcium ions during repetitive firing (Luscher et al., 1994a) and slow inactivation of sodium channels (Blair and Bean, 2003;Choi et al., 2007;Fleidervish et al., 1996). Our previous studies in the surgically induced model of OA have revealed significant changes in the rising phase of the AP in myelinated Aβ-fibre neurons, which suggests changes in the properties of sodium channels (Wu and Henry, 2006;Wu and Henry, 2009).

There are two basic forms of inactivation of sodium channels, fast and slow, which are disctinct and distinguishable. For example, fast inactivation occurs during a single AP whereas slow inactivation can last tens of seconds. Each is also under distinct regulation, fast inactivation being largely dictated by the voltage sensing S4 segment whereas slow inactivation is significantly regulated by auxiliary β-subunits, (for review, see (Vilin and Ruben, 2001). In fact, modifying slow sodium channel inactivation has emerged as a promising solution in chronic pain management; specifically inducing voltage gated sodium channels into slow inactivation state by therapeutic agents, such as lacosamine, has been shown to have broad spectrum suppressive effect on mechanical and thermal hypersensitization in various chronic pain syndromes (Beyreuther et al., 2007a). Particularly inspiring for patients suffering from OA pain, this strategy is

effective in relieving chronic muscle pain, a common symptoms in OA (Beyreuther et al., 2007b).

Sodium channel kinetics may therefore yield a novel avenue for development of new therapeutic agents for the treatment of OA pain. In the present study we aimed to investigate the role of sodium channel inactivation in conduction failure in Aβ-fibre neurons in a rat model of OA.

## 5.2. METHODS

All experimental procedures were approved by the McMaster University Animal Review Ethics Board and conform to the Guide to the Care and Use of Laboratory Animals of the Canadian Council of Animal Care, Vols.1 and 2. At the end of the acute electrophysiological experiment each animal was euthanized without recovery by an overdose of the anesthetic.

### 5.2.1. Surgical induction of the model and experimental setup for in vivo intracellular recording

Details of the induction of the animal model of OA, animal preparation for acute electrophysiological recording and in vivo intracellular recording have been published (Wu and Henry, 2009). Briefly, female Sprague Dawley rats (180-225 g) from Charles River Inc. (St. Constant, QC, Canada) were used. Animals were anesthetized with a

ketamine based anesthetic. The medial meniscus was removed, and the ACL was cut. During the first three post operation days, the animals were given Trimel and Temgesic.

For the acute electrophysiological experiments, four weeks after the model induction the animal was anesthetized. The right jugular vein was cannulated for i.v. infusion of drugs. A laminectomy was performed to expose the $L_4$ DRG ipsilateral to the surgical derangement. The animal was fixed and suspended in a stereotaxic frame. The exposed spinal cord and DRG were covered with warm paraffin oil to prevent drying. The dorsal root of the $L_4$ DRG was cut to allow a 12-15 mm length for electrical stimulation, and one pair of bipolar platinum stimulating electrodes was placed underneath. Rectal temperature was maintained at 37°C, and the animal was mechanically ventilated to achieve an end tide $CO_2$ concentration around 40 mmHg. An initial 1 mg/kg dose of pancuronium (Sandoz, Boucherville, QC, Canada) was given to eliminate muscle tone. Supplements of pentobarbital (CEVA SANTE ANIMALE, La Ballastière, Libourne, France; 20 mg/kg) were added as needed to maintain a surgical level of anesthesia. Principle of decision making for pentobarbital and pancuronium administration has been described in detail previously (Wu and Henry, 2009). Briefly, supplements of pentobarbital and pancuronium (1/3 of the initial dose) were added every hour.

Intracellular recordings from somata in the $L_4$ DRG were made with micropipettes fabricated from filament-containing borosilicate glass tubing filled with 3 M KCl solution, with DC resistance 40-70MΩ. The microelectrode was advanced by an EXFO IW-800 micromanipulator (EXFO, Montreal, QC, Canada). Intracellular recording was established when a hyperpolarization of at least -40 mV suddenly occurred and an AP could be evoked by electrical stimulation of the dorsal root. Evoked APs were recorded with a Multiclamp 700B amplifier (Molecular Devices, Union City, CA, USA) and digitized on-line via a Digidata 1322A interface (Molecular Devices) with *pClamp 9.2* software (Molecular Devices).

5.2.2. Scope of the study and neuronal type involved

The sensory receptive properties of neurones were identified by various mechanical stimuli, and classified as previously described (Lawson et al., 1997). The criterion for an Aδ-fibre was mainly based on dorsal root CVs, which were faster than 6.5 mm/ms (Fang et al., 2005). Aβ-fiber LTMs were identified using soft brush, light pressure with a blunt object and light tap. These neurons included various subtypes, such as guard hair, field hair, Pacinian, glabrous rapidly adapting, slowly adapting types I and II, and muscle spindle types I and II. Guard and field hair neurons were both rapidly adapting cutaneous hair follicle units and are included together. Pacinian and glabrous neurons were both rapidly adapting non-hair follicle neurones, and were named

rapidly adapting neurones. Slowly adapting neurons adapted slowly to light tactile stimuli to the cutaneous receptive fields. Muscle spindle neurons were slowly adapting neurones with subcutaneous receptive fields. Aβ-fiber HTMs were identified using pain-evoking mechanical stimuli, such as pinch, needle prick.

5.2.3. Stimulation protocols

Two pairs of bipolar stimulating electrodes were used, one under the dorsal root and the other one under the sciatic nerve. Two stimulation protocols were delivered either antidromically along dorsal root, orthodromically along sciatic nerve or both depending on the availability of evoked AP from each nerve. The stimulating pulse was delivered from the S940/S910 stimulus adaptor/isolator (Dagan, Minneapolis, MN, USA). The stimulating strength was set to be around 2 times activation threshold. Based on our pilot study, the current strength is normally around 0.8 mA for the dorsal root stimulation protocol, and around 2 mA for the sciatic nerve stimulation protocol.

Paired-pulse stimulation started with search sweeps with coarse interval steps at 0.2-1 ms, and then followed with testing sweeps with fine interval steps at 0.1 ms. Each sweep was separated by a pause of 4 seconds. From each original recording (Figure. 5.1A) and its differentiated derivative, the duration, amplitude and the rate of voltage change for various components of the second spikes were measured (Figure. 5.1B). For each neuron, the recording with the smallest RI was chosen for the above analyses.

Train stimuli with variable frequencies were programmed using the pClamp protocol editor. The stimulation lasted for 200 ms, with frequencies of 40-1200 Hz. The frequency of the stimulation was increased gradually with 30 Hz increments for stimulating Aβ-fibre LTMs and with 10 Hz increments for stimulating Aβ-fibre HTMs. A pause of 4 seconds separated each sweep of train stimuli. The ratio of frequency following (FF) was determined by the ratio of the frequency of evoked action potentials to the preset frequency of the stimulation (Figure. 5.2A). For each neuron, a curve of frequency following was plotted against a range of frequencies, and 100% FF, 80% FF, 50% FF were determined from the fitted curve (Figure. 5.2B).

5.2.4. Statistical analysis

Numerical data are presented as mean ± S.E.M. Electrophysiological data were tested for normality using the D'Agostino and Pearson omnibus normality test. Student's *t*-test or Mann-Whitney *U*-test was used in comparisons between the control and OA model animals, where appropriate. All tests and graphing were done using Prism 4 software (GraphPad, La Jolla, CA, USA). The *P* values of the *t*-tests are indicated in the figures, where appropriate, and $P< 0.05$ was set as the level of statistical significance.

**5.3. RESULTS:**

5.3.1. Patterns of response to repetitive stimuli in Aβ-fiber neurons

To investigate the fast process of recovery from repetitive firings in each type of neuron, paired pulse stimuli were delivered to the dorsal root; to investigate the slow process of recovery from repetitive firings in each type of neuron, a 200ms train pulse was delivered to the dorsal root. There are two basic types of response to repetitive firings, which we name as Type I and Type II responses. Representatives of each response are showed in Figure. 5.1, 5.2.

Type I response is featured as having an inflection on the rising phase of the second spike as the interval between paired pulses is gradually shortened. In corresponding differentiated recordings, two components on the rising phase become gradually separated as the interval is gradually shortened, the amplitude of the initiation component remains relatively constant, and the amplitude of the second component gradually decreases. When the interval is short enough, the second spike fails and leaves only the initiation component of the spike. Their properties are illustrated in Figure. 5.1. Moreover, during the stimulation of the 200ms train, conduction failure of some of the APs appears as stimulation frequency is gradually increased. Failed APs are manifested as non-invading APs or electronically conducted potential increase. Their properties are illustrated in Figure. 5.2. The majority of naïve control hair follicle neurons, glabrous rapidly adapting neurons, roughly half of Pacinian neurons and small portion of muscle spindle neurons show Type I response to repetitive stimulation.

Type II response is featured as having no inflection on the rising phase of the second spike and the abrupt failure of the second spike as the interval between paired pulses is gradually shortened. In corresponding differentiated recordings, no obvious separation of components on the rising phase can be found. When the interval is short enough, the second spike is completely abolished without any partial AP, as illustrated in Figure. 5.1. Conduction failure during train stimulation is manifested as the complete absence of evoked APs. This is illustrated in Figure. 5.2. The majority of naïve control muscle spindle neurons, roughly half of Pacinian neurons, very few hair follicle neurons and glabrous rapidly adapting neurons showed Type II response to repetitive stimulation.

5.3.2. Changes in the fast process of recovery from repetitive firings in OA

RI is a measurement for the refractory period which limits the rate of firing. Mechanisms regulating the duration of this insensitive period mainly include the recovery of sodium currents from inactivation following the action potential and the activation of potassium currents.

In naive control animals, the dorsal root of each type of neuron was stimulated with ~0.8 mA constant current (antidromically). Aβ-fibre nociceptors had the longest RI (1.82 ± 0.263 ms, $N = 21$). Muscle spindle neurons, which normally have ongoing discharge had the shortest RI (0.52 ± 0.051 ms, $N = 44$). Other types of Aβ-fibre

non-nociceptors have an intermediate RI: hair follicle neurons, 1.08 ± 0.131 ms ($N$ = 15); glabrous rapidly adapting neurons, 0.96 ± 0.082 ms ($N$ = 17); slowly adapting neurons, 0.96 ± 0.082 ($N$ = 4); Pacinian neurons, 0.77 ± 0.06 ms ($N$ = 24). If the RI ≥ 1.2 ms is arbitrarily assigned as long RI, the RI 0.8-1.2 ms as medium, and the RI ≤ 0.8 ms as short, Aβ-fibre nociceptors belong to long RI category, hair follicle, glabrous rapidly adapting and slowly adapting neurons belong to the medium RI category, whereas Pacinian and muscle spindle neurons belong to short RI category (Figure. 5.3A). RI in muscle spindle neurons was significantly shorter than the other types of neuron, except for Pacinian and slowly adapting neurons (one way ANOVA with Dunn's post hoc test, vs. hair follicle neurons and vs. glabrous rapidly adapting neuron, both with $P < 0.01$; vs. A-fibre HTMs, $P < 0.001$).

In OA animals, under the same stimulation conditions, it was found that RIs in Aβ-fibre nociceptors were significantly greater compared with their naïve control counterpart (1.82 ± 0.263 ms, $N$ = 21 in control vs. 2.29 ± 0.242 ms, $N$ = 24 in OA; $P$ = 0.047). RIs in Aβ-fibre LTMs were significantly shorter (0.74 ± 0.041 ms, N=104 in control vs. 0.64 ± 0.042 ms, N=112 in OA; $P$ = 0.044, Mann-Whitney $U$-test; Figure. 3B). Among Aβ-fibre LTMs, muscle spindle neurons were identified with the greatest change. RIs in muscle spindle neurons in OA were significantly shorter (0.52 ± 0.051 ms, $N$ = 44 in control vs. 0.31 ± 0.032 ms, $N$ = 47 in OA; $P$ = 0.003, Mann-Whitney $U$-test). Any

differences in the other types of A-fiber LTM did not reach significance (data not shown). Aβ-fibre nociceptors in OA animals demonstrated significantly increased RIs compared with their naïve control counterpart (1.82 ± 0.265 ms, $N = 21$ in control vs. 2.29 ± 0.239 ms, $N = 24$ in OA; $P = 0.047$, Whitney $U$-test; Figure. 3B).

In order to reveal further mechanisms underlying the shortened refractory interval in OA Aβ-fibre LTMs, we obtained data allowing us to infer the dynamics of sodium channels. During the action potential, TTX-sensitive sodium currents activate around the resting potential and inactivate almost completely by the time of the peak (Blair and Bean, 2002). However, TTX-resistant sodium currents activate slower, decrease near the peak but with much slower rate and have incomplete inactivation at the end of repolarization (Blair and Bean, 2002). However, in contrast to their activation patterns, TTX-sensitive currents are slow in recovery from inactivation, while TTX-resistant currents recover quickly from inactivation (Blair and Bean, 2002). Two components on the rising phase of the second AP of Type I become gradually separated as the interspike interval is gradually shortened. The amplitude of the initiation component remains relatively constant, even when the second spike fails. At that time only the initial component remains and forms a residue of potential increase. However, the amplitude of the second component gradually decreases. We speculated that the initiation component might represent fast kinectics TTX-sensitive sodium currents, whereas the

second component might represent slow kinetics TTX-sensitive sodium currents, rather than the differentiation between TTX-sensitive and TTX-resistant currents. There are two reasons: first, TTX-resistant currents only present in a very small number of Aβ-fibre LTMs (Djouhri and Lawson, 2004;Fukuoka et al., 2008), which does not agree with the commonness of the "inflected second spike" in these neurons in our observation; second, there are different TTX-sensitive sodium channel subtypes that recover from inactivation at vary rates, with Nav1.6 recovering fastest while Nav1.3, Nav1.7 much slow (Cummins et al., 2001;Herzog et al., 2003).

As an initial step, we measured the maximum rising rate and the amplitude of the action potential immediately after the second component of the second spike fails. Maximum rising rate of the residual AP was 107.71 ± 3.082 mV/ms in control ($N$ = 44). This value was significantly increased in OA animals, and was 122.72 ± 4.021 mV/ms ($N$ = 46; $P$ = 0.004, Student's $t$-test; Figure. 3C). However, no difference was found between the control and OA animal in the action potential amplitude of the residual AP (23.11 ± 0.881 mV, $N$ = 44 in control vs. 25.14 ± 1.082 mV, $N$ = 46 in OA; $P$ = 0.132, Student's $t$-test). These results suggest that there were more fast kinestics TTX-sensitive sodium currents (likely Nav1.6) contributing to the second spike in the OA animals that promoted recovery evoked AP. These results further imply that there is either an

increase in the absolute number of fast kinectics TTX-sensitive sodium channels or in the recovery kinetics of TTX-sensitive sodium channels in Aβ-fibre LTMs in OA animals.

Subsequently, we investigated the dynamics of the second component of the second spike by comparing the extent of decay in the maximum rising rate and action potential amplitude of the two spikes. The extent of decay in each parameter was defined as a ratio, the measurement of the second spike vs. that of the first spike. The smaller the ratio is, the greater the extent of decay. For each type of neuron, the comparison between control and OA animals was made at the same selected refractory intervals. For example, hair follicle and Pacinian neurons were tested at an interval of 1ms, glabrous rapidly adapting and slowly adapting neurons at 1.2 ms, and muscle spindle neurons at 0.4 ms. In some recordings, the stimulus artifact masked the rising phase of the first spike, and prevented accurate measurements. In these cases, measurements from single evoked action potentials under lower current strength (usually 0.3 mA of the evoked action potential protocol vs. 0.8 mA of the paired pulse protocol) were taken as substitution. We found that an inter-pair interval as short as 4 seconds in our paired pulse protocol was sufficient to allow full recovery from previous discharges. Measurements of each electrophysiological parameter of the first spikes in each sweep remained constant, and were basically interchangeable with those from single evoked action potential under lower current strength, provided that the resting potentials were

stable. The extent of decay in the maximum rising rate was significantly greater in OA animals (0.81 ± 0.016, $N$ = 54 in control vs. 0.75 ± 0.017, $N$ = 60 in OA; $P$ = 0.017, Mann-Whitney $U$-test; Figure. 3D). Also, the extent of decay in the action potential amplitude was significantly greater in OA (0.94 ± 0.007, $N$ = 51 in control vs. 0.9 ± 0.008, $N$ = 60 in OA animals; $P$ = 0.003, Mann-Whitney $U$-test). These results suggest that there were significantly less slow kinetics TTX-sensitive sodium currents (likely Nav1.7) remaining in the second spike after recovery from the first discharge in Aβ-fibre LTMs in OA animals.

Therefore, shortened refractory interval in OA Aβ-fibre LTMs might be a result of the shift towards more prominent fast kinetics TTX-sensitive currents in these neurons.

5.3.3. Changes in the slow process of recovery mechanisms from repetitive firings in OA animals

Once the train frequency exceeded the maximum frequency a neuron could follow, conduction failure occured. Conduction failure in terms of fibre following ratio was fitted well with a single exponential decay function. We determined the quality of the fit by calculating the $R^2$ value of the fitting curve. The $R^2$ value was 0.99 ± 0.001 in all control neurons stimulated from the dorsal root ($N$ = 99). No difference was found in the $R^2$ value between control neurons and OA neurons ($R^2$ = 0.99 ± 0.001, $N$ = 111; $P$ = 0.301).

In control animals, the maximum FFF along the dorsal root for each type of neurons was as follows: Aβ-fibre HTM, 149.4 ± 18.12 Hz, $N$ = 15, slowly adapting neurons 341.2 ± 43.81 Hz, $N$ = 4, hair follicle neurons 343.2 ± 25.62 Hz, $N$ = 13, glabrous rapidly adapting neurons 353.6 ± 25.22 Hz, $N$ = 15, Pacinian neurons 355.8 ± 28.73 Hz, $N$ = 21, and muscle spindle neurons 574.6 ± 19.12 Hz, $N$ = 35 (Figure. 4A). It was found that the Aβ-fibre HTM had significantly lower maximum FFF than other neuronal types (one way ANOVA with Bonferroni's post hoc test, $P < 0.001$), whereas muscle spindle neurons had significantly higher maximum FFF than other neuronal types (one way ANOVA with Bonferroni's post hoc test, $P < 0.001$). No difference was found among hair follicle, Pacinian, slowly adapting or glabrous rapidly adapting neurons. In OA animals, it was found that there were significant increases in the maximum FFF in Aβ-fibre LTMs in OA animals. The maximum frequency was 440.0 ± 16.55 Hz in control animals ($N$ = 88), and was increased to 486.1 ± 16.17 Hz in OA (N=94; $P$ = 0.041, Mann-Whitney $U$-test; Figure. 4B). The greatest changes were observed in Pacinian neurons (355.8 ± 28.73 Hz, $N$ = 21 in control vs. 443.6 ± 25.32 Hz, $N$ = 21 in OA; $P$ = 0.027) and muscle spindle neurons (574.6 ± 19.12 Hz, $N$ = 35 in control vs. 632.1 ± 14.22 Hz, $N$ = 38 in OA, $P$ = 0.017). Differences in the other types of neuron, including Aβ-fibre HTMs, did not reach significance (data not shown).

During train stimulation, when the stimulation frequency was increased, the interspike interval was approaching the refractory interval, which could lead to failure of spike electrogenesis. However, the interspike interval at which conduction failure initiated was actually several times the refractory interval. For example, estimated minimum interspike interval without conduction failure was 6.7, 2.9, 2.9, 2.8, 2.8 and 1.7 ms in HTMs, slowly adapting neurons, hair follicle neurons, glabrous rapidly adapting neurons, Pacinian neurons and muscle spindle neurons, respectively, which was 3.8, 2.9, 2.6, 2.8, 3.5 and 3.4 times the respective refractory interval.

In order to determine whether the conduction failure was due to the limiting effect of the refractory period, we compared the decay in the maximum rising rate of spikes elicited by the 200ms train at the maximum FFF with the decay in the second spike elicited by the paired pulse at 2-3 times refractory interval. To determine the decay induced by train stimulation, maximum rising rate of all evoked spikes in a selective sweep were averaged and then standardized according to the initial spike. In control animals, 42 recordings stimulated with interspike intervals equivalent to 2-3 times the refractory interval were included in this analysis (11 HTMs, 5 hair follicle neurons, 9 Pacinian neurons, 1 glabrous rapidly adapting neuron, and 16 muscle spindle neurons). The decay in the maximum rising rate in the second spike was 0.85 ± 0.014 from the paired pulse protocol ($N$ = 42), which was significantly less than the decay calculated

from the train stimulation (0.77 ± 0.007, $N = 97$; $P < 0.0001$, Student's $t$-test; Figure. 4C). This result strongly suggests that the additional decay from the train pulse protocol was due to other mechanisms besides a fast inactivation mechanism of sodium currents identified by the paired pulse protocol. We speculated that slow inactivation of sodium currents may be one of the candidate mechanisms, as prolonged repetitive stimulation has been shown to induce slow inactivation of sodium currents (Fleidervish et al., 1996).

Thus, we compared the decay in maximum rising rate in sweeps with the same stimulation frequency between control and OA neurons. It was decided that the stimulation frequencies were in the range of 515-588 Hz for muscle spindle neurons, and in the range of 280-340 Hz for the rest of the Aβ-fibre LTMs. Only recordings having the selected sweeps were chosen. The decay in MRR in these sweeps in control animals was 0.83 ± 0.011 ($N = 60$), and was the same in OA (0.83 ± 0.011, $N = 60$; $P = 0.933$, Student's $t$-test; Figure. 4D). This result did not suggest a difference in the recovery of slow inactivation of sodium currents, at least for slow kinectics TTX-sensitive currents in Aβ-fibre LTMs in OA animals.

Our conclusion is that slow inactivation of sodium currents seemed not be different between control and OA animals, although it induced a greater decay in MRR in train spikes than in pair spikes.

5.3.4. Responses to repetitive stimuli from dorsal root axons vs. peripheral axons in

Aβ-fibre LTMs

The aim here was to determine whether the response to repetitive stimuli is different between the peripheral nerve (sciatic nerve) and the central nerve (dorsal root) in OA. In order to qualify for the study, each Aβ LTM included exhibited reliable recordings evoked from the dorsal root axon and its corresponding peripheral axon. Ideally, each DRG neuron can be evoked from its dorsal root axon and its peripheral axon. In fact, only some of recordings exhibited responses induced from both nerve ends. Some neurons exhibited only a sciatic nerve evoked AP but not a dorsal root evoked AP due to possible dorsal root injury during microsurgical procedure on the DRG prior to recording. Some neurons exhibited only a dorsal root evoked AP due to a variety of reasons including fiber damage during surgical procedures and poor contact of the stimulating electrode with certain portion of the sciatic nerve.

It has been reported that conduction velocity along the dorsal root is significantly slower than that along sciatic nerve (Villiere and McLachlan, 1996). Surprisingly, we did not see a difference between the response to repetitive stimuli along dorsal root and sciatic nerve in control animals. RIs were 0.79 ± 0.07 ms along dorsal root and 0.9 ± 0.07 ms along sciatic nerve in control Aβ LTMs ($N = 23$; paired $t$-test, $P = 0.165$; Figure. 5A). Maximum FFFs were 414.3 ± 32.01 Hz along dorsal root and 373.1 ± 26.65 Hz along sciatic nerve in control Aβ LTMs ($N = 18$; paired $t$-test, $P = 0.082$; Figure. 5A).

However, we saw a significant difference between the response to repetitive stimuli along dorsal root and sciatic nerve in OA animals. RIs were shorter along the dorsal root (0.62 ± 0.061 ms) than along the sciatic nerve (0.87 ± 0.073 ms) in OA Aβ LTMs ($N$ = 29; paired $t$-test, $P$ = 0.004; Figure. 5B). Higher maximum FFFs were observed with dorsal root stimulation (417.3 ± 30.05 Hz) than with the sciatic nerve stimulation (371.9 ± 32.92 Hz) in OA Aβ LTMs ($N$ = 24; paired $t$-test, $P$ = 0.047; Figure. 5B). These results suggest that central and peripheral axons might differ in their capacities to transmit repetitive firings in OA Aβ LTMs.

## 5.4. Discussion

### 5.4.1. Cell type specific response patterns to repetitive stimuli

We observed three characteristic patterns of response to repetitive firing in DRG neurons: nociceptor, LTM and proprioceptor patterns. Typical nociceptor pattern was observed only in Aβ-fibre HTMs, which was characterized by a Type I response to paired pulse stimuli and train stimulation, long RI over 1.2 ms and low following frequency less than 200 Hz. Typical LTM pattern was mainly observed in non-muscle spindle Aβ-fibre LTMs, which was characterized by Type I response to paired-pulse stimuli and train stimulation, short to medium RI less than 1.2 ms and medium to fast following frequency of around 300-400 Hz. Typical proprioceptor pattern was observed exclusively in muscle spindle neurons, which was characterized by Type II response to

paired-pulse stimuli and train stimulation, short RI less than 0.8 ms and high following frequency over 500 Hz.

Different patterns of response to repetitive stimuli characterized by differently sized residual action potentials during conduction failure in DRG neurons have been reported and explained in previous studies (Svaetichin, 1958;Ito and Saiga, 1959;Ito, 1959;Lu and Miletic, 1990;Luscher et al., 1994a;Luscher et al., 1994b;Djouhri et al., 2001;Fang et al., 2005). Type I response to either paired pulse or train stimulation is characterized by the appearance of a 20 – 30 mV residual AP. The residual AP is analogous to previously described non-medullated spike (Brock et al., 1953;Ito, 1959), which is the result of an AP propagating through the non-medullated segments of the T-junction but failing to invade the soma of a DRG neuron. Our stimulating protocols and the *in vivo* setting prevented us from differentiating noise from the medullated spike having amplitude that could be as low as 1 mV (Brock et al., 1953).

Cell morphological factors, such as length of axon stem of the pseudo-unipolar DRG neuron (Luscher et al., 1994b), diameter, branching and mylination status of the nerve fibre (Khodorov and Timin, 1975), have been simulated and shown to shape impulse propagation from the periphery to the spinal cord. It remains unknown whether there is substantial difference in the cell morphology, especially the T-junction structure among subtypes of Aβ-fibre neurons. Therefore, we cannot preclude that these

morphological differences might account for different patterns of response to repetitive stimuli in the present study. However, it is also possible that this difference in the reliability of spike invasion of the soma during repetitive firing is determined by different electrogensis mechanisms resulting from different assembly of ion channels, especially sodium and potassium channels. For example, increased $Na^+$ ion permeability of the soma and initial segment has been shown to facilitate spike invasion of the soma (Amir and Devor, 2003). Moreover, action potential configuration which is a result of overall summation of electrogenesis has been suggested as a reliable predictor of spike invasion of the soma. Cell type specificity in conduction failure depends on functional classification rather than morphological classification: neurons with long-duration somatic action potentials with a shoulder on the falling phase invariably have a relatively long refractory period; neurons with brief, smooth action potentials have relatively short refractory period regardless of conduction velocity (CV) (Stoney, 1990). Thus, we suggest that cell type specificity in both the dynamic of action potential genesis and the cell morphology collectively determine the response pattern to repetitive stimuli in neurons with different sensory modalities.

Neurotrophic factors render neurons different firing properties due to this regulatory effect on the expression of voltage-gated ion channels (Lesser et al., 1997). The cell type specific pattern of the response to repetitive firing in the present study

might imply a pattern of neurotrophic factor dependency in these neurons. TrkA, the receptor for nerve growth factor (NGF), is expressed in nociceptive and thermoceptive sensory neurons; TrkC, the high-affinity receptor for neurotrophin-3, is expressed in proprioceptive neurons; and TrkB, the receptor for brain derived neurotrophic factor (BDNF) and neurotrophin (NT)-4, is expressed in touch neurons (Huang and Reichardt, 2001;Moqrich et al., 2004).

5.4.2. Proposed ionic mechanisms for conduction failure in OA Aβ-fibre neurons

In naive animals, when the interspike interval was gradually shortened during paired pulse stimuli, the amplitude of the 2$^{nd}$ spike was gradually reduced, and the onset of the 2$^{nd}$ spike was gradually increased. In OA animals, RI was decreased in Aβ-fibre LTMs, especially in muscle spindle neurons, whereas it was increased in Aβ-fibre HTMs. Maximum FFF was increased in Pacinian neurons and muscle spindle neurons.

Ionic mechanisms for spike-frequency adaptation have been proposed as being due to changes in the dynamics of sodium, potassium and calcium currents during repetitive stimuli (Blair and Bean, 2003;Choi et al., 2007;Luscher et al., 1994a;Momin and McNaughton, 2009;Viana et al., 1993). The present experimental setting does not identify any detailed ionic mechanism. Thus, the following discussion is merely an explanation of possible ionic mechanisms underlying conduction failure in OA neurons. In our previous studies on the electrophysiological properties of single evoked AP in

Aβ-fiber LTMs, prominent changes were observed in the rising phase of the action potential at one month following model induction, including a longer rising time to peak, a wider duration of AP at base and a slower maximum rising rate (Wu and Henry, 2006;Wu and Henry, 2009). These changes were mainly associated with the phase dominated by sodium currents. Thus, it is very likely that changes in the dynamic of sodium currents also leads to changes in the conduction of the somatic spike in the same set of neurons.

From previous *in vivo* and *in vitro* studies on the distribution of voltage-gated sodium channel subunits in subgroups of DRG neurons (Djouhri et al., 2003a;Djouhri et al., 2003b;Fang et al., 2002;Rush et al., 1998;Fukuoka et al., 2008), we deduce the following patterns of sodium channel expression. Muscle spindle neurons express merely TTX-sensitive Nav1.6 and Nav1.1 channels; the majority of Aβ-fiber LTMs express TTX-sensitive Nav1.1, Nav1.6 and Nav1.7 channels, whereas a small portion of those neurons also co-express TTX-resistant Nav1.8 channels; Aβ-fiber HTMs express both TTX-sensitive and TTX-resistant species, including Nav1.1, 1.6, 1.7, 1.8 and Nav1.9 channels. The intensity of TTX-resistant sodium channel expressed in Aβ-fiber neurons, even nociceptive neurons, is much less than that of C- and Aδ-fiber neurons. During the action potential, TTX-sensitive sodium currents activate first, inactivate almost completely by the time of the peak, and are slow to recover (at least for Nav1.7).

Although TTX-resistant sodium currents activate slower, incompletely inactivate at the end of repolarization, they recover nearly completely in 4 ms following maximal inactivation (Blair and Bean, 2002). TTX-sensitive sodium currents are most effectively inactivated by repetitive stimuli, whereas TTX-resistant currents are effectively inactivated by a single steady depolarization (Blair and Bean, 2003). Therefore, decreased RI in muscle spindle neurons in OA animals predominantly reflects an increase in the recovery from fast inactivation of fast kinectics TTX-sensitive sodium currents (likely Nav1.6). An alternative explanation is that the re-expression of the fast priming embryonic TTX-sensitive Nav1.3, as documented in neuropathic states (Black et al., 1999;Cummins and Waxman, 1997;Fukuoka et al., 2008). However, the expression of Nav1.3 channels in DRG neurons has yet to be studied in OA animals. Unlike LTMs, double pulse stimulation in nociceptive neurons is mainly governed by the fast inactivation of the dominating TTX-resistant current. Increased RI in Aβ-fibre HTMs might reflect a decrease in the recovery from fast inactivation of TTX-resistant currents.

The minimal interval defining the maximum FFF is between 1.5-2.8 ms in Aβ-fibre LTMs, and about 7 ms in Aβ-fibre HTMs. During the lowest intervals, the recovery from fast inactivation is not complete for TTX-sensitive currents, but is complete for TTX-resistant currents. Our data show that a train of stimuli effectively promotes slow inactivation in sodium currents. However, our data do not support a role

of slow inactivation mechanism of sodium currents in the increased maximum FFF in Aβ-fibre LTMs in OA. The increase might be due to the same mechanism responsible for the shortened refractory interval.

5.4.3. Differential impulse conduction along peripheral and central axons in OA Aβ-fibre neuron

The degree of conduction failure was comparable along peripheral nerve and along central nerve in naive control animals. Interestingly, a difference was observed in the conduction failure between peripheral and central processes in the OA model.

Our observation in naive animals agrees with the details provided in previous studies regarding the comparison of the conduction failure along both peripheral and central processes (Lu and Miletic, 1990;Luscher et al., 1994b). Lu and Miletic (1990) reported that most of the response patterns to stimulation of their peripheral and central processes were "in the same manner", although they also mentioned that 4 out of 10 neurons were different. However, the apparently different orders of FFF from either process (such as, 200 Hz vs. 2-10 Hz) raised a question about the integrity of both process. It is known that subtle fibre injury during surgical preparation for recordings could severely reduce the capability of an axon to follow high frequency firing, which was not discussed in their study.

One possible explanation for the increased discrepancy of conduction failure between peripheral and central processes in OA could be the differential regulation of neurotrophin expression between peripheral and central nerve after nerve injury. A fundamental difference in the immune response initiated by nerve injury between peripheral and central mylinated fibres has been well documented, involving distinct patterns of immune cell infiltration, cytokine release and adaptive transformation of myelin forming cells in peripheral and central nerves (Fenrich and Gordon, 2004). The distinct immune responses trigger distinct molecular events. For example, up-regulation of NGF expression following nerve axotomy was found exclusively in peripheral but not in central myelinated fibres (Avellino et al., 1995). As a result, peripheral and central nerve could take up different assemblies of ion channels following the same initiator, such as knee afferent injury, due to a different neurotrophin milieu.

Peripheral and central mylinated fibres are also different in myelination, including distinct types of myelin secreting cells, distinct myelin wrapping patterns (Sherman and Brophy, 2005) and different myelin thickness. However, this degree of difference seems not to account for the discrepancy between peripheral and central processes we observed in OA animals. As in naive animals, these differences existed but did not lead to significant difference in conduction failure between peripheral and central processes.

5.4.4. Conclusions

During the progress of OA, there were significant changes in the repetitive firing behaviors in heavily myelinated Aβ-fiber DRG neurons. Our data suggests that these changes might be important in the initiation and maintenance of central plasticity, and thus contribute to chronic pain in OA.

**5.5. Tables, Figures**

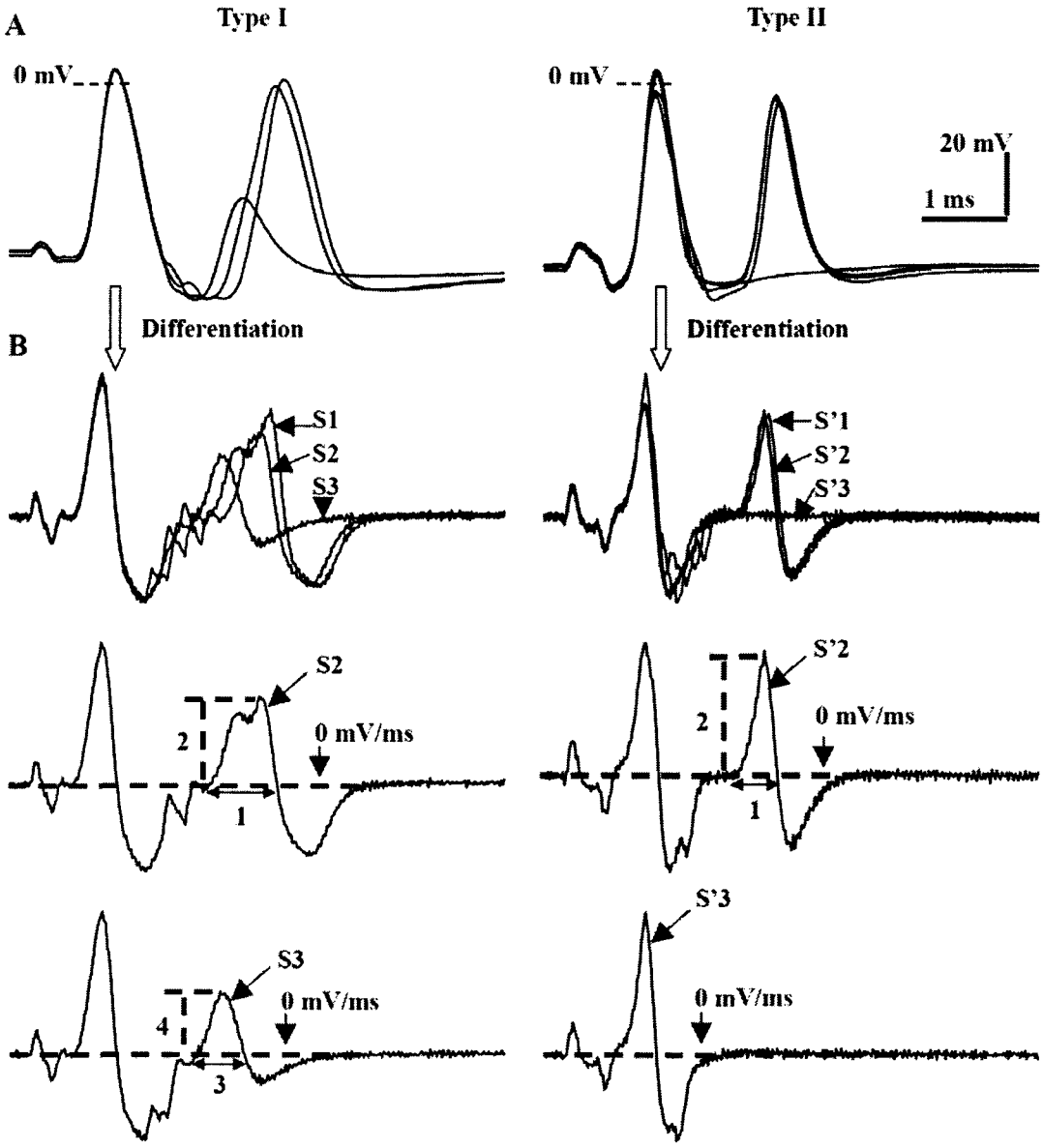


**Figure 5.1. Types of response of Aβ-fiber DRG neurons to paired pulses to dorsal roots.** Figure. 1A shows recordings from a glabrous rapidly adapting neuron (left panel), and in a muscle spindle neuron (right panel) in control each stimulated with paired pulses.

These responses represent two types of response to paired pulse stimulation in Aβ-fiber neurons. Type I response is characterized by a variable amplitude and residue of the second action potential as it fails, whereas Type II response is characterized by an all-or-none response of the second action potential. Figure. 1B shows differentials of the original recording in Figure. 1A. The sweeps before and after failure of the second action potential are shown separately. Left panels represent differentiated recordings and corresponding measurements typical for Type I response, and right panels for Type II response. Parameters 1-4 are measurements of the rise time and the maximum rising rate of the second spike and the residual AP.

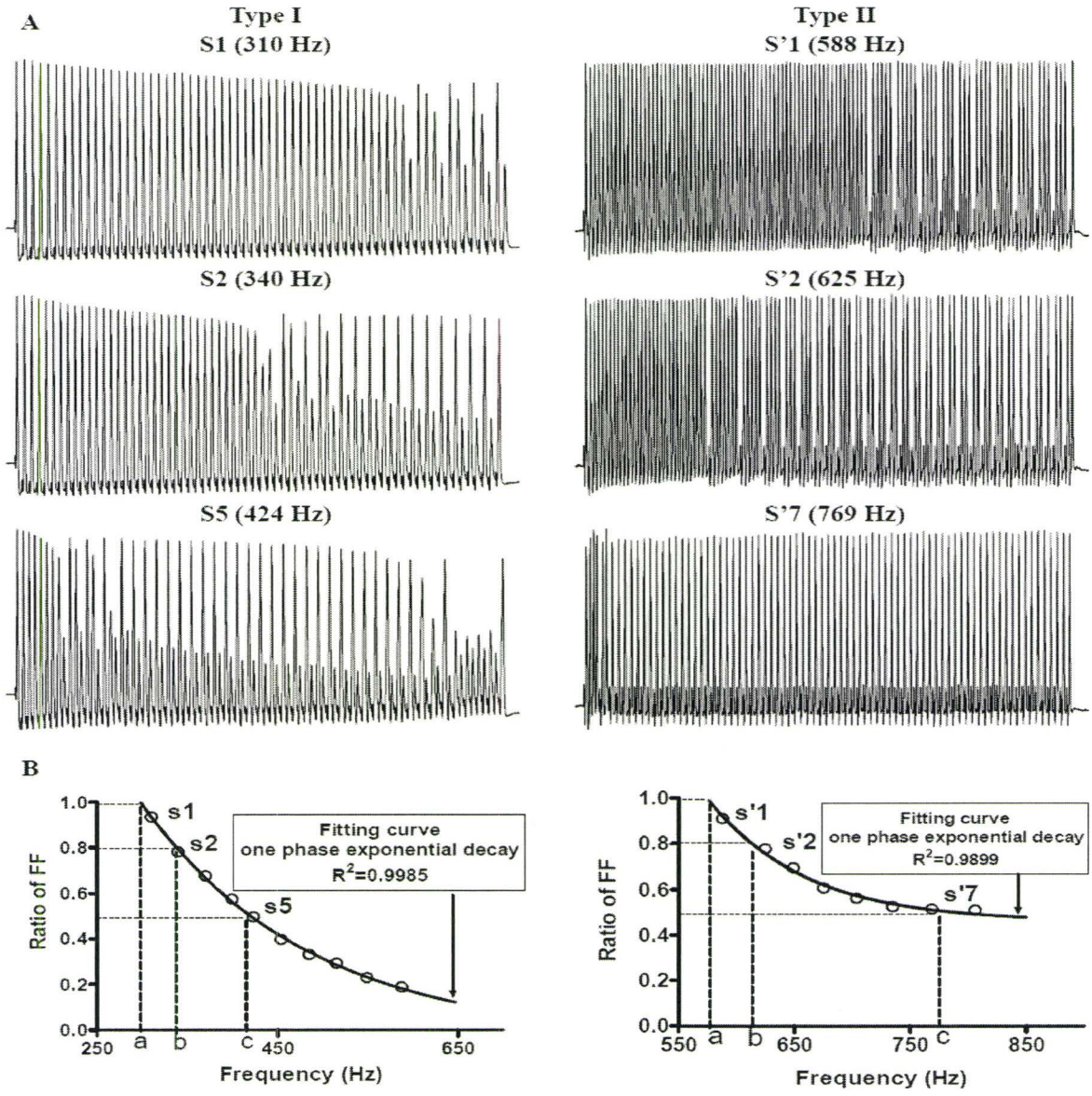


**Figure 5.2. Patterns of response and measurements from recordings resulting from train pulse stimulation along dorsal root.** Figure. 2A shows actual recordings from a glabrous rapidly adapting neuron (left panel), and in a muscle spindle neuron (right panel) in control stimulated with a 200 ms pulse train of Type I and Type II neurons. Three

selective recordings in each neuron (top, middle, and bottom in the panel) were actual sweeps with ratio of fiber following close to 1, 0.8, and 0.5, respectively. Figure. 2B shows two curves of frequency following from the recordings in the glabrous rapidly adapting and the muscle spindle neurons stimulated with train pulses. It also shows how the maximum (a), 80% (b) and 50% (c) fiber following frequencies were determined from the curve. The curve of frequency following was plotted for a range of frequencies which was later fitted with the one phase exponential decay function. $R^2$ values shown represent the goodness of fitting.

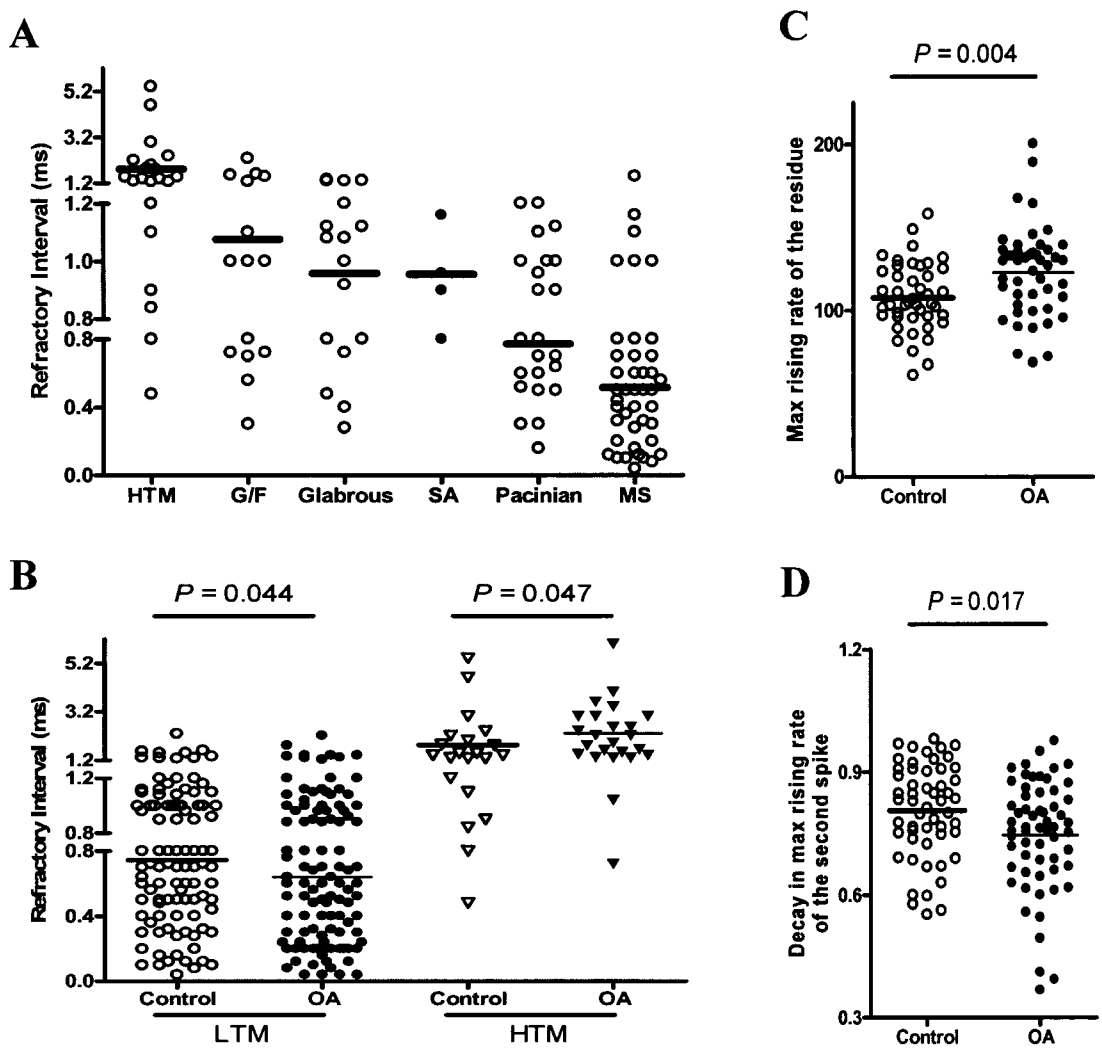


**Figure 5.3. Changes in the response to paired pulse stimulation in Aβ-fiber low threshold and high threshold mechanoreceptors in the OA model.** Each dot represents a recording from a neuron. In each case the median (horizontal line) is superimposed. (A) In naive animals, the refractory interval in high threshold mechanoreceptors (HTMs) is the longest, whereas that of muscle spindle (MS) neurons is

the shortest. "G/F", "Glabrous" and "Pacinian" represent hair follicle neurons, glabrous rapidly adapting neurons and Pacinian neurons, respectively. (B) The refractory interval was shorter in low threshold mechanoreceptors (LTMs) in OA animals ($N$ = 104 in control vs. $N$ = 112 in OA, Mann-Whitney $U$-test), but was increased in HTMs in OA animals ($N$ = 21 in control vs. $N$ = 24 in OA animals, Mann-Whitney $U$-test). (C) The maximum rising rate of the residual AP when the second spike fails was increased in OA animals ($N$ = 44 in control vs. $N$ = 46 in OA animals, Student's $t$-test). (D) The degree of decay in maximum rising rate of the second spike was greater in OA animals ($N$ = 54 in control vs. $N$ = 60 in OA animals, Mann-Whitney $U$-test).

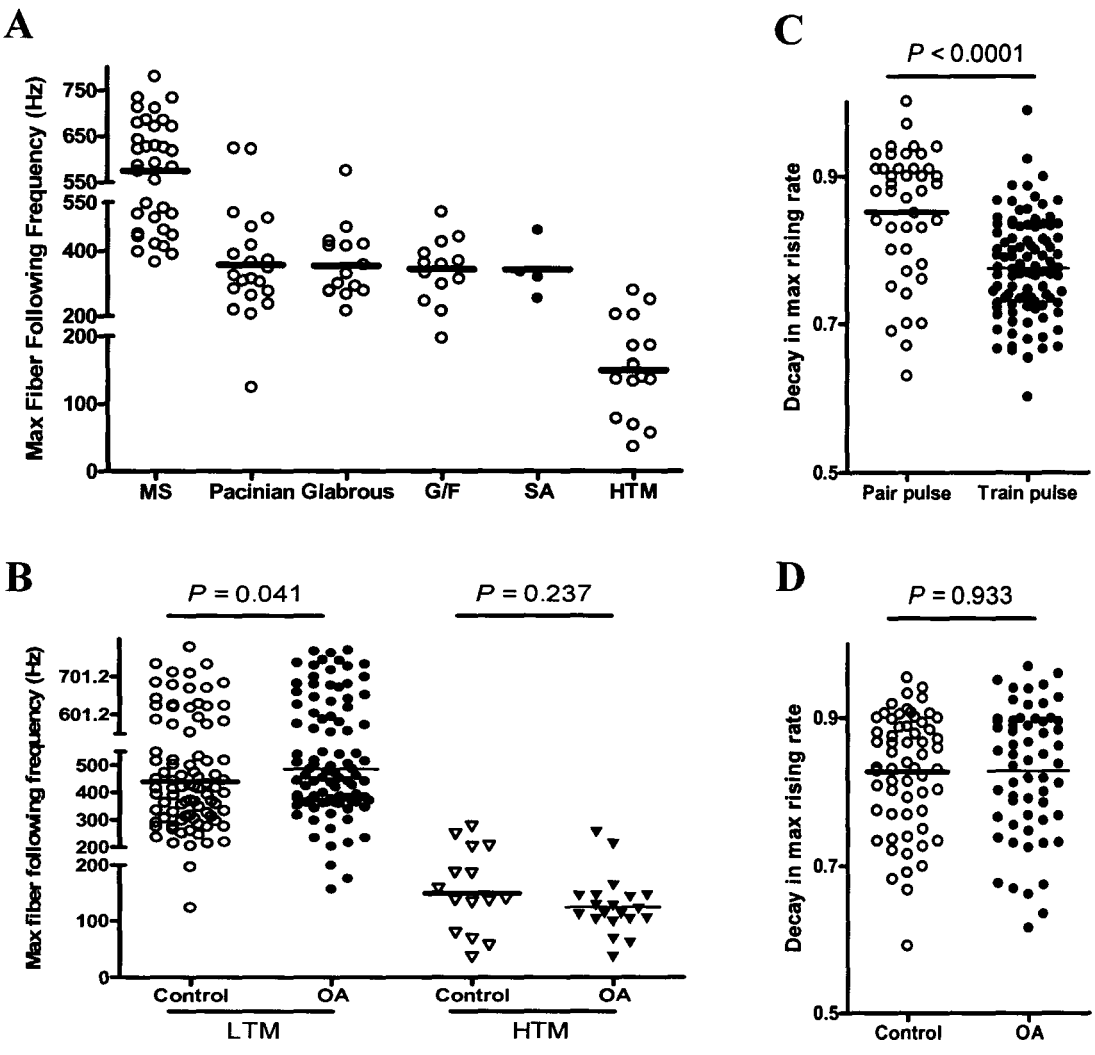


**Figure 5.4. Changes in the response to train stimulation in A beta low threshold and high threshold mechanoreceptors in the OA model.** Labeling is otherwise the same as in Figure 3. (A) Maximum fiber following frequencies (FFF) in various neuronal types are shown. (B) The maximum FFF was increased in LTMs in OA animals ($N$ = 88 in control vs. $N$ = 94 in OA animals, Mann-Whitney $U$-test), but was unaltered in HTMs in OA animals ($N$ = 15 in control vs. $N$ = 20 in OA animals, Mann-Whitney $U$-test). (C) In

naive animals, the decay in maximum rising rate in train pulse was greater than in paired pulse recordings ($N = 42$ of paired pulse recordings vs. $N = 97$ of train pulse recordings, Student's *t*-test). (D) The decay in MRR in sweeps at the same selected stimulation frequencies was not different in control from that of OA animals ($N = 60$ in control vs. $N = 60$ in OA animals, Student's *t*-test).

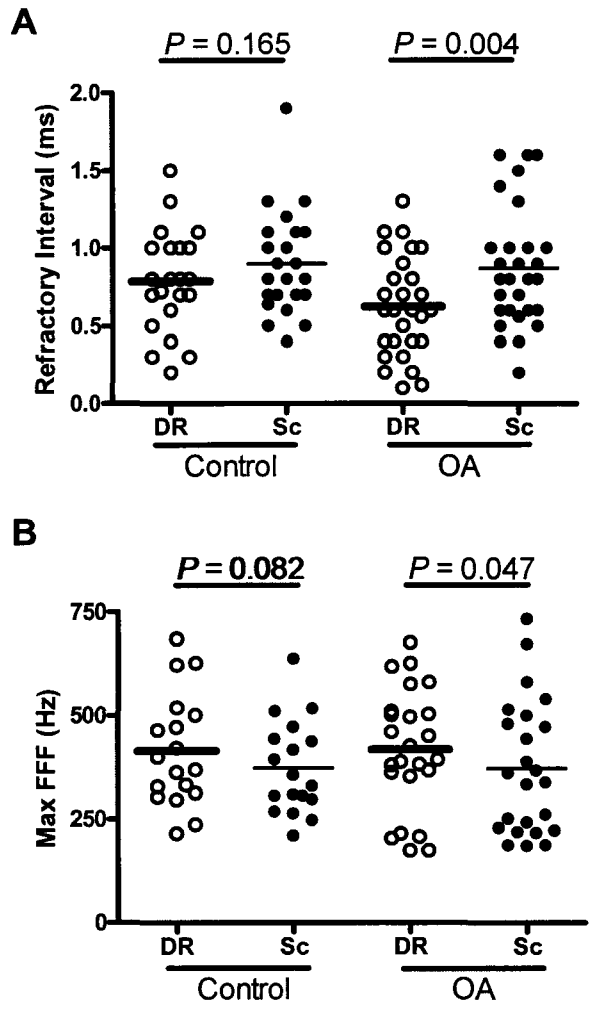


**Figure 5.5. Differentiation of the response to repetitive stimulation from the central and peripheral axon of Aβ-fiber low threshold mechanorecetors in osteoarthritis.** Each dot represents a recording from a neuron. In each case the median (horizontal line) is superimposed. Paired *t*-tests were used in the comparisons between dorsal root (DR) and sciatic nerve (Sc) elicited measurements. In naive control Aβ-fiber low threshold mechanorecetors, there was no significant difference between repetitive firing along

dorsal root and sciatic nerve in terms of refractory interval and maximum fiber following frequency (FFF). However, in OA neurons, significant discrepancies between dorsal root and sciatic nerve were seen, in term of two conduction-related measurements, refractory interval and maximum fiber following frequency.

## References

Amir R, Devor M (2003) Electrical excitability of the soma of sensory neurons is required for spike invasion of the soma, but not for through-conduction. Biophys J 84:2181-2191.

Avellino AM, Hart D, Dailey AT, MacKinnon M, Ellegala D, Kliot M (1995) Differential macrophage responses in the peripheral and central nervous system during wallerian degeneration of axons. Exp Neurol 136:183-198.

Beyreuther BK, Freitag J, Heers C, Krebsfanger N, Scharfenecker U, Stohr T (2007a) Lacosamide: a review of preclinical properties. CNS Drug Rev 13:21-42.

Beyreuther BK, Geis C, Stohr T, Sommer C (2007b) Antihyperalgesic efficacy of lacosamide in a rat model for muscle pain induced by TNF. Neuropharmacology 52:1312-1317.

Black JA, Cummins TR, Plumpton C, Chen YH, Hormuzdiar W, Clare JJ, Waxman SG (1999) Upregulation of a silent sodium channel after peripheral, but not central, nerve injury in DRG neurons. J Neurophysiol 82:2776-2785.

Blair NT, Bean BP (2002) Roles of tetrodotoxin (TTX)-sensitive Na+ current, TTX-resistant Na+ current, and Ca2+ current in the action potentials of nociceptive sensory neurons. J Neurosci 22:10277-10290.

Blair NT, Bean BP (2003) Role of tetrodotoxin-resistant Na+ current slow inactivation in adaptation of action potential firing in small-diameter dorsal root ganglion neurons. J Neurosci 23:10338-10350.

Brock LG, Coombs JS, Eccles JC (1953) Intracellular recording from antidromically activated motoneurones. J Physiol 122:429-461.

Choi JS, Dib-Hajj SD, Waxman SG (2007) Differential slow inactivation and use-dependent inhibition of Nav1.8 channels contribute to distinct firing properties in IB4+ and IB4- DRG neurons. J Neurophysiol 97:1258-1265.

Cummins TR, Aglieco F, Renganathan M, Herzog RI, Dib-Hajj SD, Waxman SG (2001) Nav1.3 sodium channels: rapid repriming and slow closed-state inactivation display quantitative differences after expression in a mammalian cell line and in spinal sensory neurons. J Neurosci 21:5952-5961.

Cummins TR, Waxman SG (1997) Downregulation of tetrodotoxin-resistant sodium currents and upregulation of a rapidly repriming tetrodotoxin-sensitive sodium current in small spinal sensory

neurons after nerve injury. J Neurosci 17:3503-3514.

Dalal A, Tata M, Allegre G, Gekiere F, Bons N, be-Fessard D (1999) Spontaneous activity of rat dorsal horn cells in spinal segments of sciatic projection following transection of sciatic nerve or of corresponding dorsal roots. Neuroscience 94:217-228.

Djouhri L, Dawbarn D, Robertson A, Newton R, Lawson SN (2001) Time course and nerve growth factor dependence of inflammation-induced alterations in electrophysiological membrane properties in nociceptive primary afferent neurons. J Neurosci 21:8722-8733.

Djouhri L, Fang X, Okuse K, Wood JN, Berry CM, Lawson SN (2003a) The TTX-resistant sodium channel Nav1.8 (SNS/PN3): expression and correlation with membrane properties in rat nociceptive primary afferent neurons. J Physiol 550:739-752.

Djouhri L, Lawson SN (2004) Abeta-fiber nociceptive primary afferent neurons: a review of incidence and properties in relation to other afferent A-fiber neurons in mammals. Brain Res Brain Res Rev 46:131-145.

Djouhri L, Newton R, Levinson SR, Berry CM, Carruthers B, Lawson SN (2003b) Sensory and electrophysiological properties of guinea-pig sensory neurones expressing Nav 1.7 (PN1) Na+ channel alpha subunit protein. J Physiol 546:565-576.

Fang X, Djouhri L, Black JA, Dib-Hajj SD, Waxman SG, Lawson SN (2002) The presence and role of the tetrodotoxin-resistant sodium channel Na(v)1.9 (NaN) in nociceptive primary afferent neurons. J Neurosci 22:7425-7433.

Fang X, McMullan S, Lawson SN, Djouhri L (2005) Electrophysiological differences between nociceptive and non-nociceptive dorsal root ganglion neurones in the rat in vivo. J Physiol 565:927-943.

Fenrich K, Gordon T (2004) Canadian Association of Neuroscience review: axonal regeneration in the peripheral and central nervous systems--current issues and advances. Can J Neurol Sci 31:142-156.

Fields RD (2006) Nerve impulses regulate myelination through purinergic signalling. Novartis Found Symp 276:148-158.

Fleidervish IA, Friedman A, Gutnick MJ (1996) Slow inactivation of Na+ current and slow cumulative spike adaptation in mouse and guinea-pig neocortical neurones in slices. J Physiol 493 ( Pt 1):83-97.

Fukuoka T, Kobayashi K, Yamanaka H, Obata K, Dai Y, Noguchi K (2008) Comparative study of the distribution of the alpha-subunits of voltage-gated sodium channels in normal and axotomized rat dorsal root ganglion neurons. J Comp Neurol 510:188-206.

Herzog RI, Cummins TR, Ghassemi F, Dib-Hajj SD, Waxman SG (2003) Distinct repriming and closed-state inactivation kinetics of Nav1.6 and Nav1.7 sodium channels in mouse spinal sensory neurons. J Physiol 551:741-750.

Huang EJ, Reichardt LF (2001) Neurotrophins: roles in neuronal development and function. Annu Rev Neurosci 24:677-736.

Ito M (1959) An analysis of potentials recorded intracellularly from the spinal ganglion cell. Jpn J Physiol 9:20-32.

Ito M, Saiga M (1959) The mode of impulse conduction through the spinal ganglion. Jpn J Physiol 9:33-42.

Jeftinija S, Urban L (1994) Repetitive stimulation induced potentiation of excitatory transmission in the rat dorsal horn: an in vitro study. J Neurophysiol 71:216-228.

Kadekaro M, Crane AM, Sokoloff L (1985) Differential effects of electrical stimulation of sciatic nerve on metabolic activity in spinal cord and dorsal root ganglion in the rat. Proc Natl Acad Sci U S A 82:6010-6013.

Khodorov BI, Timin EN (1975) Nerve impulse propagation along nonuniform fibres. Prog Biophys Mol Biol 30:145-184.

Lawson SN, Crepps BA, Perl ER (1997) Relationship of substance P to afferent characteristics of dorsal root ganglion neurones in guinea-pig. J Physiol 505:177-191.

Lesser SS, Sherwood NT, Lo DC (1997) Neurotrophins differentially regulate voltage-gated ion channels. Mol Cell Neurosci 10:173-183.

Lu GW, Miletic V (1990) Responses of type A cat spinal ganglion neurons to repetitive stimulation of their central and peripheral processes. Neuroscience 39:259-270.

Luscher C, Streit J, Lipp P, Luscher HR (1994a) Action potential propagation through embryonic dorsal root ganglion cells in culture. II. Decrease of conduction reliability during repetitive stimulation. J Neurophysiol 72:634-643.

Luscher C, Streit J, Quadroni R, Luscher HR (1994b) Action potential propagation through embryonic

dorsal root ganglion cells in culture. I. Influence of the cell morphology on propagation properties. J Neurophysiol 72:622-633.

Momin A, McNaughton PA (2009) Regulation of firing frequency in nociceptive neurons by pro-inflammatory mediators. Exp Brain Res 196:45-52.

Moqrich A, Earley TJ, Watson J, Andahazy M, Backus C, Martin-Zanca D, Wright DE, Reichardt LF, Patapoutian A (2004) Expressing TrkC from the TrkA locus causes a subset of dorsal root ganglia neurons to switch fate. Nat Neurosci 7:812-818.

Pitcher GM, Henry JL (2004) Nociceptive response to innocuous mechanical stimulation is mediated via myelinated afferents and NK-1 receptor activation in a rat model of neuropathic pain. Exp Neurol 186:173-197.

Pitcher GM, Henry JL (2008) Governing role of primary afferent drive in increased excitation of spinal nociceptive neurons in a model of sciatic neuropathy. Exp Neurol 214:219-228.

Rush AM, Brau ME, Elliott AA, Elliott JR (1998) Electrophysiological properties of sodium current subtypes in small cells from adult rat dorsal root ganglia. J Physiol 511 ( Pt 3):771-789.

Seltzer Z, Cohn S, Ginzburg R, Beilin B (1991) Modulation of neuropathic pain behavior in rats by spinal disinhibition and NMDA receptor blockade of injury discharge. Pain 45:69-75.

Sherman DL, Brophy PJ (2005) Mechanisms of axon ensheathment and myelin growth. Nat Rev Neurosci 6:683-690.

Sotgiu ML, Biella G, Riva L (1994) A study of early ongoing activity in dorsal horn units following sciatic nerve constriction. Neuroreport 5:2609-2612.

Stoney SD (1990) Limitations on impulse conduction at the branch point of afferent axons in frog dorsal root ganglion. Exp Brain Res 80:512-524.

Svaetichin G (1958) Component analysis of action potentials from single neurons. Exp Cell Res 14:234-261.

Udina E, Furey M, Busch S, Silver J, Gordon T, Fouad K (2008) Electrical stimulation of intact peripheral sensory axons in rats promotes outgrowth of their central projections. Exp Neurol 210:238-247.

Viana F, Bayliss DA, Berger AJ (1993) Multiple potassium conductances and their role in action potential repolarization and repetitive firing behavior of neonatal rat hypoglossal motoneurons. J

Neurophysiol 69:2150-2163.

Vilin YY, Ruben PC (2001) Slow inactivation in voltage-gated sodium channels: molecular substrates and contributions to channelopathies. Cell Biochem Biophys 35:171-190.

Villiere V, McLachlan EM (1996) Electrophysiological properties of neurons in intact rat dorsal root ganglia classified by conduction velocity and action potential duration. J Neurophysiol 76:1924-1941.

Wu Q, Henry JL (2009) Delayed onset of changes in soma action potential genesis in nociceptive A-beta DRG neurons in vivo in a rat model of osteoarthritis. Mol Pain 5:57.

Wu Q, Henry JL (2006) Electrophysiological properties of dorsal root ganglion neurons in vivo in a derangement rat model of osteoarthritis. pp http://www.abstractsonline.com/viewer/viewAbstractPrintFriendly.asp?CKey={62CC52E5-A052-4CBF-993D-078F39D1E5AD}&SKey={0FC269E7-500A-45A8-8180-8C63E377FA93}&MKey={D1974E76-28AF-4C1C-8AE8-4F73B56247A7}&AKey={3A7DC0B9-D787-44AA-BD08-FA7BB2FE9004}.

# CHAPTER 6.

# General Discussion

Osteoarthritis (OA) is the most common form of arthritis and it is a major health issue. It is estimated that by age 65 over 80% of adults will develop radiographic evidence of OA. In Canada, about 10% of adults are affected. Pain is the major complaint of patients with OA, and pain is more disabling than loss of joint function. Various therapeutic approaches are available to treat OA pain, and the management strategy starts with nonpharmacologic interventions (e.g. diet, exercise, bracing and corrective footwear), followed by pharmacologic means (e.g. non-steriodal anti-inflammatory drugs (NSAIDs), opioids, psychotropic drugs, intra-articular steroids and hyaluronic acid), and ultimately by surgical intervention (e.g. arthroscopic debridement and joint replacement). Yet, the effectiveness of existing drug therapies for OA pain is poor, with only moderate effectiveness. Moreover, there is a lack of effective pain therapies that have a known mechanistic basis of action. A review of the literature revealed a number of evidence-based hypotheses regarding the etiology of OA pain. These mechanisms tend to focus on changes in excitability or activation of nerve terminals in the joint or on central sensitization, including peripheral mechanisms proposing activation of sensitized nociceptors in the knee by local inflammation (McDougall et al., 2006;Schaible and Schmidt, 1985;Schuelert and McDougall, 2006), bone marrow lesions or microfractures and increased intra-osseous pressure (Mach et al., 2002), as well as central mechanisms proposing altered spinal sensory processing (Felson,

2005;Kidd, 2006;Niv et al., 2003;Rowbotham M.C et al., 2006). However these divergent hypotheses have not led to any unified theory of OA pain. Furthermore, none can account for the relatively poor management of OA pain by currently available analgesics, none can explain the lack of strict correlation between structural loss and the severity of the pain, the loss of proprioception in people with OA, or the commonness of referred pain to areas beyond the arthritic joint in people with OA.

Therefore, the current thesis project was designed to investigate changes in nociceptive mechanisms in a recently developed rodent model of OA. The focus was on possible changes in primary sensory neurons. This was because these neurons have been shown to undergo changes in animal models of other types of chronic pain, yet a survey of the literature revealed a lack of any in-depth study on possible changes in these neurons in an animal model of OA.

## 6.1. Novel hypotheses of the cause of OA sensory deficits initiated from the deranged knee

I propose that OA sensory deficits including the pain and the loss of proprioception are due to a neurological disorder resulting from changes in the properties of large diameter heavily myelinated primary afferent neurons that normally serve a non-nociceptive function.

### 6.1.1. OA pain has a neuropathic component

Based on the results of my thesis research I propose that OA pain has a neuropathic component. Neuropathic pain is initiated or caused by a primary lesion or dysfunction in the nervous system, and is one of the two main forms of chronic pain, the other being inflammatory pain. There are continuing efforts to understand neural mechanisms of the pain in OA (reviewed in Hunter et al., 2008;McDougall, 2006;Kidd, 2006). One important question is whether OA pain should be considered a neuropathic or an inflammatory pain. Our data presented in Chapter 2 showed that barely any changes were found in C- or Aδ-fiber neurons in OA rats, whereas significant changes in action potential (AP) configurations were in Aβ-fiber non-nociceptive low-threshold mechanoreceptors (LTMs). These findings are strongly supportive of the hypothesis that OA pain has a neuropathic component, as the pattern of prominent changes in large Aβ-fiber neurons and less prominent or no change in small C-fiber neurons is commonly seen in neuropathic models of chronic pain, and is rarely seen in inflammation models of chronic pain. More evidence regarding changes in AP configuration in dorsal root ganglia (DRG) neurons in various neuropathic and inflammation models of chronic pain is provided in Chapter 1. There is some further evidence of a neuropathic component in OA pain and is described in the next two paragraphs.

Histological evidence reveals an injury of the primary sensory neurons during the progress of OA. Activating transcription factor-3 (ATF-3), a marker of neuropathy

(Tsujino et al., 2000), is significantly increased in the $L_5$ DRG one week following mono iodoacetate (MIA) injection into the knee joint, and remains increased for 5 weeks (Ivanavicius et al., 2007). The up-regulation of activating transcription factor-3 (ATF-3) in specific DRGs agrees with the anatomy of the innervation of the knee joint. The DRGs that manifest most changes likely innervate medial and lateral compartments of the knee joint, where significant histopathological changes are also identified. Potential mechanisms of nerve injury might be related to osteoclast-induced injury and mechanical compression (Ivanavicius et al., 2007).

Pharmacological evidence shows that the pain in OA responds better to therapeutic drugs primary for neuropathic pain, rather than to anti-inflammatory drugs. Pain in early stage OA is sensitive to NSAIDs, such as cyclooxygenase (COX)-2 inhibitors. However, with the progression of OA, the responsiveness to NSAIDs is lost (Bove et al., 2003;Pomonis et al., 2005;Fernihough et al., 2004;Ivanavicius et al., 2007). In contrast, drugs typically used to relieve experimental and clinical neuropathic pain, such as gabapentin and amitriptyline are effective to reverse OA sensory deficits throughout the entire time course (Ivanavicius et al., 2007).

6.1.2. OA pain is progressive

OA is a chronic and progressive disorder that develops longitudinally in time (Oddis, 1996). OA is accompanied by alterations in sensory function, including pain.

There is an early predictable dull, aching, throbbing "background" pain. During the progression of OA, pain evolves from this "background" pain that is use-related in early OA (Kidd, 2006) into unpredictable short episodes of intense pain on top of the "background" pain in advanced OA (Hawker et al., 2008).

Our data presented in Chapter 2 and Chapter 3 show that Aß-fiber LTMs undergo significant changes one month following the model induction when histopathological changes of the knee joint and the nocifensive behaviors of the affected lower limb favor OA. Importantly, Aβ-fiber HTMs begin to manifest significant changes between one and two months after model induction. These data provide the neuronal basis in support of the concept that the pain in OA is dynamic and progressive.

Detailed mechanisms of the progression of the pain in OA remain largely unknown. We speculate that they might be related to changes in the chemical environment that is bathing primary sensory neurons. Changes in the host immune response in the peripheral nervous system (PNS) that is initiated by damages to knee joint afferents (nociceptive and/or proprioceptive) may also account for the pathogenesis of OA pain. This issue is also covered in more detail in Chapter 2.

6.1.3. Chronic pain in OA develops as a disease different from OA rather than being a symptom of OA

Recent advances have led to our understanding of pain as a process rather than a phenomenon (Stucky et al., 2001). The earliest pains are brought about by a set of processes that trigger additional mechanisms, including plastic changes in the nervous system. Thus, those processes that underlie acute pain can eventually trigger mechanisms that lead to chronic pain, where pain becomes unnecessary and debilitating (Woolf and Salter, 2000). In the past, it was not understood that to treat a disease-related pain we need to treat the mechanisms that produce the pain, rather than just the disease itself. Previous thought was that if the disease were treated successfully, the pain would disappear. This is not consistent with current thought among pain specialists, who would cite phantom limb pain as a striking example; the pain persists even after amputation of the affected site (Flor, 2003;Haigh et al., 2003). Chronic neuropathic pain is thus seen as a disorder of the nervous system. In osteoarthritic conditions, there is an obvious relationship between OA and the symptoms of OA. However, OA symptoms, in particular, pain and loss of proprioception, cannot be predicted from radiologic changes (Hannan et al., 2000). Knee injury might initiate two distinct yet interacting processes, one leading to sensory plasticity and the other to cartilage degeneration and remodeling of subchondral bone. The concept that the pain in OA is a disease different from OA rather than a symptom of OA has profound therapeutic implications. It provides a novel perspective to examine some difficult

decisions in OA patients, such as whether or not to recommend exercise. Exercise has been proven to preserve joint function in OA patients. However, exercise also worsens histopathological changes in the joint (Appleton et al., 2007b) and initiates peripheral and central sensitization, which intensifies the pain in OA.

6.1.4. Statements of our hypotheses for OA sensory deficits

Changes occur in primary afferents, but they are in the large diameter heavily myelinated neurons not in the small diameter lightly myelinated neurons that are commonly thought to be the primary mediators of nociception and pain. In fact, many or most of the neurons displaying altered properties were activated from sites remote from the deranged joint. This is consistent with Wallerian degeneration of axons adjacent to degradation of the myelin sheath. This in turn can account for referred pain as neurons originating in areas surrounding or even remote from an OA joint could be affected.

I repeat here that it is primarily the large diameter proprioceptive neurons that undergo the greatest change. A change in properties may be associated with a change in function. Therefore I am proposing that, while most proprioceptive primary afferent neurons may retain their original proprioceptive function, they may also adopt a nociceptive function, while other proprioceptive neurons may change to serve a wholly

nociceptive function. This could explain the loss of proprioception reported in people with OA.

Given that changes were observed mainly in large diameter primary afferent neurons that originated at sites remote from the deranged joint, and that changes were occurring long after loss of joint cartilage and other structural changes had occurred, I propose that at time points after the stabilization of structural change, changes in neural function continue to occur, and therefore that at these time points, and afterward, OA pain becomes a wholly neurological disorder. As a result, total replacement of the joint would not necessarily alleviate the joint pain. This is because joint pain is no longer being generated from the joint. Rather, joint pain is being generated by ectopic activity in axons or cell bodies of primary afferent neurons that originate from the joint and other regions of the limb.

It also follows that beyond these time points, structural change and neuronal change are two different processes and thereby diverge in disease progression. As a result, one would not expect there to be a faithful correlation between the degree of structural change and the severity of OA pain.

These hypotheses are proposed in order to foster a number of research topics. For example, what pathological changes occur in primary sensory neurons in OA? Of these pathological changes, which one or ones contribute to the pain? What are the

mechanisms inducing these pathological changes? Which of these pain-inducing mechanisms can be modified or controlled by intervention? What time in the development of OA do these changes occur? The answer to these questions may have an important impact on the pursuit of innovative approaches to treating the pain in OA, and ultimately the life habits and quality of life for those who suffer the burden of OA pain.

I shall now proceed to explain how the knee derangement initiates changes in primary afferent neurons, how changes in large diameter heavily myelinated neurons are determined, and how these changes in primary sensory neurons lead to pain.

**6.2. Proposed neural mechanisms of the pathogenesis of chronic pain in OA**

6.2.1. Functional changes in primary sensory neurons in knee OA are the result of the activation of innate immunity initiated by the damage to the innervated structures in the knee joint, which is mediated via Toll-like receptors (TLRs).

One month following the knee surgery to remove the medial meniscus and cut the ACL, significant functional changes were found in L4 DRG neurons innervating extensive regions from toe to hip, and various tissue types including hairy skin, glabrous skin, muscle spindles and other subcutaneous tissues. How do the injuries cause these extensive changes in sensory neurons?

During tissue injury, a variety of damage-associated molecules are released, including hyaluronic acid, heparan sulfate, fibrinogen, high-mobility group box1 (HMGB1), heat shock protein (HSP) 60, host mRNA, host chromatin and small ribonucleoprotein particles (Beg, 2002). The immune system is capable of processing the information of these molecules and then the governing of the nature of injury, mainly via TLRs (Mollen et al., 2006). TLRs are a group of pattern recognition receptors (Barton and Medzhitov, 2002). They are the most important interface initiating the release of cytokines following exposure to distinct pathogen- or damage-associated molecular patterns. Their limited subtype-dependent activation leads to specific activation of intracellular signaling pathways. They were originally shown to recognize specific patterns of microbial ligands (Akira and Takeda, 2004;Kawai and Akira, 2005), and later were found to recognize endogenous damage-associated molecules as well.

A sundry of signaling pathways, such as protein kinase A (PKA), PKC, PKG, extracellular signal-regulated kinase (ERK), P38 mitogen-activated protein kinase (MAPK), NF-κB and Janus kinases/ signal transducers and activators of transcription (JAK/STAT), have been implicated in the development of chronic pain (Ji and Woolf, 2001;Hanada and Yoshimura, 2002;Obata and Noguchi, 2004). Among them, NF-κB, JAK/STAT and MAPK pathways are of particular importance in chronic pain: the NF-κB pathway is the most important cellular pathway responsible for the production of

inflammatory cytokines (Nguyen et al., 2002), the JAK/STAT pathway is the primary pathway responsible for cytokine receptor signaling (Ihle, 1995) and MAPKs play a pivotal role in transducing extracellular stimuli into intracellular posttranslational and transcriptional responses, and are hot topics in recent pain mechanism studies, particularly ERK and p38 (Obata and Noguchi, 2004;Ma and Quirion, 2005;Ji and Suter, 2007). The activation of Toll-like receptor (TLR) signaling pathways produces critical intermediates including NF-κB, IRF and AP-1 that could initiate these pain-related pathways. TLRs adopt either the myeloid differentiation (MyD)88-dependent or MyD88-independent pathway following activation. Three most common TLR-mediated signaling pathways are the MyD88-dependent and MyD88-independent release of NF-κB, and the MyD88-independent production of IRF. Each of the TLRs seems to recruit different subsequent signaling pathways (Akira and Takeda, 2004).

Increasing evidence supports TLR4 as the main TLR sensing tissue damage in that it responds to a number of endogenous ligands, such as HSP 60, fibrinogen, heparan sulfate and hyaluronic acid (Ohashi et al., 2000;Smiley et al., 2001;Termeer et al., 2002;Johnson et al., 2002;Taylor et al., 2004). The TLR4-dependent signaling pathway has been linked to sterile inflammation resulting from various neural and non-neural tissue injuries (Bettinger et al., 1994;Prince et al., 2006;Boivin et al., 2007)). TLR2 is implicated in the pathogenesis of arthritis (Cho et al., 2007). HMGB1 has been

proposed as the primary putative endogenous TLR2 ligand (Park et al., 2004;Yu et al., 2006;van Beijnum et al., 2008). HMGB1 is up-regulated at the same time frame in arthritic joints in human (Kokkola et al., 2002;Taniguchi et al., 2003). TLR-3 and TLR-9 are involved in the immune response initiated by host chromatin and RNA (Leadbetter et al., 2002;Jackson et al., 2006).

Our surgically induced knee derangement model of OA involves transection of the ACL and removal of the medial meniscus. Both structures are innervated (De Avila et al., 1989;Krauspe et al., 1995;Zimny et al., 1986;Zimny et al., 1988;Assimakopoulos et al., 1992;O'Connor and McConnaughey, 1978;Haus and Halata, 1990). Therefore, any surgical procedure could cause axonal injuries in heavily myelinated A-fiber knee afferents and the release of axon injury-associated molecules, including cytoskeletal proteins, heat shock proteins, resident endoplasmic reticulum proteins, and other proteins associated with neurodegenerative diseases (Willis et al., 2005). These molecules activate immune cells and immune-like glial cells (e.g. Schwann cells) through TLR activation, and stimulate the expression of proinflammation genes (Lee et al., 2006). Moreover, meniscectomy directly causes greater cartilage degeneration. Meniscal injuries are highly and positively associated with cartilage degeneration (Cicuttini et al., 2002;Lindhorst et al., 2005). One mechanism is by chronic deformation and dehydration of cartilage resulting from the extraordinary strain and load change following

meniscectomy (Song et al., 2008). The other mechanism is via TLRs, whose activation induces catabolic responses in chondrocytes (Kim et al., 2006). The up-regulation of TLR receptors (TLR2 and TLR4) has been confirmed in OA cartilage (Kim et al., 2006).

In summary, traumatic injuries of knee components is the first step activating several important cell types, including immune cells, immune-like Schwann cells and chrondrocytes. TLR signaling might play an important role in the activation of these cells, which induces significant changes in the expression of proinflammation genes and eventually changes the chemical milieu that peripheral terminals of primary sensory neurons bath in. This may account for how knee surgery initiates functional changes in primary sensory neurons in our OA model.

6.2.2. Specific sensory innervation patterns and the nature of the knee injury determine that functional changes in OA are preferentially in Aβ-fiber LTMs, especially muscle spindle afferents.

In our studies, changes in the electrophysiological properties in Aβ-fiber LTMs, especially proprioceptive muscle spindle afferents were prominent. Here, we propose two different possible mechanisms for these changes.

One explanation is that changes in Aβ-fiber LTMs, especially proprioceptive muscle spindle afferents are secondary to the change in the pattern of load distribution, resulting from either bone or ligament remodeling or due to a voluntary change in the

manner in which the knee is used due to pain (Hurley, 1999). Our data presented in Chapter 3 shows that transection of the ACL and removal of the medial meniscus cause significantly less weight placed on the ipsilateral leg even long after initial knee surgery, similar to what is reported in previous studies (Fernihough et al., 2004;Bove et al., 2006). Muscular atrophy following chronic hindlimb unloading is a logical possibility. There have been reports about the correlation of muscular atrophy with the development of OA (DePalma and Gilchrist, 2007;Amaro et al., 2007;Laban, 2006;Hall et al., 2006). However, the causal relationship remains controversial, as muscle weakness itself could be a risk factor leading to OA (Herzog and Longino, 2007). Muscle atrophy during the progression of OA causes a reduction in the production of neurotrophins. This may lead to altered neuronal function in large myelinated mechanoreceptors, as neurotrophins modulate neuronal function through regulating the expression of a variety of ion channels (Lesser et al., 1997). Proprioceptive DRG neurons are maintained mainly by neurotrophin (NT)-3. However, NT-4 and BDNF are also survival signals that support a full spectrum of proprioceptive neurons (Snider, 1994). NT-4 and BDNF signaling through TrkB receptors are the main survival signals for Aβ-fiber LTMs (Bibel and Barde, 2000;Huang and Reichardt, 2001). These neurotrophins can be synthesized in DRG neurons or produced by various non-neuronal cell types including satellite cells (Yamamoto et al., 1996;Wetmore and Olson, 1995;Zhou et al., 1999). During

peripheral neuropathies, the increase in BDNF and NT-3 mRNA levels is proportional to the extent of invasion of the nerves by T cells and macrophages (Sobue et al., 1998), suggesting that immune cells are also important sources of neurotrophins (Kobayashi et al., 2002). Moreover, treadmill exercise is effective in up-regulating the production of neurotrophins, such as glial cell derived neurotrophic factor (GDNF) and BDNF in skeletal muscles of the lower extremities (Cuppini et al., 2007;Dupont-Versteegden et al., 2004).

However, there is other evidence contrary to these mechanisms. First, muscular atrophy is mild, if any, during the two-month observation period in our studies. Second, when put on a rotating drum, OA animals remain on the drum for similar times as naive animals, suggesting a normal muscular strength (Schwartz, 2005). Third, "treadmill" exercise counteracts muscular atrophy, but it does not retrieve sensory abnormalities close to normal. Rather, putting OA animals on a rotating drum exaggerates nocifensive behaviors and is associated with functional changes in wide dynamic range (WDR) spinal neurons, including an increase in the spontaneous firing rate, an increase in low threshold spiking and an increase in the response to ionophoretic application of glutamate and substance P (Schwartz, 2005). Therefore, muscular atrophy is unlikely to account for the changes observed in muscle spindle neurons.

The other explanation for the preferential changes in Aβ-fiber LTMs, especially proprioceptive muscle spindle afferents, rests on neural injuries of these neurons during the knee injury and the ensuing neuroinflammation. Injuries of ACL, menisci and the surrounding joint capsule not only mechanically destabilize the joint but also result in potential damage to the nerve fibers innervating these structures. These lesions lead to intermingling of damaged and intact peripheral nerves, which is similar to partial nerve injuries in spinal nerve ligation models. Nerve damage results in immune activation and the release of a variety of neuroactive substances along the length of the degenerating fibers (Watkins and Maier, 2002). Uninjured peripheral nerves are exposed to immune-derived substances released in their vicinity as a result of Wallerian degeneration of injured peripheral nerves and from the intermingling of their receptive fields, and could be sensitized by these processes. Moreover, immune-derived substances such as leukemia inhibitory factors (LIF), interleukin (IL)-6 and neurotrophins are released at the injury site and are retrogradely transported by both uninjured and injured axons (Watkins and Maier, 2002). These retrogradely transported signals in uninjured nerves may up-regulate DRG neuronal expression of various neuropeptides, neurotrophins and ion channels, and account for the increased neuronal excitability. There is debate about whether injured or uninjured nerves account for neuropathic pain following partial nerve injury. Some researchers suggested that injured nerves play a

critical role in ectopic and spontaneous discharge, and interruption of the input from these fibers attenuates certain "pain" behaviors (Liu et al., 2000b;Sheen and Chung, 1993;Han et al., 2000). However, other researchers have confirmed that following nerve injury, changes in uninjured afferents including large diameter myelinated Aβ-fibers would be sufficient to initiate and maintain neuropathic "pain" behaviors (Ali et al., 1999;Li et al., 2000;Wu et al., 2002;Wu et al., 2001;Michaelis et al., 2000;Boucher et al., 2000; for review see Gold, 2000).

Like the orderly organized dorsal horn (Rexed, 1954;Rexed, 1952), sensory axons in peripheral nerves are not randomly distributed (Honig, 1982). But, peripheral axons are not somatotopically organized. Rather, neighboring axons often have the same sensory modality (Roberts and Elardo, 1986), suggesting that fibers with the same modality tend to be clustered together. However, it is still easy to identify axons with different sensory modalities running close to each other (Wu et al., 1998). ACL, menisci and even joint capsule have been shown to receive innervation from large diameter myelinated fibers (De Avila et al., 1989;Krauspe et al., 1995;Zimny et al., 1986;Zimny et al., 1988;Assimakopoulos et al., 1992;O'Connor and McConnaughey, 1978;Haus and Halata, 1990). Thus, injuries of articular mechanoreceptors might lead to preferential changes in neighbouring Aβ-fiber LTMs, especially proprioceptive muscle

spindle afferents, due to proximity and same-modality-ensheathing pattern in peripheral nerves.

The correlation of proprioception deficit with changes in proprioceptive muscle spindle afferents is documented during the progression of OA. Evidence from peripheral neuropathy supports neural deficit as a direct cause of deficit in proprioception, and maybe changes in gait as well. Several forms of peripheral neuropathy have been shown to lead to a prioprioception deficit (Kanade et al., 2008;Goldberg et al., 2008;DeMott et al., 2007;Oki et al., 2007).

In summary, previous observations about the muscular atrophy in our OA model do not support an altered pattern of hind limb load distribution as the mechanism for preferential electrophysiological changes in Aβ-fiber LTMs, especially muscle spindle afferents. A more likely mechanism rests on the specific organization of the peripheral nerves and the nature of knee-injury-initiated neural injury.

6.2.3. Functional changes in Aβ-fiber LTMs are capable to induce chronic pain in OA.

Pain is different from nociception. The former is the perceptual consequence of afferent activation, whereas the latter is the response of the nervous system to a noxious stimulus without necessarily triggering pain (Devor, 2009). Although pain originates in sensory endings in peripheral tissues, the ultimate conscious perception of pain is the result of elaborate processing in the central nervous system (CNS). Before pain

perception can be generated, nociceptive signals from the periphery must be conveyed along specific neural routes towards a matrix of regions in the brain for proper processing. Abnormal sensory input from DRG neurons is necessary for central plasticity in chronic pain states, but is not necessarily a determinant for ultimate pain sensation.

At the early phase of OA when behavioural evaluation indicates changes in nociception, functional changes in primary sensory neurons are preferentially precipitated in Aβ-fiber LTMs rather than in classic C-fiber nociceptors. This is seen in other neuropathic types of chronic pain (Kim et al., 1998;Liu et al., 2000a;Ma et al., 2003;Sapunar et al., 2005;Stebbing et al., 1999). Devor proposed that abnormal discharge in Aβ afferents evokes neuropathic pain (Devor, 2009). Our data suggest that Devor's hypothesis might be able to explain the pain in OA. Here, we propose two related yet sequential mechanisms to further explain how changes in Aβ-fiber LTMs lead to pain; one is a peripheral mechanism and the other is central.

Peripheral mechanisms focus on phenotypic changes in Aβ-fiber LTMs, which endow them novel pain-provoking properties. Phenotypic changes in Aβ-fiber LTMs are essential in the pain in OA. As in other chronic pain states, central changes are initiated and maintained by peripheral input (Gracely et al., 1992;Koltzenburg et al., 1994). Primary afferents use glutamate as an excitary neurotransmitter in the communication with dorsal horn neurons. However, it has been shown that some of

these neurons express de novo a variety of peptidergic neuromodulators including substance P and calcitonin gene related peptide (CGRP) in neuropathic states, and induce the up-regulation of corresponding receptors in the spinal cord (Weissner et al., 2006;Noguchi et al., 1995;Miki et al., 1998a). Studies in osteoarthritic joints also identified an increase in the percentage of substance P or CGRP immunopositive knee afferents (Salo et al., 2002;Saxler et al., 2007). However, subpopulation expression is either not studied or thought to be associated with smaller nociceptive neurons. Our pilot study to investigate substance P expression in functionally identified Aβ-fiber neurons in OA in rats failed to observe an increase of this peptide in either muscle spindle neurons or other low threshold neurons. But, out priliminary data are not conclusive, and would be most appropriate being considered as an invitation for further research of the expression of various neuropeptides including CGRP and vasoactive intestinal polypeptide (VIP) in these neurons. Phenotypic changes in primary sensory neurons could lead to ectopic and/or prolonged discharge, which greatly increases the excitability of postsynaptic neurons in the spinal cord. This is expected to increase the spontaneous activity in pain-relaying dorsal horn neurons, and their response to peripheral input. Previous studies in the same OA model in our lab identified significant functional changes in WDR neurons located in deep dorsal horn layers (Rexed laminae III-V). WDR neurons in OA have higher spontaneous discharge rates and exhibit significantly

different patterns of spontaneous activity. Repetitive articulation of the treated knee within the normal range causes an increase in the spontaneous firing rate, an increase in low threshold spiking and an increase in the response to iontophoretic application of glutamate and substance P without altering the responsiveness to inhibitory amino acids (Schwartz, 2005). Brief activation of low threshold Aβ afferents induces prolonged afterdischarge in spinal WDR neurons in neuropathic states, and its emergence accompanies tactile allodynia. NK-1 antagonists abolish both (Pitcher and Henry, 2008;Pitcher and Henry, 2004).

Central mechanisms focus on changes in the properties of the "pain network" in the CNS, which result in not only gain of ascending signals but also changes in signal modality – for example, innocuous touch input now becomes effective in activating nociceptive ascending pathways. Without plasticity of the "pain network" in the CNS, signals from primary sensory neurons with altered phenotype could undergo either simple amplification or brief, localized central sensitization. One example of rerouting of nociceptive information under neuropathic states is the transmission of tactile allodynia by the dorsal column-medial lemniscus system (DCMLS) (Saade et al., 2002;Sun et al., 2001). In physiological conditions, DCMLS is responsible for signalling touch, vibration and conscious proprioceptive sense of upper limbs, but not cutaneous pain (Willis and Coggeshall, 2004), and receives direct somatosensory projection only from

low threshold Aβ afferents (Willis and Westlund, 1997). However, spontaneous activity and the response to low threshold stimuli are increased in gracile neurons ipsilateral to a neuropathic leg (Miki et al., 1998b). Ipsilateral but not contralateral dorsal column lesion blocks tactile allodynia in spinal nerve ligation rats (Sun et al., 2001). DCMLS terminates in the contralateral thalamic ventrobasal complex, where the spinothalamic tract transmitting nociceptive information in naive animals also terminates (Ma et al., 1987). Dorsal column lesion greatly alters the neuronal firing in ventral posterolateral nucleus (VPL) (Miki et al., 2000), suggesting that DCMLS contributes to the ascending transmission or modulation of nociceptive responses of VPL nucleus neurons under neuropathic conditions.

Another example of rerouting is the proposed sprouting of the Aβ afferents to superficial laminae of the dorsal horn known to be involved in the processing of nociceptive signals (Woolf et al., 1995;Woolf et al., 1992;Kohama et al., 2000;Koerber et al., 1999;Lekan et al., 1996). Thus, LTMs may play a major role in producing pain-related behavior by activating normally nociceptive-specific projection neurons in the CNS. Supportive evidence shows that under neuropathic pain states, low intensity stimuli in the neuropathic dermatome induce c-fos (normally elicited by nociceptive stimuli) expression in the superficial dorsal horn and the parabrachial area of the brainstem (Bester et al., 2000), evoke excitatory postsynaptic potentials (EPSPs) in

Rexed lamina II that normally do not occur (Kohama et al., 2000) and resemble the low threshold stimuli elicited EPSPs in normal lamina III (Kohama et al., 2000). The rerouting of Aβ afferents under neuropathic states is under the control of neurotrophins. IL-6 in the presence of either NGF or NT-3 has been demonstrated to enhance injury-induced spinal axon regeneration (Cafferty et al., 2004). Cytokines and neurotrophins are locally available to injured and neighbouring sensory neurons after nerve injuries (Zhou et al., 1999;Murphy et al., 1995;Bolin et al., 1995).

In summary, it is proposed that abnormal pain sensation in OA can only be elicited once two prerequisites are met: phenotype switch in some of the Aβ-fiber LTMs so that they are equipped with novel pain-relaying properties, and modification of the "pain network" in the CNS so that not only gain of ascending signals occur but also changes in signal modality can take place.

Based on the results in this thesis project, and within the context of the current literature, I am proposing a novel concept regarding the mechanism underlying the pain in OA induced by traumatic injuries. Following an initial trauma to the joint, two distinct yet interacting processes are initiated. One is neural injury of joint afferents and ensuing maladaptive changes of the nervous system. The other is the cartilage degradation and bony changes in the joint. The former process starts with neuropathic types of change in non-nociceptive/low threshold myelinated afferents, which is the

peripheral drive for the sustained central plasticity. The latter process creates a dynamic chemical environment in which joint afferents bath. The chemical milieu provides continuing molecular signalling at different phases of OA progression, orchestrating functional adjustments in distinct populations of primary afferents that are intermingled with joint afferents, and therefore contributes to the progression of OA pain. Host immune response to joint trauma is the common ground for the maladaptive changes in the nervous system and in the joint, and also governs their interaction.

## 6.3. Limitations of the thesis project

### 6.3.1. Sham surgery

In this thesis project, naïve rats served as control. Sham surgeries, both simple exposure of joint capsule or even skin incision over the joint were considered inappropriate controls for this chronic model of OA pain. The former sham surgical procedure likely causes mild OA, and results in the comparison between severe and mild OA. Simple surgical exposure of the joint capsule, regardless of the size of the surgical exposure has been reported to cause joint instability (Hsu et al., 1997) and articular cartilage degeneration (Hsu et al., 2003), and therefore induces an animal model of OA. The latter sham surgical procedure is a proper control for acute or subacute models, but is equivalent to a naive control for a chronic model lasting a month and more, such as our OA model. Surgical incision normally induces a brief inflammatory phase lasting only

days (Baum and Arpey, 2005;Rook et al., 2008), but is fully repaired with scar tissue devoid of inflammatory infiltration by the end of the first month (Mitchell and Cotran, 2003).

There are different needs to set up a control group. One is to determine whether OA is induced by the damage to ACL and menisci. Therefore, a control group is expected to rule out the role of surgical exposure. Another is to determine whether sensory changes in the surgically-induced OA model are associated with changes within the joint but not with cutaneous inflammation. Thus, a control group is expected to exclude the role of cutaneous inflammation. From our point of view, OA is induced by the derangement of the joint initiated by the damage to the ACL and the medial meniscus, but not limited to merely these two structures. Muscle strength, gait and joint stability all play a role in the development of OA. As a result, there is no appropriate control for our model.

6.3.2. Behavioral evaluation

In this thesis project, behavioral studies and eletrophysiological studies were done separately, sometimes in different animal groups. Behavioral evaluation before recordings was rarely done. One limitation is that more animals are required to reveal any difference in sensory function between the OA and the naive group. Because there was considerable variance in nocifensive symptoms following the knee injury, range

from severe to mild. Some variance might be due to subtle variances, such as housing conditions, number of animals per cage, etc. These factors have been shown to induce variance in immuno-endocrine responses (Bartolomucci et al., 2003;D'Arbe et al., 2002), which could be consequential in chronic pain pathogenesis.

Another limitation is that it is difficult to comment on the correlation of changes in nociception and electrophysiological properties of sensory neurons within an individual animal. However, even if we had done behavioral testings prior to recordings, we might still face the difficulty of lacking a behavioral test that can faithfully and effectively gauge the pain in OA. In human subjects, pain in the early stage of OA is mainly use-dependant during normal range activities, such as walking, whereas static form of pain, such as mechanical allodynia of the affected limb is mild (Creamer et al., 1998). There is no effective means to evaluate this dynamic form of pain. Some might suggest the voluntary open field test. However, it is a test more appropriate for the evaluation of emotionality (Ramos and Mormede, 1998). Moreover, each OA rat does not have exactly the same set of symptoms, varying in types or extents. Thus, it remains a big challenge to assign an overall "pain" score for each animal, as we normally do in human subjects.

6.3.3. Repetitive stimulation protocols

There were two stimulation protocols used in the thesis projects, the paired-pulse stimulation with gradually shortened inter-stimulus intervals and train stimulation with gradually increased stimulation frequencies. The former protocol aimed to study the kinetics of fast inactivation of sodium channels. The time course of the process is normally within several milliseconds. The latter protocol is comprised of a series of 200 ms stimulation trains, which aimed to study a much slower process – the slow inactivation of sodium channels with the time course of hundreds of milliseconds. Limitations of the train-pulse protocol include that the frequency of each stimulation sweep is variable, that the duration of the stimulation pulse is relatively brief. Spike frequency adaption did occur during the delivery of the train-pulse stimulation protocol. However, it became more challenging to differentiate the effect of fast inactivation due to gradually shortening stimulus interval and the effect of slow inactivation due to prolonged firing when the frequency of each stimulation sweep is variable. Moreover, spike adaption might have several phases, each with a distinct time course. In a previous study in neocortical neurons, a one second depolarizing pulse produces an initial phase of rapid adaptation lasting 50-100 ms, followed by a second phase of slow adaptation and a third phase of adaptation late in the course of the pulse (Fleidervish et al., 1996). Therefore, stimulation trains longer than the currently adopted 200ms might be

advantageous to reveal more details about this slow process of the inactivation of sodium channels.

**6.4. Future work**

On the basis of current data it is suggested that injury-induced OA pain likely includes a neuropathic component. Even A-fiber LTMs that are activated by innocuous stimuli in naive animals might be involved in the pathogenesis of chronic pain in OA. Changes in AP configuration and the response to repetitive stimulation in these neurons indicate alterations in the kinetics of sodium currents. As a result, there are several directions worthy of future studies.

6.4.1. Comparisons between MIA and surgically induced OA

In this project, the pattern of the changes in DRG neurons in OA resembles those typically seen in neuropathic models. However, OA has come to be viewed more as a syndrome with many complex etiologies rather than a single disease entity (Creamer and Hochberg, 1997). MIA-induced OA is another commonly used OA model, which has a totally different etiology from the surgical knee derangement model of OA. The procedure of injecting monoacetate into the joint *pe se* does not cause neural injury, although neural injury is identified at the later course of the MIA-induced OA (Ivanavicius et al., 2007). Therefore, it will be informative to use a similar electrophysiological approache to determine changes in DRG neurons in the

focused on small nociceptors, mostly C- and Aδ-fiber neurons. Considering the fact that large myelinated neurons including LTMs now appear to play an important role in the pathogenesis of neuropathic type of pain, as suggested here, it is compelling to conduct studies to reveal detailed ion channel distribution in these large myelinated LTMs, ideally in functionally identified neuronal types. *In vivo* intracellular recording and labeling followed by single cell RT-PCR amplification should be considered as a primary strategy to reveal details on ion channel expression in functionally identified A-fiber LTMs.

6.4.4. The role of immune response in the initiation of the pain in OA

In the present surgical OA model, it is suggested that an initial injury in some of the mechanoreceptors innervating joint structures causes significant ensuing changes particularly in larger Aβ-fiber DRG neurons. Host immune response has been suspected to play a central role to bridge tissue injury and sensory plasticity. As cell types activated during the process, for example, macrophages and Schwann cells, and bioactive molecules released during the process, for example, cytokines and neurotrophic factors, have been proven to be involved in sensory plasticity in chronic pain conditions. However, it remains unknown how specific immune response leads to distinct sets of sensory abnormalities as seen in inflammatory pain and neuropathic pain. Therefore, it will advance our understanding about the role of immune response in the initiation of the pain in OA if we compare the immune response during the earliest stage following tissue

injury between the present surgically induced OA, cutaneous inflammation and peripheral neuropathy. RNA silencing for TLRs, cytokine assay and pain behavioral testing should be conducted in the comparison between the pain in OA and other chronic pain conditions.

### 6.5. Closing remarks

OA is the most common arthritis in human. In OA, pain remains the central issue, from impact to diagnosis to treatment. Continuing efforts have been made to understand the mechanisms of the pain in OA. However, none of the current concepts of the cause of OA pain complements the clinical picture, and the management of the pain in OA is poor. Driven by this unmet medical need, this thesis project was designed to investigate the possible role of primary sensory neurons in the pathogenesis of the pain in OA, as sensory neurons have been proven crucial for the development of other chronic pain conditions. *In vivo* intracellular recording technique, the technical basis of this thesis project, enabled me to comment on physiological changes in functionally identified primary sensory neurons. Several important findings have been made: LTMs rather than C- and Aδ-fiber nociceptors are altered in functional properties at the stage when signs of nocifensive behavior and the histology of the knee joint indicate the presence of OA and the pain in OA. Muscle spindle neurons, proprioceptive neurons are the most affected LTMs, in terms of AP configurations and the pattern of the response to repetitive

stimulation. During the progression of OA, distinct populations of DRG neurons are affected: Aβ-fiber LTMs are affected earlier in model development, whereas Aβ-fiber HTMs are affected later. Changes in electrophysiological properties in this project strongly suggest the alteration of the kinetics of sodium currents. These findings constitute the neuronal basis upon which clinical presentation of sensory deficits in OA patients might be explained. Moreover, these findings might lead to novel therapeutic avenues in the management of the pain in OA, as this pain is likely a form of neuropathic pain rather than inflammatory pain as implicated by the name of the mother disease, "osteoarthritis".

**6.6. Claims of originality**

✧ First effort to systematically examine the role of Aβ-fiber low threshold sensory neurons in OA pain. The findings from this effort challenge the long standing hypothesis that OA pain is initiated by nociceptive articular afferents.

✧ First effort to study the neural basis underlying the progression of OA pain syndromes. This study furthers our understanding of cellular mechanisms underlying clinical presentations of OA pain.

✧ First study to reveal a central role of muscle spindle neurons (proprioceptive neurons) in the pathogenesis of sensory abnormalities in OA, including pain and loss of

proprioception. This study reveals a novel cellular target in the management of OA sensory disorders.

✧ First effort to investigate dynamics of sodium currents, including a slow inactivation mechanism in functionally identified neurons. This effort is the first step towards the ultimate precise understanding of ion channel kinetics in individual neurons whose sensory properties are clearly identified.

# BIBLIOGRAPHY

Aigner T, Kim HA (2002) Apoptosis and cellular vitality: issues in osteoarthritic cartilage degeneration. Arthritis Rheum 46:1986-1996.

Akira S, Takeda K (2004) Toll-like receptor signalling. Nat Rev Immunol 4:499-511.

Ali Z, Ringkamp M, Hartke TV, Chien HF, Flavahan NA, Campbell JN, Meyer RA (1999) Uninjured C-fiber nociceptors develop spontaneous activity and alpha-adrenergic sensitivity following L6 spinal nerve ligation in monkey. J Neurophysiol 81:455-466.

Alloui A, Zimmermann K, Mamet J, Duprat F, Noel J, Chemin J, Guy N, Blondeau N, Voilley N, Rubat-Coudert C, Borsotto M, Romey G, Heurteaux C, Reeh P, Eschalier A, Lazdunski M (2006) TREK-1, a K+ channel involved in polymodal pain perception. EMBO J 25:2368-2376.

Amaro A, Amado F, Duarte JA, Appell HJ (2007) Gluteus medius muscle atrophy is related to contralateral and ipsilateral hip joint osteoarthritis. Int J Sports Med 28:1035-1039.

Appleton CT, McErlain DD, Henry JL, Holdsworth DW, Beier F (2007a) Molecular and histological analysis of a new rat model of experimental knee osteoarthritis. Ann N Y Acad Sci 1117:165-174.

Appleton CT, McErlain DD, Pitelka V, Schwartz N, Bernier SM, Henry JL, Holdsworth DW, Beier F (2007b) Forced mobilization accelerates pathogenesis: characterization of a preclinical surgical model of osteoarthritis. Arthritis Res Ther 9:R13.

Appleton CT, Pitelka V, Henry J, Beier F (2007c) Global analyses of gene expression in early experimental osteoarthritis. Arthritis Rheum 56:1854-1868.

Assimakopoulos AP, Katonis PG, Agapitos MV, Exarchou EI (1992) The innervation of the human meniscus. Clin Orthop Relat Res232-236.

Averill S, McMahon SB, Clary DO, Reichardt LF, Priestley JV (1995) Immunocytochemical localization of trkA receptors in chemically identified subgroups of adult rat sensory neurons. Eur J Neurosci 7:1484-1494.

Bahia PK, Suzuki R, Benton DC, Jowett AJ, Chen MX, Trezise DJ, Dickenson AH, Moss GW (2005) A functional role for small-conductance calcium-activated potassium channels in sensory pathways including nociceptive processes. J Neurosci 25:3489-3498.

Bajaj P, Bajaj P, Graven-Nielsen T, rendt-Nielsen L (2001) Osteoarthritis and its association with muscle hyperalgesia: an experimental controlled study. Pain 93:107-114.

Barrett DS, Cobb AG, Bentley G (1991) Joint proprioception in normal, osteoarthritic and replaced knees. J Bone Joint Surg Br 73:53-56.

Bartolomucci A, Palanza P, Sacerdote P, Ceresini G, Chirieleison A, Panerai AE, Parmigiani S (2003) Individual housing induces altered immuno-endocrine responses to psychological stress in male mice. Psychoneuroendocrinology 28:540-558.

Barton GM, Medzhitov R (2002) Toll-like receptors and their ligands. Curr Top Microbiol Immunol 270:81-92.

Baum CL, Arpey CJ (2005) Normal cutaneous wound healing: clinical correlation with cellular and molecular events. Dermatol Surg 31:674-686.

Beg AA (2002) Endogenous ligands of Toll-like receptors: implications for regulating inflammatory and immune responses. Trends Immunol 23:509-512.

Belmonte C, Viana F (2008) Molecular and cellular limits to somatosensory specificity. Mol Pain 4:14.

Bergsteinsdottir K, Kingston A, Jessen KR (1992) Rat Schwann cells can be induced to express major histocompatibility complex class II molecules in vivo. J Neurocytol 21:382-390.

Bester H, Beggs S, Woolf CJ (2000) Changes in tactile stimuli-induced behavior and c-Fos expression in the superficial dorsal horn and in parabrachial nuclei after sciatic nerve crush. J Comp Neurol 428:45-61.

Bettinger DA, Pellicane JV, Tarry WC, Yager DR, Diegelmann RF, Lee R, Cohen IK, DeMaria EJ (1994) The role of inflammatory cytokines in wound healing: accelerated healing in endotoxin-resistant mice. J Trauma 36:810-813.

Bibel M, Barde YA (2000) Neurotrophins: key regulators of cell fate and cell shape in the vertebrate nervous system. Genes Dev 14:2919-2937.

Bielefeldt K, Jackson MB (1993) A calcium-activated potassium channel causes frequency-dependent action-potential failures in a mammalian nerve terminal. J Neurophysiol 70:284-298.

Birder LA, Nakamura Y, Kiss S, Nealen ML, Barrick S, Kanai AJ, Wang E, Ruiz G, de Groat WC, Apodaca G, Watkins S, Caterina MJ (2002) Altered urinary bladder function in mice lacking the vanilloid receptor TRPV1. Nat Neurosci 5:856-860.

Black JA, Dib-Hajj S, McNabola K, Jeste S, Rizzo MA, Kocsis JD, Waxman SG (1996) Spinal sensory neurons express multiple sodium channel alpha-subunit mRNAs. Brain Res Mol Brain Res 43:117-131.

Black JA, Renganathan M, Waxman SG (2002) Sodium channel Na(v)1.6 is expressed along nonmyelinated axons and it contributes to conduction. Brain Res Mol Brain Res 105:19-28.

Blair NT, Bean BP (2002) Roles of tetrodotoxin (TTX)-sensitive Na+ current, TTX-resistant Na+ current, and Ca2+ current in the action potentials of nociceptive sensory neurons. J Neurosci 22:10277-10290.

Boiko T, Rasband MN, Levinson SR, Caldwell JH, Mandel G, Trimmer JS, Matthews G (2001) Compact myelin dictates the differential targeting of two sodium channel isoforms in the same axon. Neuron 30:91-104.

Boivin A, Pineau I, Barrette B, Filali M, Vallieres N, Rivest S, Lacroix S (2007) Toll-like receptor signaling is critical for Wallerian degeneration and functional recovery after peripheral nerve injury. J Neurosci 27:12565-12576.

Bolin LM, Verity AN, Silver JE, Shooter EM, Abrams JS (1995) Interleukin-6 production by Schwann cells and induction in sciatic nerve injury. J Neurochem 64:850-858.

Borzi RM, Mazzetti I, Macor S, Silvestri T, Bassi A, Cattini L, Facchini A (1999) Flow cytometric analysis of intracellular chemokines in chondrocytes in vivo: constitutive expression and enhancement in osteoarthritis and rheumatoid arthritis. FEBS Lett 455:238-242.

Bosco G, Poppele RE (2001) Proprioception from a spinocerebellar perspective. Physiol Rev 81:539-568.

Boucher TJ, Okuse K, Bennett DL, Munson JB, Wood JN, McMahon SB (2000) Potent analgesic effects of GDNF in neuropathic pain states. Science 290:124-127.

Bove SE, Calcaterra SL, Brooker RM, Huber CM, Guzman RE, Juneau PL, Schrier DJ, Kilgore KS (2003) Weight bearing as a measure of disease progression and efficacy of

anti-inflammatory compounds in a model of monosodium iodoacetate-induced osteoarthritis. Osteoarthritis Cartilage 11:821-830.

Bove SE, Laemont KD, Brooker RM, Osborn MN, Sanchez BM, Guzman RE, Hook KE, Juneau PL, Connor JR, Kilgore KS (2006) Surgically induced osteoarthritis in the rat results in the development of both osteoarthritis-like joint pain and secondary hyperalgesia. Osteoarthritis Cartilage 14:1041-1048.

Braz JM, Nassar MA, Wood JN, Basbaum AI (2005) Parallel "pain" pathways arise from subpopulations of primary afferent nociceptor. Neuron 47:787-793.

Brenn D, Richter F, Schaible HG (2007) Sensitization of unmyelinated sensory fibers of the joint nerve to mechanical stimuli by interleukin-6 in the rat: an inflammatory mechanism of joint pain. Arthritis Rheum 56:351-359.

Brody DL, Yue DT (2000) Release-independent short-term synaptic depression in cultured hippocampal neurons. J Neurosci 20:2480-2494.

Brown AG (1981) The spinocervical tract. Prog Neurobiol 17:59-96.

Brown AG, Fyffe RE, Noble R (1980) Projections from Pacinian corpuscles and rapidly adapting mechanoreceptors of glabrous skin to the cat's spinal cord. J Physiol 307:385-400.

Brown AG, Rose PK, Snow PJ (1978) Morphology and organization of axon collaterals from afferent fibres of slowly adapting type I units in cat spinal cord. J Physiol 277:15-27.

Brown AG, Rose PK, Snow PJ (1977) The morphology of hair follicle afferent fibre collaterals in the spinal cord of the cat. J Physiol 272:779-797.

Buffington AL, Hanlon CA, McKeown MJ (2005) Acute and persistent pain modulation of attention-related anterior cingulate fMRI activations. Pain 113:172-184.

Burgess PR, Petit D, Warren RM (1968) Receptor types in cat hairy skin supplied by myelinated fibers. J Neurophysiol 31:833-848.

Cafferty WB, Gardiner NJ, Das P, Qiu J, McMahon SB, Thompson SW (2004) Conditioning injury-induced spinal axon regeneration fails in interleukin-6 knock-out mice. J Neurosci 24:4432-4443.

Caldwell JH, Schaller KL, Lasher RS, Peles E, Levinson SR (2000) Sodium channel Na(v)1.6 is localized at nodes of ranvier, dendrites, and synapses. Proc Natl Acad Sci U S A 97:5616-5620.

Campana WM (2007) Schwann cells: activated peripheral glia and their role in neuropathic pain. Brain Behav Immun 21:522-527.

Cardenas CG, Del Mar LP, Scroggs RS (1995) Variation in serotonergic inhibition of calcium channel currents in four types of rat sensory neurons differentiated by membrane properties. J Neurophysiol 74:1870-1879.

Caterina MJ, Rosen TA, Tominaga M, Brake AJ, Julius D (1999) A capsaicin-receptor homologue with a high threshold for noxious heat. Nature 398:436-441.

Caterina MJ, Schumacher MA, Tominaga M, Rosen TA, Levine JD, Julius D (1997) The capsaicin receptor: a heat-activated ion channel in the pain pathway. Nature 389:816-824.

Catterall WA, Goldin AL, Waxman SG (2003) International Union of Pharmacology. XXXIX. Compendium of voltage-gated ion channels: sodium channels. Pharmacol Rev 55:575-578.

Catterall WA, Perez-Reyes E, Snutch TP, Striessnig J (2005) International Union of Pharmacology. XLVIII. Nomenclature and structure-function relationships of voltage-gated calcium channels. Pharmacol Rev 57:411-425.

Chen AI, de Nooij JC, Jessell TM (2006a) Graded activity of transcription factor Runx3 specifies the laminar termination pattern of sensory axons in the developing spinal cord. Neuron 49:395-408.

Chen CL, Broom DC, Liu Y, de Nooij JC, Li Z, Cen C, Samad OA, Jessell TM, Woolf CJ, Ma Q (2006b) Runx1 determines nociceptive sensory neuron phenotype and is required for thermal and neuropathic pain. Neuron 49:365-377.

Chen S, Rio C, Ji RR, Dikkes P, Coggeshall RE, Woolf CJ, Corfas G (2003) Disruption of ErbB receptor signaling in adult non-myelinating Schwann cells causes progressive sensory loss. Nat Neurosci 6:1186-1193.

Chen S, Velardez MO, Warot X, Yu ZX, Miller SJ, Cros D, Corfas G (2006c) Neuregulin 1-erbB signaling is necessary for normal myelination and sensory function. J Neurosci 26:3079-3086.

Chi XX, Jiang X, Nicol GD (2007) ATP-sensitive potassium currents reduce the PGE2-mediated enhancement of excitability in adult rat sensory neurons. Brain Res 1145:28-40.

Cho ML, Ju JH, Kim HR, Oh HJ, Kang CM, Jhun JY, Lee SY, Park MK, Min JK, Park SH, Lee SH, Kim HY (2007) Toll-like receptor 2 ligand mediates the upregulation of angiogenic factor, vascular endothelial growth factor and interleukin-8/CXCL8 in human rheumatoid synovial fibroblasts. Immunol Lett 108:121-128.

Cicuttini FM, Forbes A, Yuanyuan W, Rush G, Stuckey SL (2002) Rate of knee cartilage loss after partial meniscectomy. J Rheumatol 29:1954-1956.

Clapham DE, Montell C, Schultz G, Julius D (2003) International Union of Pharmacology. XLIII. Compendium of voltage-gated ion channels: transient receptor potential channels. Pharmacol Rev 55:591-596.

Coggeshall RE, Hong KA, Langford LA, Schaible HG, Schmidt RF (1983) Discharge characteristics of fine medial articular afferents at rest and during passive movements of inflamed knee joints. Brain Res 272:185-188.

Cooper BY, Johnson RD, Rau KK (2004) Characterization and function of TWIK-related acid sensing K+ channels in a rat nociceptive cell. Neuroscience 129:209-224.

Coward K, Plumpton C, Facer P, Birch R, Carlstedt T, Tate S, Bountra C, Anand P (2000) Immunolocalization of SNS/PN3 and NaN/SNS2 sodium channels in human pain states. Pain 85:41-50.

Creamer P (2000) Osteoarthritis pain and its treatment. Curr Opin Rheumatol 12:450-455.

Creamer P, Hochberg MC (1997) Osteoarthritis. Lancet 350:503-508.

Creamer P, Hunt M, Dieppe P (1996) Pain mechanisms in osteoarthritis of the knee: effect of intraarticular anesthetic. J Rheumatol 23:1031-1036.

Creamer P, Lethbridge-Cejku M, Hochberg MC (1998) Where does it hurt? Pain localization in osteoarthritis of the knee. Osteoarthritis Cartilage 6:318-323.

Cummins TR, Dib-Hajj SD, Herzog RI, Waxman SG (2005) Nav1.6 channels generate resurgent sodium currents in spinal sensory neurons. FEBS Lett 579:2166-2170.

Cunha FQ, Poole S, Lorenzetti BB, Ferreira SH (1992) The pivotal role of tumour necrosis factor alpha in the development of inflammatory hyperalgesia. Br J Pharmacol 107:660-664.

Cuppini R, Sartini S, Agostini D, Guescini M, Ambrogini P, Betti M, Bertini L, Vallasciani M, Stocchi V (2007) Bdnf expression in rat skeletal muscle after acute or repeated exercise. Arch Ital Biol 145:99-110.

Czeschik JC, Hagenacker T, Schafers M, Busselberg D (2008) TNF-alpha differentially modulates ion channels of nociceptive neurons. Neurosci Lett 434:293-298.

D'Arbe M, Einstein R, Lavidis NA (2002) Stressful animal housing conditions and their potential effect on sympathetic neurotransmission in mice. Am J Physiol Regul Integr Comp Physiol 282:R1422-R1428.

De Avila GA, O'Connor BL, Visco DM, Sisk TD (1989) The mechanoreceptor innervation of the human fibular collateral ligament. J Anat 162:1-7.

De CF, Dassencourt L, Anract P (2004) The inflammatory side of human chondrocytes unveiled by antibody microarrays. Biochem Biophys Res Commun 323:960-969.

DeMott TK, Richardson JK, Thies SB, shton-Miller JA (2007) Falls and gait characteristics among older persons with peripheral neuropathy. Am J Phys Med Rehabil 86:125-132.

DePalma TB, Gilchrist JM (2007) Unilateral thigh atrophy and weakness in hip osteoarthritis. J Clin Neuromuscul Dis 9:313-317.

Devaux JJ, Kleopa KA, Cooper EC, Scherer SS (2004) KCNQ2 is a nodal K+ channel. J Neurosci 24:1236-1244.

Devor M (1999) Unexplained peculiarities of the dorsal root ganglion. Pain Suppl 6:S27-S35.

Devor M (2009) Ectopic discharge in Abeta afferents as a source of neuropathic pain. Exp Brain Res 196:115-128.

Dib-Hajj SD, Tyrrell L, Black JA, Waxman SG (1998) NaN, a novel voltage-gated Na channel, is expressed preferentially in peripheral sensory neurons and down-regulated after axotomy. Proc Natl Acad Sci U S A 95:8963-8968.

Djouhri L, Fang X, Okuse K, Wood JN, Berry CM, Lawson SN (2003) The TTX-resistant sodium channel Nav1.8 (SNS/PN3): expression and correlation with membrane properties in rat nociceptive primary afferent neurons. J Physiol 550:739-752.

Djouhri L, Lawson SN (2001) Differences in the size of the somatic action potential overshoot between nociceptive and non-nociceptive dorsal root ganglion neurones in the guinea-pig. Neuroscience 108:479-491.

Dupont-Versteegden EE, Houle JD, Dennis RA, Zhang J, Knox M, Wagoner G, Peterson CA (2004) Exercise-induced gene expression in soleus muscle is dependent on time after spinal cord injury in rats. Muscle Nerve 29:73-81.

Edgley SA, Jankowska E (1988) Information processed by dorsal horn spinocerebellar tract neurones in the cat. J Physiol 397:81-97.

Everill B, Rizzo MA, Kocsis JD (1998) Morphologically identified cutaneous afferent DRG neurons express three different potassium currents in varying proportions. J Neurophysiol 79:1814-1824.

Fang X, Djouhri L, McMullan S, Berry C, Waxman SG, Okuse K, Lawson SN (2006) Intense isolectin-B4 binding in rat dorsal root ganglion neurons distinguishes C-fiber nociceptors with broad action potentials and high Nav1.9 expression. J Neurosci 26:7281-7292.

Felson DT (2005) The sources of pain in knee osteoarthritis. Curr Opin Rheumatol 17:624-628.

Felson DT, McAlindon TE, Anderson JJ, Naimark A, Weissman BW, Aliabadi P, Evans S, Levy D, LaValley MP (1997) Defining radiographic osteoarthritis for the whole knee. Osteoarthritis Cartilage 5:241-250.

Fernihough J, Gentry C, Malcangio M, Fox A, Rediske J, Pellas T, Kidd B, Bevan S, Winter J (2004) Pain related behaviour in two models of osteoarthritis in the rat knee. Pain 112:83-93.

Ferreira SH, Lorenzetti BB, Bristow AF, Poole S (1988) Interleukin-1 beta as a potent hyperalgesic agent antagonized by a tripeptide analogue. Nature 334:698-700.

Fjell J, Hjelmstrom P, Hormuzdiar W, Milenkovic M, Aglieco F, Tyrrell L, Dib-Hajj S, Waxman SG, Black JA (2000) Localization of the tetrodotoxin-resistant sodium channel

NaN in nociceptors. Neuroreport 11:199-202.

Fleidervish IA, Friedman A, Gutnick MJ (1996) Slow inactivation of Na+ current and slow cumulative spike adaptation in mouse and guinea-pig neocortical neurones in slices. J Physiol 493 ( Pt 1):83-97.

Flor H (2003) Remapping somatosensory cortex after injury. Adv Neurol 93:195-204.

Fukuoka T, Kobayashi K, Yamanaka H, Obata K, Dai Y, Noguchi K (2008) Comparative study of the distribution of the alpha-subunits of voltage-gated sodium channels in normal and axotomized rat dorsal root ganglion neurons. J Comp Neurol 510:188-206.

Gao XF, Zhang HL, You ZD, Lu CL, He C (2007) G protein-coupled inwardly rectifying potassium channels in dorsal root ganglion neurons. Acta Pharmacol Sin 28:185-190.

Garcia-Anoveros J, Samad TA, Zuvela-Jelaska L, Woolf CJ, Corey DP (2001) Transport and localization of the DEG/ENaC ion channel BNaC1alpha to peripheral mechanosensory terminals of dorsal root ganglia neurons. J Neurosci 21:2678-2686.

Geiger JR, Jonas P (2000) Dynamic control of presynaptic Ca(2+) inflow by fast-inactivating K(+) channels in hippocampal mossy fiber boutons. Neuron 28:927-939.

George A, Schmidt C, Weishaupt A, Toyka KV, Sommer C (1999) Serial determination of tumor necrosis factor-alpha content in rat sciatic nerve after chronic constriction injury. Exp Neurol 160:124-132.

Gnanadesigan N, Smith RL (2003) Knee pain: osteoarthritis or anserine bursitis? J Am Med Dir Assoc 4:164-166.

Gold MS (2000) Spinal nerve ligation: what to blame for the pain and why. Pain 84:117-120.

Gold MS, Shuster MJ, Levine JD (1996) Characterization of six voltage-gated K+ currents in adult rat sensory neurons. J Neurophysiol 75:2629-2646.

Gold R, Toyka KV, Hartung HP (1995) Synergistic effect of IFN-gamma and TNF-alpha on expression of immune molecules and antigen presentation by Schwann cells. Cell Immunol 165:65-70.

Goldberg A, Russell JW, Alexander NB (2008) Standing balance and trunk position sense in impaired glucose tolerance (IGT)-related peripheral neuropathy. J Neurol Sci

270:165-171.

Goldstein SA, Bayliss DA, Kim D, Lesage F, Plant LD, Rajan S (2005) International Union of Pharmacology. LV. Nomenclature and molecular relationships of two-P potassium channels. Pharmacol Rev 57:527-540.

Gorke K, Pierau FK (1980) Spike potentials and membrane properties of dorsal root ganglion cells in pigeons. Pflugers Arch 386:21-28.

Gracely RH, Lynch SA, Bennett GJ (1992) Painful neuropathy: altered central processing maintained dynamically by peripheral input. Pain 51:175-194.

Grigg P, Schaible HG, Schmidt RF (1986) Mechanical sensitivity of group III and IV afferents from posterior articular nerve in normal and inflamed cat knee. J Neurophysiol 55:635-643.

Grissmer S, Nguyen AN, Aiyar J, Hanson DC, Mather RJ, Gutman GA, Karmilowicz MJ, Auperin DD, Chandy KG (1994) Pharmacological characterization of five cloned voltage-gated K+ channels, types Kv1.1, 1.2, 1.3, 1.5, and 3.1, stably expressed in mammalian cell lines. Mol Pharmacol 45:1227-1234.

Grossman Y, Parnas I, Spira ME (1979) Mechanisms involved in differential conduction of potentials at high frequency in a branching axon. J Physiol 295:307-322.

Grubb BD, Stiller RU, Schaible HG (1993) Dynamic changes in the receptive field properties of spinal cord neurons with ankle input in rats with chronic unilateral inflammation in the ankle region. Exp Brain Res 92:441-452.

Guler AD, Lee H, Iida T, Shimizu I, Tominaga M, Caterina M (2002) Heat-evoked activation of the ion channel, TRPV4. J Neurosci 22:6408-6414.

Gutman GA, Chandy KG, Grissmer S, Lazdunski M, McKinnon D, Pardo LA, Robertson GA, Rudy B, Sanguinetti MC, Stuhmer W, Wang X (2005) International Union of Pharmacology. LIII. Nomenclature and molecular relationships of voltage-gated potassium channels. Pharmacol Rev 57:473-508.

Haigh RC, McCabe CS, Halligan PW, Blake DR (2003) Joint stiffness in a phantom limb: evidence of central nervous system involvement in rheumatoid arthritis. Rheumatology (Oxford) 42:888-892.

Hall MC, Mockett SP, Doherty M (2006) Relative impact of radiographic osteoarthritis and pain on quadriceps strength, proprioception, static postural sway and lower limb function. Ann Rheum Dis 65:865-870.

Han HC, Lee DH, Chung JM (2000) Characteristics of ectopic discharges in a rat neuropathic pain model. Pain 84:253-261.

Hanada T, Yoshimura A (2002) Regulation of cytokine signaling and inflammation. Cytokine Growth Factor Rev 13:413-421.

Hannan MT, Felson DT, Pincus T (2000) Analysis of the discordance between radiographic changes and knee pain in osteoarthritis of the knee. J Rheumatol 27:1513-1517.

Harper AA, Lawson SN (1985) Electrical properties of rat dorsal root ganglion neurones with different peripheral nerve conduction velocities. J Physiol 359:47-63.

Haus J, Halata Z (1990) Innervation of the anterior cruciate ligament. Int Orthop 14:293-296.

Hawker GA, Stewart L, French MR, Cibere J, Jordan JM, March L, Suarez-Almazor M, Gooberman-Hill R (2008) Understanding the pain experience in hip and knee osteoarthritis--an OARSI/OMERACT initiative. Osteoarthritis Cartilage 16:415-422.

Herzog RI, Cummins TR, Waxman SG (2001) Persistent TTX-resistant Na+ current affects resting potential and response to depolarization in simulated spinal sensory neurons. J Neurophysiol 86:1351-1364.

Herzog W, Longino D (2007) The role of muscles in joint degeneration and osteoarthritis. J Biomech 40 Suppl 1:S54-S63.

Hill CL, Gale DG, Chaisson CE, Skinner K, Kazis L, Gale ME, Felson DT (2001) Knee effusions, popliteal cysts, and synovial thickening: association with knee pain in osteoarthritis. J Rheumatol 28:1330-1337.

Hongo T, Kudo N, Sasaki S, Yamashita M, Yoshida K, Ishizuka N, Mannen H (1987) Trajectory of group Ia and Ib fibers from the hind-limb muscles at the L3 and L4 segments of the spinal cord of the cat. J Comp Neurol 262:159-194.

Honig MG (1982) The development of sensory projection patterns in embryonic chick

hind limb. J Physiol 330:175-202.

Horch KW, Tuckett RP, Burgess PR (1977) A key to the classification of cutaneous mechanoreceptors. J Invest Dermatol 69:75-82.

Hsu HC, Luo ZP, Cofield RH, An KN (1997) Influence of rotator cuff tearing on glenohumeral stability. J Shoulder Elbow Surg 6:413-422.

Hsu HC, Luo ZP, Stone JJ, Huang TH, An KN (2003) Correlation between rotator cuff tear and glenohumeral degeneration. Acta Orthop Scand 74:89-94.

Huang CL (2004) The transient receptor potential superfamily of ion channels. J Am Soc Nephrol 15:1690-1699.

Huang EJ, Reichardt LF (2001) Neurotrophins: roles in neuronal development and function. Annu Rev Neurosci 24:677-736.

Hui W, Rowan AD, Richards CD, Cawston TE (2003) Oncostatin M in combination with tumor necrosis factor alpha induces cartilage damage and matrix metalloproteinase expression in vitro and in vivo. Arthritis Rheum 48:3404-3418.

Hunt SP, Rossi J (1985) Peptide- and non-peptide-containing unmyelinated primary afferents: the parallel processing of nociceptive information. Philos Trans R Soc Lond B Biol Sci 308:283-289.

Hunter DJ, McDougall JJ, Keefe FJ (2008) The symptoms of osteoarthritis and the genesis of pain. Rheum Dis Clin North Am 34:623-643.

Hurley MV (1999) The role of muscle weakness in the pathogenesis of osteoarthritis. Rheum Dis Clin North Am 25:283-98, vi.

Hurley MV, Scott DL, Rees J, Newham DJ (1997) Sensorimotor changes and functional performance in patients with knee osteoarthritis. Ann Rheum Dis 56:641-648.

Hylden JL, Nahin RL, Traub RJ, Dubner R (1989) Expansion of receptive fields of spinal lamina I projection neurons in rats with unilateral adjuvant-induced inflammation: the contribution of dorsal horn mechanisms. Pain 37:229-243.

Iggo A (1985) Sensory receptors in the skin of mammals and their sensory functions. Rev Neurol (Paris) 141:599-613.

Ihle JN (1995) Cytokine receptor signalling. Nature 377:591-594.

Inoue K, Ozaki S, Shiga T, Ito K, Masuda T, Okado N, Iseda T, Kawaguchi S, Ogawa M, Bae SC, Yamashita N, Itohara S, Kudo N, Ito Y (2002) Runx3 controls the axonal projection of proprioceptive dorsal root ganglion neurons. Nat Neurosci 5:946-954.

Ivanavicius SP, Ball AD, Heapy CG, Westwood FR, Murray F, Read SJ (2007) Structural pathology in a rodent model of osteoarthritis is associated with neuropathic pain: increased expression of ATF-3 and pharmacological characterisation. Pain 128:272-282.

Jackson AC, Rossiter JP, Lafon M (2006) Expression of Toll-like receptor 3 in the human cerebellar cortex in rabies, herpes simplex encephalitis, and other neurological diseases. J Neurovirol 12:229-234.

Jasmin L, Burkey AR, Card JP, Basbaum AI (1997) Transneuronal labeling of a nociceptive pathway, the spino-(trigemino-)parabrachio-amygdaloid, in the rat. J Neurosci 17:3751-3765.

Jerng HH, Shahidullah M, Covarrubias M (1999) Inactivation gating of Kv4 potassium channels: molecular interactions involving the inner vestibule of the pore. J Gen Physiol 113:641-660.

Ji RR, Suter MR (2007) p38 MAPK, microglial signaling, and neuropathic pain. Mol Pain 3:33.

Ji RR, Woolf CJ (2001) Neuronal plasticity and signal transduction in nociceptive neurons: implications for the initiation and maintenance of pathological pain. Neurobiol Dis 8:1-10.

Johnson GB, Brunn GJ, Kodaira Y, Platt JL (2002) Receptor-mediated monitoring of tissue well-being via detection of soluble heparan sulfate by Toll-like receptor 4. J Immunol 168:5233-5239.

Johnson K, Terkeltaub R (2004) Upregulated ank expression in osteoarthritis can promote both chondrocyte MMP-13 expression and calcification via chondrocyte extracellular PPi excess. Osteoarthritis Cartilage 12:321-335.

Julius D, Basbaum AI (2001) Molecular mechanisms of nociception. Nature 413:203-210.

Kanade RV, Van Deursen RW, Harding KG, Price PE (2008) Investigation of standing balance in patients with diabetic neuropathy at different stages of foot complications. Clin Biomech (Bristol , Avon ) 23:1183-1191.

Kang D, Kim D (2006) TREK-2 (K2P10.1) and TRESK (K2P18.1) are major background K+ channels in dorsal root ganglion neurons. Am J Physiol Cell Physiol 291:C138-C146.

Katz WA. (2001) Osteoarthritis: clinical presentations. In: Osteoarthritis: diagnosis and medical/surgical management (Moskowitz RW, Howell DS, Altman RD, Buckwalter JA, Goldberg V, eds), pp 231-238. W.B. Saunders.

Kawai T, Akira S (2005) Toll-like receptor downstream signaling. Arthritis Res Ther 7:12-19.

Kawano T, Zoga V, Gemes G, McCallum JB, Wu HE, Pravdic D, Liang MY, Kwok WM, Hogan Q, Sarantopoulos C (2009) Suppressed Ca2+/CaM/CaMKII-dependent K(ATP) channel activity in primary afferent neurons mediates hyperalgesia after axotomy. Proc Natl Acad Sci U S A 106:8725-8730.

Kean WF, Kean R, Buchanan WW (2004) Osteoarthritis: symptoms, signs and source of pain. Inflammopharmacology 12:3-31.

Kerr NC, Gao Z, Holmes FE, Hobson SA, Hancox JC, Wynick D, James AF (2007) The sodium channel Nav1.5a is the predominant isoform expressed in adult mouse dorsal root ganglia and exhibits distinct inactivation properties from the full-length Nav1.5 channel. Mol Cell Neurosci 35:283-291.

Kidd BL (2006) Osteoarthritis and joint pain. Pain 123:6-9.

Kikuchi T, Sakuta T, Yamaguchi T (1998) Intra-articular injection of collagenase induces experimental osteoarthritis in mature rabbits. Osteoarthritis Cartilage 6:177-186.

Kim HA, Cho ML, Choi HY, Yoon CS, Jhun JY, Oh HJ, Kim HY (2006) The catabolic pathway mediated by Toll-like receptors in human osteoarthritic chondrocytes. Arthritis Rheum 54:2152-2163.

Kim YI, Na HS, Kim SH, Han HC, Yoon YW, Sung B, Nam HJ, Shin SL, Hong SK (1998) Cell type-specific changes of the membrane properties of peripherally-axotomized dorsal root ganglion neurons in a rat model of neuropathic pain. Neuroscience 86:301-309.

Kobayashi H, Gleich GJ, Butterfield JH, Kita H (2002) Human eosinophils produce neurotrophins and secrete nerve growth factor on immunologic stimuli. Blood 99:2214-2220.

Koerber HR, Mendell LM (1992) Functional heterogeneity of dorsal root ganglion cells. In: Sensory neurons (Scott SA, ed), pp 77-96. New York: Oxford University Press.

Koerber HR, Druzinsky RE, Mendell LM (1988) Properties of somata of spinal dorsal root ganglion cells differ according to peripheral receptor innervated. J Neurophysiol 60:1584-1596.

Koerber HR, Mirnics K, Kavookjian AM, Light AR (1999) Ultrastructural analysis of ectopic synaptic boutons arising from peripherally regenerated primary afferent fibers. J Neurophysiol 81:1636-1644.

Kohama I, Ishikawa K, Kocsis JD (2000) Synaptic reorganization in the substantia gelatinosa after peripheral nerve neuroma formation: aberrant innervation of lamina II neurons by Abeta afferents. J Neurosci 20:1538-1549.

Kokkola R, Sundberg E, Ulfgren AK, Palmblad K, Li J, Wang H, Ulloa L, Yang H, Yan XJ, Furie R, Chiorazzi N, Tracey KJ, Andersson U, Harris HE (2002) High mobility group box chromosomal protein 1: a novel proinflammatory mediator in synovitis. Arthritis Rheum 46:2598-2603.

Koltzenburg M, Stucky CL, Lewin GR (1997) Receptive properties of mouse sensory neurons innervating hairy skin. J Neurophysiol 78:1841-1850.

Koltzenburg M, Torebjork HE, Wahren LK (1994) Nociceptor modulated central sensitization causes mechanical hyperalgesia in acute chemogenic and chronic neuropathic pain. Brain 117 ( Pt 3):579-591.

Kosek E, Ordeberg G (2000) Lack of pressure pain modulation by heterotopic noxious conditioning stimulation in patients with painful osteoarthritis before, but not following, surgical pain relief. Pain 88:69-78.

Kramer I, Sigrist M, de Nooij JC, Taniuchi I, Jessell TM, Arber S (2006) A role for Runx transcription factor signaling in dorsal root ganglion sensory neuron diversification. Neuron 49:379-393.

Krauspe R, Schmitz F, Zoller G, Drenckhahn D (1995) Distribution of

neurofilament-positive nerve fibres and sensory endings in the human anterior cruciate ligament. Arch Orthop Trauma Surg 114:194-198.

Krzemien DM, Schaller KL, Levinson SR, Caldwell JH (2000) Immunolocalization of sodium channel isoform NaCh6 in the nervous system. J Comp Neurol 420:70-83.

Kubo Y, Adelman JP, Clapham DE, Jan LY, Karschin A, Kurachi Y, Lazdunski M, Nichols CG, Seino S, Vandenberg CA (2005) International Union of Pharmacology. LIV. Nomenclature and molecular relationships of inwardly rectifying potassium channels. Pharmacol Rev 57:509-526.

Laban MM (2006) Atrophy and clinical weakness of the iliopsoas muscle: a manifestation of hip osteoarthritis. Am J Phys Med Rehabil 85:629.

Lawrence RC, Helmick CG, Arnett FC, Deyo RA, Felson DT, Giannini EH, Heyse SP, Hirsch R, Hochberg MC, Hunder GG, Liang MH, Pillemer SR, Steen VD, Wolfe F (1998) Estimates of the prevalence of arthritis and selected musculoskeletal disorders in the United States. Arthritis Rheum 41:778-799.

Lawson SN, Crepps BA, Perl ER (1997) Relationship of substance P to afferent characteristics of dorsal root ganglion neurones in guinea-pig. J Physiol 505 ( Pt 1):177-191.

Leadbetter EA, Rifkin IR, Hohlbaum AM, Beaudette BC, Shlomchik MJ, Marshak-Rothstein A (2002) Chromatin-IgG complexes activate B cells by dual engagement of IgM and Toll-like receptors. Nature 416:603-607.

Lee H, Jo EK, Choi SY, Oh SB, Park K, Kim JS, Lee SJ (2006) Necrotic neuronal cells induce inflammatory Schwann cell activation via TLR2 and TLR3: implication in Wallerian degeneration. Biochem Biophys Res Commun 350:742-747.

Leem JW, Willis WD, Chung JM (1993a) Cutaneous sensory receptors in the rat foot. J Neurophysiol 69:1684-1699.

Leem JW, Willis WD, Weller SC, Chung JM (1993b) Differential activation and classification of cutaneous afferents in the rat. J Neurophysiol 70:2411-2424.

Lekan HA, Carlton SM, Coggeshall RE (1996) Sprouting of A beta fibers into lamina II of the rat dorsal horn in peripheral neuropathy. Neurosci Lett 208:147-150.

Lesser SS, Sherwood NT, Lo DC (1997) Neurotrophins differentially regulate voltage-gated ion channels. Mol Cell Neurosci 10:173-183.

Levanon D, Bettoun D, Harris-Cerruti C, Woolf E, Negreanu V, Eilam R, Bernstein Y, Goldenberg D, Xiao C, Fliegauf M, Kremer E, Otto F, Brenner O, Lev-Tov A, Groner Y (2002) The Runx3 transcription factor regulates development and survival of TrkC dorsal root ganglia neurons. EMBO J 21:3454-3463.

Li W, Gao SB, Lv CX, Wu Y, Guo ZH, Ding JP, Xu T (2007) Characterization of voltage-and Ca2+-activated K+ channels in rat dorsal root ganglion neurons. J Cell Physiol 212:348-357.

Li Y, Dorsi MJ, Meyer RA, Belzberg AJ (2000) Mechanical hyperalgesia after an L5 spinal nerve lesion in the rat is not dependent on input from injured nerve fibers. Pain 85:493-502.

Lindhorst E, Wachsmuth L, Kimmig N, Raiss R, Aigner T, Atley L, Eyre D (2005) Increase in degraded collagen type II in synovial fluid early in the rabbit meniscectomy model of osteoarthritis. Osteoarthritis Cartilage 13:139-145.

Liu CN, Wall PD, Ben-Dor E, Michaelis M, Amir R, Devor M (2000a) Tactile allodynia in the absence of C-fiber activation: altered firing properties of DRG neurons following spinal nerve injury. Pain 85:503-521.

Liu W, Burton-Wurster N, Glant TT, Tashman S, Sumner DR, Kamath RV, Lust G, Kimura JH, Cs-Szabo G (2003) Spontaneous and experimental osteoarthritis in dog: similarities and differences in proteoglycan levels. J Orthop Res 21:730-737.

Liu X, Eschenfelder S, Blenk KH, Janig W, Habler H (2000b) Spontaneous activity of axotomized afferent neurons after L5 spinal nerve injury in rats. Pain 84:309-318.

Lu GW, Miletic V (1990) Responses of type A cat spinal ganglion neurons to repetitive stimulation of their central and peripheral processes. Neuroscience 39:259-270.

Lumpkin EA, Bautista DM (2005) Feeling the pressure in mammalian somatosensation. Curr Opin Neurobiol 15:382-388.

Lumpkin EA, Caterina MJ (2007) Mechanisms of sensory transduction in the skin. Nature 445:858-865.

Luscher C, Streit J, Lipp P, Luscher HR (1994) Action potential propagation through embryonic dorsal root ganglion cells in culture. II. Decrease of conduction reliability during repetitive stimulation. J Neurophysiol 72:634-643.

Lynn B, Carpenter SE (1982) Primary afferent units from the hairy skin of the rat hind limb. Brain Res 238:29-43.

Ma C, Shu Y, Zheng Z, Chen Y, Yao H, Greenquist KW, White FA, LaMotte RH (2003) Similar electrophysiological changes in axotomized and neighboring intact dorsal root ganglion neurons. J Neurophysiol 89:1588-1602.

Ma Q, Fode C, Guillemot F, Anderson DJ (1999) Neurogenin1 and neurogenin2 control two distinct waves of neurogenesis in developing dorsal root ganglia. Genes Dev 13:1717-1728.

Ma W, Peschanski M, Ralston HJ, III (1987) The differential synaptic organization of the spinal and lemniscal projections to the ventrobasal complex of the rat thalamus. Evidence for convergence of the two systems upon single thalamic neurons. Neuroscience 22:925-934.

Ma W, Quirion R (2005) The ERK/MAPK pathway, as a target for the treatment of neuropathic pain. Expert Opin Ther Targets 9:699-713.

Mach DB, Rogers SD, Sabino MC, Luger NM, Schwei MJ, Pomonis JD, Keyser CP, Clohisy DR, Adams DJ, O'Leary P, Mantyh PW (2002) Origins of skeletal pain: sensory and sympathetic innervation of the mouse femur. Neuroscience 113:155-166.

Maingret F, Lauritzen I, Patel AJ, Heurteaux C, Reyes R, Lesage F, Lazdunski M, Honore E (2000) TREK-1 is a heat-activated background K(+) channel. EMBO J 19:2483-2491.

Marchand F, Perretti M, McMahon SB (2005) Role of the immune system in chronic pain. Nat Rev Neurosci 6:521-532.

McDougall JJ (2006) Arthritis and pain. Neurogenic origin of joint pain. Arthritis Res Ther 8:220.

McDougall JJ, Watkins L, Li Z (2006) Vasoactive intestinal peptide (VIP) is a modulator of joint pain in a rat model of osteoarthritis. Pain 123:98-105.

McKemy DD, Neuhausser WM, Julius D (2002) Identification of a cold receptor reveals

a general role for TRP channels in thermosensation. Nature 416:52-58.

Melton L (2003) Osteoarthritis pain goes central. Lancet Neurol 2:524.

Michaelis M, Liu X, Janig W (2000) Axotomized and intact muscle afferents but no skin afferents develop ongoing discharges of dorsal root ganglion origin after peripheral nerve lesion. J Neurosci 20:2742-2748.

Miki K, Fukuoka T, Tokunaga A, Noguchi K (1998a) Calcitonin gene-related peptide increase in the rat spinal dorsal horn and dorsal column nucleus following peripheral nerve injury: up-regulation in a subpopulation of primary afferent sensory neurons. Neuroscience 82:1243-1252.

Miki K, Iwata K, Tsuboi Y, Morimoto T, Kondo E, Dai Y, Ren K, Noguchi K (2000) Dorsal column-thalamic pathway is involved in thalamic hyperexcitability following peripheral nerve injury: a lesion study in rats with experimental mononeuropathy. Pain 85:263-271.

Miki K, Iwata K, Tsuboi Y, Sumino R, Fukuoka T, Tachibana T, Tokunaga A, Noguchi K (1998b) Responses of dorsal column nuclei neurons in rats with experimental mononeuropathy. Pain 76:407-415.

Mitchell RN, Cotran RS (2003) Tissue repair: Cell regeneration and fibrosis. In: Robbins and Cotran: Pathologic Basis of Disease (Kumar V, Cotran RS, Robbins SL, eds), pp 61-78. Philadelphia: ELSEVIER SAUNDERS.

Mitsou A, Vallianatos P (1988) Meniscal injuries associated with rupture of the anterior cruciate ligament: a retrospective study. Injury 19:429-431.

Moalem G, Grafe P, Tracey DJ (2005) Chemical mediators enhance the excitability of unmyelinated sensory axons in normal and injured peripheral nerve of the rat. Neuroscience 134:1399-1411.

Mollen KP, Anand RJ, Tsung A, Prince JM, Levy RM, Billiar TR (2006) Emerging paradigm: toll-like receptor 4-sentinel for the detection of tissue damage. Shock 26:430-437.

Molliver DC, Wright DE, Leitner ML, Parsadanian AS, Doster K, Wen D, Yan Q, Snider WD (1997) IB4-binding DRG neurons switch from NGF to GDNF dependence in early postnatal life. Neuron 19:849-861.

Mongan LC, Hill MJ, Chen MX, Tate SN, Collins SD, Buckby L, Grubb BD (2005) The distribution of small and intermediate conductance calcium-activated potassium channels in the rat sensory nervous system. Neuroscience 131:161-175.

Munoz-Guerra MF, gado-Baeza E, Sanchez-Hernandez JJ, Garcia-Ruiz JP (2004) Chondrocyte cloning in aging and osteoarthritis of the hip cartilage: morphometric analysis in transgenic mice expressing bovine growth hormone. Acta Orthop Scand 75:210-216.

Murphy PG, Grondin J, Altares M, Richardson PM (1995) Induction of interleukin-6 in axotomized sensory neurons. J Neurosci 15:5130-5138.

Murphy PG, Ramer MS, Borthwick L, Gauldie J, Richardson PM, Bisby MA (1999) Endogenous interleukin-6 contributes to hypersensitivity to cutaneous stimuli and changes in neuropeptides associated with chronic nerve constriction in mice. Eur J Neurosci 11:2243-2253.

Nakayama K, Niwa M, Sasaki SI, Ichikawa T, Hirai N (1998) Morphology of single primary spindle afferents of the intercostal muscles in the cat. J Comp Neurol 398:459-472.

Nguyen MD, Julien JP, Rivest S (2002) Innate immunity: the missing link in neuroprotection and neurodegeneration? Nat Rev Neurosci 3:216-227.

Nikolajsen L, Brandsborg B, Lucht U, Jensen TS, Kehlet H (2006) Chronic pain following total hip arthroplasty: a nationwide questionnaire study. Acta Anaesthesiol Scand 50:495-500.

Niv D, Gofeld M, Devor M (2003) Causes of pain in degenerative bone and joint disease: a lesson from vertebroplasty. Pain 105:387-392.

Noel J, Zimmermann K, Busserolles J, Deval E, Alloui A, Diochot S, Guy N, Borsotto M, Reeh P, Eschalier A, Lazdunski M (2009) The mechano-activated K+ channels TRAAK and TREK-1 control both warm and cold perception. EMBO J 28:1308-1318.

Noguchi K, Kawai Y, Fukuoka T, Senba E, Miki K (1995) Substance P induced by peripheral nerve injury in primary afferent sensory neurons and its effect on dorsal column nucleus neurons. J Neurosci 15:7633-7643.

Noyes FR, Bassett RW, Grood ES, Butler DL (1980) Arthroscopy in acute traumatic

hemarthrosis of the knee. Incidence of anterior cruciate tears and other injuries. J Bone Joint Surg Am 62:687-95, 757.

O'Connor BL, McConnaughey JS (1978) The structure and innervation of cat knee menisci, and their relation to a "sensory hypothesis" of meniscal function. Am J Anat 153:431-442.

Obata K, Noguchi K (2004) MAPK activation in nociceptive neurons and pain hypersensitivity. Life Sci 74:2643-2653.

Oddis CV (1996) New perspectives on osteoarthritis. Am J Med 100:10S-15S.

Oh Y, Waxman SG (1995) Differential Na+ channel beta 1 subunit mRNA expression in stellate and flat astrocytes cultured from rat cortex and cerebellum: a combined in situ hybridization and immunocytochemistry study. Glia 13:166-173.

Ohashi K, Burkart V, Flohe S, Kolb H (2000) Cutting edge: heat shock protein 60 is a putative endogenous ligand of the toll-like receptor-4 complex. J Immunol 164:558-561.

Oki Y, Koike H, Iijima M, Mori K, Hattori N, Katsuno M, Nakamura T, Hirayama M, Tanaka F, Shiraishi M, Yazaki S, Nokura K, Yamamoto H, Sobue G (2007) Ataxic vs painful form of paraneoplastic neuropathy. Neurology 69:564-572.

Okuse K (2007) Pain signalling pathways: from cytokines to ion channels. Int J Biochem Cell Biol 39:490-496.

Pap G, Eberhardt R, Sturmer I, Machner A, Schwarzberg H, Roessner A, Neumann W (1998) Development of osteoarthritis in the knee joints of Wistar rats after strenuous running exercise in a running wheel by intracranial self-stimulation. Pathol Res Pract 194:41-47.

Park JS, Svetkauskaite D, He Q, Kim JY, Strassheim D, Ishizaka A, Abraham E (2004) Involvement of toll-like receptors 2 and 4 in cellular activation by high mobility group box 1 protein. J Biol Chem 279:7370-7377.

Patapoutian A, Reichardt LF (2001) Trk receptors: mediators of neurotrophin action. Curr Opin Neurobiol 11:272-280.

Pearce RJ, Duchen MR (1994) Differential expression of membrane currents in dissociated mouse primary sensory neurons. Neuroscience 63:1041-1056.

Peier AM, Moqrich A, Hergarden AC, Reeve AJ, Andersson DA, Story GM, Earley TJ, Dragoni I, McIntyre P, Bevan S, Patapoutian A (2002a) A TRP channel that senses cold stimuli and menthol. Cell 108:705-715.

Peier AM, Reeve AJ, Andersson DA, Moqrich A, Earley TJ, Hergarden AC, Story GM, Colley S, Hogenesch JB, McIntyre P, Bevan S, Patapoutian A (2002b) A heat-sensitive TRP channel expressed in keratinocytes. Science 296:2046-2049.

Peles E, Salzer JL (2000) Molecular domains of myelinated axons. Curr Opin Neurobiol 10:558-565.

Pellegrino RG, Spencer PS, Ritchie JM (1984) Sodium channels in the axolemma of unmyelinated axons: a new estimate. Brain Res 305:357-360.

Pelletier JP, Martel-Pelletier J, Abramson SB (2001) Osteoarthritis, an inflammatory disease: potential implication for the selection of new therapeutic targets. Arthritis Rheum 44:1237-1247.

Petruska JC, Napaporn J, Johnson RD, Cooper BY (2002) Chemical responsiveness and histochemical phenotype of electrophysiologically classified cells of the adult rat dorsal root ganglion. Neuroscience 115:15-30.

Petruska JC, Napaporn J, Johnson RD, Gu JG, Cooper BY (2000) Subclassified acutely dissociated cells of rat DRG: histochemistry and patterns of capsaicin-, proton-, and ATP-activated currents. J Neurophysiol 84:2365-2379.

Pitcher GM, Henry JL (2004) Nociceptive response to innocuous mechanical stimulation is mediated via myelinated afferents and NK-1 receptor activation in a rat model of neuropathic pain. Exp Neurol 186:173-197.

Pitcher GM, Henry JL (2008) Governing role of primary afferent drive in increased excitation of spinal nociceptive neurons in a model of sciatic neuropathy. Exp Neurol 214:219-228.

Poliak S, Peles E (2003) The local differentiation of myelinated axons at nodes of Ranvier. Nat Rev Neurosci 4:968-980.

Pomonis JD, Boulet JM, Gottshall SL, Phillips S, Sellers R, Bunton T, Walker K (2005) Development and pharmacological characterization of a rat model of osteoarthritis pain. Pain 114:339-346.

Poole AR (1999) An introduction to the pathophysiology of osteoarthritis. Front Biosci 4:D662-D670.

Price MP, Lewin GR, McIlwrath SL, Cheng C, Xie J, Heppenstall PA, Stucky CL, Mannsfeldt AG, Brennan TJ, Drummond HA, Qiao J, Benson CJ, Tarr DE, Hrstka RF, Yang B, Williamson RA, Welsh MJ (2000) The mammalian sodium channel BNC1 is required for normal touch sensation. Nature 407:1007-1011.

Price MP, McIlwrath SL, Xie J, Cheng C, Qiao J, Tarr DE, Sluka KA, Brennan TJ, Lewin GR, Welsh MJ (2001) The DRASIC cation channel contributes to the detection of cutaneous touch and acid stimuli in mice. Neuron 32:1071-1083.

Prince JM, Levy RM, Yang R, Mollen KP, Fink MP, Vodovotz Y, Billiar TR (2006) Toll-like receptor-4 signaling mediates hepatic injury and systemic inflammation in hemorrhagic shock. J Am Coll Surg 202:407-417.

Ramos A, Mormede P (1998) Stress and emotionality: a multidimensional and genetic approach. Neurosci Biobehav Rev 22:33-57.

Rasband MN, Park EW, Vanderah TW, Lai J, Porreca F, Trimmer JS (2001) Distinct potassium channels on pain-sensing neurons. Proc Natl Acad Sci U S A 98:13373-13378.

Rasband MN, Trimmer JS, Schwarz TL, Levinson SR, Ellisman MH, Schachner M, Shrager P (1998) Potassium channel distribution, clustering, and function in remyelinating rat axons. J Neurosci 18:36-47.

Rau KK, Cooper BY, Johnson RD (2006) Expression of TWIK-related acid sensitive K+ channels in capsaicin sensitive and insensitive cells of rat dorsal root ganglia. Neuroscience 141:955-963.

Reid G, Flonta M (2001) Cold transduction by inhibition of a background potassium conductance in rat primary sensory neurones. Neurosci Lett 297:171-174.

Renganathan M, Cummins TR, Waxman SG (2001) Contribution of Na(v)1.8 sodium channels to action potential electrogenesis in DRG neurons. J Neurophysiol 86:629-640.

Rexed B (1952) The cytoarchitectonic organization of the spinal cord in the cat. J Comp Neurol 96:414-495.

Rexed B (1954) A cytoarchitectonic atlas of the spinal cord in the cat. J Comp Neurol

100:297-379.

Ritchie JM, Rogart RB (1977) Density of sodium channels in mammalian myelinated nerve fibers and nature of the axonal membrane under the myelin sheath. Proc Natl Acad Sci U S A 74:211-215.

Roberts WJ, Elardo SM (1986) Clustering of primary afferent fibers in peripheral nerve fascicles by sensory modality. Brain Res 370:149-152.

Rook JM, Hasan W, McCarson KE (2008) Temporal effects of topical morphine application on cutaneous wound healing. Anesthesiology 109:130-136.

Rowbotham M.C, Kidd BL, Porreca F (2006) Role of central sensitization in chronic pain: Osteoarthritis and rheumatoid arthritis compared to neuropathic pain. In: Proceedings of the 11th World Congress on Pain (Flor H, Kalso E, Dostrovsky JO, eds), pp 231-249. Seattle: IASP Press.

Rudy B (1988) Diversity and ubiquity of K channels. Neuroscience 25:729-749.

Rush AM, Cummins TR, Waxman SG (2007) Multiple sodium channels and their roles in electrogenesis within dorsal root ganglion neurons. J Physiol 579:1-14.

Saade NE, Baliki M, El-Khoury C, Hawwa N, Atweh SF, Apkarian AV, Jabbur SJ (2002) The role of the dorsal columns in neuropathic behavior: evidence for plasticity and non-specificity. Neuroscience 115:403-413.

Sah DW, Ossipo MH, Porreca F (2003) Neurotrophic factors as novel therapeutics for neuropathic pain. Nat Rev Drug Discov 2:460-472.

Sah P, Faber ES (2002) Channels underlying neuronal calcium-activated potassium currents. Prog Neurobiol 66:345-353.

Saito T, Koshino T (2000) Distribution of neuropeptides in synovium of the knee with osteoarthritis. Clin Orthop Relat Res172-182.

Salo PT, Seeratten RA, Erwin WM, Bray RC (2002) Evidence for a neuropathic contribution to the development of spontaneous knee osteoarthrosis in a mouse model. Acta Orthop Scand 73:77-84.

Sangameswaran L, Delgado SG, Fish LM, Koch BD, Jakeman LB, Stewart GR, Sze P, Hunter JC, Eglen RM, Herman RC (1996) Structure and function of a novel

voltage-gated, tetrodotoxin-resistant sodium channel specific to sensory neurons. J Biol Chem 271:5953-5956.

Sapunar D, Ljubkovic M, Lirk P, McCallum JB, Hogan QH (2005) Distinct membrane effects of spinal nerve ligation on injured and adjacent dorsal root ganglion neurons in rats. Anesthesiology 103:360-376.

Sarantopoulos C, McCallum B, Sapunar D, Kwok WM, Hogan Q (2003) ATP-sensitive potassium channels in rat primary afferent neurons: the effect of neuropathic injury and gabapentin. Neurosci Lett 343:185-189.

Sarantopoulos CD, McCallum JB, Rigaud M, Fuchs A, Kwok WM, Hogan QH (2007) Opposing effects of spinal nerve ligation on calcium-activated potassium currents in axotomized and adjacent mammalian primary afferent neurons. Brain Res 1132:84-99.

Saxler G, Loer F, Skumavc M, Pfortner J, Hanesch U (2007) Localization of SP- and CGRP-immunopositive nerve fibers in the hip joint of patients with painful osteoarthritis and of patients with painless failed total hip arthroplasties. Eur J Pain 11:67-74.

Saxne T, Lindell M, Mansson B, Petersson IF, Heinegard D (2003) Inflammation is a feature of the disease process in early knee joint osteoarthritis. Rheumatology (Oxford) 42:903-904.

Schafers M, Brinkhoff J, Neukirchen S, Marziniak M, Sommer C (2001) Combined epineurial therapy with neutralizing antibodies to tumor necrosis factor-alpha and interleukin-1 receptor has an additive effect in reducing neuropathic pain in mice. Neurosci Lett 310:113-116.

Schafers M, Svensson CI, Sommer C, Sorkin LS (2003) Tumor necrosis factor-alpha induces mechanical allodynia after spinal nerve ligation by activation of p38 MAPK in primary sensory neurons. J Neurosci 23:2517-2521.

Schaible HG, Grubb BD (1993) Afferent and spinal mechanisms of joint pain. Pain 55:5-54.

Schaible HG, Schmidt RF (1985) Effects of an experimental arthritis on the sensory properties of fine articular afferent units. J Neurophysiol 54:1109-1122.

Schaible HG, Schmidt RF (1988) Time course of mechanosensitivity changes in articular afferents during a developing experimental arthritis. J Neurophysiol 60:2180-2195.

Scholz A, Gruss M, Vogel W (1998) Properties and functions of calcium-activated K+ channels in small neurones of rat dorsal root ganglion studied in a thin slice preparation. J Physiol 513 ( Pt 1):55-69.

Scholz J, Woolf CJ (2002) Can we conquer pain? Nat Neurosci 5 Suppl:1062-1067.

Schuelert N, McDougall JJ (2006) Electrophysiological evidence that the vasoactive intestinal peptide receptor antagonist VIP6-28 reduces nociception in an animal model of osteoarthritis. Osteoarthritis Cartilage 14:1155-1162.

Schwartz N (2005) Altered buffering capacity of spinal wide dynamic range neurons in a chronic model of osteoarthritis. M.Sc. Thesis. The University of Western Ontario.

Schwarz JR, Glassmeier G, Cooper EC, Kao TC, Nodera H, Tabuena D, Kaji R, Bostock H (2006) KCNQ channels mediate IKs, a slow K+ current regulating excitability in the rat node of Ranvier. J Physiol 573:17-34.

Scroggs RS, Fox AP (1992a) Calcium current variation between acutely isolated adult rat dorsal root ganglion neurons of different size. J Physiol 445:639-658.

Scroggs RS, Fox AP (1992b) Multiple Ca2+ currents elicited by action potential waveforms in acutely isolated adult rat dorsal root ganglion neurons. J Neurosci 12:1789-1801.

Segev I, Schneidman E (1999) Axons as computing devices: basic insights gained from models. J Physiol Paris 93:263-270.

Shakoor N, Moisio K (2004) A biomechanical approach to musculoskeletal disease. Best Pract Res Clin Rheumatol 18:173-186.

Shamash S, Reichert F, Rotshenker S (2002) The cytokine network of Wallerian degeneration: tumor necrosis factor-alpha, interleukin-1alpha, and interleukin-1beta. J Neurosci 22:3052-3060.

Sharma L (1999) Proprioceptive impairment in knee osteoarthritis. Rheum Dis Clin North Am 25:299-314.

Sharma L, Pai YC (1997) Impaired proprioception and osteoarthritis. Curr Opin Rheumatol 9:253-258.

Sheen K, Chung JM (1993) Signs of neuropathic pain depend on signals from injured

nerve fibers in a rat model. Brain Res 610:62-68.

Shirakura K, Terauchi M, Fukasawa N, Kimura M, Shimizu T (1995) Clinical and arthroscopic findings of acute anterior cruciate ligament tears of the knee. Diagn Ther Endosc 2:107-112.

Simkin PA (2004) Bone pain and pressure in osteoarthritic joints. Novartis Found Symp 260:179-186.

Smiley ST, King JA, Hancock WW (2001) Fibrinogen stimulates macrophage chemokine secretion through toll-like receptor 4. J Immunol 167:2887-2894.

Smith GD, Gunthorpe MJ, Kelsell RE, Hayes PD, Reilly P, Facer P, Wright JE, Jerman JC, Walhin JP, Ooi L, Egerton J, Charles KJ, Smart D, Randall AD, Anand P, Davis JB (2002) TRPV3 is a temperature-sensitive vanilloid receptor-like protein. Nature 418:186-190.

Snider WD (1994) Functions of the neurotrophins during nervous system development: what the knockouts are teaching us. Cell 77:627-638.

Sobue G, Yamamoto M, Doyu M, Li M, Yasuda T, Mitsuma T (1998) Expression of mRNAs for neurotrophins (NGF, BDNF, and NT-3) and their receptors (p75NGFR, trk, trkB, and trkC) in human peripheral neuropathies. Neurochem Res 23:821-829.

Sommer C, Petrausch S, Lindenlaub T, Toyka KV (1999) Neutralizing antibodies to interleukin 1-receptor reduce pain associated behavior in mice with experimental neuropathy. Neurosci Lett 270:25-28.

Song Y, Greve JM, Carter DR, Giori NJ (2008) Meniscectomy alters the dynamic deformational behavior and cumulative strain of tibial articular cartilage in knee joints subjected to cyclic loads. Osteoarthritis Cartilage 16:1545-1554.

Stebbing MJ, Eschenfelder S, Habler HJ, Acosta MC, Janig W, McLachlan EM (1999) Changes in the action potential in sensory neurones after peripheral axotomy in vivo. Neuroreport 10:201-206.

Story GM, Peier AM, Reeve AJ, Eid SR, Mosbacher J, Hricik TR, Earley TJ, Hergarden AC, Andersson DA, Hwang SW, McIntyre P, Jegla T, Bevan S, Patapoutian A (2003) ANKTM1, a TRP-like channel expressed in nociceptive neurons, is activated by cold temperatures. Cell 112:819-829.

Stucky CL, Gold MS, Zhang X (2001) Mechanisms of pain. Proc Natl Acad Sci U S A 98:11845-11846.

Sun H, Ren K, Zhong CM, Ossipov MH, Malan TP, Lai J, Porreca F (2001) Nerve injury-induced tactile allodynia is mediated via ascending spinal dorsal column projections. Pain 90:105-111.

Suri S, Gill SE, Massena de CS, Wilson D, McWilliams DF, Walsh DA (2007) Neurovascular invasion at the osteochondral junction and in osteophytes in osteoarthritis. Ann Rheum Dis 66:1423-1428.

Swagerty DL, Jr., Hellinger D (2001) Radiographic assessment of osteoarthritis. Am Fam Physician 64:279-286.

Takahashi N, Kikuchi S, Dai Y, Kobayashi K, Fukuoka T, Noguchi K (2003) Expression of auxiliary beta subunits of sodium channels in primary afferent neurons and the effect of nerve injury. Neuroscience 121:441-450.

Taniguchi N, Kawahara K, Yone K, Hashiguchi T, Yamakuchi M, Goto M, Inoue K, Yamada S, Ijiri K, Matsunaga S, Nakajima T, Komiya S, Maruyama I (2003) High mobility group box chromosomal protein 1 plays a role in the pathogenesis of rheumatoid arthritis as a novel cytokine. Arthritis Rheum 48:971-981.

Taylor KR, Trowbridge JM, Rudisill JA, Termeer CC, Simon JC, Gallo RL (2004) Hyaluronan fragments stimulate endothelial recognition of injury through TLR4. J Biol Chem 279:17079-17084.

Termeer C, Benedix F, Sleeman J, Fieber C, Voith U, Ahrens T, Miyake K, Freudenberg M, Galanos C, Simon JC (2002) Oligosaccharides of Hyaluronan activate dendritic cells via toll-like receptor 4. J Exp Med 195:99-111.

Thacker MA, Clark AK, Marchand F, McMahon SB (2007) Pathophysiology of peripheral neuropathic pain: immune cells and molecules. Anesth Analg 105:838-847.

Theriault FM, Roy P, Stifani S (2004) AML1/Runx1 is important for the development of hindbrain cholinergic branchiovisceral motor neurons and selected cranial sensory neurons. Proc Natl Acad Sci U S A 101:10343-10348.

Tominaga M, Caterina MJ, Malmberg AB, Rosen TA, Gilbert H, Skinner K, Raumann BE, Basbaum AI, Julius D (1998) The cloned capsaicin receptor integrates multiple

pain-producing stimuli. Neuron 21:531-543.

Tsujino H, Kondo E, Fukuoka T, Dai Y, Tokunaga A, Miki K, Yonenobu K, Ochi T, Noguchi K (2000) Activating transcription factor 3 (ATF3) induction by axotomy in sensory and motoneurons: A novel neuronal marker of nerve injury. Mol Cell Neurosci 15:170-182.

van Beijnum JR, Buurman WA, Griffioen AW (2008) Convergence and amplification of toll-like receptor (TLR) and receptor for advanced glycation end products (RAGE) signaling pathways via high mobility group B1 (HMGB1). Angiogenesis 11:91-99.

varez de la RD, Zhang P, Shao D, White F, Canessa CM (2002) Functional implications of the localization and activity of acid-sensitive channels in rat peripheral nervous system. Proc Natl Acad Sci U S A 99:2326-2331.

Viana F, De La PE, Belmonte C (2002) Specificity of cold thermotransduction is determined by differential ionic channel expression. Nat Neurosci 5:254-260.

Voets T, Nilius B (2003) TRPs make sense. J Membr Biol 192:1-8.

Watkins LR, Maier SF (2002) Beyond neurons: evidence that immune and glial cells contribute to pathological pain states. Physiol Rev 82:981-1011.

Watkins LR, Milligan ED, Maier SF (2001) Glial activation: a driving force for pathological pain. Trends Neurosci 24:450-455.

Waxman SG, Kocsis JD, Black JA (1994) Type III sodium channel mRNA is expressed in embryonic but not adult spinal sensory neurons, and is reexpressed following axotomy. J Neurophysiol 72:466-470.

Wei AD, Gutman GA, Aldrich R, Chandy KG, Grissmer S, Wulff H (2005) International Union of Pharmacology. LII. Nomenclature and molecular relationships of calcium-activated potassium channels. Pharmacol Rev 57:463-472.

Weissner W, Winterson BJ, Stuart-Tilley A, Devor M, Bove GM (2006) Time course of substance P expression in dorsal root ganglia following complete spinal nerve transection. J Comp Neurol 497:78-87.

Wetmore C, Olson L (1995) Neuronal and nonneuronal expression of neurotrophins and their receptors in sensory and sympathetic ganglia suggest new intercellular trophic

interactions. J Comp Neurol 353:143-159.

Willis D, Li KW, Zheng JQ, Chang JH, Smit A, Kelly T, Merianda TT, Sylvester J, van MJ, Twiss JL (2005) Differential transport and local translation of cytoskeletal, injury-response, and neurodegeneration protein mRNAs in axons. J Neurosci 25:778-791.

Willis WD, Coggeshall RE (2004) Sensory Mechanisms of the Spinal Cord. New York: Kluwer Academic/Plenum Publishers.

Willis WD, Westlund KN (1997) Neuroanatomy of the pain system and of the pathways that modulate pain. J Clin Neurophysiol 14:2-31.

Wilson P, Meyers DE, Snow PJ (1986) The detailed somatotopic organization of the dorsal horn in the lumbosacral enlargement of the cat spinal cord. J Neurophysiol 55:604-617.

Woolf CJ, Salter MW (2000) Neuronal plasticity: increasing the gain in pain. Science 288:1765-1769.

Woolf CJ, Shortland P, Coggeshall RE (1992) Peripheral nerve injury triggers central sprouting of myelinated afferents. Nature 355:75-78.

Woolf CJ, Shortland P, Reynolds M, Ridings J, Doubell T, Coggeshall RE (1995) Reorganization of central terminals of myelinated primary afferents in the rat dorsal horn following peripheral axotomy. J Comp Neurol 360:121-134.

Wu G, Ekedahl R, Hallin RG (1998) Clustering of slowly adapting type II mechanoreceptors in human peripheral nerve and skin. Brain 121 ( Pt 2):265-279.

Wu G, Ringkamp M, Hartke TV, Murinson BB, Campbell JN, Griffin JW, Meyer RA (2001) Early onset of spontaneous activity in uninjured C-fiber nociceptors after injury to neighboring nerve fibers. J Neurosci 21:RC140.

Wu G, Ringkamp M, Murinson BB, Pogatzki EM, Hartke TV, Weerahandi HM, Campbell JN, Griffin JW, Meyer RA (2002) Degeneration of myelinated efferent fibers induces spontaneous activity in uninjured C-fiber afferents. J Neurosci 22:7746-7753.

Xu H, Ramsey IS, Kotecha SA, Moran MM, Chong JA, Lawson D, Ge P, Lilly J, Silos-Santiago I, Xie Y, DiStefano PS, Curtis R, Clapham DE (2002) TRPV3 is a calcium-permeable temperature-sensitive cation channel. Nature 418:181-186.

Yamamoto M, Sobue G, Yamamoto K, Terao S, Mitsuma T (1996) Expression of mRNAs for neurotrophic factors (NGF, BDNF, NT-3, and GDNF) and their receptors (p75NGFR, trkA, trkB, and trkC) in the adult human peripheral nervous system and nonneural tissues. Neurochem Res 21:929-938.

Yelin E, Callahan LF (1995) The economic cost and social and psychological impact of musculoskeletal conditions. National Arthritis Data Work Groups. Arthritis Rheum 38:1351-1362.

Yin XF, Fu ZG, Zhang DY, Jiang BG (2007) Alterations in the expression of ATP-sensitive potassium channel subunit mRNA after acute peripheral nerve and spinal cord injury. Eur Neurol 57:4-10.

Yoshimura N, White G, Weight FF, de Groat WC (1996) Different types of Na+ and A-type K+ currents in dorsal root ganglion neurones innervating the rat urinary bladder. J Physiol 494 ( Pt 1):1-16.

Yu M, Wang H, Ding A, Golenbock DT, Latz E, Czura CJ, Fenton MJ, Tracey KJ, Yang H (2006) HMGB1 signals through toll-like receptor (TLR) 4 and TLR2. Shock 26:174-179.

Yusaf SP, Goodman J, Pinnock RD, Dixon AK, Lee K (2001) Expression of voltage-gated calcium channel subunits in rat dorsal root ganglion neurons. Neurosci Lett 311:137-141.

Zhou XF, Deng YS, Chie E, Xue Q, Zhong JH, McLachlan EM, Rush RA, Xian CJ (1999) Satellite-cell-derived nerve growth factor and neurotrophin-3 are involved in noradrenergic sprouting in the dorsal root ganglia following peripheral nerve injury in the rat. Eur J Neurosci 11:1711-1722.

Zimny ML, Albright DJ, Dabezies E (1988) Mechanoreceptors in the human medial meniscus. Acta Anat (Basel) 133:35-40.

Zimny ML, Schutte M, Dabezies E (1986) Mechanoreceptors in the human anterior cruciate ligament. Anat Rec 214:204-209.